

CHARACTERISATION AND STRUCTURE/FUNCTION
STUDIES OF THE LIVER-TYPE AND BRAIN-TYPE
GLUCOSE TRANSPORTERS

A thesis submitted to the
FACULTY OF SCIENCE
for
the degree of
DOCTOR OF PHILOSOPHY

BY

MICHAEL JOHN SEATTER

Division of Biochemistry & Molecular Biology
Institute of Biomedical & Life Sciences
University of Glasgow
November 1994

ProQuest Number: 11007895

All rights reserved

INFORMATION TO ALL USERS

The quality of this reproduction is dependent upon the quality of the copy submitted.

In the unlikely event that the author did not send a complete manuscript and there are missing pages, these will be noted. Also, if material had to be removed, a note will indicate the deletion.



ProQuest 11007895

Published by ProQuest LLC (2018). Copyright of the Dissertation is held by the Author.

All rights reserved.

This work is protected against unauthorized copying under Title 17, United States Code
Microform Edition © ProQuest LLC.

ProQuest LLC.
789 East Eisenhower Parkway
P.O. Box 1346
Ann Arbor, MI 48106 – 1346

GLASGOW
UNIVERSITY
LIBRARY

Thesis
10,003
Copy 1

Abstract.

K_m values were measured for zero-*trans* entry of 2-deoxy-D-glucose and β -D-fructose into *Xenopus* oocytes heterologously expressing GLUT2. GLUT2 transports 2-deoxy-D-glucose with a K_m of 11 mM and D-fructose with a K_m of 67 mM. K_i values for D-glucose, maltose, D-fructose and cytochalasin B inhibition of 2-deoxy-D-glucose transport by GLUT2 were measured. Inhibition of 2-deoxy-D-glucose transport by D-glucose, maltose and D-fructose was competitive, with K_i values of 6.5 mM, 125 mM and 200 mM, respectively. Inhibition by cytochalasin B was non-competitive, with a K_i of 6.9 μ M. In addition, K_i values were measured for D-glucose, maltose, and cytochalasin B inhibition of D-fructose transport by GLUT2. D-glucose and maltose were competitive inhibitors displaying K_i values of 15.3 mM and 116 mM, respectively. Inhibition by cytochalasin B was non-competitive, with a K_i value of 6.1 μ M.

The inhibitory effects of L-sorbose and 2,5-anhydro-D-mannitol, β -D-fructopyranose and β -D-fructofuranose analogues, respectively, on 2-deoxy-D-glucose transport into *Xenopus* oocytes by heterologously expressed GLUT2, were investigated. L-sorbose and 2,5-anhydro-D-mannitol both competitively inhibited 2-deoxy-D-glucose transport with K_i values of 170 mM and 26 mM, respectively, suggesting that β -D-fructose is likely to interact with GLUT2 in the furanose ring form.

The structural basis of sugar binding to GLUT2 has been investigated using a range of hexoses, halogeno- and deoxy-D-glucose analogues to inhibit the transport of 2-deoxy-D-glucose by GLUT2 expressed heterologously in *Xenopus* oocytes. Results indicate that hydrogen bonding is important at the C-1, C-3, and to a lesser extent at the C-4 and C-6 hydroxyls of D-glucose, and that hydrophobic interactions at the C-6 position may also prove important.

The results obtained for GLUT2 have been compared with those published for GLUT1 and GLUT4, and with GLUT3 in oocytes, and the binding patterns of the transporters were found to be broadly similar but this varied subtly between isoforms. A model has been produced to show the interactions of D-glucose and D-fructose with the exofacial binding site of GLUT2.

Site-directed mutagenesis and recombinant polymerase chain reaction (PCR) technology have been used to construct a series of nineteen mutant GLUT3 cDNAs. These contain single codon changes such that each cDNA encodes a protein with a single transmembrane helix 8 residue substituted with alanine. These transporter cDNAs have been used as a template for *in vitro* synthesis of mRNA which has been injected into *Xenopus* oocytes. Each of these mutants has been found to transport 2-deoxy-D-glucose at levels between 40-200% of that measured with wild-type GLUT3, but expression levels have not yet been determined.

Acknowledgements.

I would primarily like to thank Dr. Gwynedd Gould, for his excellent supervision and helpful advice over the last three years, which have proved essential. I could only wish that his advice on the subject of spelling was as rewarding.

I would also like to thank: Dr. Carol Colville, whose GLUT3 data is referred to frequently in this thesis; Dr. Margaret MacClean, for some practical tips on the "black magic" of Molecular Biology; Thomas Jess, for helping me get started with the automatic sequencer and generally keeping me in my place (and because he told me to mention him); Dr. Alison Brant, for the timely loan of her thesis so that I could get my own write-up off the ground; and all other members of Lab. C36 (Susie, Sally, Ian, Lisa, Callum & Fiona), who have suffered my inane drivel for the past three years- especially while writing this Sme.....Sme.....thesis.

I would especially like to thank Sandra Gardner, who has put up with me for the majority of my time in Glasgow, and whose encouragement and support I have greatly appreciated.

Lastly, I would like to thank to my mum, dad and paternal grandparents, all of whom encouraged me ever onward but never demanded. It is to them that I dedicate this thesis - it'll make a damn fine doorstep!

Abbreviations.

Ac	Acetate
Amp	Ampicillin
ASA-BMPA	2-N-(4-azidosalicyl)-1,3-bis(D-mannos-4-yloxy)propyl-2-amine
ATB-BMPA	2-N-[4-azi-2,2,2-trifluoroethyl)benzoyl]-1,3-bis(D-mannos-4-yloxy)-2-propylamine
ATP	adenosine 5'-triphosphate
BMPA	1,3-bis-(D-mannos-4-yloxy)-2-propylamine
bp	base pairs
C-1	carbon position number 1.
cDNA	complementary deoxyribonucleic acid
CD	circular dichroism
CIP	calf intestinal phosphatase
CTP	cytidine 5'-triphosphate
DNA	deoxyribonucleic acid
dsDNA	double-stranded deoxyribonucleic acid
dNTPs	deoxyribonucleic nucleoside 5'-triphosphates
dpm	disintegrations per minute
dTTP	deoxyribonucleic thymidine 5'-triphosphate
DTT	dithiothreitol
EDTA	Diaminoethanetetra-acetic acid, disodium salt
FDNB	1-fluoro-2,4-dinitrobenzene
FTIR	fourier-transforming infra-red
g _{av}	average gravitational force
GLUT	glucose transporter
GTP	guanosine 5'-triphosphate

HEPES	<i>N</i> -2-hydroxyethylpiperazine- <i>N'</i> -2-ethane sulphonic acid
IAPS-forskolin	iodo-4-azidophenethylamido-7- <i>O</i> -succinyldeacetyl forskolin
IR	infra-red
K_i	inhibitory affinity constant
K_m	affinity constant
LB	Luria-Bertani
min	minutes
MOPS	3'-(<i>N</i> -morpholino)propanesulphonic acid
mRNA	messenger ribonucleic acid
NHS-LC-biotin	sulphosuccinimidyl-6-(biotinamido)-hexano-oate
NIDDM	non-insulin-dependent diabetes mellitus
NMR	nuclear magnetic resonance
PBS	phosphate-buffered saline
pCMBS	<i>p</i> -chloro-mercuribenzenesulphonate
PCR	polymerase chain reaction
PEG	polyethylene glycol
PEP	phospho-enol-pyruvate
pfu	plaque-forming units
rfDNA	replicating form deoxyribonucleic acid
RNA	ribonucleic acid
RNase A	ribonuclease A
rNTPs	ribonucleoside 5'-triphosphates
rpm	revolutions per minute
sec	seconds
SD	standard deviation
SDS-PAGE	sodium dodecyl sulphate polyacrylamide gel electrophoresis

SGLT1	sodium-glucose-linked transporter 1
ssDNA	single-stranded deoxyribonucleic acid
STE	saline-Tris-EDTA
TACS	terminator ammonium cycle sequencing
TAE	Tris-acetate-EDTA
TBE	Tris-borate-EDTA
TE	Tris-EDTA
TEMED	<i>N, N, N', N'</i> -tetramethylenediamine
Tris	tris(hydroxymethyl)aminoethane
rUTP	uridine 5'-triphosphate
UTR	untranslated regions
V_{\max}	theoretical maximum velocity
v/v	volume/volume ratio
w/v	weight/volume ratio

Contents.

	Page.
Title	i
Abstract	ii
Acknowledgements	iv
Abbreviations	v
Contents	viii
List of figures	xvii
List of tables	xx
Chapter 1. Introduction.	1
1.1 General Background.	2
1.2 Tissue-specific Distribution of the Facilitative Glucose Transporter Family.	 4
1.2.1 General.	4
1.2.2 GLUT1.	5
1.2.3 GLUT2.	7
1.2.4 GLUT3.	9
1.2.5 GLUT4.	11
1.2.6 GLUT5.	13
1.2.7 GLUT6.	13
1.2.8 GLUT7.	14
1.3 Structure of the Mammalian Facilitative Glucose Transporter Family.	 15

1.3.1	General Studies.	15
1.3.2	Topology Studies.	16
1.3.3	Spectroscopic Studies.	19
1.4	Homologous Transporter Proteins in other Organisms.	20
1.5	The Dynamics of D-Glucose Transport.	22
1.5.1	Kinetic Parameters of GLUT1 D-Glucose Transport.	22
1.5.1.1	<i>Zero-trans</i> Entry.	23
1.5.1.2	<i>Zero-trans</i> Exit.	23
1.5.1.3	<i>Infinite-cis</i> Entry.	24
1.5.1.4	<i>Infinite-cis</i> Exit.	24
1.5.1.5	<i>Infinite-trans</i> Entry.	24
1.5.1.6	<i>Infinite-trans</i> Exit.	24
1.5.1.7	Equilibrium Exchange.	25
1.5.2	Mechanistic Models for D-Glucose Transport.	26
1.5.2.1	The Single-Site Alternating Conformer Model.	26
1.5.2.2	Measurement of Rate Constants for Transport Events.	27
1.5.2.3	Multiple Site Models.	29
1.6	Conformational Changes in GLUT1.	30
1.6.1	Detection of GLUT1 Conformational Changes by Measurement of Transporter Intrinsic Fluorescence.	31
1.6.2	Sensitivity of Different Transporter Conformations to Chemical Inactivation.	32
1.6.3	Effects of GLUT1 Conformational State on Proteolytic Cleavage.	33

1.7	D-Glucose-Inhibitable Photoaffinity Labelling.	35
1.7.1	Photoaffinity Labels Proposed to Interact with the Endofacial D-Glucose Binding Site.	36
1.7.2	Photoaffinity Labels Proposed to Interact with the Exofacial D-Glucose Binding Site.	37
1.8	Oligomerisation of GLUT1.	38
1.9	Aims of this Study.	41
Chapter 2.	Materials and Methods.	49
2.1	Materials.	50
2.2	<i>In Vitro</i> Synthesis of mRNA from Plasmid cDNA.	53
2.3	Using <i>Xenopus</i> Oocytes.	54
2.3.1	Handling <i>Xenopus</i> .	54
2.3.2	Anaesthesia.	55
2.3.3	Surgery.	55
2.3.4	Oocyte Isolation and Injection.	56
2.4	Sugar Transport in <i>Xenopus</i> Oocytes.	57
2.5	General Techniques for the Manipulation of cDNA.	58
2.5.1	Plasmid Construction.	58
2.5.2	Linearisation of Plasmid cDNA.	59
2.5.3	Agarose Gel Electrophoresis of cDNA.	60

2.5.4	Restriction Digestion of cDNA.	61
2.5.5	Dephosphorylation of Double-Stranded cDNA using Calf Intestinal Phosphatase.	62
2.5.6	Ligation of Double-Stranded cDNA.	62
2.5.7	Preparation of Competent Cells.	63
2.5.8	Transformation of Competent <i>E. coli.</i> with M13.	64
2.5.9	Transformation of Competent <i>E. coli.</i> with Plasmid cDNA.	65
2.5.10	Preparation of Small Amounts of Plasmid cDNA. (Calculation to Determine Plasmid cDNA Concentration and Purity.)	66
2.5.11	Preparation of Small Amounts of Bacteriophage M13 "Replicative Form" cDNA.	68
2.5.12	QIAGEN Plasmid Midi/Maxi Preparation Protocol.	68
2.5.12.a	M13mp18GT3 Midi Preparation Procedure.	69
2.5.12.b	Plasmid Maxi Preparation Procedure.	70
2.5.13	Preparation of Small Amounts of Single Stranded cDNA from M13.	71
2.6	Site-Directed Mutagenesis.	73
2.6.1	Components.	73
2.6.2	Phosphorylation of Oligonucleotides.	74
2.6.3	Sculptor Protocol.	75
2.7	Recombinant Polymerase Chain Reaction.	76
2.7.1	Primary Polymerase Chain Reactions using <i>Taq</i> Polymerase.	76
2.7.1.a	Synthesis of Oligonucleotides.	76

2.7.1.b	Reaction Conditions.	77
2.7.1.c	Thermal Cycling.	78
2.7.2	Secondary Polymerase Chain Reactions using <i>Taq</i> Polymerase.	79
2.7.2.a	Reaction Conditions.	79
2.7.2.b	Thermal Cycling.	80
2.7.3	Polymerase Chain Reactions using Native <i>Pfu</i> Polymerase.	80
2.7.3.a	Conditions for Primary Reactions.	80
2.7.3.b	Conditions for Secondary Reactions.	81
2.7.3.c	Thermal Cycling.	82
2.7.4	Elution of DNA from Gel Fragments by Electrophoresis.	83
2.7.5	Preparation of Dialysis Tubing.	83
2.7.6	Purification of DNA using Elutip-D Affinity Columns.	84
2.8	<i>Taq</i> DyeDeoxy™ Terminator Cycle Sequencing Protocol.	85
2.8.1.a	Kit Reagents.	85
2.8.1.b	Other Reagents.	86
2.8.2	Preparation of Templates.	87
2.8.3	Thermal Cycling.	88
2.8.4	Acrylamide Gel Preparation.	88
2.8.4.a	Preparing the Gel Plates.	89
2.8.4.b	Casting the Gel- Methods 1 & 2.	89
2.8.5	Setting up for a Run.	90
2.8.6	Sample Extraction and Precipitation.	91
2.8.7	Preparing and Loading the Samples.	91

2.8.8	Analysis of Samples.	92
Chapter 3.	Measurement of the Kinetic Parameters of 2-Deoxy-D-glucose and D-Fructose Transport by GLUT2 Expressed in <i>Xenopus</i> Oocytes.	103
3.1	Aims.	104
3.2	Background.	105
3.2.1	Kinetic Characterisation of Glucose Transporters.	105
3.2.2	Use of <i>Xenopus</i> Oocytes for the Expression of Glucose Transporters.	106
3.3	Results.	109
3.3.1	Measurement of K_m Values for 2-Deoxy-D-glucose and D-fructose Transport by GLUT2 and the Effects of the Presence of Various Sugars and Cytochalasin B.	109
3.3.2	Measurement of the Effects of the Presence of 2,5-Anhydro-D-mannitol and L-Sorbose on 2-Deoxy-D-glucose Transport by GLUT2.	111
3.4	Conclusions.	138
3.4.1	Effects of Various Sugars on <i>Zero-trans</i> Entry of 2-Deoxy-D-glucose and D-Fructose by GLUT2 and D-Galactose by GLUT3.	138
3.4.2	β -D-Fructose Transport Conformation.	142
3.5	Summary.	144

Chapter 4.	Analysis of the Structural Requirements of Sugar Binding to the Liver-type Glucose Transporter (GLUT2) Expressed in <i>Xenopus</i> Oocytes.	146
4.1	Aims.	147
4.2	Background.	148
4.3	Results.	153
4.3.1	Effects of C-1 and C-2 Position Analogues on 2-Deoxy-D-glucose Transport.	154
4.3.2	Effects of C-3 Position Analogues on 2-Deoxy-D-glucose Transport.	154
4.3.3	Effects of C-4 and C-6 Position Analogues on 2-Deoxy-D-glucose Transport.	154
4.4	Discussion.	173
4.4.1	Binding at the C-1 Position.	175
4.4.2	Binding at the C-2 Position.	175
4.4.3	Binding at the C-3 Position.	176
4.4.4	Binding at the C-4 Position.	178
4.4.5	Binding at the C-6 Position.	179
4.4.6	Models of the Interaction of β -D-Glucose with the Exofacial Binding Sites of GLUT2 and GLUT3.	181
4.5	Summary.	183

Chapter 5.	Analysis of the Role of Putative Transmembrane Helix 8 in GLUT3, the Brain-type Transporter.	184
5.1	Aims.	185
5.2	Introduction.	186
5.2.1	Structure-Function Analyses of GLUT1 using Mutagenic Techniques.	186
5.2.1.1	Substitution of Conserved Polar Residues.	186
5.2.1.2	Substitution of Conserved Tryptophan Residues.	189
5.2.1.3	Substitution of Conserved Proline Residues.	191
5.2.1.4	Substitution of GLUT1 Cysteine Residues.	192
5.2.1.5	Substitution of Residues Predicted to Lie in Extramembranous Loops.	193
5.2.1.6	Naturally-Occurring Mutations.	194
5.2.1.7	Mutations Induced in the Yeast SNF3 Transporter.	195
5.2.2	Transmembrane Helix 8.	196
5.3	Mutagenesis, Subcloning and Sequencing of cDNA.	197
5.3.1	Vectors.	198
5.3.2	Site-Directed Mutagenesis.	198
5.3.2.1	Results.	200
5.3.3	Recombinant Polymerase Chain Reaction.	201
5.3.3.1	Primary Reactions.	202
5.3.3.2	Secondary Reactions.	203
5.3.3.3	Results using <i>Taq</i> Polymerase.	203
5.3.3.4	Further Subcloning.	204

5.3.3.5	Results using <i>Pfu</i> DNA Polymerase.	205
5.3.4	Sequencing of Subclones.	206
5.4	Transport of 2-Deoxy-D-glucose by GLUT3 Mutants into <i>Xenopus</i> Oocytes.	207
5.5	Discussion.	237
5.6	Summary.	240
Chapter 6.	Final Discussion.	242
	References.	248

List of Figures.

	Page.
Figure 1.1	2-Dimensional Structure and Topology of GLUT1. 44
Figure 1.2	King-Altman Representation of the Alternating Conformation Model for Sugar Transport by GLUT1. 46
Figure 1.3	Schematic Diagram showing the Conformational Changes Occurring during D-Glucose Transport as Predicted by the Alternating Conformation Model. 48
Figure 2.1	<i>In Vitro</i> Synthesised mRNA after Electrophoresis on a 1% Agarose Gel. 96
Figure 2.2	Schematic Representation of pSPGT3. 98
Figure 2.3	Schematic Representation of M13mp18GT3. 103
Figure 2.4	Diagram showing the Pattern Observed on a 1% Agarose Gel after Electrophoresis of Samples from Various Stages of a Site-Directed Mutagenesis Reaction. 102
Figure 3.1	Accumulation of 2-Deoxy-D-glucose by GLUT2-injected Oocytes with Time. 116
Figure 3.2	Lineweaver-Burk Plot of Transport of 2-Deoxy-D-glucose into GLUT2-injected Oocytes in the Presence and Absence of Cytochalasin B. 118
Figure 3.3	Lineweaver-Burk Plot of Transport of 2-Deoxy-D-glucose into GLUT2-injected Oocytes in the Presence and Absence of D-Glucose. 120
Figure 3.4	Lineweaver-Burk Plot of Transport of 2-Deoxy-D-glucose into GLUT2-injected Oocytes in the Presence of Maltose or D-Fructose or in the Absence of Inhibitors. 122

Figure 3.5	Lineweaver-Burk Plot of Transport of D-Fructose into GLUT2-injected Oocytes in the Presence and Absence of Cytochalasin B.	124
Figure 3.6	Lineweaver-Burk Plot of Transport of D-Fructose into GLUT2-injected Oocytes in the Presence and Absence of Maltose.	126
Figure 3.7	Lineweaver-Burk Plot of Transport of D-fructose into GLUT2-injected Oocytes in the Presence and Absence of D-Glucose.	128
Figure 3.8	Dose Response of Cytochalasin B on the Inhibition of Transport Rates in GLUT2 and GLUT3- injected Oocytes.	130
Figure 3.9	Lineweaver-Burk Plot of Transport of 2-Deoxy-D-glucose into GLUT2-injected Oocytes in the Presence of 2,5-Anhydro-D-mannitol or L-Sorbose or in the Absence of Inhibitors.	132
Figure 3.10	Structures of Pyranose and Furanose Sugars.	134-135
Figure 3.11	Model for the Interaction of β -D-Fructose with GLUT2.	137
Figure 4.1	Model for the Interaction of β -D-Glucose with GLUT1.	166
Figure 4.2	Model for the Interaction of β -D-Glucose with GLUT2.	168
Figure 4.3	Model for the Interaction of β -D-Glucose with GLUT3.	170
Figure 4.4	Model for the Interaction of β -D-Fructose with GLUT2.	172
Figure 5.1.a	Comparison of Amino Acid Sequences in Putative Transmembrane Helix 8 of the Facilitative Glucose Transporter Family.	216
Figure 5.1.b	Predicted α - Helical Structure of GLUT3 Transmembrane Helix 8.	218

Figure 5.2	Diagram showing Sculptor™ Site-directed Mutagenesis Procedure.	220
Figure 5.3.a	Recombinant PCR used for the Construction of GLUT3 Mutants.	222
Figure 5.3.b	Diagram showing Secondary PCR Products.	224
Figure 5.4	A Photograph of a 1% Agarose gel with Samples of Various PCR products and Vector cDNAs used in Recombinant PCR and Cloning.	226
Figure 5.5	Digestion of Secondary PCR Products and Cloning into pSPGT3.	228
Figure 5.6	Excision of Misincorporated Bases from Mutant GLUT3 by Digestion with <i>StuI</i> and <i>PvuI</i> and Re-cloning into pSPGT3.	230
Figure 5.7	Excision of Misincorporated Bases from Mutant GLUT3 by Digestion with <i>SacI</i> and Re-cloning into pSPGT3.	232
Figure 5.8	Diagram showing the Binding Positions of Various Oligonucleotides used for Sequencing and Mutagenesis.	234
Figure 5.9	2-Deoxy-D-glucose Transport Levels of GLUT3 Mutants Expressed as a Percentage of Wild-type GLUT3 Levels.	236

List of Tables.

	Page.
Table 2.1	Table of Buffers. 93
Table 2.2	Bacterial Media and Agar. 94
Table 3.1	Kinetic Parameters for Transport of Sugars by GLUT2 and GLUT3. 113
Table 3.2	Effects of D-Fructose, D-Glucose and D-Galactose on 2-Deoxy-D-glucose Transport by GLUT2. 114
Table 4.1	Effects of C-1 and C-2 Position Analogues on 2-Deoxy-D-glucose Transport by GLUTs 2 and 3. 157
Table 4.2	Effects of C-3 Position Analogues on 2-Deoxy-D-glucose Transport by GLUTs 2 and 3. 159
Table 4.3.	Effects of C-4 position Analogues on 2-Deoxy-D-glucose Transport by GLUTs 2 and 3. 161
Table 4.4.	Effects of C-6 Position Analogues on 2-Deoxy-D-glucose Transport by GLUTs 2 and 3. 163
Table 4.5.	Comparison of the Inhibitions Induced by C-3-Substituted Sugars of 2-Deoxy-D-glucose Transport Mediated by GLUT2 and GLUT3 . 164
Table 5.1	Oligonucleotides used in Recombinant PCR and Site-directed Mutagenesis. 210-212
Table 5.2	Oligonucleotides used in Automated Sequencing. 214

CHAPTER 1.

Introduction.

1.1 General Background.

The utilisation of glucose as an energy source by mammalian cells has been a subject of great interest for many years. One important aspect of glucose metabolism relates to the transport of glucose across the cellular plasma membrane. There are three methods by which this event can occur (reviewed in Carruthers, 1990). The first is simple, bidirectional diffusion which, due to the polar nature of the glucose molecule, is predicted to be much too slow to meet the energy requirements of cells. Therefore, a protein-mediated method of uptake was thought to be responsible for the bulk of sugar uptake. The second method of uptake is rapid, bidirectional, protein-mediated facilitated diffusion; and the third is rapid, active protein-mediated transport. Facilitated transport does not require a coupled energy-providing reaction such as ATP hydrolysis, or cotransport of an ion. Although facilitated transport is bidirectional, net transport always occurs down the sugar's concentration gradient, i.e. from high to low concentration.

Both types of protein-mediated transport have been observed in mammalian cells, but although almost all cells exhibit sugar uptake by facilitated diffusion, only those of the absorptive epithelia of the gut and reabsorptive epithelia of the kidney possess the ability to actively transport glucose, which is coupled to the cotransport of sodium. Active transporters are not required elsewhere since blood glucose levels are kept roughly constant at the relatively high concentration of 5-10 mM, thus enabling passive uptake by cells as glucose can be transported down its concentration gradient.

The observations of saturation of sugar transport by erythrocytes at high sugar concentrations (Widdas, 1952) and competition between different sugars (reviewed in LeFevre, 1961) for transport, suggested that transporters

follow simple Michaelis-Menten saturation kinetics and behave like enzymes, with D-glucose as the substrate on one side of a membrane and the product on the other. The kinetics of D-glucose uptake were also found to vary subtly between tissues, predicting the existence of more than one facilitative transporter.

The existence of a protein moiety responsible for the uptake of glucose, was demonstrated by Jung who showed that the transport capacity of the erythrocyte was retained by erythrocyte ghosts but not by erythrocyte lipids alone (Jung, 1971). This finding was reinforced by the observation that very low concentrations of two compounds, cytochalasin B and phloretin, are capable of inhibiting transport very efficiently with K_i values of 140 nM and 200 nM, respectively (Bloch, 1973; Zoccoli *et al.*, 1978; LeFevre & Marshall, 1959).

Although protein-mediated uptake of sugar had been detected in many tissue types, all the early kinetic studies were performed on human erythrocytes, since they could be obtained easily and in great quantity. They also provided a simple experimental system which could be easily manipulated. The transporter protein content of human erythrocytes has since been determined to be 5% of the total membrane protein (Allard & Lienhard, 1985). Studies were performed by several groups in the early 1970s, investigating the nature of the transporter's sugar binding site, which was predicted to utilise hydrogen bonding to reversibly bind glucose (Barnett *et al.*, 1973; Kahlenberg & Dolansky, 1972). These studies are reviewed in Chapter 4.

The functional purification of the erythrocyte transporter was achieved independently by two groups. The first group based their purification on the ability of reconstituted fractionated erythrocyte membrane proteins to transport glucose (Kasahara & Hinkle, 1977). The second group used the specific binding of the transport inhibitor cytochalasin B as a basis for the

purification procedure (Baldwin *et al.*, 1979; Baldwin *et al.*, 1981). Both studies revealed a heterogeneously glycosylated integral membrane protein which migrated on SDS-polyacrylamide gels as a broad band with an approximate molecular mass of 55 kDa, which was reduced to a mass of 46 kDa upon treatment with Endoglycosidase H. When this protein was reconstituted into phospholipid vesicles it behaved in an identical fashion kinetically to native protein (Wheeler & Hinkle, 1981). Additionally, when present in vesicles this protein binds cytochalasin B at a stoichiometric ratio of 1: 1 (Baldwin & Lienhard, 1989). The purification of the erythrocyte transporter led to the production of antibody probes (Sogin & Hinkle, 1978) and its partial protein sequencing. This in turn led to cloning and sequencing of the transporter from human hepatoma G2 (HepG2) cells (Mueckler *et al.*, 1985). This glucose transporter has been named GLUT1 (Fukumoto *et al.*, 1989). Other members of the facilitative glucose transporter family have been named GLUTs 2-7, in the chronological order of the isolation of cDNAs.

1.2 Tissue-specific Distribution of the Facilitative Glucose Transporter Family.

1.2.1 General.

The unique requirements of different mammalian tissues for glucose, and the varying needs of each tissue for glucose at distinct stages of development, suggests the necessity for one or more regulatory mechanisms. A family of glucose transporters had been suspected to exist for many years, reinforced by the observation that different tissues display unique kinetics for D-glucose uptake. This family comprises six members to date (GLUTs 1-7, of

which GLUT6 is a pseudo-gene sequence) which are structurally very similar and distinct from the mammalian active sodium-linked transporters of the intestinal and kidney absorptive epithelia.

1.2.2 GLUT1.

GLUT1 is the most extensively studied member of the family to date and is the only member of the family to be purified in a functional form (Kasahara & Hinkle, 1977). GLUT1 is otherwise referred to as the erythrocyte/brain or HepG2 transporter since clones encoding it were first isolated from rat brain and HepG2 cDNA libraries using antibodies raised against purified GLUT1 (Birnbaum *et al.*, 1986; Mueckler *et al.*, 1985). These cDNAs were found to encode 492-residue proteins, which are more than 97% identical in sequence, and were predicted to span the membrane bilayer 12 times by hydrophathy analysis (Mueckler *et al.*, 1985). Since then GLUT1 has been cloned from mice (Kaestner *et al.*, 1989), rabbits (Asano *et al.*, 1988) and pigs (Weiler Guttler *et al.*, 1989). All cDNAs encode a 492-residue protein with 97% sequence identity to human GLUT1.

The isolation of a human GLUT1 cDNA clone led to the production of oligonucleotides which enabled the screening of tissues for the presence of GLUT1 mRNA. This paralleled studies performed with anti-GLUT1 antibodies looking at the relative protein levels in the various tissue types. Highest levels of GLUT1 protein in human adults were found in erythrocytes (Allard & Lienhard, 1985). It was also abundant in blood-tissue barriers (reviewed in Takata *et al.*, 1990) such as the blood-brain barrier, the blood-nerve barrier, the placenta syncytiotrophoblast and various blood-eye barriers, although it was found in almost every tissue. Only very low levels were found in the liver. High concentrations were found in all foetal tissues,

including heart, liver and brown fat which possess very little GLUT1 in adults (Asano *et al.*, 1988; Santalucia *et al.*, 1992). Cultured cell lines also have elevated levels of GLUT1 protein (reviewed in Gould & Holman, 1993).

Since GLUT1 is expressed at some level in most tissues it has been proposed to be a basal transporter, not responsible for the post-prandial insulin-stimulated uptake of sugar by adipose tissue and skeletal muscle, although it is also expressed at lower levels in these tissues. The K_m for zero-*trans* entry of D-glucose into cells at 37°C by GLUT1 is 7 mM (Lowe & Walmsley, 1986). This allows GLUT1 to efficiently transport glucose in its physiological concentration range. However the reason for its high expression levels in erythrocytes, where it constitutes 5% of the total membrane protein, is unclear (Allard & Lienhard, 1985).

The abundance of GLUT1 in blood-tissue barriers suggests that a primary role of this protein is the transepithelial and transendothelial transport of D-glucose.

GLUT1 is found universally at high levels in all foetal tissues (Asano *et al.*, 1988), including adipose tissue and muscle, where no GLUT4 has been found. It established that mammalian foetal erythrocytes have a high capacity for transport and that this ability is lost soon after birth (Widdas, 1955). It has been suggested that this high capacity erythrocyte transporter facilitates the transfer of glucose across the placenta into the intracellular space of the foetal erythrocyte, and that this occurs to a lesser extent across the blood-tissue barriers in adult primates (Jacquez, 1984).

The reason for the existence of elevated levels of GLUT1 protein in transformed cells and all cultured cell lines is unknown. However, it has been shown that many mitogens stimulate the transcription of the GLUT1 gene (reviewed in Merrall *et al.*, 1993), as does glucose starvation (reviewed in

Gould & Holman, 1993). Cultured cells are continually subjected to these conditions.

1.2.3 GLUT2.

Since the quantities of GLUT1 detected in liver were very low, and because this tissue displays notably different kinetics for D-glucose uptake from GLUT1, it was likely that this tissue was host to a related transporter. Hepatocyte cDNA libraries were screened by low stringency hybridisation using GLUT1 cDNA as a probe. This led to the isolation of GLUT2 clones from human (Fukumoto *et al.*, 1988), rat (Thorens *et al.*, 1988) and mouse (Suzue *et al.*, 1989) cDNA libraries. These encode proteins of 522, 523 and 524 residues, respectively, and share 80% identity. Human GLUT2 has 55% sequence identity with human GLUT1, and both proteins have virtually superimposable hydropathy plots. Most diversity occurs in the large extracellular loop and at the extreme C-terminus (Figure 1.1).

Screening of tissue types by immunocytochemical techniques showed high GLUT2 protein levels in the β -cells of the Islets of Langerhans in the pancreas (Thorens *et al.*, 1988; Orci *et al.*, 1989), in the transepithelial cells of the intestine and the kidney (Thorens *et al.*, 1990), as well as the hepatocytes of the liver itself. Here its expression was found to be restricted to the sinusoidal plasma membrane of hepatocytes, where it was expressed at high levels in the periportal area, with a steady decrease in numbers toward the perivenous area (Thorens *et al.*, 1990; Hacker *et al.*, 1991). GLUT2 protein has also been found expressed at very low levels in all brain regions (Brant *et al.*, 1993).

In the liver, GLUT2 is required for the influx of postprandial glucose, and under fasting conditions, for the release of glucose produced from

glycogenolysis and gluconeogenesis into the bloodstream. The high concentration of GLUT2 in the plasma membranes of hepatocytes, coupled with the transporter's high K_m values for D-glucose entry and exit (reviewed in Elliot & Craik, 1982), allows for a rapid, non-saturable translocation of D-glucose in either direction in times of stress.

The presence of GLUT2 in the Islets of Langerhans is strictly limited to the β -cells, which release insulin- there is no expression in the α - or γ - cells (Thorens *et al.*, 1988; Orci *et al.*, 1989). This specific distribution of expression, coupled with the high K_m value of GLUT2 led to the speculation that this isoform might allow glucokinase, which is the rate-limiting step in liver glucose metabolism (Vischer *et al.*, 1987), to act as a blood glucose level sensor (Thorens *et al.*, 1988; Orci *et al.*, 1989) over the range of blood sugar levels which stimulate insulin secretion (5- 15 mM). Presumably the high K_m would ensure that the uptake of glucose into the β -cell would be linear over a large range of concentrations rather than saturating at low levels like GLUT1. This would allow the production of an intracellular metabolite of D-glucose to be a rate-limiting step in an unidentified pathway leading to the release of insulin. Simulations of the transport of D-glucose by cells possessing glucose transporters with a range of K_m values and similar capacities for glucose transport suggest that those with high K_m values are less efficient at producing rapid equilibration of D-glucose between interstitial and cytosolic water (Herbert & Carruthers, 1991). Therefore it is likely to be the high capacity (V_{max}) of GLUT2-expressing β -cells for D-glucose that enables them to act as a glucose sensor, not the low affinity property (high K_m) of GLUT2 . Results obtained from studies with two insulinoma cell lines, one of which expresses GLUT1 in addition to GLUT2, show that only the cell line which expressed GLUT2 alone secreted insulin in response to elevated glucose levels (Miyazaki *et al.*, 1990). Both cell lines produced insulin mRNA, so this would

suggest that the defect in the GLUT1-containing cell-line occurs due to the presence of that isoform, which may lead to non-linear influxes of sugar. However, there might also be some other undefined defect in the GLUT1-expressing cell line which leads to this phenotype.

GLUT2 is also found in the basolateral surfaces of the transepithelial cells of the intestine and of the proximal tubule of the kidney (Thorens *et al.*, 1990). In the intestine, it is proposed to work in conjunction with SGLT1, the active glucose transporter, which is present on the apical surface of the same cells. SGLT1 actively transports glucose against its concentration gradient from the lumen of the gut into the cell, utilising the energy obtained from the cotransport of sodium ions. This leads to the build-up of high glucose concentrations in the cell which are released down the concentration gradient into the blood by GLUT2. A similar situation occurs in the proximal tubule of the kidney, where SGLT1 is responsible for the reabsorption of D-glucose, and GLUT2 functions to translocate it from the epithelial cells into the blood.

Wherever it is expressed, GLUT2 seems to play an important role in glucose homeostasis.

1.2.4 GLUT3.

GLUT3 clones were isolated and cloned from a human foetal skeletal muscle (Kayano *et al.*, 1988) and mouse (Nagamatsu *et al.*, 1992) cDNA libraries, encoding proteins with 496 and 493 residues, respectively. These share 83% identity and the human isoform has 64% identity with human GLUT1. An avian homologue of GLUT3 has also been cloned (White *et al.*, 1991).

Northern analysis of human tissues showed that GLUT3 mRNA was expressed in almost every tissue type, but was found at particularly high

levels in neurones and brain, especially in the cerebrum (Kayano *et al.*, 1988). Surprisingly, very little was found in skeletal muscle itself, so GLUT3 was ruled out as a candidate for insulin-stimulated glucose uptake by that tissue.

This ubiquitous distribution of human mRNA contrasted strongly with the same analysis of monkey, rat, rabbit and mouse tissues (Nagamatsu *et al.*, 1992; Maher *et al.*, 1992; Yano *et al.*, 1991), which showed that GLUT3 mRNA was confined to neural tissue and brain. Immunological studies show that GLUT3 protein is expressed in most areas of rat brain, and also in primary cultured rat cerebellar neurones and neuronal cell lines (Maher *et al.*, 1992).

Studies screening human tissues using anti-GLUT3 antibodies showed that GLUT3 protein was present at high levels in neural tissue and brain, and at lower levels in placenta, liver, heart and kidney (Gould *et al.*, 1992; Shepherd *et al.*, 1992). None was found in skeletal muscle. GLUT3 expression is expressed in virtually all regions of the brain, but is expressed at different levels in different sections (Brant *et al.*, 1993). The apparent differences between human GLUT3 protein and mRNA levels in other human tissues may be due to neural contamination of tissues used for Northern analysis, or to post-transcriptional regulation of the mRNA in non-neural tissues. The differences in tissue-specific mRNA and protein expression levels measured in humans and other species are not known.

The brain is dependent on glucose as an energy source since it is unable to derive energy from fatty acid hydrolysis. It is documented that the glucose concentrations of the extracellular fluid of the brain are lower than those found in the plasma (Lund-Andersen, 1979). GLUT3 has been shown to exhibit relatively low K_m values for 2-deoxy-D-glucose *zero-trans* entry (1.4 mM) (Colville *et al.*, 1993) and 3-O-methyl-D-glucose under equilibrium exchange conditions (10 mM) (Gould *et al.*, 1991). This leads to the speculation that this glucose transporter is probably responsible for the more

efficient uptake of glucose by the brain under hypoglycaemic conditions, where its low K_m value allows it to transport glucose more efficiently. GLUT3 is probably not responsible for transport under hyperglycaemic conditions, since GLUT1, which is co-expressed in brain, can transport glucose more efficiently at higher concentrations.

1.2.5 GLUT4.

GLUT4 cDNA was finally obtained in 1989, where its isolation was reported simultaneously by five separate groups. It was cloned from human (Fukumoto *et al.*, 1989; James *et al.*, 1989), rat (Birnbaum, 1989; Charron *et al.*, 1989), and mouse (Kaestner *et al.*, 1989) cDNA libraries. These encode proteins of 509, 509 and 510 residues, respectively, and share about 95% sequence identity. The human GLUT1 and GLUT4 isoforms are 65% identical. Again, hydropathy analysis of the primary sequence is superimposable with those of the other members of the family. The major differences in sequence occur at the N-terminus, where GLUT4 is 12 residues longer, in the central loop and the C-terminus.

Subsequent immunolabelling studies with various tissue samples showed that GLUT4 is predominantly present in brown and white adipose tissue, skeletal muscle and heart, those tissues which exhibit insulin-stimulated uptake of glucose (James *et al.*, 1988; James *et al.*, 1989), although it has been discovered at low levels in the cerebellum, hypothalamus, and the pituitary (Brant *et al.*, 1993).

Measurement of the rate of glucose transport into rat adipose cells has shown that transport is increased 20- to 30-fold above basal levels in response to insulin (Taylor & Holman, 1981; May & Mikulecky, 1982; Whitesell & Gliemann, 1979; Simpson & Cushman, 1986; Holman *et al.*, 1990). Rat muscle

transport is increased 7-fold on exposure to insulin (Ploug *et al.*, 1987). The effect of insulin on human adipocytes and skeletal muscle are only 2- to 4-fold (Pederson & Glieman, 1981) and 2-fold (Dohm *et al.*, 1988) stimulations of transport, respectively.

These effects were found to be caused primarily by an increase of the V_{\max} of these tissues for glucose (Taylor & Holman 1981; May & Mikulecky, 1982; Whitesell & Gliemann, 1979; Simpson & Cushman, 1986). This has been found to be caused by a rapid translocation of GLUT4 transporters from an intracellular location to the plasma membrane after insulin exposure both in fat (Cushman & Wardzala, 1980; Suzuli & Kono, 1980) and skeletal muscle (Klip *et al.*, 1987; Hirshman *et al.*, 1990; Klip *et al.*, 1992). It has been shown that these transporters cycle continuously in the absence of insulin but at any point in time most are present in an endosomal-like compartment. Upon stimulation, the exocytosis of transporter is stimulated and it appears in large quantities on the cell surface (reviewed in Holman *et al.*, 1994).

When expressed in *Xenopus* oocytes, GLUT4 has been found to display equilibrium exchange K_m values for 3-O-methyl-D-glucose of 1.8 mM (Keller *et al.*, 1989). and 4.3 mM (Nishimura *et al.*, 1993) compared to a value of 26.2 mM obtained with GLUT1 (Nishimura *et al.*, 1993). Turnover numbers were calculated to be similar for both transporter isoforms ($20,000 \text{ min}^{-1}$) (Nishimura *et al.*, 1993), which is comparable to the figure of $10,000 \text{ min}^{-1}$ previously observed with GLUT1 (Gould & Lienhard, 1989). This would indicate that at low substrate concentrations, GLUT4 would be responsible for the majority of glucose uptake in human tissues, and that insulin-stimulation increases the quantity of GLUT4 to increase the uptake at higher concentrations (Nishimura *et al.*, 1993).

1.2.6 GLUT5.

GLUT5 cDNA was isolated from human small intestine (Kayano *et al.*, 1990). It encodes a 501 residue transporter which has 40% identity with human GLUT1. GLUT5 mRNA and protein has been found at highest levels in the small intestine, but low levels have been found in kidney, skeletal muscle, brain and adipose tissue (Davidson *et al.*, 1992; Shepherd *et al.*, 1992). Its distribution in the intestine is limited to the apical brush border of the transepithelial cells, where it is co-expressed with SGLT1, the active, sodium-linked transporter. The function of GLUT5 in this location is probably the absorption of dietary fructose from the lumen. This conclusion is based on the finding that GLUT5, when expressed in *Xenopus* oocytes, transports D-fructose with a K_m value of 6 mM (Burant & Bell, 1992) but has very poor affinity for D-glucose.

The presence of low levels of GLUT5 in other tissues might enable these to transport D-fructose, but it is not known whether other fructose transporters also exist.

1.2.7 GLUT6.

A GLUT6 cDNA clone was isolated at the same time as GLUT5 (Kayano *et al.*, 1990). The cDNA sequence had 80% identity with human GLUT3, but also was found to contain multiple stop codons and frame shift mutations, so was unlikely to encode a functional transporter protein. It was suggested that the transcript was formed by the insertion of a reverse-transcribed copy of a ubiquitously expressed gene (Kayano *et al.*, 1990).

1.2.8 GLUT7.

GLUT7 cDNA was cloned from a rat cDNA library (Waddell *et al.*, 1992). It encodes a 528 residue protein which has 68% identity with rat GLUT2. A major difference between the amino acid sequences of these two isoforms is the presence of a six amino acid endoplasmic reticulum targeting motif (K K X K X X) at the C-terminus of GLUT7. GLUT2 and GLUT7 cDNA sequences are completely identical at three locations and there is very little base-drift over large sequences of the cDNA. Although the sequences do not coincide with the intron-exon boundaries (Bell *et al.*, 1990), it is possible that GLUTs 2 and 7 mRNA are generated by an unknown splicing mechanism (Waddell *et al.*, 1992).

Western blotting experiments have shown that GLUT7 is expressed in the microsomal fraction of rat hepatocytes (Waddell *et al.*, 1991), and is also localised to the endoplasmic reticulum when expressed in COS-7 cells (Waddell *et al.*, 1992).

The expression of a glucose transporter localised in the endoplasmic reticulum of hepatocytes is an important discovery. The liver is a key factor in the regulation of blood glucose levels. It is responsible for the uptake and release of glucose (mediated by GLUT2) under hyperglycaemic and hypoglycaemic conditions respectively. However the terminal step in both glycogenolysis and gluconeogenesis, the dephosphorylation of glucose-6-phosphate by glucose-6-phosphatase, occurs in the lumen of the hepatocyte endoplasmic reticulum. To be released from the cell, glucose must traverse the endoplasmic reticulum membrane to the cytosol from which it is transported into the bloodstream by GLUT2. Until the discovery of GLUT7, it was not understood how this initial transport event occurred.

1.3 Structure of the Mammalian Facilitative Glucose Transporter Family.

1.3.1 General Studies.

After the purification of GLUT1 (Kasahara & Hinkle, 1977) and the isolation of the cDNAs encoding the members of the human glucose transporter family (section 1.2), it was possible to predict a common membrane-spanning topology for each of the transporter isoforms. Using hydropathy analysis of the primary sequence of GLUT1 (Mueckler *et al.*, 1985) a pattern was obtained where twelve regions were long enough (21 residues) and sufficiently hydrophobic to form hydrophobic or amphipathic membrane-spanning α -helices (Figure 1.1). The N- and C-termini and the large loop between transmembrane helices 6 and 7 are predicted to lie on the cytoplasmic side of the membrane and the other loop, between helices 1 and 2, on the extracellular side. The other transporter sequences align together very closely and have very similar hydropathy plots. The sequences predicted to be transmembrane helices are most conserved between transporter isoforms and the extramembranous regions, especially the two large loops and the N- and C-termini are least conserved. Five of the transmembrane helices are predicted to be amphipathic; helices 3, 5, 7, 8 and 11 (Mueckler *et al.*, 1985), which could form a hydrophilic "pore" through the membrane bilayer allowing the passage of D-glucose.

The structure is divided into two halves by the large intracellular loop between helices 6 and 7, although it is not known whether this division is significant in the tertiary structure. The other cytoplasmic loops are uniformly short (eight residues long) and probably serve to restrict the movement of the transmembrane helices. The extracellular loops are not so

conserved in size and sequence as those on the cytoplasmic side. This may allow the protein some flexibility of movement during transport.

Conserved sequence motifs in the glucose transporters include: GRR(K) between transmembrane helices 1 and 2, which is repeated between transmembrane helices 7 and 8; EXXXXXXR between transmembrane helices 4 and 5, and again between helices 10 and 11; and PESPR present in the cytoplasmic loop between helices 6 and 7, which is paralleled by the PETKG motif in the C-terminal cytoplasmic loop. The repetition of these sequences in the same position of the N- and C-terminal halves of the transporters suggest that the transporters may have evolved from an ancestral 6 transmembrane helix membrane protein by a gene duplication event (Maiden *et al.*, 1987; Baldwin & Henderson, 1989). This, and the constraints imposed by the short length of the cytoplasmic loops, suggest that the transporter tertiary structure may be composed of two groups of six helices in a bilobular structure (Hodgson *et al.*, 1992) as observed with low resolution electron microscopic images of *E. coli* lactose permease (Li & Tooth, 1987). Photolabelling studies and proteolytic digestion have suggested that the glucose binding sites are located in the C-terminal half of GLUT1 (section 1.7), so transport occurs in this region, but the N-terminal half of the protein might also play a role.

An alternative topology has been described where the transporters have 16 β -sheet transmembrane helices, forming a large β -barrel structure (Fischbarg *et al.*, 1993). This is, however, not generally accepted.

1.3.2 Topology studies.

This section summarises studies aimed at delineating the topology of GLUT1. Tryptic digestion of GLUT1 (Cairns *et al.*, 1987) yields two peptides corresponding to GLUT1 residues 213-269 and residues 457-492 only when

trypsin is present on the cytoplasmic side of erythrocyte membranes. These fragments are predicted to form part of the cytoplasmically disposed large intracellular loop and C-terminal sequence respectively. Specific antibodies raised against peptides representing these sequences have also been found to bind only to the cytoplasmic side of the erythrocyte membrane (Davies *et al.*, 1987; Davies *et al.*, 1990; Haspel *et al.*, 1988). This evidence would suggest that these regions are, as predicted, intracellularly disposed.

The loop connecting putative transmembrane helices 1 and 2, which is predicted to be extracellular, contains the only site of *N*-linked glycosylation in the primary sequence, asparagine-45 (Asn⁴⁵) (Cairns *et al.*, 1987). Since the protein is heavily glycosylated, this residue must lie in an extracellular location. Indeed it has been demonstrated that the substitution of Asn⁴⁵ by Asp, Trp or Gln abolished *N*-linked glycosylation of GLUT1 (Asano *et al.*, 1991).

Cysteine-429 (Cys⁴²⁹), which is predicted to lie in the extracellular loop just before helix 12, is possibly the site of labelling with the reagent bis-(maleimidomethyl)-ether-L-[³⁵S]cysteine (May *et al.*, 1990). The impermeant thiol-group-reactive agent *p*-chloro-mercuribenzenesulphonate (pCMBS) has also been demonstrated to bind to this residue (Wellner *et al.*, 1992).

Chemical modification of GLUT1 in intact erythrocytes with the impermeant, amino-group-specific biotinylating reagent sulphosuccinimidyl-6-(biotinamido)-hexano-oate (NHS-LC-biotin), leads to the modification of a single exofacial lysine residue (Preston & Baldwin, 1993). Tryptic digestion of the protein revealed this residue to be Lys³⁰⁰, which is predicted to lie in the exofacial loop connecting transmembrane helices 7 and 8.

A recent study (Hresko *et al.*, 1994) investigated the effects of introducing cDNA sequence encoding the GLUT4 glycosylation site individually into each of the various regions of GLUT1 sequence which are

predicted to encode hydrophilic soluble loops, and injecting the *in vitro*-synthesised mRNA into *Xenopus* oocytes. Each GLUT1 cDNA had also been altered by substituting Asn⁴⁵ with Thr so that the encoded protein would not be glycosylated at its native region. These workers then assayed the glycosylation levels of each mutant by the change of mobility on SDS-PAGE after glycosidase digestion. Only proteins which presented the stretch of GLUT4 sequence to the lumen of the endoplasmic reticulum and Golgi apparatus (and hence be exofacially disposed) would be glycosylated. Insertions into each predicted exofacial loop always produced proteins which were glycosylated, and insertions into endofacial loops in each case yielded non-glycosylated proteins, thus confirming the predicted 12 transmembrane helices model (Mueckler *et al.*, 1985).

Hence, the bulk of evidence supports the model of GLUT1 which predicts that the orientation is such that it forms 12 transmembrane helices with the N- and C- termini and large loop located on the cytoplasmic side of the membrane, and the smaller loop on the extracellular side (Mueckler *et al.*, 1985). Other transporter isoforms are predicted to have identical topologies.

However, a recent study (Fischbarg *et al.*, 1993) has produced an alternative topological model. Polyclonal antibodies raised against a synthetic peptide corresponding to the highly conserved fifth endofacial loop of GLUT1 (Ile³⁸⁶ to Ala⁴⁰⁵) have been shown to increase 2-deoxy-D-glucose transport by GLUT1-, GLUT2- and GLUT4-expressing *Xenopus* oocytes when applied to extracellular medium (Fischbarg *et al.*, 1993). This result was interpreted by these authors to imply that this loop is actually exofacially orientated, and a new model of GLUT1 topology was predicted consisting of 16 β -sheet transmembrane helices with cytoplasmic hydrophilic N- and C-terminal domains. This model is based on Chou and Fassman secondary structure analyses which predict that GLUT1 exclusively contains β -sheet structure

(Carruthers, 1990). However, it is not evident how antibody binding to a supposedly exofacial sequence could increase the rate of transport. Although their results are difficult to explain, the conclusions of Fischbarg *et al* cannot be supported from their data.

1.3.3 Spectroscopic studies.

Infra-red (IR) spectroscopy is a valuable method for investigation of protein secondary structure, with which the relative proportions of α -helical, β -strand and random coil conformations can be determined from the frequency of the amide I and amide II bands. Fourier-transforming infra-red methods (FTIR) allow the analysis of protein structure in dilute aqueous media, producing spectra which can be deconvoluted to analyse the overlapping amide absorptions caused by the various secondary structures present in the protein (Carruthers, 1990). FTIR studies of GLUT1 protein in lipid bilayers have shown that α -helical structure is predominant, but there is also a proportion of β -sheet, β -turns and random coil conformation present (Alvarez *et al.*, 1987). Extensive hydrolysis of the membrane imbedded transporter with papain reduces the α -helical and random coil conformation content of the transporter, relative to the β -strand content. However the remaining protein contains a substantial amount of both α -helical and β -strand structure. Tryptic digestion of the transporter leads to a decrease in α -helical and random coil conformation content of the membrane-bound transporter (Cairns *et al.*, 1987). Trypsin digestion is predicted to remove the large intracellular loop (residues 213-269) and the cytoplasmically disposed C-terminal sequence (residues 457-492). These results suggest that the membrane-spanning regions contain both α -helical and β -strand structure, and that the large cytoplasmic domains contain α -helical structure.

Polarised FTIR spectroscopy has detected the presence of α -helical and random coil conformation in GLUT1 but no β -sheet structure (Chin *et al.*, 1986). Circular dichroism (CD) spectroscopy performed by the same group detects 82% α -helix, 10% β -turns and 8% random coil structure but no β -sheet structure (Chin *et al.*, 1987). The polarised FTIR results suggest that the α -helices are preferentially orientated perpendicular to the plane of the lipid bilayer, with a tilt of $< 38^\circ$ from the membrane normal (Chin *et al.*, 1986).

Hydrogen-deuterium exchange studies of purified GLUT1 in lipid bilayers (Alvarez *et al.*, 1987; Jung *et al.*, 1986) demonstrate that 80% of the polypeptide backbone of GLUT1 is readily accessible to solvent. The residual portion of the protein which exchanges only slowly includes α -helical structure which presumably exists in a hydrophobic environment. This suggests the presence of a hydrophilic pore-like structure, possibly surrounded by amphipathic transmembrane helices.

All the above data are consistent with the 12 transmembrane α -helix structure and further suggest that D-glucose is transported across the lipid bilayer via a hydrophilic pore formed by bundles of helices which span the bilayer.

1.4 Homologous Transporter Proteins in other Organisms.

The advent of Molecular Biology has led to the cloning and sequencing of many cDNAs and genes from diverse organisms. The amino acid sequences of the proteins encoded by these sequences can be aligned together to look for regions of similarity and identity. Griffith *et al.* searched protein databases for sequences which possessed similarity to: TetC protein (the tetracycline resistance protein of gram-negative bacteria); TetL (the tetracycline

resistance protein of gram-positive bacteria); AraE (a sugar transporter of *E. coli*); GLUT2; and CitA (the citrate transporter of gram negative bacteria) (Griffith *et al.*, 1992). Using various algorithms to analyse those transport proteins which were selected, these workers found that many of these possessed sequences which were conserved in various others. Griffith *et al* proposed that sequence information alone suggested that these transporters function by a common mechanism of action, and form a related "superfamily" of transporter proteins, despite the observed differences in sugar specificity, direction of transport and mechanism of transport.

Both active and passive eukaryotic and prokaryotic transporters are included in this "sugar transporter superfamily". It contains the mammalian facilitative glucose transporters and both passive transporters and active, sugar/H⁺ symporters from higher plants, green algae, protozoans, yeasts, cyanobacteria and eubacteria (reviewed Henderson *et al.*, 1992; Griffith *et al.*, 1992). Bacterial tetracycline and citrate transporters and fungal quinate transport proteins are also included in the "superfamily". It does not, however, contain the apparently unrelated mammalian sodium-linked glucose transporters or bacterial ATP- and PEP-utilising active transporters. All members of the family seem to yield similar hydropathy plots to those of the mammalian glucose transporters in the regions of sequence similarity, and are predicted to form 12 transmembrane α -helices, bisected by a large loop between transmembrane helices 6 and 7, despite large differences in overall length.

Sequence analysis suggest that the proteins most closely related to GLUT1 are the *E. coli* H⁺/L-arabinose symporter, AraE, and the *E. coli* H⁺/D-xylose symporter, XylE, which are 23% and 27% identical, respectively, in sequence to human GLUT1. These proteins even bind the same ligands as the mammalian facilitative glucose transporters (section 1.7).

More distantly related to GLUT1, for example, are tetracycline/H⁺ antiporters, the citrate transporter, and maltose and lactose transporters (Griffith *et al.*, 1992). It is not known whether the lactose/H⁺ transporter of *E. coli* (*lac* permease) is a member of the "superfamily". Although it bears little sequence similarity to GLUT1, it has been predicted to contain 12 transmembrane helices (Büchel *et al.*, 1980), and does contain many identical or conserved residues in regions that are also conserved in the "sugar transporter superfamily".

1.5 The Dynamics of D-Glucose Transport.

The majority of kinetic, thermodynamic and ligand binding studies have been carried out investigating GLUT1, due to its availability from human erythrocytes and its functional purification (Kasahara & Hinkle, 1977). Many properties measured with GLUT1 will undoubtedly apply to all the members of the glucose transporter family since they all share very similar structures, although sugar specificities, kinetic parameters, targeting patterns, ligand binding, and both acute and chronic hormonal regulation of expression is found to vary widely between different transporter isoforms.

1.5.1 Kinetic Parameters of GLUT1 D-Glucose Transport.

Transport of D-glucose by GLUT1 has generally been measured in erythrocytes using a variety of methods (reviewed in Carruthers, 1990), usually by the accumulation of radiolabelled sugar, henceforth referred to as "tracer". Other methods include chemical analysis of cellular sugar content, spectrophotometric measurement of glucose induced changes in cell volume,

and coupled secondary enzyme-linked assays. There are several categories of assay which can be employed to measure different parameters of the transport process. These are listed below. The terms *cis* and *trans* refer to the same side of the membrane from which transport is measured and the opposite side, respectively.

1.5.1.1 Zero-*trans* entry.

The simplest study to perform involves measuring the uptake of trace amounts of radioactively labelled D-glucose into cells which have been stored in a medium without glucose for a certain period of time, so that the cytosolic sugar concentration is as low as possible. The external sugar concentration is varied for each measurement. The initial transport of glucose into the cell should be linear since the cytosolic sugar concentration is zero. Only measurements of initial rates are recorded, before reverse-flow of sugar occurs. Therefore, what is being measured is sugar binding affinity of the exofacial binding site (K_m outside) and the maximum velocity of sugar entry under infinitely high substrate concentrations (V_{max} entry).

1.5.1.2 Zero-*trans* exit.

In this case, cells are preincubated with varying concentrations of sugar plus tracer until equilibrium is reached. Then the medium is rapidly removed and replaced with one without sugar. Initial rates of sugar exit are measured by testing the amount of radioactivity in the external medium. This assay measures the affinity of the endofacial sugar binding site (K_m inside) and the V_{max} for sugar exit.

1.5.1.3. Infinite-*cis* entry.

As in section 1.5.1.2 above, the cells are preincubated in variable concentrations of sugar plus tracer until equilibration. The assay is begun by the addition of a saturating concentration of sugar plus tracer. This assay measures the K_m of the internal binding site and the V_{max} for entry.

1.5.1.4 Infinite-*cis* exit.

This is the opposite of infinite-*cis* entry. The cells are preincubated with saturating concentrations of sugar and tracer, then the exit of tracer into variable concentrations of sugar plus tracer is measured. The K_m of the exofacial binding site and the V_{max} for exit are measured.

1.5.1.5 Infinite-*trans* entry.

In this assay the cells are incubated with saturating concentrations of sugar. Uptake of tracer from varied concentrations of sugar gives a measure of the K_m for the exofacial binding site and the V_{max} for sugar exchange i.e. the maximum rate for a complete transporter cycle where two molecules of sugar are exchanged.

1.5.1.6 Infinite-*trans* exit.

The initial concentration of sugar inside the cells is variable and the exit of tracer into a saturating concentration of sugar is measured. This measures the K_m for the endofacial binding site and the V_{max} for sugar exchange.

1.5.1.7 Equilibrium Exchange.

This is the most common type of assay. Cells are preincubated with various concentrations of sugar and the uptake of tracer measured from external media with the same concentration of sugar. Alternatively, the exit of tracer could be measured, although both methods would give values of K_m and V_{max} for sugar exchange.

The results of many sugar transport assays performed by different groups with erythrocytes under conditions outlined above at both 0°C and 20°C have been reviewed recently (Carruthers, 1990). The kinetics of glucose transport by GLUT1 are very temperature dependent, generally displaying lower K_m and V_{max} values at lower temperatures. All transport profiles show simple, hyperbolic Michaelis-Menten kinetics, but also display very different K_m and V_{max} values depending on the conditions used. For example, at 0°C, under *zero-trans* entry conditions the K_m and V_{max} values are approximately 0.15-0.2 mM and 0.0035-0.0055 mM s^{-1} , respectively; whereas these values under *zero-trans* exit conditions are 1.6-3.4 mM and 0.071-0.150 mM s^{-1} , respectively. Thus, the kinetic values for *zero-trans* exit are substantially greater (12-fold) than those for *zero-trans* entry. This asymmetry of transport is reduced somewhat at 20°C, to a 3-fold difference in kinetic values for entry and exit. One physiologically significant function of GLUT1 utilising this observed asymmetry might be the preferential transport of D-glucose in one direction across blood-tissue barriers, such as the blood-brain barrier, under hypoglycaemic conditions. Studies in oocytes suggest that the kinetic properties of GLUT2 and GLUT4 are symmetrical (reviewed in Gould & Holman, 1993).

The equilibrium exchange K_m and V_{max} values are even larger than those measured for *zero-trans* exit (8.7 mM and 0.73 mM s^{-1} , respectively, at 0°C). This observation is due to a phenomenon named *trans*-acceleration, which describes the stimulation of sugar transport by the presence of sugar on the opposite (*trans*) side of the membrane.

1.5.2 Mechanistic Models for D-Glucose Transport.

1.5.2.1 The Single-Site Alternating Conformer Model.

The simplest model for the transport event is the single-site alternating conformer, or, as it is otherwise known, the simple asymmetric model (Figure 1.2). This model was developed initially by Widdas (Widdas, 1952) as a symmetric carrier model and adjusted to account for the observed asymmetry of GLUT1-mediated glucose transport (Geck, 1971). This model also explains the phenomenon of *trans*-acceleration.

This model kinetically describes the re-orientation of the transporter between two conformations: one which exposes the D-glucose-binding site to the extracellular medium, T_o ; and one which exposes the D-glucose-binding site to the cytoplasm, T_i . This re-orientation can occur in the presence or absence of D-glucose. The outward-facing and inward-facing transporters with D-glucose bound are labelled T_oS and T_iS , respectively (Figures 1.2 & 1.3). This re-orientation event might involve just the substrate-binding site, or a large proportion of the transporter structure (Hodgson *et al.*, 1992). The dissociation constants of the substrates at the exofacial (K_{s_o}) and endofacial binding sites (K_{s_i}) are not necessarily equal and the rate constants describing the movement of the loaded carrier (k_1, k_{-1}) are greater than those relating to

the movement of the empty carrier (k_2 , k_{-2}). The rates of association and dissociation of D-glucose from the transporter are also much greater than either re-orientation step, as shown by NMR measurements (Wang *et al.*, 1986). During *zero-trans* transport, the initial unidirectional flux of D-glucose is rate-limited by the slow re-orientation of the unloaded carrier molecule. This does not occur under equilibrium exchange conditions when the dissociation of a D-glucose molecule is followed by the rapid association of another. This accounts for the phenomenon of *trans*-acceleration.

1.5.2.2 Measurement of Rate Constants for Transport Events.

The rate constants for the re-orientation of the transporter in the presence and absence of D-glucose have been measured. Steady-state values have been evaluated by the measurement of the *zero-trans* entry *zero-trans* exit and equilibrium exchange transport of radiolabelled D-glucose by erythrocytes over a range of temperatures (Lowe & Walmsley, 1986), utilising the temperature dependence of transport. Pre-steady-state values for these steps have been measured with purified GLUT1, reconstituted in "leaky" lipid vesicles, in the presence and the absence of D-glucose (Appleman & Lienhard, 1989) by measuring the differences of intrinsic fluorescence at 336 nm displayed by the two transporter conformations. This fluorescence is quenched in the presence of the external ligand 4,6-*O*-ethylidene-D-glucose or the internal ligand phenyl β -D-glucoside. Rapid changes in the conformational state at 10°C were induced by the addition of saturating concentrations of 4,6-*O*-ethylidene-D-glucose, which binds to the exofacial binding site (T_0) and traps the transporter in that conformation, thus measuring single half turnovers (k_{-2} in the presence of glucose or k_{-1} in the absence of glucose), or phenyl β -D-glucoside, which binds the endofacial

binding site (T_i) and traps the transporter in that conformation, thus measuring single half turnovers (k_1 in the presence of glucose and k_2 in its absence).

Values obtained for these rate constants are shown in the Figure 1.2 legend. To summarise, the relative values of each rates constant are $k_2 > k_{-2} > k_1 > k_{-1}$. The results support the existence of the alternating conformer model.

The dissociation constants for substrate at the exofacial and endofacial binding sites can also be calculated from knowledge of the rate constants and the observed transport kinetics. These values for the exofacial binding site were found to be $K_{s0} = \sim 10$ mM for all temperatures from 0°C to 37°C, but the dissociation for the endofacial binding site was found to vary from $K_{si} = 13$ mM, at 0°C, to $K_{si} = 23$ mM, at 37°C (Lowe & Walmsley, 1986). Therefore at low temperatures the affinity of both endofacial and exofacial binding sites for glucose are similar, which contrasts sharply with the measured 10-fold lower affinity (K_m) of the endofacial binding site at 0°C. This difference must be due to the differences in rate constants, which preferentially orientate the transporter to the inward-facing conformation, hence reducing the exit of glucose relative to its entry. Indeed only 7.5% of the loaded and 6% unloaded transporter molecules are predicted to be in an outward-facing conformation at 0°C. At 37°C, these values increase to 40% unloaded and 60% loaded transporters in an outward-facing conformation (Walmsley & Lowe, 1987). The reason for this temperature-dependence of distribution has been suggested to be caused by large positive entropy and endothermic enthalpy changes required for the attainment of an outward-facing conformation, perhaps due to the salt-bridge induced stability of the inward-facing conformation (Walmsley & Lowe, 1987).

1.5.2.3 Multiple Site Models.

There are inconsistencies in the data obtained by kinetic studies with GLUT1, and predicted values derived from integrated rate equations using the simple one-site alternating conformation model, as described by Carruthers and others (Carruthers, 1990). They postulate that the alternating conformer model is an incorrect simplification. Carruthers has proposed several alternative models including the iso two-site model, and the allosteric two-site model. These two-site or fixed-site models assume that each carrier molecule possesses two simultaneously existing glucose binding sites. Re-orientation of the transporter can occur in the presence of two, one or no glucose molecules. The mechanism of transport is such that re-orientation of one binding site to the opposite side of the membrane is accompanied by the simultaneous and opposite re-orientation of the other site, such that both sites are always located on opposite sides of the membrane (Carruthers, 1991).

Evidence for the existence of a two-site model includes the observation that erythrocyte glucose transporters have been shown to bind the endofacial ligand cytochalasin B and then exofacial ligands, such as maltose, 4,6-O-ethylidene-D-glucose or phloretin, simultaneously (Helgerson & Carruthers, 1987). The effects of each inhibitor on the inhibition of transport (K_i) of D-glucose by the other inhibitor suggest that as well as existing simultaneously, the binding of one ligand exhibits negative co-operativity on the binding of the second ligand (Carruthers & Helgerson, 1991).

On the other hand, the bulk of the kinetic data does agree with the single-site model, if allowances for differences in measuring techniques and the fact that sugars do not exhibit "ideal" behaviour, such that measured values for kinetic parameters do not always agree with values obtained with integrated rate equations (Baldwin, 1993).

Other evidence for the single-site model is derived from studies in which erythrocytes are incubated with the non-transported reversible exofacial ligand maltose, which has the effect of pulling transporters into an outward-facing conformation (if the alternating model is correct) (Lowe & Walmsley, 1987). Rapid dilution of maltose and the simultaneous addition of D-glucose induces a change in the intrinsic fluorescence of the transporter, which corresponds to the formation of the inward-facing conformation, prior to the attainment of steady-state transport levels. This single-half turnover supports the existence of the single-site model, since no initial fluorescence change would be predicted in a two-site model, where the maltose could bind to one of two binding sites, and hence could not pull the transporters into an outward-facing conformation.

The results of different analyses support either of the two models. It is far more likely that neither of these models are correct, and that in reality the mechanism of transport incorporates elements of both models. However, for the sake of simplicity, all work done in this study assumes that the single-site model is correct.

1.6 Conformational Changes in GLUT1.

Although the mechanism of transport by GLUT1 is unknown and the number of distinct glucose binding sites is still unresolved, it is certain that the transport of glucose involves a change in transporter conformation.

Sugars with large substituent C-4 groups (compared to D-glucose) such as maltose or 4,6-*O*-ethylidene-D-glucose or large C-6 groups such as 6-*O*-propyl-D-glucose were found to inhibit erythrocyte D-glucose transport only when present outside the cell (Baker & Widdas, 1973; Barnett *et al.*, 1975), and thus were proposed to bind the exofacial glucose binding site. Moreover, n-

propyl- β -D-glucopyranoside only inhibited transport when present inside the cell, and thus was proposed to bind the endofacial binding site (Barnett *et al.*, 1975). This demonstrates the asymmetry of GLUT1 and supports the alternating conformation model of transport.

1.6.1 Detection of GLUT1 Conformational Changes by Measurement of Transporter Intrinsic Fluorescence.

There is a difference in the intrinsic fluorescence of outward-facing and inward-facing conformations of GLUT1 at 336 nm, as observed whilst using ligands which interact with either the exofacial binding site or the endofacial binding site (Appleman & Lienhard, 1989; section 1.5.1.2). The fluorescence observed with native exofacially-orientated transporters is 20% less than those in the inward-facing conformation. The fluorescence spectrum corresponds to that emitted by tryptophan residues in polar and non-polar environments (Gorga & Lienhard, 1982). The fluorescence is quenched in the presence of D-glucose and ligands proposed to bind the exofacial and endofacial binding sites (Gorga & Lienhard, 1982; Chin *et al.*, 1992), and this effect is strongest at wavelengths corresponding to that emitted by tryptophan residues in a polar environment. Thus it is possible that tryptophan residues are present in one or both of the glucose binding sites. Indeed, substitution of GLUT1 Trp³⁸⁸ or Trp⁴¹² leads to a decrease in transport activity and perturbation of cytochalasin B binding, which is proposed to bind to the endofacial binding site (Inukai *et al.*, 1994). Of course, fluorescence quenching by ligands need not occur by direct interaction with a glucose binding site.

Moreover, GLUT1 intrinsic fluorescence is only partially quenched by the addition of potassium iodide, indicating that these tryptophan residues are located both in the membrane bilayer and in a more accessible hydrophilic

environment (Pawagi & Deber, 1990). In the presence of D-glucose, this quenching is reduced at longer wavelengths, and increased at shorter wavelengths (Pawagi & Deber, 1990; Chin *et al.*, 1992). This suggests that the transport of D-glucose causes the movement of one or more tryptophan residues from a hydrophilic environment to a hydrophobic environment, presumably representing a transition state in the transport process.

1.6.2 Sensitivity of Different Transporter Conformations to Chemical Inactivation.

1-fluoro-2,4-dinitrobenzene (FDNB) is an amino group-modifying reagent which has been found irreversibly inactivate glucose transport by erythrocyte GLUT1. Moreover the rate of this inactivation is increased in the presence of extracellular glucose but reduced in the presence of intracellular glucose (Edwards, 1973). Similarly, in the presence of the intracellular n-propyl- β -D-glucopyranoside the inactivation is accelerated (Barnett *et al.*, 1975). However, protection from inactivation is afforded by extracellular ligands such as maltose, 4,6-O-ethylidene-D-glucose, phloretin (Krupka, 1971; Baker & Widdas, 1973) and 6-O-alkyl-D-galactoses (Barnett *et al.*, 1975). Although it is not known precisely where this reagent binds, it apparently binds the transporter whilst in an inward-facing orientation, probably at the external surface. The protection afforded by intracellular glucose is likely due to the increase in steady-state levels of outward-facing transporter achieved by the increased rate of re-orientation toward an outward-facing conformation due to bound glucose (Figure 1.2).

The modification of the exofacial residue Cys⁴²⁹ by impermeant sulphhydryl group-modifying reagents [bis-(maleimidomethyl)-ether-L-[³⁵S]cysteine, (May *et al.*, 1990); pCMBS (Wellner *et al.*, 1992)] also leads to

transporter inactivation. It has been demonstrated that modification by these reagents has been increased in the presence of substances which interact with the exofacial binding site, such as maltose and phloretin. However, the presence of cytochalasin B leads to a reduction in the effectiveness of the reagents (Krupka, 1971; May, 1988; May, 1989). Cytochalasin B has been proposed to stabilise the transporter in an inward-facing conformation by binding at or close to the endofacial glucose binding site (Deves & Krupka, 1978). Cys⁴²⁹ probably lies in a location that is structurally distinct from the exofacial binding site, since the binding of substances known to interact with the exofacial binding site actually increase its modification. This increase of modification in the presence of exofacial ligands and the inhibitory effect of cytochalasin B on modification suggest that this residue lies in a position that is buried when the transporter adopts the inward-facing conformation.

1.6.3 Effects of GLUT1 Conformational State on Proteolytic Cleavage.

As described in section 1.3.2, trypsin cleaves membrane-inserted GLUT1 at three sites, yielding two fragments corresponding to fragments of the large cytoplasmic loop and the hydrophilic C-terminal sequence. Thermolysin is predicted to cleave off the transporter's large cytoplasmic loop. The rate of proteolytic cleavage is reduced in the presence of reversibly binding exofacial ligands such as maltose, 4,6-*O*-ethylidene-*D*-glucose and phloretin (Gibbs *et al.*, 1988; King *et al.*, 1991). In addition, the photoaffinity-labelling of the transporter by exofacial ligands such as the bis-mannose derivative ATB-BMPA (section 1.7), almost completely protects GLUT1 from thermolysin cleavage (Clark & Holman, 1990). These results suggest that the increase in the steady-state levels of outward-facing transporters protect against proteolytic cleavage of the cytoplasmic loops by indirectly causing them to

adopt an orientation that is less susceptible to proteolytic cleavage. Moreover, the presence of reversible endofacial ligands such as n-propyl- β -D-glucopyranoside and methyl- α -D-glucopyranoside increase the rate of thermolytic cleavage relative to native transporter. This is presumably due to the increase in the steady-state levels of inward-facing transporters which are orientated such that the cytoplasmic loops are in a position that is susceptible to proteolysis. The presence of intracellular D-glucose increases the rate of proteolysis (Gibbs *et al.*, 1988; King *et al.*, 1991). Since kinetic theory applied to the alternating conformation model predicts an increase in the numbers of outward-facing, proteolytic-resistant transporters in the presence of glucose (Lowe & Walmsley, 1986), this susceptibility to digestion must occur during the transport process.

Surprisingly, binding of cytochalasin B, which is predicted to stabilise the inward-facing conformation, had no effect on proteolysis (Gibbs *et al.*, 1988; King *et al.*, 1991). Perhaps the increased steady-state levels of inward-facing transporters is balanced by partial steric hindrance by the bulky cytochalasin B molecule, or the lack of effect might be due to the formation of a second distinct inward-facing conformation which binds cytochalasin B.

However, cytochalasin B was found to successfully bind to GLUT1 which had previously been completely digested with trypsin (Cairns *et al.*, 1984; Karim *et al.*, 1987). Conversely, the binding of the exofacial ligand, ATB-BMPA, to this transporter is much reduced (Clark & Holman, 1990). Similar behaviour is exhibited by a GLUT1 mutant which lacks the C-terminal 37 residues (Oka *et al.*, 1990; section 5.2.1.5), but not with one which has only the C-terminal 12 residues removed (Lin *et al.*, 1992). These data would suggest that removal of the GLUT1 C-terminal residues 455-480 causes the formation of a transport-deficient mutant which is locked in the inward-facing conformation.

Taken together, these results suggest that the conformational changes which occur in the transporter are very dynamic, causing movement of at least some of the transmembrane helices and the cytoplasmic loops.

As described in section 5.2.1.3, molecular modelling and molecular dynamics techniques suggest that transmembrane helix 10 of GLUT1 may undergo large conformational changes which could account for the ability of the transporter to assume two distinct glucose-binding conformations (Hodgson *et al.*, 1992). The same modelling predicts that Pro³⁸³, Pro³⁸⁵ and Pro³⁸⁷ would probably act as the pivot necessary for this conformational change. Substitution of Pro³⁸⁵ with isoleucine (Tamori *et al.*, 1994) produced a mutant which was locked into the inward-facing conformation, indeed suggesting that this region is important in the conformational change.

1.7 D-Glucose-Inhibitable Photoaffinity labelling.

The location of the D-glucose binding site, or sites, is unknown, but much work has been done with photoaffinity ligands, the binding of which inhibit, and are inhibited by D-glucose transport. Limited proteolysis of the transporter followed by radiolabelled ligand photoaffinity labelling should reveal the approximate position of the glucose binding site, given that the site of photoaffinity labelling does not merely sterically hinder glucose binding, whether directly or by affecting transporter conformation, and assuming that the site of photoaffinity binding and the site of reversible inhibition of glucose transport are the same.

1.7.1 Photoaffinity Labels Proposed to Interact with the Endofacial D-Glucose Binding Site.

One such ligand is the fungal metabolite cytochalasin B, which binds GLUT1 in a D-glucose-sensitive manner at the ratio of one molecule per polypeptide chain (Baldwin & Lienhard, 1989) with a K_d of 120 nM (Zoccoli *et al.*, 1978). It binds GLUT2 [K_d of $\sim 1 \mu\text{M}$ (Axelrod & Pilch, 1983)] and GLUT7 (Waddell *et al.*, 1991) with relatively weak affinity, and does not appreciably bind GLUT5 (Burant *et al.*, 1992).

Cytochalasin B binds GLUT1 at the intracellular surface of the membrane (Deves & Krupka, 1978). Photolabelling with [^3H]cytochalasin B after tryptic cleavage (Cairns *et al.*, 1984; Deziel & Rothstein, 1984) yields a labelled fragment corresponding to residues 270-456, which comprises most of the C-terminal half of the protein. The site of photoaffinity labelling has been proposed to lie within residues 389-412, which comprises the loop connecting helices 10 and 11, and helix 11 itself (Holman & Rees, 1987). Recent studies suggest that Trp³⁸⁸ is included in this sequence too (Inukai *et al.*, 1994). This sequence is believed to contain the endofacial glucose binding site. The D-glucose inhibitable binding of cytochalasin B and forskolin derivatives to GLUT1 (and other transporters) is proposed to occur to the endofacial binding site since the oxygen atoms of these molecules are superimposable with those of D-glucose, hence allowing these inhibitors to interact with the binding site via hydrogen bonding. The *E. coli* galactose/ H^+ symporter, GalP, and the arabinose/ H^+ symporter, AraE, both bind cytochalasin B but the xylose/ H^+ symporter, Xyl E, does not (Henderson *et al.*, 1992). It has recently been found that cytochalasin B and 4,6-O-ethylidene-D-glucose can bind GLUT1 simultaneously (Carruthers & Helgersen, 1991), a finding which casts doubts on the accuracy of the alternating conformation model (section 1.5.2.3).

Forskolin has been found to inhibit D-glucose transport by GLUT1. It is also found to bind to the intracellular surface of the membrane and bind GLUT1 in a cytochalasin B and D-glucose inhibitable manner (Sergeant & Kim, 1985). Therefore it binds close to the cytochalasin B binding site. Proteolytic digestion and labelling with the photoactivatable derivative [³H]IAPS-forskolin, followed by proteolytic and chemical cleavage have suggested that it binds within helix 10, that is, residues 369-389 (Wadzinski *et al.*, 1990). This may also comprise part of the endofacial binding site, since forskolin binding is inhibitable by cytochalasin B. GalP of *E. coli* binds [³H]IAPS-forskolin and its sugar transport is inhibited by forskolin (Henderson *et al.*, 1992). AraE and XylE do not bind forskolin.

1.7.2 Photoaffinity Labels Proposed to Interact with the Exofacial D-Glucose Binding Site.

The requirement for a membrane impermeant affinity label to participate in the quantitation of cell surface glucose transporters led Holman and colleagues to develop a series of bis-hexoses (Midgley *et al.*, 1985; Holman & Midgley, 1985) with the rationale that these should bind the exofacial D-glucose binding site. The bis-mannose-derivative, 1,3-bis-(D-mannos-4-yloxy)-2-propylamine (BMPA), a hydrophilic impermeable compound consisting of two mannose moieties, bisected by an amino group which can be linked to a photoactivatable group, was found to be useful. Although derivatives of this were found to bind to GLUT1 with lower affinity than cytochalasin B or IAPS-forskolin, they bound with greater affinity than D-mannose itself.

The derivative 2-N-(4-azidosalicyl)-1,3-bis(D-mannos-4-yloxy)propyl-2-amine (ASA-BMPA), which possesses an azidosalicyl photoactivatable

group, was found to selectively label the extracellular surface of GLUT1 (Holman *et al.*, 1986). This compound was found to bind to GLUT1 the region between residues 347-388, probably at the extracellular end of helix 9, which was proposed to be the exofacial glucose binding site (Holman & Rees, 1987).

However, ASA-BMPA was found not to selectively label plasma membrane glucose transporters when they were in low abundance. Therefore a new photoaffinity probe, 2-*N*-[4-azi-2,2,2-trifluoroethyl)benzoyl]-1,3-bis(D-mannos-4-yloxy)-2-propylamine (ATB-BMPA), was developed (Clark & Holman, 1990). This compound, which incorporates an azitrifluoroethylbenzoyl reactive group was found to exhibit better selectivity than its predecessor, allowing its use even with membrane fractions. The site of ATB-BMPA labelling has been localised to residues 301-330, within transmembrane helix 8 (Davies *et al.*, 1991).

Thus, the site of the exofacial binding site is propose to include helices 8 and 9, whereas the endofacial binding site is proposed to include helices 10 and 11. Therefore there seems to be some structural separation between the endofacial and exofacial binding sites. The results of several mutagenesis studies have supported the proposed position of the endofacial binding site, and suggested that helix 7 is also included as part of the exofacial binding site (section 5.2).

1.8 Oligomerisation of GLUT1.

It has been shown that the application of size-exclusion chromatography and sucrose gradient ultracentrifugation to cholate-solubilised GLUT1, and reconstitution of the resulting complexes into proteoliposomes, leads to the formation of transporter complexes which display D-glucose inhibitable-cytochalasin B binding (Herbert & Carruthers,

1991). The sizes of these particles indicate that GLUT1 can exist as a tetramer or a dimer under different reducing conditions. Further hydrodynamic studies, chemical cross-linking and use of conformational-specific antibodies suggest that the tetramer binds 1 mole of cytochalasin B/2 moles GLUT1, presenting at least two binding sites to D-glucose; and the dimer binds 1 mole of cytochalasin B/mole GLUT1, presenting a single population of binding sites to D-glucose (Herbert & Carruthers, 1992).

Furthermore, Carruthers has suggested that the tetramer is the native erythrocyte transporter, which is formed of two dimers, stabilised by intramolecular disulphide bonds (Herbert & Carruthers, 1992). He suggests that the tetrameric transporter isoform is 2-8-fold catalytically more efficient than dimeric forms, and that discrepancies in previous kinetic studies with GLUT1 arise from the fact that these have been performed on both erythrocytes (tetrameric form) and detergent-treated reconstituted transporters (dimeric form).

Carruthers proposes a model to explain this difference in efficiency between different forms. In the dimeric form, each subunit is independent of the actions of the other, and thus displays no allosteric interactions, each behaving in such a manner as explained by the single-site alternating conformation model. On the other hand, the tetramer is composed of two dimers which are bound to each other in such a way that they adopt a pseudo-D₂ symmetry, and the active region of each subunit is conformationally constrained by the isomerisation of the neighbour such that the binding sites are arranged in an antiparallel manner. Thus each "dimer" in the tetrameric structure presents one exofacial and one endofacial binding site, and the tetramer displays characteristics of a multi-site, allosteric transporter which is consistent with the two-site fixed site model. Carruthers speculates that the tetramer is intrinsically more efficient since the conformation change induced

by transport of glucose by one subunit causes the re-orientation of the neighbouring unloaded subunit, overcoming the large energy barrier required for this step (Lowe & Walmsley, 1986) in dimers and monomers. Presumably this rate-limiting re-orientation step would not occur under equilibrium exchange conditions (Carruthers, 1991), so that the steady-state kinetics observed for both tetramers and dimers would be identical.

In a further study, two chimeric transporters were individually expressed in Chinese hamster ovary (CHO) cells (Pessino *et al.*, 1991). These were mutants of GLUT1 which had the C-terminal 29 residues or the C-terminal 294 residues substituted with those of GLUT4. Both mutants were found to quantitatively co-immunoprecipitate native GLUT1 from CHO cells using an anti-GLUT4 C-terminal peptide antibody, as detected by immunoblotting the precipitates with an anti-GLUT1 C-terminal peptide antibody. No co-immunoprecipitation of native GLUT4 with native GLUT1 was observed from 3T3-L1 adipocytes using the same antibody. These results demonstrate that GLUT1 forms at least homodimers *in vivo*, but not heterodimers with GLUT4, and that the sequence responsible for the interaction of dimer subunits is present in the first 199 residues of GLUT1.

Studies performed with GLUT2 and GLUT3 expressed heterologously in *Xenopus* oocytes show that the kinetics of these two transporters are distinguishable (Burant & Bell, 1992; Colville *et al.*, 1993; see also Chapter 3). It has been shown that co-expression of these two transporters in oocytes displays a kinetic profile that can be separated into two components attributable to each of the individual transporters, indicating that no heterodimers are formed (Burant & Bell, 1992). Co-expression of heterologous GLUT3 and a transport-defective GLUT3 transporter in oocytes, displayed kinetics associated with wild-type GLUT3, even when a 3-fold excess of mutant GLUT3 mRNA was injected, suggesting that GLUT3 also behaves

as a monomer in oocytes (Burant & Bell, 1992). It is impossible to tell whether it is the intrinsic nature of the GLUT3 transporter to form monomers, or whether this is due to the conditions in oocytes that accounts for these data. It is interesting to note that dimers could still be formed and have subunits that are independent of each other, as suggested by Carruthers (Herbert & Carruthers, 1992). Additionally, factors such as temperature might influence oligomerisation. The suitability of the oocyte system for oligomerisation studies could be tested by the co-expression of GLUT1 and the constructs described by Pessino *et al.*.

1.9 Aims of this Study.

The objectives of this work are to characterise kinetic parameters of sugar transport by GLUT2 and GLUT3 in *Xenopus* oocytes, with particular attention to interactions at the exofacial binding sites. This should help gain some insight into their respective *in vivo* functions. In addition, basic kinetic values for zero-*trans* entry should provide standard kinetic values as baselines for comparison with transporters which have substitutions of specific residues that are believed to be involved in their exofacial binding sites. Since it is not currently known how GLUT2 binds D-fructose, investigation of which ring form of this sugar that is transported by GLUT2 is necessary. Further aims include an investigation of the effects of substituting various hydroxyl groups of D-glucose on the ability the sugar to bind to the exofacial binding sites of GLUT2 and GLUT3, and thus investigate the interactions at that sugar group.

Some of the work in this study has been performed by Dr. Carol Colville, and is noted where it is included. This is for the purposes of comparison only.

Lastly, an investigation of the importance of the residues of transmembrane helix 8 is necessary. In GLUT1 this helix is proposed to be the site of binding of the external ligand ATB-BMPA, and possibly comprises part of the exofacial D-glucose binding site. It is likely to have a similar function in GLUT3, since the this transporter isoform has a high identity, a similar substrate specificity, and not dissimilar kinetic properties to GLUT1. Therefore an objective of this study is to systematically alter each of the residues of GLUT3 helix 8 to alanine and measure any perturbation of sugar transport or exofacial ligand binding caused by the mutations, and to assess which residues are involved in D-glucose binding and/or transport.

Figure 1.1

Model for the Orientation of Mammalian Facilitative Glucose Transporters in the Membrane.

This model is based mainly on studies performed with human GLUT1, and so this model corresponds to that transporter. However, it is predicted from hydropathy analysis of the primary sequence of other mammalian transporters (Mueckler *et al.*, 1985) and numerous other studies that they will adopt an identical conformation. The 12 transmembrane α -helices are shown as boxes, numbered from 1-12. The site marked "CHO" between transmembrane helices 1 and 2 represents the potential site of *N*-linked glycosylation in the large exofacial loop. The amino- and carboxy-termini (NH_2 and COOH , respectively) are cytoplasmically disposed. Invariant residues are shown by their single-letter abbreviations, and filled circles represent invariant polar residues which are predicted to reside in the lipid bilayer. Residues which have been implicated to be important for transporter function by mutagenesis studies are shown as red circles (section 5.2). This diagram was taken from Bell *et al.*, 1993).

Figure 1.2

This shows a King-Altman representation of the Alternating-Conformation Model of D-glucose transport. T_o and T_i represent the unloaded transporter in outward-facing and inward-facing conformations, respectively. T_oS and T_iS represent the transporter with bound substrate (D-glucose), in outward-facing and inward-facing conformations, respectively. K_{S_o} and K_{S_i} represent the dissociation constants for substrate (D-glucose), at the exofacial and endofacial binding sites, respectively. Rate constants for the re-orientation transporter are denoted as k_1 , k_{-1} , k_2 and k_{-2} . Re-orientation of unloaded transporter from outward-facing conformation to inward-facing conformation is represented by k_1 . Re-orientation of unloaded transporter from inward-facing conformation to outward-facing conformation is represented by k_{-1} . Re-orientation of loaded transporter from outward-facing conformation to inward-facing conformation is represented by k_2 . Re-orientation of loaded transporter from inward-facing conformation to outward-facing conformation is represented by k_{-2} . Values of these constants for GLUT1 at 0°C are shown below (Lowe & Walmsley, 1986).

Rate Constant	Value at 0°C (s ⁻¹)
k_1	12.1 ± 0.98
k_{-1}	0.726 ± 0.498
k_2	1113 ± 498
k_{-2}	90.3 ± 3.47

Figure 1.2-

King-Altman Representation of the Alternating-Conformation Model for Sugar Transport by GLUT1.

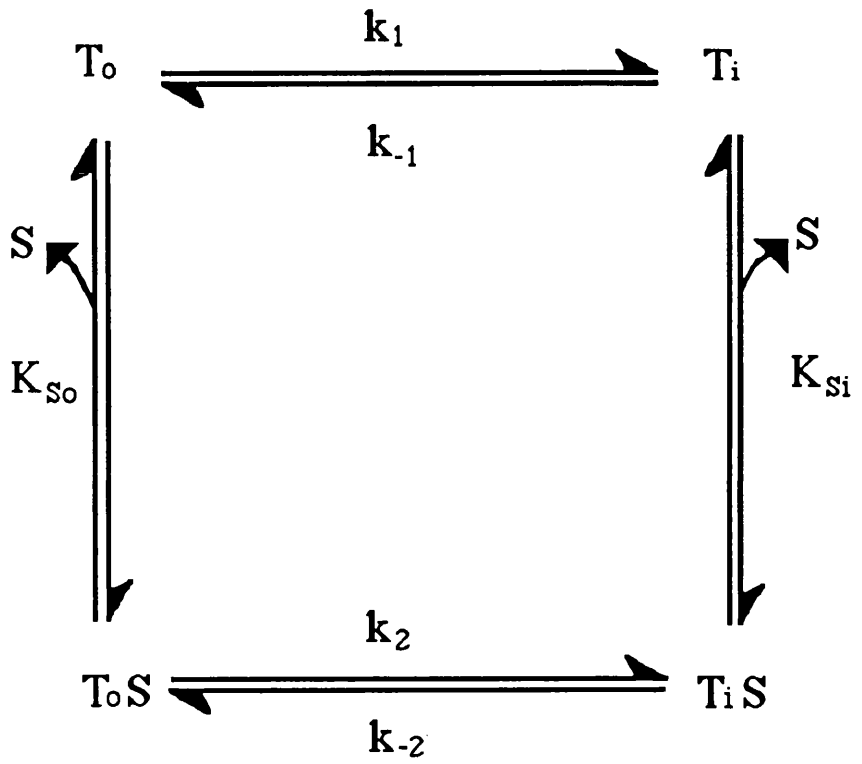
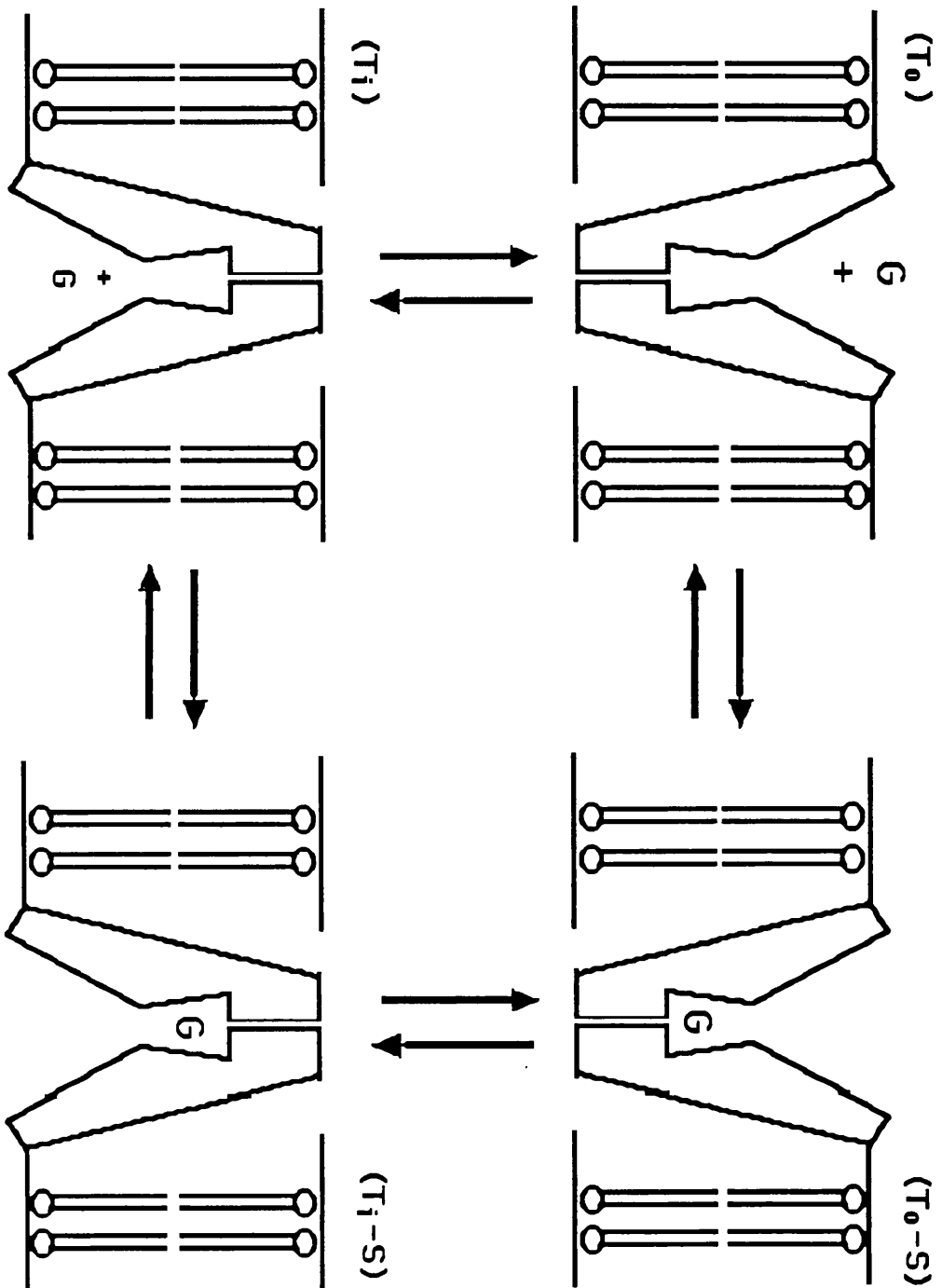


Figure 1.3

This is a schematic diagram representing the Alternating Conformation Model depicting the conformational changes occurring during D-glucose transport. T_o and T_i represent the unloaded transporter in outward-facing and inward-facing conformations, respectively. T_oS and T_iS represent the transporter with bound substrate (D-glucose), in outward-facing and inward-facing conformations, respectively. Note that this diagram does not in any way attempt to represent the actual transporter conformations.

Figure 1.3-

Schematic Diagram Showing the Conformational Changes Occurring during D-Glucose Transport as Predicted by the Alternating Conformation Model.



CHAPTER 2.

Materials and Methods.

2.1 Materials.

Adult female *Xenopus laevis* were obtained from either Blades Biologicals, Edenbridge, Kent, UK, or directly from South Africa, (African *Xenopus* Facility, PO Box 118, Noordhoek, Republic of South Africa). "Frog Brittle" was also obtained from Blades Biologicals.

Recrystallised 4,6-*O*-ethylidene-D-glucose was a gift of Prof. G. E. Lienhard (Dartmouth Medical School, Hanover, NH, USA).

3-*O*-propyl-D-glucose, 1-deoxy-D-glucose, 6-deoxy-D-glucose, 6-*O*-propyl-D-galactose, 6-fluoro-D-galactose, 6-*O*-methyl-D-galactose and 3-fluoro-D-glucose were the gift of Dr. G. D. Holman (University of Bath, UK).

All other sugars and analogues were the gift of Prof. Mohammed Akhtar (University of Southampton, UK).

Tricaine Methane Sulphonate, MS222 was supplied by Thompson & Joseph Ltd., Norwich, UK.

Chromic sterile catgut[®] was supplied by Ethicon Ltd., London, UK.

2-deoxy-D-glucose, 3-*O*-methyl-D-glucose, 3-deoxy-D-glucose, 3-fluoro-3-deoxy-D-glucose, maltose, D-galactose, β -D-fructose, β -lactose, D-cellobiose, L-arabinose, D-mannose, D-xylose, phloretin, kanamycin, ampicillin, tetracycline, dithiothreitol, collagenase, cytochalasin B, and 2,5-anhydro-D-mannitol were supplied by Sigma Chemical Company, Poole, Dorset, UK.

D-allose, D-fucose, and L-sorbose were supplied by Pfanstiehl Laboratories Inc., Waukegan, IL, USA.

Ammonium formate, calcium chloride-6-hydrate, and chloroform (Analytical Reagent) were supplied by BDH, Poole, UK.

Bacto[®]-tryptone, Bacto[®]-agar and Bacto[®]-yeast extract were supplied by Difco, East Molesey, Surrey, UK.

Tris was supplied by Boehringer Mannheim GmbH., Lewes, East Sussex, UK.

Agarose (electrophoresis grade), DNA ligase and 5x ligase buffer were supplied by Gibco BRL, Paisley, UK.

Lambda ladder (*Bst*E II digested) and ribonuclease A were supplied by New England Biolabs, Hitchin, Herts, UK.

Sequencing grade urea, Tris, EDTA, de-ionised formamide, TEMED and Mixed Bed Resin were obtained from International Biotechnologies Inc. Ltd. (IBI), Cambridge, UK.

National Diagnostics Sequagel-6™ 6% sequencing gel solution and Sequagel™ Complete Buffer Reagent were obtained from BS&S, Edinburgh, UK.

Ultima-flo AF scintillant was obtained from Canberra Packard Ltd., Pangbourne, Berks., UK.

Taq DyeDeoxy™ Terminator Cycle Sequencing kits and sequencing-grade phenol/chloroform/H₂O (68:18:14) was obtained from Applied Biosystems Inc. (ABI), Warrington, Cheshire, UK.

Plasmid Midi and Maxi Preparation Kits were supplied by QIAGEN, UK.

Elutip-D DNA purification columns (Schleicher & Schuell) were obtained from Anderman Ltd, London, UK.

Permacel™ tape was obtained from Genetic Research Instruments, Dunmow, Essex, UK.

Alconox™ detergent was supplied by Aldrich Chemical Company Ltd., Gillingham, Dorset, UK.

'Native' *Pfu* DNA polymerase and 'Native' *Pfu* polymerase 10x buffer were obtained from Stratagene, Cambridge, UK.

All restriction enzymes and corresponding 10x buffers, *Taq* DNA polymerase with supplied 10x buffer and MgCl₂, calf intestinal alkaline phosphatase and 10x buffer, polynucleotide kinase and polynucleotide kinase 10x buffer, rNTPs, dNTPs, nuclease-free H₂O, 5x transcription buffer, dithiothreitol (DTT), RNasin, RNA ladder (360-9,490 bases) and SP6 RNA polymerase were supplied by Promega, Southampton, UK.

[2,6-³H]2-deoxy-D-glucose, [U-¹⁴C]D-fructose and [U-³H]D-galactose were supplied by DuPont NEN, Stevenage, Herts, UK.

"Sculptor™ *in vitro* mutagenesis system- RPN 1526" kits and [³²P]dATP (5000 Ci/mmol; 10 mCi/ml) were supplied by Amersham International plc., Aylesbury, Bucks, UK.

Dialysis tubing (Visking size 1-8/32") was supplied by Medicell International Ltd, London, UK.

Sterile Acrodisc® 0.2 µm filters were supplied by Gelman Sciences Ltd., Northampton, UK.

DE-81 filter paper was supplied by Whatman Scientific Ltd., Maidstone, Kent, UK.

Sodium diguanosine triphosphate, GpppG (5' Cap) was supplied by Pharmacia, Milton Keynes, UK.

All oligonucleotides (Tables 5.1 and 5.2) were synthesised by Dr. V. Math, Department of Biochemistry, University of Glasgow.

Unless indicated otherwise, all remaining chemicals were supplied by Fisons, Loughborough, UK.

2.2 *In Vitro* Synthesis of mRNA from Plasmid cDNA.

All work with mRNA was conducted with sterile equipment whilst wearing gloves since ribonucleases which can degrade mRNA can be found on the skin and elsewhere, and as they are very stable enzymes, care was taken to avoid potential degradation of the mRNA. All reagents were thawed on ice. A nucleotide stock (2.5 mM rATP, 2.5 mM rCTP, 2.5 mM rUTP and 0.5 mM rGTP) was diluted from stock 100 mM ribonucleotides. The following reagents were added to a sterile microfuge tube in the order shown, at room temperature:-

- 75 μ l ribonuclease-free H₂O
- 40 μ l 5x transcription buffer
- 20 μ l 100 mM dithiothreitol (DTT)
- 5 μ l RNasin (a synthetic inhibitor of ribonuclease)
- 40 μ l nucleotide mix (see above)
- 10 μ l GpppG (5' Cap) (25 units/100 μ l).
- 10 μ l linearised plasmid cDNA (~ 1 μ g/ml; see section 2.5.2).
- 2.5 μ l SP6 polymerase (25 units)

This gave a total volume of 200 μ l. The tube was placed in a 37°C water bath for 1 hour, after which a further 0.5 μ l of SP6 polymerase was added, mixed and incubated at 37°C for 30 min. At this point the reaction was centrifuged in a microfuge to collect the condensate and then 1 volume of phenol/chloroform [1:1 (v/v)] added. This was vortexed for 1 min and centrifuged in a microfuge for a further 1 min. The upper aqueous phase, which contained both mRNA and cDNA, was carefully collected into a clean tube. 100 μ l of chloroform/isoamyl-alcohol (24:1) was added to the solution, before vortexing, centrifuging, and again collecting the aqueous phase. This procedure was repeated, before finally adding 0.3 volumes of 5 M potassium

acetate and 2.5 volumes of ice-cold absolute ethanol to precipitate the nucleic acid. The reaction was mixed and placed at -20°C for approximately 1 hour, then centrifuged in a microfuge for 30 min. The pellet was washed with 0.5 ml 70% ethanol and centrifuged as above. All traces of ethanol were removed from the pellet by drying under vacuum. The pellet was resuspended in 20 µl of ribonuclease-free H₂O. 1 µl of this was mixed with 3 µl of 5x DNA gel loading buffer (see Table 2.1) and loaded into a 1% agarose gel overlaid with 1x TAE running buffer (see Table 2.1). 5 µl of 100 µg/ml *BstE* II-cut lambda ladder DNA was loaded into an adjacent well and the current adjusted to 50 mA so that negatively charged nucleic acids migrated toward the positive electrode. Electrophoresis was carried out until the dye-front was half to two thirds across the gel, then 20 µl of 10 mg/ml ethidium bromide added per litre of running buffer. The bands were visualised by viewing the gel under ultraviolet light, and the size of any mRNA band checked by its relative migration to the lambda ladder. A typical photograph of mRNA on a 1% agarose gel can be seen in Figure 2.1.

2.3 Using *Xenopus* Oocytes.

2.3.1 Handling *Xenopus*.

Adult female *Xenopus laevis* (average length 15 cm) were kept in aquaria at a constant temperature of 16-18°C on a 12 hour day/night cycle. The animals were housed 2-4 per tank, in distilled water in a quiet environment. They were fed once weekly with raw chopped sheep heart and the aquaria cleaned the following day. Alternatively they were fed Blades Biologicals "Frog Brittle". Each animal was kept for at least one month before

operating to allow acclimatisation to its new environment. Oocytes were generally satisfactory after this initial period, however during the summer poor oocytes were occasionally encountered, coincident with seasonal variability of the female cycle in these animals.

2.3.2 Anaesthesia.

The anaesthetic was prepared by dissolving 0.75 g Tricaine Methane Sulphonate (MS222) in 500 ml distilled water. 25 ml of 0.5 M sodium bicarbonate was added to ensure that the pH of the anaesthetic approached neutrality and hence was acceptable for the animal. The animal to be operated on was placed in the tank with the anaesthetic and supervised to ensure that it did not drown. Typically, animals were unconscious after 5-10 min. The animal was placed on its back and observed. If it did not move, it was judged to be unconscious.

2.3.3 Surgery.

Home Office Project and Individual Animal Handling Licenses were required for work on *Xenopus*. The animal was placed on its back and, using a sharp scalpel, a centimetre-long incision was made in the dermis and then another one directly underneath in the abdominal wall. A small clump of oocytes was removed using fine watchmaker's forceps and small scissors. These were placed into a petri-dish containing Barths buffer (Table 2.1). Oocytes were determined to be healthy if they fulfilled several important criteria. Oocytes had to be approximately 1 mm in diameter; required well-defined animal and vegetable poles, with a sharp distinction at the boundary; required no discoloured patches; and had to exhibit a certain robustness when

manipulated. These were defined as stage V and VI oocytes. If the oocytes were judged to be healthy, enough were removed from the toad as required for injection and non-injected controls. The animal was then sewn up using chromic sterile catgut, with a single stitch in the abdominal wall and two stitches in the dermis. The animal was then placed on its front in a recovery tank containing 2-3 mm of distilled water until it fully regained consciousness, when it was returned to its own holding tank. A minimum period of no less than three months was allowed to pass before operating on the same animal.

2.3.4 Oocyte Isolation and Injection.

Oocytes were removed from adult female *Xenopus laevis* and individually dissected. This involved removing the oocytes from the connective tissue and blood vessels which provide the oocytes with nutrients and remove toxic wastes. Oocytes were placed into a petri-dish, immersed in Barths buffer (see Table 2.1), to maintain the environment as close to *in vivo* conditions as possible. Using a binocular microscope and fine watchmakers forceps, stage V and VI oocytes were removed from their stalks and then transferred to a container with fresh Barths buffer. Damaged oocytes were immediately discarded to minimise the exposure of healthy oocytes to proteases. Generally, 2-3 times as many oocytes were isolated than actually required since a percentage of the population would be expected to die before they were assayed. Oocytes were selected as required for injection with 40 nl of *in vitro* transcribed mRNA encoding GLUT2, GLUT3 or a mutant transporter, or to act as non-injected "control" oocytes.

The injection apparatus consisted of a 10 µl micro-injector (Drummond Scientific Co.); six inch long capillary tubes; a micro-manipulator (Narishige,

Japan); a needle-puller (World Precision Instruments); a binocular microscope with separate light source; a petri-dish with a SpectraMesh grid (Fischer); and paraffin oil. Gloves were worn at all times to prevent contamination of the mRNA by ribonuclease present on fingertips. A capillary tube was placed in the needle-puller and by a combination of heating and pulling produced needles with a bore size of about 2 μm . The tip of one was broken off near the end with fine forceps and, using a syringe and 25 gauge needle, filled with paraffin oil. This was attached to the micropipette (set at about 3 μl) and secured in the micro-manipulator. GLUT mRNA was placed into a 1.5 ml microfuge tube and pulsed for 30 sec in a microfuge to remove any debris or insoluble material. About 7 μl of mRNA was taken from the supernatant and placed onto a sterile microfuge tube lid. The micropipette was lowered so that the end of the needle was submerged in the droplet, and the mRNA taken up slowly into the needle. Oocytes were placed on a grid in a petri-dish with Barths buffer and orientated so that the pale vegetable pole was uppermost. They were injected with a precise volume of mRNA (10-50 nl) and then removed to a separate container. The oocytes were incubated in Barths buffer for 48-72 hours prior to assay, transferring to fresh buffer every 12 hours. Non-injected oocytes were treated in an identical fashion. After this period, oocytes were assayed for the ability to transport 2-deoxy-D-glucose.

2.4 Sugar Transport in *Xenopus* oocytes.

Groups of 6 oocytes were incubated in 0.45 ml Barths buffer (Table 2.1) at room temperature in 13.5 ml centrifuge tubes. Transport (*zero-trans* entry) was initiated by the addition of 50 μl of [2,6- ^3H]2-deoxy-D-glucose, [U- ^{14}C]D-fructose or [U- ^3H]D-galactose to give a specified final sugar concentration with an activity of ~ 1 $\mu\text{Ci/ml}$. After a designated time, usually 15 or 30 min, the

transport of sugar into the oocytes was quenched by rapid aspiration of the media and three washes with 5 ml ice-cold 150 mM phosphate buffered saline, pH 7.4, (1xPBS, Table 2.1) containing 0.1 mM phloretin (a potent transport inhibitor). The oocytes were dispensed individually into scintillation vials using a pipette and a tip which had the end cut off, and then 0.5 ml of 1% sodium dodecyl sulphate (SDS) added. The vials were left for an 1 hour at room temperature then vortexed to solubilise the oocytes, before the addition of 4 ml scintillation fluid and subsequent measurement of radioactive uptake by a scintillation counter. For each group of GLUT-injected oocytes assayed at a particular sugar concentration, a group of non-injected oocytes were assayed under identical conditions. This control gave a value for radioactive sugar transport by native oocyte glucose transporters plus background radiation levels. Hence, the rate of uptake in GLUT-injected oocytes less the rate of transport in control (non-injected) oocytes gave a value corresponding to specific transport by heterologous transporters. Transport with a variety of sugar concentrations was measured for each assay so that Lineweaver-Burk plots could be constructed, and K_m and K_i values determined. For assays involving the inhibition of radioactive sugar uptake by another sugar or the fungal metabolite cytochalasin B, the inhibitor was added to the oocytes in 0.45 ml Barths buffer at least 15 min prior to addition of labelled sugar.

2.5 General Techniques for the Manipulation of DNA.

2.5.1 Plasmid Construction.

The human glucose transporter constructs used for the preparation of mRNA have been described previously (Kayano *et al.*, 1990). Human GLUTs

2 and 3 and mutant GLUT3 were in pSP64T (Krieg & Melton, 1984) and named pHTL217 and pSPGT3, respectively. These constructs contain the protein coding region of the cDNA (and various amounts of 5'- and 3'-untranslated regions) flanked by 89 bp of 5'- and 141 bp of 3'-untranslated sequence from the *Xenopus* β -globin gene (Kayano *et al.*, 1990) (Figure 2.2). The plasmid contains a SP6 RNA polymerase promoter at the 5' end of the transporter sequence and a sequence encoding ampicillin resistance.

GLUT3 cDNA was also present in M13mp18GT3, cloned as a *Bam*H I/*Xba* I fragment into the multiple cloning site of M13mp18 (Figure 2.3). This bacteriophage vector has no RNA polymerase promoters, and hence was not used as a template for the synthesis of mRNA.

2.5.2 Linearisation of Plasmid cDNA.

pHTL217 or pSPGT3, or a derivative thereof, was specifically restricted once at the 3' end of the cDNA, downstream of the coding sequence. This had the effect of linearising the plasmid, so that the efficiency of subsequent mRNA synthesis reactions were increased by ensuring that the SP6 RNA polymerase used did not continue synthesis of mRNA after transcription of the transporter. The choice of restriction enzyme depended on the particular plasmid and transporter. GLUT3 and its point mutants were linearised using *Xba* I, and GLUT2 by *Sal* I. 10 μ g of plasmid cDNA was digested in a total volume of 20 μ l overnight at 37°C (section 2.5.4). 1 μ l of this reaction was loaded onto a 1% agarose gel and electrophoresed to confirm linearisation (section 2.5.3). From this point onwards, all work was done using sterile microfuge tubes whilst wearing gloves. 70 μ l of ribonuclease-free H₂O was added to the tube, the solution extracted with 1 volume of phenol/chloroform (1:1), then twice with chloroform/isoamyl-alcohol (24:1).

The cDNA was precipitated by the addition of 0.3 volumes of 5 M potassium acetate and 2.5 volumes of absolute ethanol, and incubation at -20°C for at least 1 hour. The tube was centrifuged in a microfuge for 30 min at 4°C, the pellet resuspended in 0.5 ml 70% ethanol, centrifuged again in a microfuge for 30 min, and the pellet finally resuspended in 10 µl of ribonuclease-free H₂O. This was ready to be used in a mRNA synthesis reaction (section 2.2).

2.5.3 Agarose Gel Electrophoresis of cDNA.

Various gel volumes, combs and agarose concentrations were used. The gel volume was governed by the number of samples, the volume of the samples and to a lesser extent the required degree of separation of the cDNA bands. The choice of comb depended only on the volume of the samples. The concentration of agarose used varied depending on the molecular weight of the cDNA band to be visualised- high agarose concentrations aided the separation of low molecular weight bands, and lower agarose concentrations give better separation with higher molecular weight bands. Typical concentrations used were 1.0% and 1.5% (w/v).

Example:- for a 100 ml 1.0% Agarose Gel.

An appropriate gel base was selected and the ends secured with tape to prevent gel leakage. 1.0 g of agarose was weighed out and distilled water added to a total volume of 100 ml. This was heated in a microwave oven until the solution just boiled and left to cool until hand hot. 2 ml of 50xTAE buffer (Table 2.1) was added to the gel solution and mixed. The contents were poured onto the gel base, the comb inserted and the gel left to set for about 10 min. The tape was then removed and the entire gel/ gel base placed into the

electrophoresis tank so that the wells were nearest to the negative electrode. About 1 litre of 1xTAE buffer (40 mM Tris-acetate, 1 mM EDTA, pH 8.0) was added to the chamber so that the entire gel was submerged, and then the comb was removed. To each sample, 1/4 volume of 5x DNA gel-loading buffer (Table 2.1) was added and mixed. The samples were loaded into the wells by pipetting directly above them- the glycerol in the sample buffer ensured that the samples were more dense than the buffer and therefore the samples sank into the wells. 10 μ l of loading buffer containing 25 μ g/ml *Bst*E II-cut lambda ladder cDNA was loaded into an adjacent well. The electrodes were connected so that the negative electrode was closest to the sample wells. The samples were electrophoresed at 50-100 mA using an LKB 2197 power supply until the dye front had migrated two thirds of the way along the gel towards the positive electrode, then 50 μ l of 10 mg/ml ethidium bromide was added per litre of running buffer, and left at room temperature for 30- 45 min. The DNA was visualised by ultra-violet light using an Ultraviolet Products Inc. transilluminator, and the size of any cDNA band checked by its relative migration to the lambda ladder. The gel was then photographed using a Mitsubishi video copy processor.

2.5.4 Restriction Digestion of cDNA.

Restriction digestion of cDNA was performed by the addition of restriction enzymes to cDNA in the appropriate buffer, optimising salt concentration and pH for individual enzymes. Generally, from 0.5-10 μ g of cDNA was digested per reaction. The total reaction volume was 10 μ l per 1 μ g cDNA and the quantity of enzyme added equal to 1 unit per 1 μ g cDNA. The reaction was carried out by the addition of 1 volume of 10x buffer to 9 volumes diluted cDNA solution, before the addition of enzyme. This was

incubated for 1 hour at 37°C (or otherwise depending on the particular enzyme). For digestions with more than one enzyme, the reaction was carried out as usual with the first enzyme (the one which utilises lower salt concentrations), and then salt added to the reaction to optimise conditions for the second digestion which was subsequently carried out. Alternatively, if both enzymes utilised approximately the same optimum reaction conditions, both digests could be carried out simultaneously. The reactions were then added to 1/4 volume of 5x DNA gel loading buffer and the solution loaded onto an appropriate agarose gel. This was electrophoresed, stained with ethidium bromide and cDNA bands visualised as described above (section 2.5.3). Any bands of interest were excised from the gel with a scalpel and purified as described (sections 2.7.4; 2.7.5; 2.7.6).

2.5.5 Dephosphorylation of Double-Stranded cDNA using Calf Intestinal Phosphatase.

Plasmid cDNA was digested with the appropriate restriction enzyme for 60 min and then treated with RNase A for 15 min at 37°C (section 2.5.10). The mix was then made up to a volume of 100 µl with dephosphorylation buffer (1 mM ZnCl₂, 1 mM MgCl₂, 10 mM Tris-HCl pH 8.8) and 1 unit of Calf Intestinal Phosphatase (CIP) was added. After incubation at 37°C for 60 min, plasmid cDNA was isolated from the enzyme reagents by phenol extraction and precipitation (section 2.5.2), and cDNA was resuspended in 20 µl of H₂O.

2.5.6 Ligation of Double-Stranded cDNA.

cDNA fragments were ligated to plasmid cDNA by the following procedure. In order to increase the efficiency of ligation, the reaction was

performed with a high GLUT cDNA: plasmid cDNA molar ratio, (10:1). 100 ng of plasmid cDNA which had been CIP-treated was added to GLUT cDNA at a molar ratio of 1:10 and the mix incubated at 60°C for 5 min. After pulsing the samples briefly in a microfuge, an aliquot of 5x concentrated ligation buffer and 3 units of T4 DNA ligase were added, and the samples then incubated overnight at 16°C. Competent bacteria were then transformed with 5- 10 µl of the ligation reaction as described (section 2.5.9).

2.5.7 Preparation of Competent Cells.

Lyophilised *E. coli* XL1-Blue MRF' cells were resuspended in 3 ml of LB medium (Table 2.2) with 10 µg/ml tetracycline and grown overnight at 37°C. These were then streaked onto a LB plate containing 10 µg/ml tetracycline and again incubated overnight at 37°C. This culture was then streaked onto glucose/minimal medium plates (Table 2.2) and left for about 48 hours at 37°C. This procedure selected for bacteria possessing the "F pilus", via which M13 bacteriophage enter the cell upon infection. This plate was used as a master plate for making both competent cells and "lawn cells" for transformation protocols involving M13 (2.5.8). A single *E. coli* XL1-Blue MRF' colony was picked from a glucose/minimal medium plate using a sterile pipette tip and dropped into 3 ml LB medium containing 10 µg/ml tetracycline. This was grown overnight in a shaking 37°C incubator. Two 40 ml cultures of LB medium (10 µg/ml tetracycline) in sterile flasks were inoculated with 400 µl of overnight culture and grown at 37°C for approximately 2 hours until the A_{600} reached a value of 0.3. One flask was stored at 4°C as lawn cells. The contents of the other were transferred to a chilled 50 ml centrifuge tube and centrifuged at 4°C for 5 min at 2500x g_{av} in a prechilled rotor. The supernatant was gently poured off and the pellet

resuspended in 20 ml of cold sterile 100 mM CaCl₂ and incubated on ice for 40 min. The cells were centrifuged again and resuspended in 4 ml of 100 mM CaCl₂. Cells were left at 4°C for at least one hour before the addition of cDNA, however the cells reached maximum transforming efficiency after several hours, only decreasing after 24 hours.

When preparing competent cells for use with plasmid cDNA (section 2.5.9), the procedure was identical except that it was not necessary to include the growth on a glucose/minimal medium plate since the F pilus was not required for simple transformation. Plasmid transformations do not require "lawn cells".

2.5.8 Transformation of Competent *E. coli*. with M13mp18GT3.

M13mp8 rfdNA (100 ng/μl) was included in the Amersham Sculptor™ site-directed mutagenesis kit. This was used as a positive control for transformation. 1 ng of rfdNA (double stranded replicating form) produced 200-300 plaques if the cells were competent. Each control and transformation reaction was carried out in duplicate.

For each transformation reaction a 15 ml polypropylene Falcon tube was placed on ice and 300 μl of competent *E. coli* XL1-Blue MRF' cells added (section 2.5.7). 100 μl of M13 rfdNA was added to the competent cells. This was mixed by stirring while adding the rfdNA and then left on ice for 40 min. The cells were heat shocked in a 42°C waterbath for 45 sec, returned to ice for 5 min, then allowed to reach room temperature. 200 μl of noncompetent *E. coli* XL1-Blue MRF' lawn cells and 3 ml of molten LB top agar (Table 2. 2) at 45°C were subsequently added to each tube. The contents of the tube were mixed vigorously and immediately poured onto a LB plate with 10 μg/ml tetracycline, gently rolling the plate to ensure that the top agar covered its

entire surface. This was left to set for 10 min and then the plates were inverted and incubated overnight at 37°C. Plaques were isolated, and single-stranded or double-stranded cDNA was isolated as described (sections 2.5.11 and 2.5.13).

2.5.9 Transformation of Competent *E. coli* with Plasmid cDNA.

This process was similar to that of section 2.5.8. 100 ng of purified pSPGT3 plasmid cDNA was used as a positive control for transformation. Sterile H₂O was used as a negative control.

For each transformation reaction a 15 ml polypropylene Falcon tube was placed on ice and 200 µl of competent *E. coli* XL1-Blue MRF' cells added. 10 µl of cDNA was added to the competent cells. This was mixed by gently rolling the tube while adding the cDNA, then left on ice for 40 min. The cells were heat shocked in a 42°C waterbath for 45 sec, returned to ice for 5 min, and finally allowed to reach room temperature. 0.8 ml or 0.98 ml of LB medium was added to 200 µl and 20 µl samples, respectively, of each transformation reaction and incubated in a shaking 37°C incubator for 1 hour to "pre-grow" the cells. Ampicillin was used consistently for selection of cells transformed with pHTL217 and pSPGT3 plasmid cDNA. This pre-growth step allows the cells to establish plasmid encoded ampicillin resistance, after which the cells were harvested by centrifugation in a Beckman CPR benchtop centrifuge for 5 min at 4000 rpm at 4°C. The supernatant was removed, except for the last 100 µl, in which the cells were resuspended by gentle pipetting. The cells were spread onto LB agar plates with 10 µg/ml tetracycline and 50 µg/ml ampicillin and grown overnight at 37°C. Colonies were selected and used to prepare double-stranded cDNA (section 2.5.10).

2.5.10 Preparation of Small Amounts of Plasmid cDNA.

Colonies of interest were picked with sterile tips and dropped into universals, each containing 3 ml of 2xYT medium containing 10 µg/ml tetracycline and 50µg/ml ampicillin. These were grown overnight at 37°C in a shaking incubator. 1.5 ml of culture was removed, placed in a microfuge tube and centrifuged for 15 min in a microfuge to pellet the cells. The supernatant was discarded and the pellet resuspended in 100 µl of glucose buffer (50 mM glucose, 25 mM Tris, pH 7-8 and 12.5 mM EDTA) with extensive vortexing. This was incubated on ice for 5 min, then 200 µl of 1% SDS in 0.2 M NaOH was added and the tube gently inverted 5 times. The tube was incubated on ice for 10- 20 min, or until viscous. 300 µl of 3 M K⁺/5 M Ac was added, the tube inverted gently 5 times, and incubated on ice for another 5 min before centrifuging in a microfuge for 5 min. The supernatant was removed to a fresh tube, 5 µl of 1 mg/ml RNase A was added and incubated at 37°C for 15 min. One phenol extraction, two phenol/chloroform (1:1 v/v) extractions, and two chloroform/ isoamylalcohol (24:1 v/v) washes of the supernatants were performed, retaining each time the upper aqueous phase. After the final wash, 0.3 volumes of 3 M sodium acetate and 2.5 volumes of 100% ethanol were added to precipitate the cDNA. This was incubated at -20°C for at least an hour before pelleting the cDNA by centrifugation for 30 min in a microfuge. The ethanol was removed, the pellet washed with 70% ethanol and centrifuged for a further 30 min, before drying under vacuum. The pellet was resuspended in 20 µl of sterile water. 1 µl of this was added to 1 ml of sterile water and the absorbance measured at 260 nm. The concentration was determined from the calculation below.

Calculation to Determine the Plasmid cDNA Concentration and Purity.

absorbance value of 1.0 at 260 nm = 50 µg/ml of dsDNA.

absorbance value of "y" at 260 nm = "y" x 50 µg/ml of dsDNA.

absorbance at 260 nm = " Z "

absorbance at 280 nm

cDNA has a lower protein concentration and has a higher purity when the value of " Z " is nearer to 2.0.

2.5.11 Preparation of Small Amounts of Bacteriophage M13 "Replicative Form" cDNA.

An appropriate plaque was picked from a recent plate (no more than 1 week old). The tip was dropped into a sterile universal with 1 ml of LB medium containing 10 µg/ml tetracycline, and left for 1 hour to allow the agar plug to diffuse into the medium. 700 µl of the medium was removed and stored as a primary stock of bacteriophage particles. A further 2 ml of LB-broth containing 10 µg/ml tetracycline and 100 µl of an overnight culture of XL1-Blue MRF' *E. coli* were added. The cells were incubated at 37°C for 5 hours with shaking. 1.5 ml was then removed, placed into a microfuge tube and centrifuged for 15 min to pellet the cells. The double-stranded rfDNA is inside the cells (i.e. in the pellet), so the supernatant was discarded. The remainder of the protocol is identical to that used for preparation of plasmid cDNA from *E. coli* (section 2.5.10).

2.5.12 QIAGEN Plasmid Midi/Maxi Preparation Kits.

These kits use various buffer reagents and columns to bind and purify cDNA from 100 ml or 300 ml cultures of plasmid-containing bacteria.

Components:-

(supplied with kits)

<u>Buffer P1</u> (Resuspension buffer)	100µg/ml RNase A, 50 mM Tris/HCl, 10 mM EDTA, pH 8.0 stored at 4°C.
<u>Buffer P2</u> (Lysis buffer)	200 mM NaOH, 1% SDS.
<u>Buffer P3</u> (Neutralisation buffer)	3 M KAc, pH 5.5, stored at 4 °C.
<u>Buffer QBT</u> (Equilibration buffer)	750 mM NaCl, 50 mM MOPS, 15% ethanol, pH 7.0, 0.15% Triton-X- 100.
<u>Buffer QC</u> (Wash buffer)	1.0 M NaCl, 50 mM MOPS, 15% ethanol, pH 7.0.
<u>Buffer QF</u> (Elution buffer)	1.25 M NaCl, 50 mM Tris/HCl, 15% ethanol, pH 8.5.
<u>TE buffer</u>	10 mM Tris/HCl, 1 mM EDTA, pH 8.0.

STE buffer

100 mM NaCl, 10 mM Tris/HCl,
1 mM EDTA, pH 8.0.

QIAGEN-tip 100 columns

These contain a patented anion-exchange resin, which is a modification of macroporous silicagel

2.5.12.a M13mp18GT3 Midi Preparation Procedure:-

An overnight culture of XL1-Blue MRF' *E. coli* was grown in LB medium containing 10 µg/ml tetracycline. 1 ml of this culture was mixed with 200 µl of the appropriate stock of M13 bacteriophage particles (pfu =10¹² particles/ml), and incubated at room temperature for 5 min. This mixture was then added to 100 ml of LB medium containing 10 µg/ml tetracycline, prewarmed to 37°C, and incubated for 6 hours at 37°C with shaking. The cells were harvested by splitting the culture into two 50 ml centrifuge tubes and centrifuging at 4000x g_{av} for 5 min at 4°C. The supernatant, which contains the bacteriophage particles, was removed and stored at 4°C. The pellets were resuspended and combined in 15 ml of STE buffer to remove residual phage and spun down at 4000x g_{av} for 5 min at 4°C. The supernatant was discarded and the pellet resuspended in 4 ml of buffer P1. 4 ml of buffer P2 was added, mixed gently, and incubated at room temperature for 5 min. Then 4 ml of buffer P3 was added, mixed quickly but gently, and incubated on ice for 15 min. The contents of the tube were placed into 50 ml Beckman centrifuge tubes and centrifuged in a JA-20 rotor at 30,000x g_{av} for 30 min at 4°C. The

supernatant was quickly removed and passed through 2 layers of muslin to remove any particles. If necessary, the centrifugation step and filtering were repeated. A QIAGEN-tip 100 was equilibrated with 4 ml of buffer QBT and the supernatant passed through the column. The tip was washed twice with 10 ml of buffer QC. The cDNA was eluted with 5 ml of buffer QF, then precipitated with 0.7 volumes of isopropanol. This was centrifuged at $15,000\times g_{av}$ for 30 min at 4°C . The supernatant was removed taking care not to disturb the pellet. 5 ml of cold 70% ethanol was added to the pellet and centrifuged as before. Lastly, the ethanol was removed and the pellet air-dried for 5 min, before dissolving in 100 μl of sterile H_2O . 4 μl of this was added to 1 μl of DNA gel-loading buffer and electrophoresed in a 1% agarose gel to check the recovery of cDNA (section 2.5.3).

2.5.12. b Plasmid Maxi Preparation Procedure.

An overnight culture of XL1-Blue MRF' *E. coli* containing the plasmid of interest was grown in 3 ml LB medium containing 10 $\mu\text{g}/\text{ml}$ tetracycline and 50 $\mu\text{g}/\text{ml}$ ampicillin. 1 ml of this culture was added to 300 ml of LB medium containing 10 $\mu\text{g}/\text{ml}$ tetracycline and 50 $\mu\text{g}/\text{ml}$ ampicillin, prewarmed to 37°C , and incubated overnight at 37°C with shaking. The cells were harvested by splitting the culture into two 250 ml centrifuge tubes and centrifuging at $4000\times g_{av}$ for 5 min at 4°C . The supernatant was discarded and the pellet resuspended in 10 ml of buffer P1. 10 ml of buffer P2 was added, mixed gently, and incubated at room temperature for 5 min. Then 10 ml of buffer P3 was added, mixed quickly but gently, and incubated on ice for 20 min. The contents of the tube were placed into 50 ml Beckman centrifuge tubes and centrifuged in a JA-20 rotor at $30,000\times g_{av}$ for 30 min at 4°C . The supernatant was quickly removed and passed through 2 layers of muslin to

remove any particles. If necessary, the centrifugation step and filtering were repeated. A QIAGEN-tip 300 was equilibrated with 10 ml of buffer QBT and the supernatant passed through the column. The tip was washed twice with 30 ml of buffer QC. The cDNA was eluted and collected with 10 ml of buffer QF, then precipitated with 0.7 volumes of isopropanol. This was centrifuged at $15,000\times g_{av}$ for 30 min at 4°C . The supernatant was removed taking care not to disturb the pellet. 5 ml of cold 70% ethanol was added to the pellet and centrifuged as before. Lastly, the ethanol was removed and the pellet air-dried for 5 min, before dissolving in 300 μl of sterile H_2O . 4 μl of this was added to 1 μl of DNA gel-loading buffer and electrophoresed in a 1% agarose gel to check the recovery of cDNA (section 2.5.3).

2.5.13 Preparation of Small Amounts of Single Stranded cDNA from M13.

A plaque of interest was selected and stabbed with a sterile pipette tip. This was dropped into 1 ml of LB medium, containing 10 $\mu\text{g}/\text{ml}$ tetracycline, in a 30 ml sterile "Universal" container. This was vortexed extensively and left at room temperature for 1 hour. 0.7 ml of this was removed and stored at 4°C as a primary phage stock. A further 2 ml of LB medium and also 100 ml of an overnight culture of MRF' *E. coli* were added to the Universal, which was then placed in a 37°C shaking incubator for 5 hours at 200 rpm. This resulted in both *E. coli* containing double-stranded rfdNA and bacteriophage particles comprising single-stranded cDNA with a protein coat. 1.5 ml of culture was removed and centrifuged for 15 min in a microfuge. The supernatant was recovered, leaving the last 100 μl and the bacterial pellet. The supernatant was centrifuged once more to remove all residual bacteria, and again the final 100 μl was left behind. 200 μl of 20% Polyethylene glycol (PEG) 6000/ 2.5 M NaCl was added to the supernatant to precipitate the phage

particles. This was mixed by inversion and left at room temperature for 20 min. The phage were harvested by 15 min centrifugation in a microfuge, discarding the supernatant. The pellet was resuspended in 100 μ l of TE buffer (Table 2.1). 5 μ l of this solution was stored as a bacteriophage stock. Ribonuclease A (1 mg/ml) was added to the remaining solution and incubated for 15 min at 37°C to remove cellular RNA. Then, 100 μ l of Tris-washed phenol was added to the tube which was vortexed for 1 min, centrifuged for 1 min in a microfuge, and the upper aqueous layer removed with a pipette. This fraction contained the ssDNA. 100 μ l of 1:1 (v/v) phenol/chloroform was added; the tube vortexed and centrifuged; and the aqueous phase saved. Lastly, 100 μ l of 24:1 (v/v) chloroform /isoamyl-alcohol was added to remove traces of phenol from the aqueous phase. This was repeated twice, each time involving extensive vortexing and centrifugation. 0.3 volumes of 3 M sodium acetate and 2.5 volumes of absolute ethanol were added to the remaining ssDNA solution. The tube was vortexed and incubated at -20°C for 1 hour. The precipitated cDNA was centrifuged for 30 min in a microfuge, the ethanol removed and 0.5 ml of 70% ethanol added to wash the pellet. The cDNA was pelleted by centrifugation for 15 min in a microfuge; the ethanol supernatant was discarded. The pellet was resuspended in 10 μ l of water by vortexing. 1 μ l in 3 μ l of gel loading buffer was run on a 1% agarose gel (section 2.5.3). Bands were visualised as described in section 2.5.3. A further 1 μ l of ssDNA was taken and diluted in 1 ml of water and its absorbance at 260 nm read by spectrophotometry to determine the concentration. However, the calculation was adjusted such that a reading at 260 nm of 1.0 = 40 μ g/ml of cDNA.

2.6 Site-Directed Mutagenesis.

The method used for site-directed mutagenesis involved use of the Amersham "Sculptor™ *in vitro* mutagenesis system- RPN 1526" kit.

2.6.1 Components.

The kit contained:-

native T7 DNA polymerase; T4 DNA ligase; T5 exonuclease; *Nci* I restriction enzyme; exonuclease III; DNA polymerase I; Buffer A (1.4 M MOPS, pH 8 and 1.4 M NaCl); Buffer B (70 mM Tris, pH 8, 10 mM MgCl₂, 45 mM NaCl); Buffer C (700 mM Tris, pH 8, 350 mM EDTA, 20 mM DTT); Buffer D (250 mM Tris, pH 8, 150 mM NaCl and 500 mM EDTA); dNTP mix A (1.01 mM dATP, dCTP γ -S, dGTP, dTTP, 2.02 mM ATP and 20 mM MgCl₂); dNTP mix B (1.25 mM dATP, dCTP, dGTP, dTTP, 2.5 mM ATP and 25 mM MgCl₂); sterile water; lyophilised *E. coli* TG1 host cells; M13mp8 control rfDNA; control template cDNA (single-stranded); and control mutagenic oligonucleotide (phosphorylated).

Besides the components of the kit, the following were required:-

ssDNA template (2 μ g); mutant oligonucleotide (1.6 pmole/ μ l); LB medium with tetracycline; glucose/minimal medium agar plates; H top agar; LB agar plates with tetracycline; 20% polyethylene glycol (6000)/2.5 M NaCl solution; TE buffer; 3 M sodium acetate solution; polynucleotide kinase and polynucleotide kinase 10x buffer; 100 mM rATP; [γ -³²P]ATP (5000 Ci/mmole; 10 mCi/ml); DE-81 filter paper; 50 mM CaCl₂ solution; 10x TAE electrophoresis buffer; ethidium bromide solution; and 5x DNA gel loading dye solution.

2.6.2 Phosphorylation of Oligonucleotides.

Oligonucleotides (18-24'mers) with sequence identical to the antisense strand of GLUT3 in the region of putative transmembrane helix 8 were synthesised (Dr. V. Math, Department of Biochemistry, University of Glasgow). However these oligonucleotides had 1-3 bases altered, compared with wild-type GLUT3, so that one amino acid was altered to alanine (Table 5.1). Oligonucleotides were supplied in an ammonium hydroxide solution. 360 μ l of each oligonucleotide solution was added to 1.2 ml of ethanol and 40 μ l of 3 M sodium acetate in a microfuge tube, mixed and incubated at -20°C for at least 1 hour. This was then centrifuged for 30 min in a microfuge, washed with 70% ethanol, centrifuged again, dried and resuspended in 360 μ l of sterile H_2O . Absorbance values at a wavelength of 260 nm (A_{260}) were measured for 25 μ l of purified oligonucleotide in 1 ml sterile H_2O . The oligonucleotide was then diluted to 1.6 pmole/ μ l, the concentration required for mutagenesis. 30 μ l of the oligonucleotide solution, 3.6 μ l of 10x kinase buffer, 2 μ l of 100 mM ATP and 2 units of polynucleotide kinase were added to a microfuge tube. This was mixed and incubated for 15 min at 37°C to phosphorylate the 5'-hydroxyl group of the first base in the oligonucleotide sequence, and then incubated at 70°C for 10 min to inactivate the kinase. Phosphorylated oligonucleotides were stored at -20°C . To confirm phosphorylation, 2 μ l of [γ - ^{32}P] dATP (10 $\mu\text{Ci}/\mu\text{l}$, 5000 Ci/mmole) was used instead of ATP in an otherwise identical reaction. The procedure was also identical, except 2 μ l of the reaction product was loaded onto the origin (about 1 cm from the bottom narrow end) of a 2 cm x 10 cm strip of DE-81 filter paper. The spot was dried using a hair-dryer and the strip suspended over a beaker so that the bottom was immersed in 3 M ammonium formate, pH 8.0. The solvent was run until almost at the top and the location of the solvent front

marked before air-drying the strip. The paper was then cut into 1 cm sections and placed into 20 ml scintillation vials. The radioactive decay (dpm) produced was measured with a program designed to measure ^{32}P emissions on a scintillation counter. If a high percentage of the counts remained at the origin, this showed that most of the label had been incorporated into the oligonucleotide since, unlike free nucleotides, this was not mobile in the solvent.

2.6.3 Sculptor Protocol.

See Figure 5.2. 2 μl of single-stranded template cDNA (1 mg/ml M13mp18GT3), 1 μl of phosphorylated oligonucleotide (1.6 pmoles/ μl), 1 μl of buffer A and 5 μl of sterile H_2O were added to a microfuge tube and mixed. The reaction mix was incubated for 3 min at 70°C , and then placed in a beaker of water at 55°C and cooled slowly to room temperature, allowing the oligonucleotide to anneal to the single-stranded template cDNA. 10 μl of dNTP mix A, 2.5 units of T4 DNA ligase, and 0.8 units of T7 DNA polymerase were added to the annealing reaction. This was incubated for 10 min at room temperature, 30 min at 37°C to allow the extension and ligation of the mutant strand (containing dCTP γ -S), and finally 15 min at 70°C to inactivate the enzymes. A 1 μl sample was removed for analysis by gel electrophoresis. 50 μl of buffer B and 2000 units of T5 exonuclease were added to the extension reaction. This was incubated for 30 min at 37°C to remove the single-stranded, non-mutant DNA and for 15 min at 70°C to inactivate the exonuclease. A 5 μl sample was removed for analysis. 5 μl of buffer C and 5 units of *Nci* I were added to the digestion. This was mixed and incubated at 37°C for 90 min to allow the nicking of the non-mutant strand. A 10 μl sample was taken for analysis. 20 μl of buffer D and 160 units of exonuclease

III were added to the nicking reaction, the tube mixed and incubated at 37°C for 30 min to digest the non-mutant strand, then heat inactivated at 70°C for 15 min. 10 µl was removed for analysis. 20 µl of dNTP mix B, 3.5 units of DNA polymerase I and 2.5 units of T4 DNA ligase were added to the tube and mixed. This was incubated for 60 min at 37°C to repolymerise the cDNA. A 15 µl sample was taken for analysis. 3 µl of 5x DNA gel-loading buffer was added to each of the five samples and mixed. These were electrophoresed on a 1% agarose gel in 1x TAE buffer (Table 2.1), and then stained with 5 µl of 10 mg/ml ethidium bromide per 100 ml buffer. The bands were analysed to check that each step of the mutagenesis reaction had proceeded as expected (Figure 2.4). 10 µl of the final reaction was diluted to 100 µl with sterile H₂O and used to transform 300 µl of competent *E. coli* XL1-Blue MRF' cells as described in section 2.5.8. M13mp8 rfDNA (100 ng/µl) was included in the Amersham Sculptor™ site-directed mutagenesis kit. This was used as a positive control for transformation. 1 ng of rfDNA produced 200-300 plaques if the cells were competent. Each control and transformation reaction was carried out in duplicate.

Plaques were isolated, and small amounts of single-stranded cDNA were isolated and sequenced as described (section 2.5.13 and section 2.8).

2.7 Recombinant Polymerase Chain Reaction.

2.7.1 Primary Polymerase Chain Reactions using *Taq* DNA Polymerase.

2.7.1.a Synthesis of Oligonucleotides.

Oligonucleotides (18-24'mers) with sequence identical to GLUT3 in the region of putative transmembrane helix 8 were synthesised (Dr. V. Math,

Department of Biochemistry, University of Glasgow). However these oligonucleotides had 1-3 bases altered, compared with wild-type GLUT3, so that one codon was altered to alanine (Table 5.1). Pairs of oligonucleotides were constructed: one sequence representing the sense strand and another the complementary sequence, both incorporating the same codon change. These will be referred to subsequently as internal primers. Additionally, one oligonucleotide (a 37' mer) was constructed which had positive polarity and a sequence complementary to the antisense strand of the untranslated region at the 5' end of GLUT3. Likewise, an antisense oligonucleotide (a 37' mer) was synthesised which bound to the positive strand of cDNA at the untranslated region at the 3' end of GLUT3 (Figure 5.3). Both these oligonucleotides incorporated a *Sal* I restriction site at their 5' ends (Table 5.1) and are subsequently referred to as external primers.

2.7.1.b Reaction Conditions.

1.6 µg	"internal" primer.
1.6 µg	"external" primer.
10 ng	template pSPGT3 dsDNA
1 µl	nucleotide mix (20 mM dATP, 20 mM dGTP, 20 mM dTTP, 20 mM dCTP)
10 µl	10x <i>Taq</i> polymerase reaction buffer (Mg-free)
6 µl	25 mM MgCl ₂
2.5 units	<i>Taq</i> polymerase
sterile water to give a final volume of 100 µl	

Reactions were carried out in 0.5 ml microfuge tubes, adding the *Taq* polymerase last. Upon completion of the thermal cycling (see below), 20 µl of

5x DNA gel loading buffer was added to each reaction and mixed, before loading the entire reaction mixture onto a 1.5% agarose gel. Following electrophoresis, cDNA bands were excised, electro-eluted (section 2.7.4), purified (section 2.7.6) and ethanol precipitated (section 2.5.1), combining the contents of 3-6 reactions, and finally resuspending each pellet into 40 μ l of sterile water. 5 μ l of this was then electrophoresed on another 1.5% agarose gel to determine the recovery of purified primary product.

2.7.1.c Thermal Cycling.

The tubes were placed in a Techne PHC-3 Thermal Cycler with a heated lid. The following procedure was programmed into the machine:-

Initial Extension	95°C	3 min
<u>Cycling-</u> (30 cycles total, with a 1°C/sec ramp rate.)		
Separation	95°C	1 min
Reannealing	X°C	1 min
Extension	72°C	2 min
Final Extension	72°C	5 min
Soak	4°C	Hold

"X" = 0-5°C below the melting temperature of the oligonucleotide having the lower melting temperature.

2.7.2 Secondary Polymerase Chain Reactions.

2.7.2.a Reaction Conditions.

0.8 µg	"external-sense" primer
0.8 µg	"external-antisense" primer
1-2 µl	template (5' primary product)
1-2 µl	template (3' primary product)
1 µl	nucleotide mix (20 mM dATP, 20 mM dGTP, 20 mM dTTP, 20 mM dCTP)
10 µl	10x <i>Taq</i> polymerase reaction buffer (Mg-free)
6 µl	25 mM MgCl ₂
2.5 units	<i>Taq</i> polymerase
sterile water to give a final volume of 100 µl	

Secondary reactions were carried out in a similar way to primary reactions except that there were two primary product templates instead of one. The 3' end of the 5' primary product (encoding the N-terminal portion of GLUT3) and the 5' end of the 3' primary product (encoding the C-terminal portion of GLUT3) were single-stranded, complementary and overlapped (Figure 5.3). The first few cycles of the chain reaction involved the association of the two primary products as well as the polymerisation between the two external primers, so the reaction protocol was modified (see below), having three cycles with lower annealing temperatures. The reactions were treated exactly in the same way as the primary reactions, except that the final pellet was resuspended in 10 µl of sterile water.

2.7.2.b Thermal Cycling.

The tubes were placed in a Techne PHC-3 Thermal Cycler with a heated lid. The following procedure was programmed into the machine:-

Initial Extension	95°C	3 min
<u>Cycling-</u> (3 cycles total, with a 1°C/sec ramp rate.)		
Separation	95°C	1 min
Reannealing	37°C	1 min
Extension	72°C	2 min
<u>Cycling-</u> (27 cycles total, with a 1°C/sec ramp rate.)		
Separation	95°C	1 min
Reannealing	X°C	1 min
Extension	72°C	2 min
Final Extension	72°C	5 min
Soak	4°C	Hold

"X" = 0-5°C below the melting temperature of the oligonucleotide having the lower melting temperature.

2.7.3 Polymerase Chain Reactions using *Pfu* DNA Polymerase.

2.7.3.a Conditions for Primary Reactions.

0.8 µg	"internal" primer.
0.8 µg	"external" primer.
100 ng	template pSPGT3 dsDNA

1 μ l nucleotide mix (20 mM dATP, 20 mM dGTP, 20 mM dTTP,
 20 mM dCTP)
 10 μ l 10x *Pfu* DNA polymerase reaction buffer
 2.5 units *Pfu* DNA polymerase
 sterile water to give a final volume of 100 μ l

Oligonucleotides used were identical to those used with reactions involving *Taq* DNA polymerase. Reactions were carried out in 0.5 ml microfuge tubes, adding the *Pfu* polymerase to the reactions after the initial 10 min annealing step. This is referred to as "Hot Start PCR". Upon completion of the thermal cycling (section 2.7.3.b), 20 μ l of 5x DNA gel loading buffer was added to each reaction and mixed, before loading the entire reaction mixture onto a 1.5% agarose gel. Following electrophoresis, DNA bands were excised, electro-eluted (section 2.7.4), purified (section 2.7.6) and ethanol precipitated (section 2.5.1), combining the contents of 3-6 reactions and finally resuspending each pellet into 40 μ l of sterile water. 5 μ l of this was then electrophoresed on another 1.5% agarose gel to determine the recovery of purified primary product.

2.7.3.b Conditions for Secondary Reactions.

0.8 μ g "external- sense" primer
 0.8 μ g "external- antisense" primer
 1-2 μ l template (5' primary product)
 1-2 μ l template (3' primary product)
 1 μ l nucleotide mix (20 mM dATP, 20 mM dGTP, 20 mM dTTP,
 20 mM dCTP)
 10 μ l 10x *Pfu* DNA polymerase reaction buffer

2.5 units *Pfu* DNA polymerase
sterile water to give a final volume of 100 µl

Secondary reactions were carried out in a similar way to primary reactions except that there were two primary product templates instead of one. The 3' end of the 5' primary product (encoding the N-terminal portion of GLUT3) and the 5' end of the 3' primary product (encoding the C-terminal portion of GLUT3) were single-stranded, complementary and overlapped (Figure 5.3). The first few cycles of the chain reaction involved the association of the two primary products as well as the polymerisation between the two external primers, but uses the same reaction protocol as that used for the generation of primary products with *Pfu* polymerase. The reactions were treated exactly in the same way as the primary reactions, except that the final pellet was resuspended in 10 µl of sterile water.

2.7.3.c Thermal Cycling.

The tubes were placed in a Techne PHC-3 Thermal Cycler with a heated lid. The following procedure was programmed into the machine:-

Initial Extension 95°C 10 min

Addition of *Pfu* DNA polymerase.

Cycling- (3 cycles total, with a 1°C/sec ramp rate.)

Separation 95°C 1 min

Reannealing 37°C 5 min

Extension 72°C 5 min

Cycling- (27 cycles total, with a 1°C/sec ramp rate.)

Separation 95°C 1 min

Reannealing	56°C	2 min
Extension	72°C	5 min
Final Extension	72°C	10 min
Soak	4°C	Hold

2.7.4 Elution of DNA from Gel Fragments by Electrophoresis.

The gel fragment containing the DNA band of interest was put into dialysis tubing (section 2.7.5) which had been clipped shut at one end. Then 1 ml of TAE buffer was added to the tubing and the other end secured, ensuring that no air bubbles remained within. This tubing was then placed into an electrophoresis tank containing 1 litre of TAE buffer. The tubing was laid at an angle perpendicular to the direction of current and the voltage increased to 150 V for 2 hours. Next, the voltage polarity was reversed so that the current flowed in the opposite direction for 30 sec to ensure that the cDNA was removed from the membrane and was present in solution. The solution was removed from the tubing with a sterile pasteur pipette and placed into a 5 ml "bijou" tube. Then a further 1 ml of TAE buffer was added to the tubing and pumped up and down vigorously to remove any residual cDNA, before adding this to the same bijou tube.

2.7.5 Preparation of Dialysis Tubing.

Dialysis tubing (Visking size 1-8/32") was cut into lengths of approximately 6 cm. 10 g of this was placed in a beaker with 500 ml of 2% sodium hydrogen carbonate, 10 mM EDTA and boiled for 10 min. The solution was then poured away and the tubing washed twice in distilled water. The tubing was

stored at 4°C in 50% ethanol, 50% water, 1 mM EDTA. When required, the tubing was washed by boiling in distilled water.

2.7.6 Purification of DNA using Elutip-D Affinity Columns.

Components:-

High salt solution (see below)

Low salt solution (see below)

Sterile 10 ml syringes

Sterile 1 ml syringes

Sterile Acrodisc® 0.2 µm filters

Elutip-D columns

Low salt solution

0.2 M NaCl

20 mM Tris, pH 7.4

1 mM EDTA

High salt solution

1 M NaCl

20 mM Tris, pH 7.4

1 mM EDTA

A 10 ml syringe was loaded with 2 ml of high salt solution, the Elutip-D column attached to the syringe and the solution passed through the column to remove any DNA which might be present. A second syringe was loaded with 5 ml low salt solution and this was passed down the column to remove all traces of high salt solution. The cDNA sample in TAE buffer (section 2.7.4) was taken up into the same syringe. A 0.2 µm filter was attached between this syringe and the column and the cDNA passed through the column at a flow

rate no faster than 1 ml/min. The column was then washed with 3 ml of low salt solution, again using the same syringe and filter. Finally the cDNA was eluted from the column in 0.4 ml of high salt solution into a sterile microfuge tube. 1.2 ml of ethanol was added to the tube, mixed and incubated at -20°C for 1 hour. The precipitated cDNA was collected by centrifugation in a microfuge tube for 30 min, washed with 70% ethanol, centrifuged again for another 30 min, the pellet dried and resuspended in a suitable volume of sterile water, generally 20 µl.

2.8 *Taq* DyeDeoxy™ Terminator Cycle Sequencing Protocol.

This protocol was used with the Applied Biosystems *Taq* DyeDeoxy™ Terminator Cycle Sequencing Kit, in conjunction with the Applied Biosystems Model 373A Automated Sequencer.

2.8.1.a Kit Reagents.

100 µl	G DyeDeoxy™ Terminator
100 µl	A DyeDeoxy™ Terminator
100 µl	T DyeDeoxy™ Terminator
100 µl	C DyeDeoxy™ Terminator
100 µl	dNTP mix- (750 µM dGTP, 150 µM dATP, 150 µM dTTP, 150 µM dCTP)
400 units	AmpliTaq® DNA Polymerase, 8 units/µl
400 µl	5x Terminator Ammonium Cycle Sequencing (TACS) Buffer- (400 mM Tris-HCl, 10 mM MgCl ₂ , 100 mM (NH ₄) ₂ SO ₄ pH 9.0)

6 μg pGEM[®]-3Zf(+) double-stranded DNA Control Template, 0.2
 $\mu\text{g}/\mu\text{l}$
50 μl -21M13 Forward Primer, 0.8 pmoles/ μl

2. 8. 1. b Other Reagents.

Distilled water

De-ionised formamide

Phenol/H₂O/Chloroform (68:18:14, v/v/v)

Alconox[™] detergent

Ethanol

A/ Gel Reagents- Sequagel-6[™] 6% Sequencing Gel Solution

Sequagel[™] Complete Buffer Reagent

10% Ammonium persulphate solution

B/ Gel Reagents- 40% Acrylamide stock solution (19:1 Acrylamide: Bis
acrylamide)

10xTBE Buffer (8.2 g EDTA, 107.8 g Tris, 55.0 g Boric acid
per litre)

10% Ammonium persulphate

50 mM EDTA

TEMED

Urea

dH₂O

Mixed Bed Resin

2.8.2 Preparation of Templates.

M13mp18GT3 ssDNA was prepared from plaques using the method described previously (section 2.5.13). The quantities of template and sequencing oligonucleotide primer used per reaction were 1 μg ssDNA template and 1.6 pmoles of primer. The primer used was invariably primer "G3 2B+" (Table 5.2).

pSPGT3 dsDNA was prepared from colonies as described previously (section 2.5.10). The quantities of template and sequencing oligonucleotide primer used per reaction were 2 μg dsDNA template and 3.2 pmoles of primer. The primers used are listed in Table 5.2.

In either case the combined volume of template and primer did not exceed 10.5 μl since 9.5 μl of reaction premix was added to bring the final volume to 20 μl . The total volume was adjusted to 20 μl by the addition of sterile water. A reaction premix sufficient for 20 reactions consisted of:-

Reagents

5x TACS Buffer	80 μl
dNTP mix	20 μl
DyeDeoxy™ A Terminator	20 μl
DyeDeoxy™ T Terminator	20 μl
DyeDeoxy™ G Terminator	20 μl
DyeDeoxy™ C Terminator	20 μl
AmpliTaq® DNA Polymerase	10 μl

The reagents were mixed in a 0.5 ml microfuge tube-

Reaction Premix	9.5 μl
* Template DNA	5.0 μl

** Primer	4.0 μ l
dH ₂ O	<u>1.5 μl</u>
Final volume	20 μ l

- * ssDNA solution concentration = 0.2 mg/ml
dsDNA solution concentration = 0.4 mg/ml
- ** Primer concentration with ssDNA template = 0.4 pmoles/ μ l
Primer concentration with dsDNA template = 0.8 pmoles/ μ l

2.8.3 Thermal Cycling.

The tubes were placed in a Techne PHC-3 Thermal Cycler with a heated lid. The following procedure was programmed into the machine:-

Initial Extension	96°C	3 min
Cycling		
Separation	96°C	30 sec
Reannealing	50°C	15 sec
Extension	60°C	4 min
(30 cycles total, with a 1°C/sec ramp rate.)		
Soak	4°C	Hold

2.8.4 Acrylamide Gel Preparation.

The gel needed at least 2 hours polymerisation time before pre-running so the gel was prepared whilst the reactions underwent thermal cycling.

2.8.4.a Preparing the Gel Plates.

The plates, spacers and comb were washed with Alconox™ and dH₂O. Only the plates were then wiped with absolute ethanol. The plates were aligned with the spacers between them along the outside of the longer edges. The plates were clamped in that position and Permacel™ tape applied along the short bottom edges of the plates and the lower ends of both longer edges so that the corners were covered and a seal was formed. The plates were balanced on a rest so that open top was raised and the angle between the plane of the plates and that of the desktop surface was 30-45°.

2.8.4.b Casting the Gel.

There were two separate methods used for casting the gel. Method 1 is the simplest method which was routinely used. Method 2 was initially used before the pre-made gel reagents used in Method 1 were made available.

Method 1.

This involved using Gel Reagents A. 80 ml of Sequagel-6™ 6% Sequencing Gel Solution was mixed with 20 ml of Sequagel™ Complete Buffer Reagent and 0.8 ml of 10% ammonium persulphate solution was added while stirring.

Method 2.

This involved using Gel Reagents B. 40 g urea, 12 ml 40% acrylamide stock solution, 23 ml of dH₂O, and 1 g of mixed bed resin were stirred together

in a beaker in a 37°C waterbath until all the ingredients had dissolved. The solution was then filtered through a 0.2 µm cellulose acetate filter unit under vacuum and then degassed for 5 min. 8 ml of filtered 10xTBE buffer was added and the solution volume increased to 80 ml by the addition of dH₂O. 400 µl of 10% ammonium persulphate and 45 µl of TEMED were added and swirled.

Here both methods were the same. The gel was immediately poured between the glass plates up to the top edge of the notched plate, with the aid of a 60 ml syringe. All air bubbles were removed by tapping the plates or with the aid of a Promega "Bubble Hook". The plates were lowered so that they were lying flat on the bench and the gel casting comb carefully inserted. The comb was secured by clamping the top of the gel with two binder clamps. It was left to polymerise completely- this took at least 2 hours.

2.8.5 Setting Up for a Run.

All the clamps and tape were removed from the gel plates and the casting comb carefully taken out. Excess acrylamide was cleaned off the plates which were then washed with Alconox™, distilled water and ethanol making sure that the plates were especially clean in the region where the laser read (about a third of the way from the bottom of the plates). A 24-well-shark's tooth comb was carefully placed on the gel surface so that it indented the gel but did not puncture it. The 373A DNA Sequencer and the Macintosh IICI computer were switched on. The gel was placed onto the lower buffer chamber and the beam-stop rack locked. The "Start Pre-run" button on the 373A keypad was pressed followed by "Plate Check". "Scan" and "Map" on the Macintosh Menu were opened. If the baselines were flat, then there was judged to be no dirt on the plates- if they were not then the plates were

cleaned again. Next, "Abort Run" was pressed and the upper buffer chamber and the alignment brace were secured. 1.5 litres of 1xTBE buffer, pH 8.3 was prepared and about half added to the upper buffer chamber and the remainder poured into the bottom chamber. The wells were rinsed with a syringe fitted with a 18-gauge needle containing 1x TBE buffer. The electrode leads were attached and "Start Pre-run" and then "Pre-run Gel" selected. Pre-running took at least 5 min but longer if required. "Abort Run" was pressed to stop.

2.8.6 Sample Extraction and Precipitation.

After the cycling (section 2.8.3) was complete, 80 µl of sterile water was added to each reaction mixture. 100 µl of phenol/water/chloroform (68:18:14, v/v/v) was added to each tube and vortexed for at least 1 min, and then centrifuged for 2 min in a microfuge. The upper aqueous phase was retained, discarding the lower organic phase. This process was repeated. The extracted aqueous phase was transferred to a fresh microfuge tube and precipitated by the addition of 15 µl of 2 M sodium acetate and 300 µl of absolute ethanol (stored at -20°C). Tubes were vortexed to mix the contents and then placed at -20°C for 30 min to ensure complete precipitation. The tubes were centrifuged in a microfuge for 15 min to pellet the cDNA, the pellets washed in 70% ethanol, and dried by centrifugation under vacuum.

2.8.7 Preparing and Loading the Samples.

4 µl of de-ionised formamide/10 mM EDTA was added to each of the samples and mixed well. This was heated at 90°C for 2 min, and placed onto ice immediately. The wells of the gel (section 2.8.5) were flushed out with 1xTBE and 4 µl of each odd-numbered sample added to its corresponding well

in the gel. The door was closed and "Start Run" pressed. This was left for 10 min. "Interrupt Run" was pressed and all the wells flushed out again. The even-numbered samples were loaded and the sequencer restarted. "Collect" on the Controller panel on the Macintosh display was clicked and the details of the samples filled out on a "New Sample Sheet".

2.8.8 Analysis of Samples.

The samples were electrophoresed at a constant temperature of 40°C for 12 hours, passing through the "read window" area of the gel where laser light was periodically passed along this area of the gel. The resulting fluorescence emitted by the DyeDeoxy™ Terminator dyes over a period of time were measured by the 373A sequencer and incorporated by the ABI Data Collection Program on the Macintosh IIfx computer. After the data was collected, it was analysed by the ABI Data Analysis Program. Sequences were determined by use of this program. When different sequences were generated by the use of various sequencing primers (Table 5.2) with the same template cDNA, these were compared using the GeneJockey II (Biosoft) program.

Table 2.1 Table of Buffers.

Buffer	Constituents
50xTris-acetate (TAE) buffer	242 g Tris base; 57.1 ml glacial acetic acid, 100 ml 0.5 M EDTA, pH 8.0
10xTris-borate (TBE) buffer	108 g Tris base; 55.0 g Boric acid; 40 ml 0.5 M EDTA, pH 8.0
TE buffer (pH 8.0)	10 mM Tris.Cl, pH 8.0, 1 mM EDTA, pH 8.0
STE buffer	0.1 M NaCl; 10 mM Tris.Cl, pH 8.0, 10 mM EDTA, pH 8.0
10xPhosphate Buffered Saline (PBS)	80 g NaCl; 2 g KCl; 14.4 g Na ₂ HPO ₄ ; 2.4 g KH ₂ PO ₄ , pH 7.4
Glucose buffer	50 mM glucose; 25 mM Tris.Cl, pH 8.0, 10 mM EDTA, pH 8.0
SDS buffer	0.2 M NaOH; 1% SDS
3 M Potassium/5 M acetate buffer	60 ml 5 M potassium acetate; 11.5 ml glacial acetic acid; 28.5 ml water
5x DNA gel-loading buffer	0.25% bromophenol blue; 30% glycerol in water
Barths buffer	88 mM NaCl; 1 mM KCl; 2.4 mM NaHCO ₃ ; 0.82 mM MgSO ₄ ; 0.41 mM CaCl ₂ ; 0.33 mM Ca(NO ₃) ₂ ; 5 mM HEPES-NaOH, pH 7.6.

Table 2. 2 Bacterial Media and Agar.

Type	Constituents (per litre)
Luria-Bertani medium (LB)	10 g Tryptone (Bactotryptone); 5 g Yeast extract; 10 g NaCl
2xYT medium	16 g Tryptone; 10 g Yeast extract; 5 g NaCl
H medium	10 g Tryptone; 8 g NaCl
H top agar	10 g Tryptone; 8 g NaCl, 7 g Agar (Bactoagar)
LB plates	10 g Tryptone; 5 g Yeast extract; 10 g NaCl, 15 g Agar
2xYT plates	16 g Tryptone; 10 g Yeast extract; 5 g NaCl, 15 g Agar
H plates	10 g Tryptone; 8 g NaCl, 15 g Agar
1x M9 Salts	6 g Na ₂ HPO ₄ , anhydrous; 3 g KH ₂ PO ₄ ; 1 g NH ₄ Cl; 0.5 g NaCl
Glucose/Minimal media plates	1 litre M9 salts; 15 g Agar (oxoid agar); 1 ml 1 M MgSO ₄ ; 1 ml thiamine HCl; 1 ml 0.1 M CaCl ₂ ; 10 ml 20% glucose

Figure 2.1

This shows a photograph of 2 μ l samples of *in vitro* synthesised mRNA which have been electrophoresed on a 1% denaturing agarose gel and stained with ethidium bromide. Lane 1 shows GLUT1 mRNA, lane 2 is GLUT3 mRNA, lane 3 is RNA markers (360-9,490 bases), and lane 4 is GLUT2 mRNA.

The size of all mRNA bands are approximately 1,700 bases.

Figure 2.1 -

In Vitro synthesised mRNA after electrophoresis on a 1% Agarose gel.

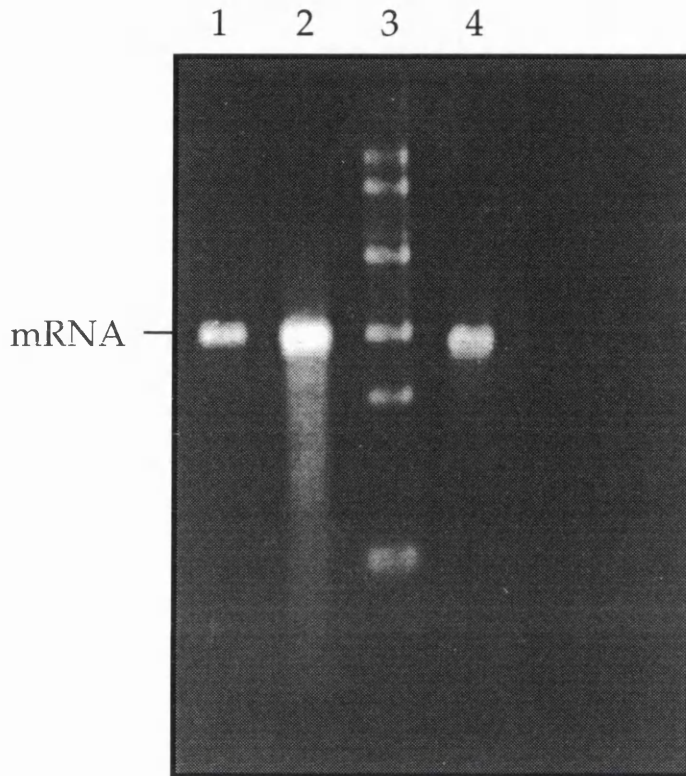


Figure 2.2

Diagrammatic Representation of pSPGT3. GLUT3 cDNA was cloned into pSP64T as a *Bgl* II/*Bam*H I fragment into the untranslated regions of the *Xenopus* β -globin gene, which had previously been cloned into the multiple cloning site of pSP64 (Krieg & Melton, 1984). The 5' untranslated region (UTR) is 89 bp long and the 3' untranslated region is 141 bp long. These function to stabilise the *in vitro* synthesised mRNA in *Xenopus* oocytes. The GLUT3 cDNA and its flanking sequences are located 3' of the SP6 polymerase promoter.

Figure 2.2

Diagrammatic Representation of pSPGT3.

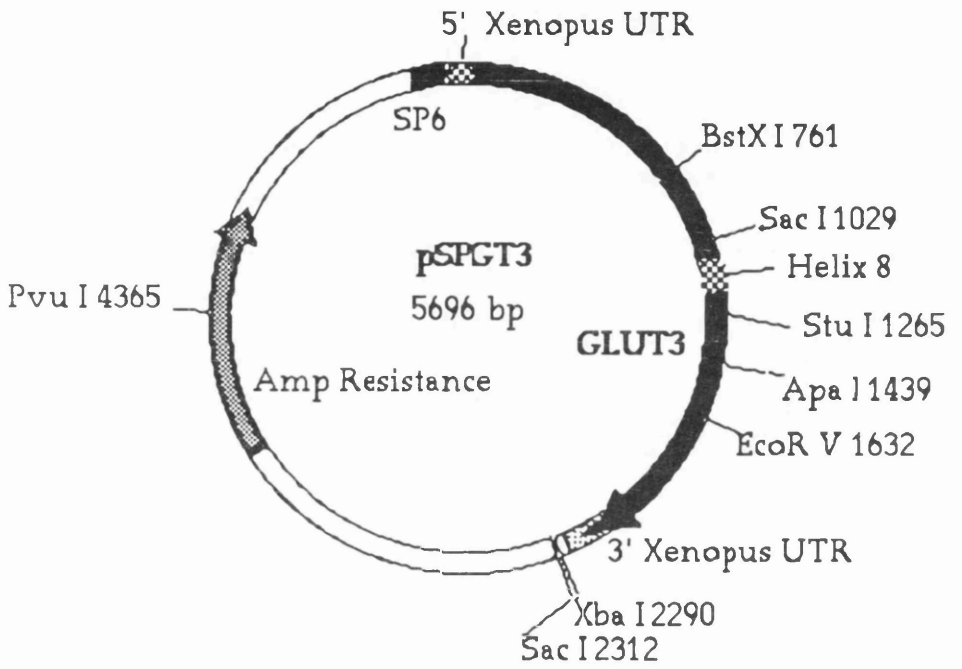


Figure 2.3

Diagrammatic Representation of M13mp18GT3. The entire GLUT3 sequence and its 5' and 3' untranslated regions are cloned into the multiple cloning site of M13mp18 rfdNA as a *Bam*H I/*Xba* I fragment. This bacteriophage vector exists as both double-stranded and single-stranded DNA forms. The various open reading frames of this vector are shown as Roman numerals. These encode enzymes necessary for phage replication and bacteriophage coat proteins. Note that this vector contains no SP6 RNA polymerase promoter, and hence GLUT3 cDNA must be subcloned into another vector to allow synthesis of its mRNA.

Figure 2.3-

Diagrammatic Representation of M13mp18GT3.

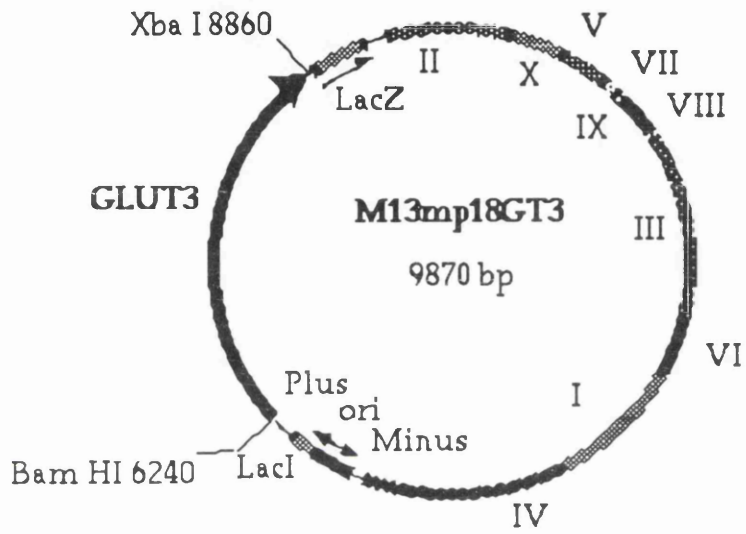


Figure 2. 4

Diagram showing the banding pattern expected at various stages of a site-directed mutagenesis reaction after electrophoresis of the samples (section 2.6) on a 1% agarose gel. The DNA species present at each stage of the reaction are shown schematically underneath each "lane". The substituted bases are indicated by an "x".

Lane 1. This shows the banding pattern on an agarose gel after annealing of the mutagenic oligonucleotide to the template and the extension reaction. Most of the ssDNA should be converted to double-stranded DNA, in relaxed and nicked forms (but not supercoiled since this is not produced by polymerase and ligase alone).

Lane 2. This is the gel pattern after the T5 exonuclease digestion has removed unpolymerised template DNA.

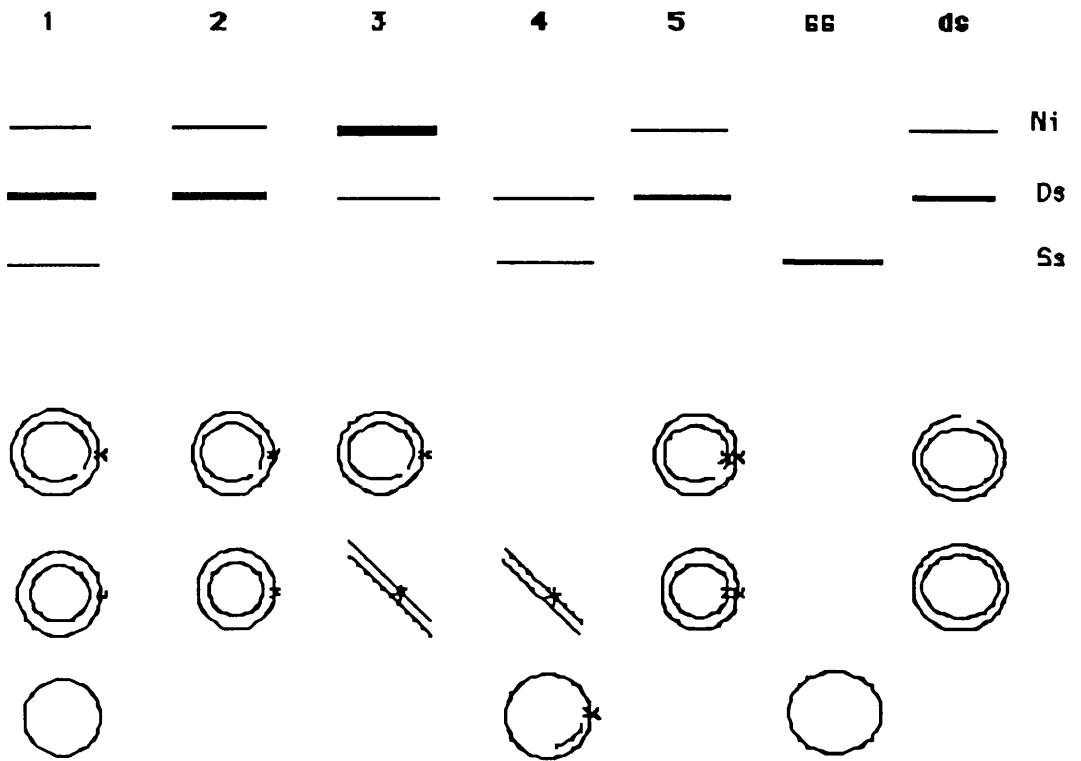
Lane 3. *Nci* I digestion produces both nicked and linear double-stranded DNA. The latter is formed from previously nicked DNA.

Lane 4. Exonuclease III digests the nicked non-mutant strand to give a smeared band which is approximately the same size as single-stranded DNA. An 800 bp fragment of the original strand remains bound to the mutant strand which acts as a primer for repolymerisation. A proportion of the linear DNA has single-stranded overhangs, which makes it Exonuclease III resistant.

Lane 5. This is the replicating form DNA (rfDNA) which is produced after repolymerisation. There is a mixed population of intact and nicked DNA.

Figure 2.4

Diagram Showing the Pattern Observed on a 1% Agarose Gel after Electrophoresis of Samples from Various Stages of a Site-Directed Mutagenesis Reaction.



CHAPTER 3.

Measurement of the Kinetic Parameters of 2-Deoxy-D-glucose and D-Fructose Transport by GLUT2 Expressed in *Xenopus* Oocytes.

3.1 Aims.

1. To investigate some basic kinetic parameters of GLUT2 to provide "baseline" values for comparison with kinetic values obtained from potential chimeric GLUT2/GLUT3 transporters and those incorporating single amino acid point mutations.

a. To measure K_m values for 2-deoxy-D-glucose and D-fructose transport (*zero-trans* entry) by GLUT2, expressed in *Xenopus* oocytes.

b. To measure K_i values for D-glucose, maltose, D-fructose and cytochalasin B on 2-deoxy-D-glucose transport by GLUT2.

c. To measure K_i values for D-glucose, maltose, and cytochalasin B on D-fructose transport by GLUT2.

2. To investigate the inhibitory effects of various D-fructose analogues on 2-deoxy-D-glucose transport by GLUT2, in an attempt to determine which ring form of D-fructose is transported.

3.2 Background.

3.2.1 Kinetic Characterisation of Glucose Transporters.

At the outset of this work, although abundant kinetic information was available for the erythrocyte-type transporter (GLUT1), relatively little was known about other transporter isoforms. This is mainly due to the fact that GLUT1 is the sole transporter isoform in erythrocytes, where it is present in as much as 5% of the total membrane protein. This provides a system which allows sugar transport kinetics to be measured unambiguously, uncomplicated by the actions of other transporter isoforms. Most native cell types express more than one isoform, hence confusing analysis. GLUT1 has also been purified (Kasahara & Hinkle, 1977) from erythrocytes and reconstituted into phospholipid vesicles (Wheeler & Hinkle, 1981) where both its steady-state and pre-steady-state kinetics for sugar transport have been measured (Lowe & Walmsley, 1986; Appleman & Lienhard, 1989; see also section 1.5.2).

However, the isolation of the GLUT1 cDNA by Mueckler *et al.* in 1985 led to the isolation of cDNAs encoding GLUTs 2, 3, 4, 5 and 7. By inserting these sequences into various expression vectors, it has been possible to express each member of the facilitative glucose transporter family in foreign cell types. Expression has been achieved in many cell systems, including 3T3-L1 adipocytes, CHO-K1 cells, and *Xenopus* oocytes (reviewed in Gould & Holman, 1993).

3.2.2 Use of *Xenopus* Oocytes for the Expression of Glucose Transporters.

The *Xenopus* oocyte expression system was initially used for kinetic analysis of GLUT1 (Gould & Lienhard, 1989). Many groups have since utilised oocytes for the expression of both wild-type and chimeric glucose transporter isoforms. The low endogenous glucose transport rates in these cells, together with the ease of microinjection of mRNA make the oocyte an ideal system with which to undertake a kinetic analysis of the heterologously expressed transporter.

Each oocyte is a large single cell of 1 mm diameter, visibly divided into two hemispheres: a dark pigmented "animal" pole, containing the large nucleus, and a lighter coloured "vegetable" pole, which is mainly cytoplasmic, densely populated with ribosomes and the machinery responsible for translation, protein processing and targeting. Stage V and VI oocytes are those which translate injected mRNA most efficiently. These are isolated from the toad by surgery and dissected manually from the surrounding vasculature network (section 2.3.4).

Expression of foreign proteins can be achieved in two ways: either by the microinjection of DNA into the nucleus, or by microinjection of mRNA into the cytoplasm. Although both methods result in adequate expression of proteins, it is much less demanding to inject mRNA into the cytoplasm, and so this is the method which has been chosen. Typically, 40 nl of ~1 mg/ml mRNA was injected into each oocyte, which are then left in physiological medium (Barths- Table 2.1) to express protein for 48 hours. *Zero-trans* entry assays were conducted by the addition of various concentrations of radiolabelled 2-deoxy-D-glucose, D-fructose or D-galactose for 30 min incubation times, for which transport has been shown to be linear (section 2.4 and Figure 3.1). Hence, by subtracting transport values for water-injected

oocytes from values obtained with oocytes injected with mRNA encoding a particular isoform, kinetic data for essentially a single transporter isoform can be generated. It has been previously shown that the rates of sugar transport into water-injected oocytes and non-injected oocytes are identical (Gould & Lienhard, 1989).

Recently, GLUTs 1, 2, 3 and 4 have been successfully expressed in *Xenopus* oocytes (Gould *et al.*, 1991). They found oocytes expressing GLUT2 or GLUT3 exhibited high 3-O-methyl-D-glucose transport rates, typically giving a 20-fold increase in transport rates over non-injected oocytes. Transport rates were much lower with GLUT4, which was thought to be consistent with the proposed intracellular distribution of GLUT4. These workers also measured transport of other radiolabelled sugars such as 2-deoxy-D-glucose, D-galactose and D-fructose, and demonstrated that the transporters have varying abilities to transport these secondary substrates. For example, only GLUT2 was found to transport D-fructose and GLUT3 transported D-galactose to a greater extent than the other transporter isoforms. The K_m value obtained for 3-O-methyl-D-glucose equilibrium exchange transport by GLUT1 (20 mM) correlated closely to that found in erythrocytes (17 mM) (Lowe & Walmsley, 1986).

The K_m value for equilibrium exchange transport of 3-O-methyl-D-glucose by GLUT4 in oocytes was measured in two separate studies and found to be 1.8 mM (Keller *et al.*, 1989) and 4.3 mM (Nishimura *et al.*, 1993). The value for zero-*trans* entry of 2-deoxy-D-glucose by GLUT4 into oocytes was found to be 4.6 mM (Burant & Bell, 1992).

GLUT2 was found to have a value of 17 mM for zero-*trans* entry of 3-O-methyl-D-glucose (Johnson *et al.*, 1990) but equilibrium exchange values were not measured. Zero-*trans* entry of 2-deoxy-D-glucose in oocytes expressing GLUT2 was determined concurrently with the work described here, and the

K_m value reported was 13 mM (Burant & Bell, 1992), which correlates well with the figure of 11 mM obtained herein (Table 3.1).

The K_m values of 3-O-methyl-D-glucose and 2-deoxy-D-glucose for zero-*trans* entry by GLUT3 have since been measured in Chinese hamster ovary cells (Asano *et al.*, 1992) and found to be about 3.5 mM and 0.9 mM, respectively. K_m values obtained for zero-*trans* entry of 2-deoxy-D-glucose into GLUT3-injected oocytes are 1.8 mM (Burant & Bell, 1992) and 1.4 mM (Colville *et al.*, 1993).

A kinetic analysis of the liver-type glucose transporter (GLUT2) expressed heterologously in *Xenopus* oocytes is presented, and contrasted with data obtained concurrently for the brain-type transporter (GLUT3) by Dr. Carol Colville. K_m values for zero-*trans* entry of 2-deoxy-D-glucose and D-fructose have been determined for GLUT2, in addition to K_i values for maltose, D-glucose, D-fructose and cytochalasin B inhibition of 2-deoxy-D-glucose transport by GLUT2. K_i values have also been measured for maltose, D-glucose and cytochalasin B inhibition of zero-*trans* D-fructose entry by GLUT2. K_m values for zero-*trans* entry of 2-deoxy-D-glucose and D-galactose by GLUT3, and the effects of inhibition by maltose, D-glucose, D-galactose and cytochalasin B are shown for the purposes of comparison.

3.3 Results.

3.3.1 Measurement of K_m Values for 2-Deoxy-D-glucose and D-Fructose Transport by GLUT2 and the Effects of the Presence of Various Sugars and Cytochalasin B.

The values for 2-deoxy-D-glucose, D-fructose and D-galactose transport by GLUTs 2 and 3 were determined by measuring the rate of transport of trace radiolabelled sugar over a range of external sugar concentrations into oocytes which had been incubated in sugar-free medium for at least 48 hours (section 2.4). By measuring the rates of *zero-trans* entry as a function of substrate concentration Lineweaver-Burk plots were constructed, and hence K_m values determined for the transport of these sugars by GLUT2. Oocytes were exposed to 2-deoxy-D-glucose for 15 min, or D-fructose or D-galactose for 30 min. It has been shown that the amount of label accumulating within the oocyte increases linearly with time, suggesting that transport of the sugar is the rate limiting step and not phosphorylation of the sugar by hexokinase (Figure 3.1). This was confirmed by the measurement of both relative and absolute levels of phosphorylated and non-phosphorylated sugars within the oocyte under the conditions used for analysis. In no case was a significant portion of the radiolabel associated with the oocyte due to non-phosphorylated sugar (Thomas *et al.*, 1993). Hence, the term 'transport' will be used here, rather than 'uptake', as the latter suggests both transport and phosphorylation processes.

Figure 3.2 shows a typical Lineweaver-Burk analysis of 2-deoxy-D-glucose transport by GLUT2 in the presence and absence of cytochalasin B, Figure 3.3 shows its transport inhibited by D-glucose, and Figure 3.4 shows the inhibitory effects of maltose and D-fructose. As can be seen from the graphs,

cytochalasin B is a non-competitive inhibitor of 2-deoxy-D-glucose transport by GLUT2, whereas maltose, D-fructose and D-glucose are competitive inhibitors. Similar results were obtained with D-fructose transport studies, its transport was non-competitively inhibited by cytochalasin B (Figure 3.5) whilst maltose and D-glucose exhibited competitive inhibition (Figures 3.6 and 3.7, respectively). The K_m values for 2-deoxy-D-glucose, D-fructose and D-galactose zero-*trans* entry by GLUT2 expressed in *Xenopus* oocytes are shown in Table 3.1. In addition, K_i values obtained for the inhibition of both 2-deoxy-D-glucose and D-fructose transport by GLUT2 using D-glucose, maltose, D-fructose and cytochalasin B are shown. K_i values for both competitive and non-competitive inhibition were calculated by application of the equation:-

$$\text{gradient of line (inhibitor)} = K_m / V_{\max} \cdot (1 + [I] / K_i)$$

For the purposes of comparison, and because of its relevance to later work, the kinetic analysis of GLUT3 is also summarised in Table 3.1. K_m values are shown for 2-deoxy-D-glucose and D-galactose transport, with K_i values for the inhibition of these sugars by cytochalasin B, D-glucose and maltose. The K_i value of D-galactose inhibition of 2-deoxy-D-glucose transport by GLUT3 is also shown. Cytochalasin B acted as a non-competitive inhibitor with 2-deoxy-D-glucose and D-galactose transport by GLUT3. Maltose, D-glucose and D-galactose acted as competitive inhibitors of 2-deoxy-D-glucose transport.

The effects of increasing concentrations of cytochalasin B on the transport of 2-deoxy-D-glucose and D-fructose by GLUT2, and 2-deoxy-D-glucose and D-galactose by GLUT3 are presented in Figure 3.8.

The effect of addition of 50 mM L-glucose, D-glucose, D-fructose and D-galactose on the transport rate of 2-deoxy-D-glucose by GLUT2-injected oocytes

is shown in Table 3.2. Note that these values are not adjusted for transporter protein levels, and show a typical experiment in which the average transport value of six oocytes has been determined.

3.3.2 Measurement of the Effects of the Presence of 2,5-Anhydro-D-mannitol and L-Sorbose on 2-Deoxy-D-glucose Transport by GLUT2.

To investigate which ring form of D-fructose is transported by GLUT2, the inhibitory effects of 2,5-anhydro-D-mannitol, a fixed-ring furan-analogue of D-fructose, and L-sorbose, which exists mainly in the pyranose ring form, on the transport of 2-deoxy-D-glucose by GLUT2-injected oocytes were compared. The Lineweaver-Burk plot of the data obtained is shown as Figure 3.9. 2,5-anhydro-D-mannitol has a K_i of 26 mM and L-sorbose has a K_i of 170 mM on 2-deoxy-D-glucose transport by GLUT2. The structures of 2,5-anhydro-D-mannitol, L-sorbose and the pyranose and furanose ring forms of D-fructose can be seen in Figure 3.10.

Table 3.1

K_m and K_i values were determined from Lineweaver-Burk plots such as that shown in Figure 3.2. All values above are the mean and standard deviations from between 3 and 10 separate experiments for each condition. Note that values for GLUT3 were obtained by Dr. Carol Colville.

Table 3.1
Kinetic Parameters for Transport of Sugars by GLUT 2 and GLUT 3.

<u>GLUT 2.</u>					
Substrate	K _m (mM)	Inhibitor: Maltose K _i (mM)	D-Glucose K _i (mM)	D-fructose K _i (mM)	Cytochalasin B K _i (μM)
2-Deoxy-D-glucose	11.2 ± 1.1	125 ± 24	6.5 ± 1.3	204 ± 35	6.9 ± 1.2
D-Fructose	66.7 ± 18.3	116 ± 5.8	15.3 ± 4.3	n.d.	6.1 ± 1.1
D-Galactose	85.5 ± 10.7	n.d.	n.d.	n.d.	n.d.
<u>GLUT 3.</u>					
	K _m (mM)	Maltose K _i (mM)	D-Glucose K _i (mM)	D-Galactose K _i (mM)	Cytochalasin B K _i (μM)
2-Deoxy-D-glucose	1.4 ± 0.06	37.0 ± 1.8	1.6 ± 0.4	15.5 ± 4.5	2.1 ± 0.47
D-Galactose	8.5 ± 2.5	29.2 ± 9.0	6.9 ± 0.3	n.d.	2.8 ± 0.72

Table 3.2

Effects of D-Fructose, D-Glucose and D-Galactose on 2-Deoxy-D-glucose Transport by GLUT2.

<u>Competing Sugar</u>	<u>Transport Rate (pmoles/min/oocyte)</u>
50 mM L-glucose	2.61 ± 0.35
50 mM D-galactose	2.25 ± 0.15
50 mM D-fructose	1.60 ± 0.10
50 mM D-glucose	0.30 ± 0.05

Groups of 6 oocytes injected with GLUT2 mRNA were incubated in 450 μ l of Barths buffer containing 50 mM of the sugars indicated. 2-deoxy-D-glucose (0.1 mM, 1 μ Ci/ml) was added and transport rates determined as described. The experiment shown is representative of three separate experiments and the values are mean \pm standard deviation of the rate of transport into six oocytes.

Figure 3.1

Each point is the mean of the transport rate determined from 6 oocytes as described in section 2.4. Uptake was determined by exposure of 2-deoxy-D-glucose* to the oocytes for 5, 10, 15, 20 and 30 min and the counts per oocyte determined as described. For each experiment parallel incubations were carried out in oocytes which were not injected with mRNA ('control oocytes'), and the values obtained from this oocyte population subtracted from the values obtained from injected oocytes to obtain the true heterologous uptake. Uptakes in 'control oocytes' were typically 5 to 10% of injected oocytes. The range of error was typically $\pm 10\%$ at each point. Error bars are omitted for clarity.

*
(0.1mM, 1 μ Ci/ml)

Figure 3. 1
| Accumulation of 2-Deoxy-D-glucose by GLUT2-Injected Oocytes with Time.

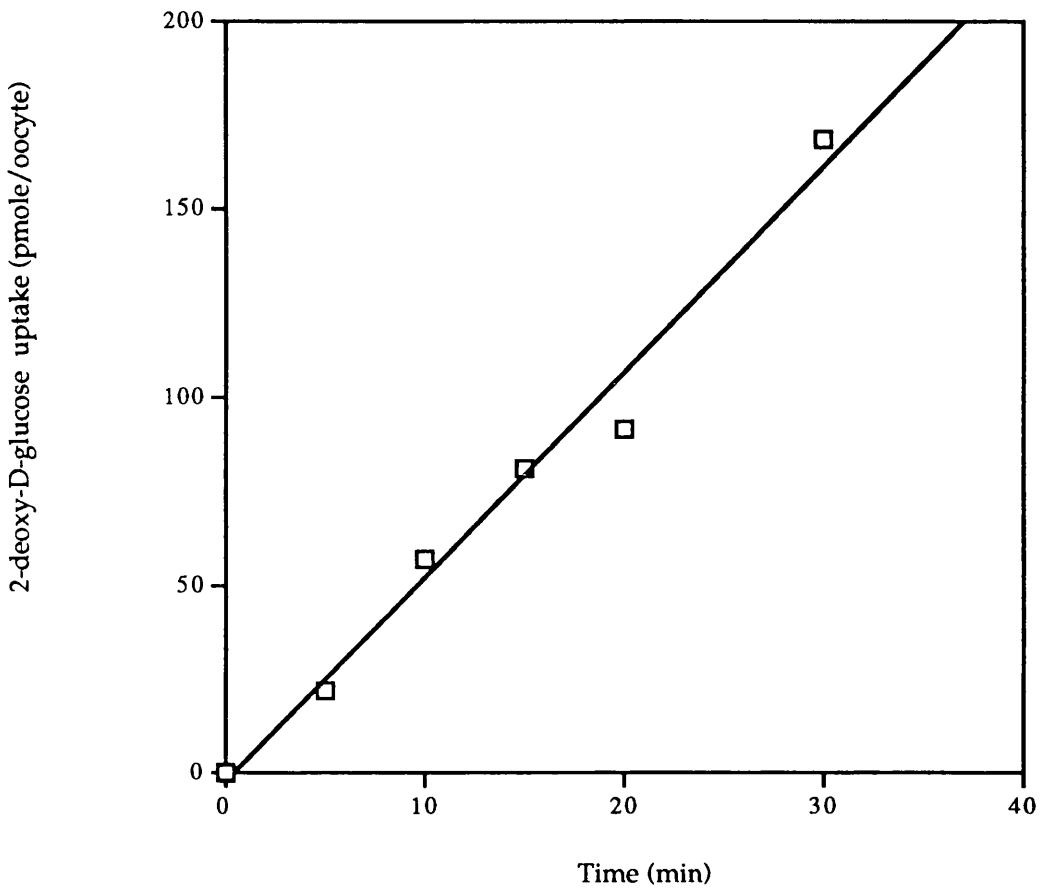


Figure 3.2

Each point is the mean of the transport rate determined from 6 oocytes as described in section 2.4. Transport was determined by 15 min exposure of the 2-deoxy-D-glucose to the oocytes and the counts per oocyte determined as described. For each experiment parallel incubations were carried out in oocytes which were not injected with mRNA ('control oocytes'), and the values obtained from this oocyte population subtracted from the values obtained from injected oocytes to obtain the true heterologous transport rate. Transport rates in 'control oocytes' were typically 5-10% of injected oocytes. The range of error was typically $\pm 10\%$ at each point. Error bars are omitted for clarity. In the above experiment, (\diamond) represents the plot obtained in the absence of inhibitors, (\square) in the presence of 10 μM cytochalasin B.

Figure 3.2
Lineweaver-Burk Plot of Transport of 2-Deoxy-D-glucose into GLUT2-Injected Oocytes in the Presence and Absence of Cytochalasin B.

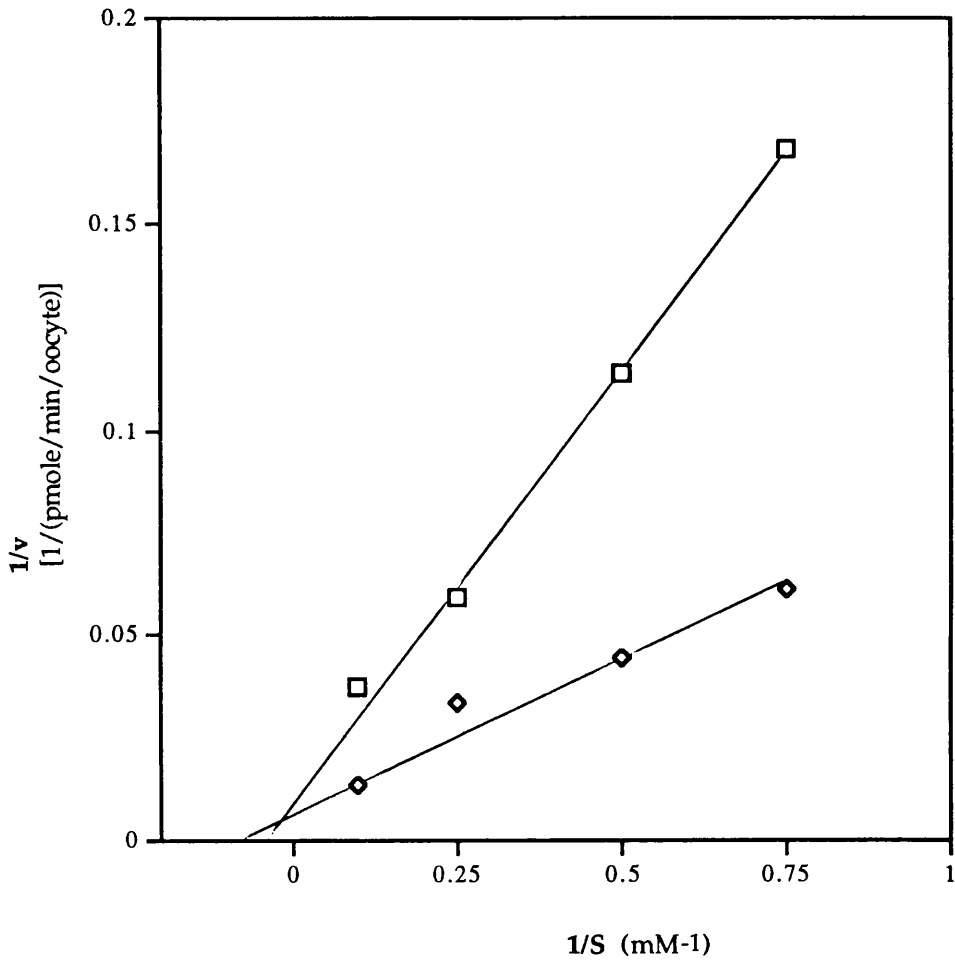


Figure 3.3

Transport rates of 2-deoxy-D-glucose into oocytes expressing GLUT2 were determined as described. Each point is the mean of six separate oocytes at each concentration of sugar. Values presented are corrected for the transport of 2-deoxy-D-glucose by non-injected oocytes as described in Figure 3.2. In the representative experiment shown, (\diamond) represents the plot obtained in the absence of inhibitors, and (\square) in the presence of 10 mM D-glucose. The range of error was typically $\pm 10\%$ at each point. Error bars are omitted for clarity.

Figure 3.3
Lineweaver-Burk Plot of Transport of 2-Deoxy-D-glucose by GLUT2-Injected Oocytes in the Presence and Absence of D-Glucose.

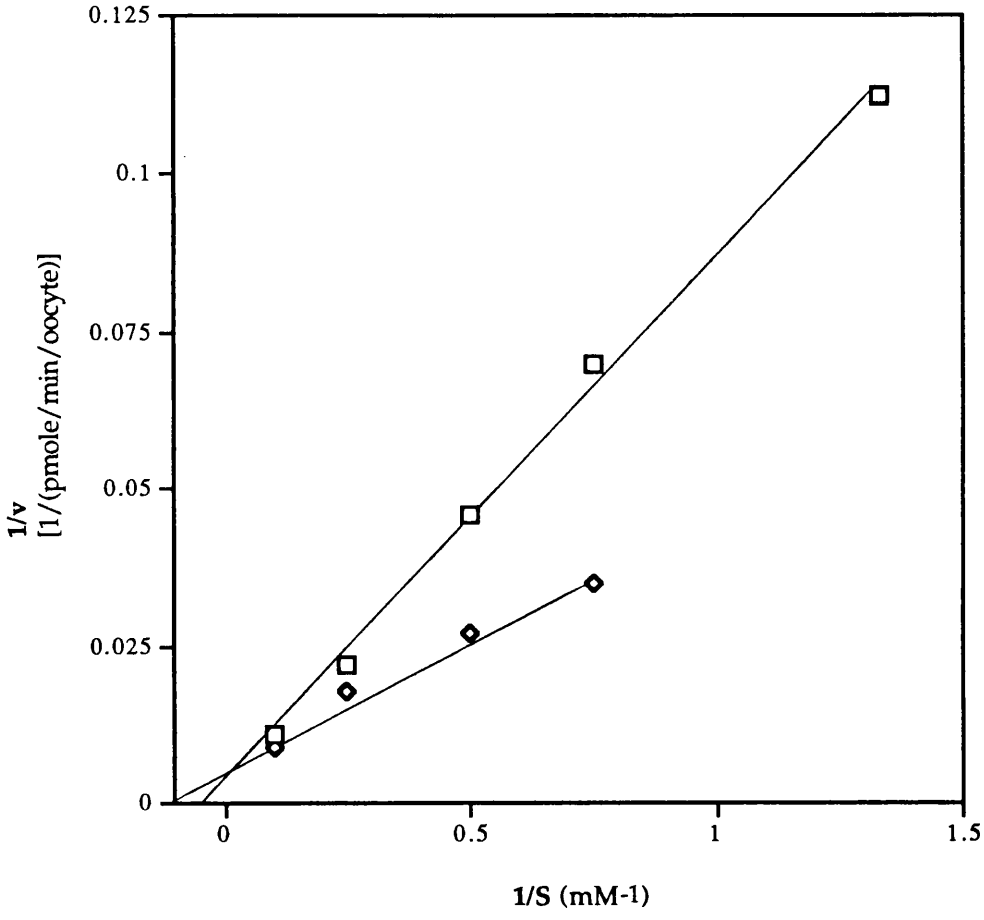


Figure 3.4

Transport rates of 2-deoxy-D-glucose into oocytes expressing GLUT2 were determined as described. Each point is the mean of six separate oocytes at each concentration of sugar. Values presented are corrected for the transport of 2-deoxy-D-glucose by non-injected oocytes as described in Figure 3.2. In the representative experiment shown, (\square) represents the plot obtained in the absence of inhibitors, (\diamond) in the presence of 50 mM D-fructose, and (\bullet) in the presence of 150 mM maltose. The range of error was typically $\pm 10\%$ at each point. Error bars are omitted for clarity.

Figure 3.4
Lineweaver-Burk Plot of Transport of 2-Deoxy-D-glucose by GLUT2-Injected Oocytes in the Presence of Maltose or D-Fructose or in the Absence of Inhibitors.

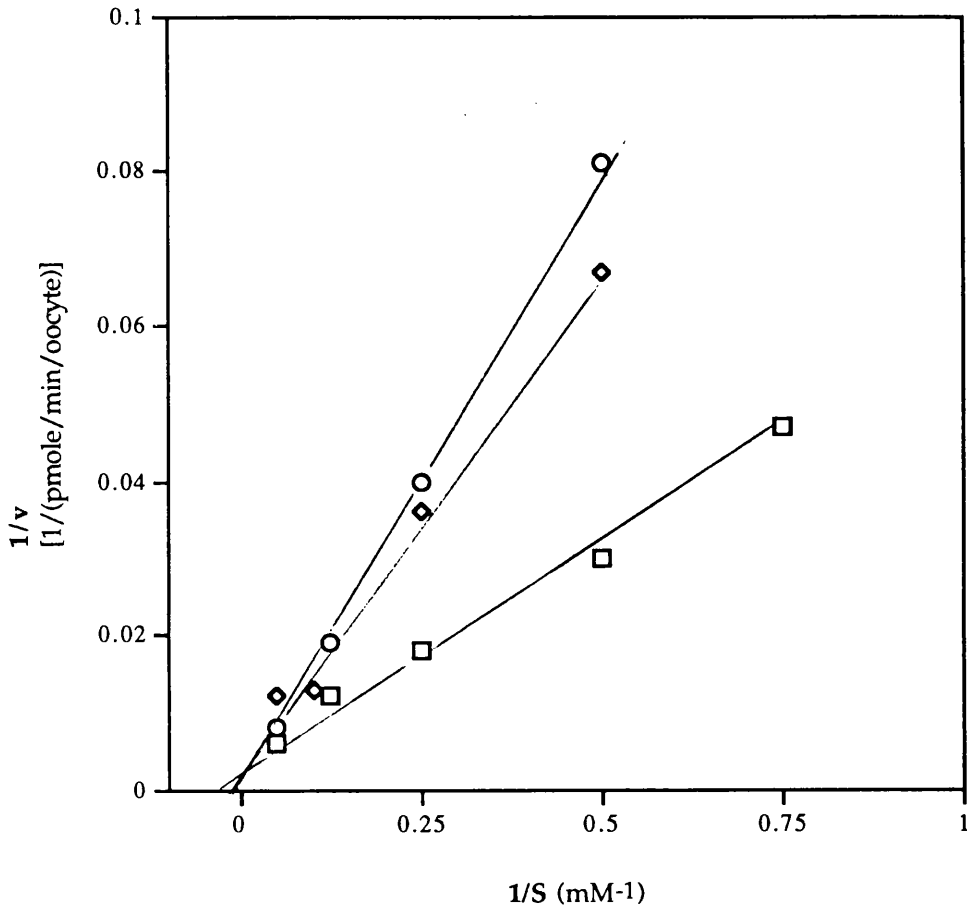


Figure 3.5

Transport rates of D-fructose into oocytes expressing GLUT2 were determined as described. Each point is the mean of six separate oocytes at each concentration of sugar. Values presented are corrected for the transport of fructose by non-injected oocytes as described in Figure 3.2 for 2-deoxy-D-glucose. In the representative experiment shown, (\square) represents the plot obtained in the absence of inhibitors, and (\diamond) in the presence of 2 μ M cytochalasin B. The range of error was typically $\pm 10\%$ at each point. Error bars are omitted for clarity.

Figure 3.5
Lineweaver-Burk Plot of Transport of D-Fructose into GLUT2-Injected Oocytes in the Presence and Absence of Cytochalasin B.

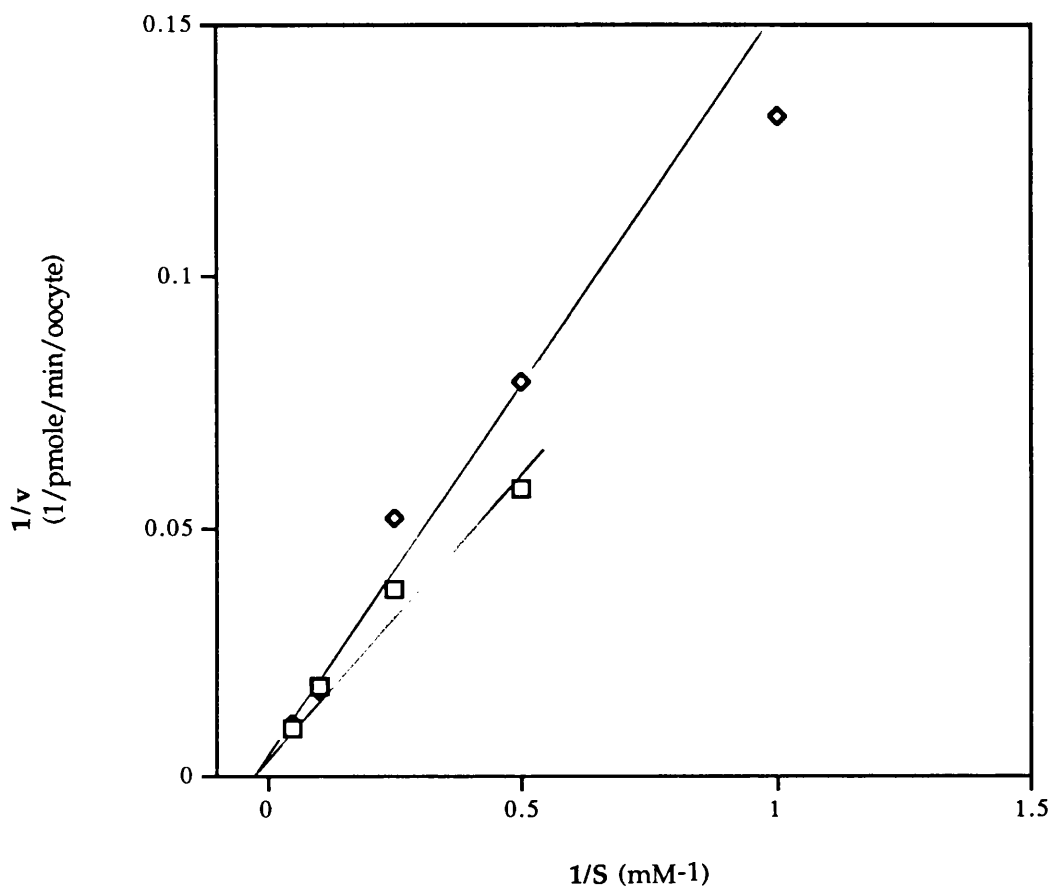


Figure 3. 6

Transport rates of D-fructose into oocytes expressing GLUT2 were determined as described. Each point is the mean of six separate oocytes at each concentration of sugar. Values presented are corrected for the transport of fructose by non-injected oocytes as described in Figure 3.2 for 2-deoxy-D-glucose. In the representative experiment shown, (□) represents the plot obtained in the absence of inhibitors, and (◇) in the presence of 150 mM maltose. The range of error was typically $\pm 10\%$ at each point. Error bars are omitted for clarity.

Figure 3.6
Lineweaver-Burk Plot of Transport of D-Fructose by
GLUT2-Injected Oocytes in the Presence and Absence
of Maltose.

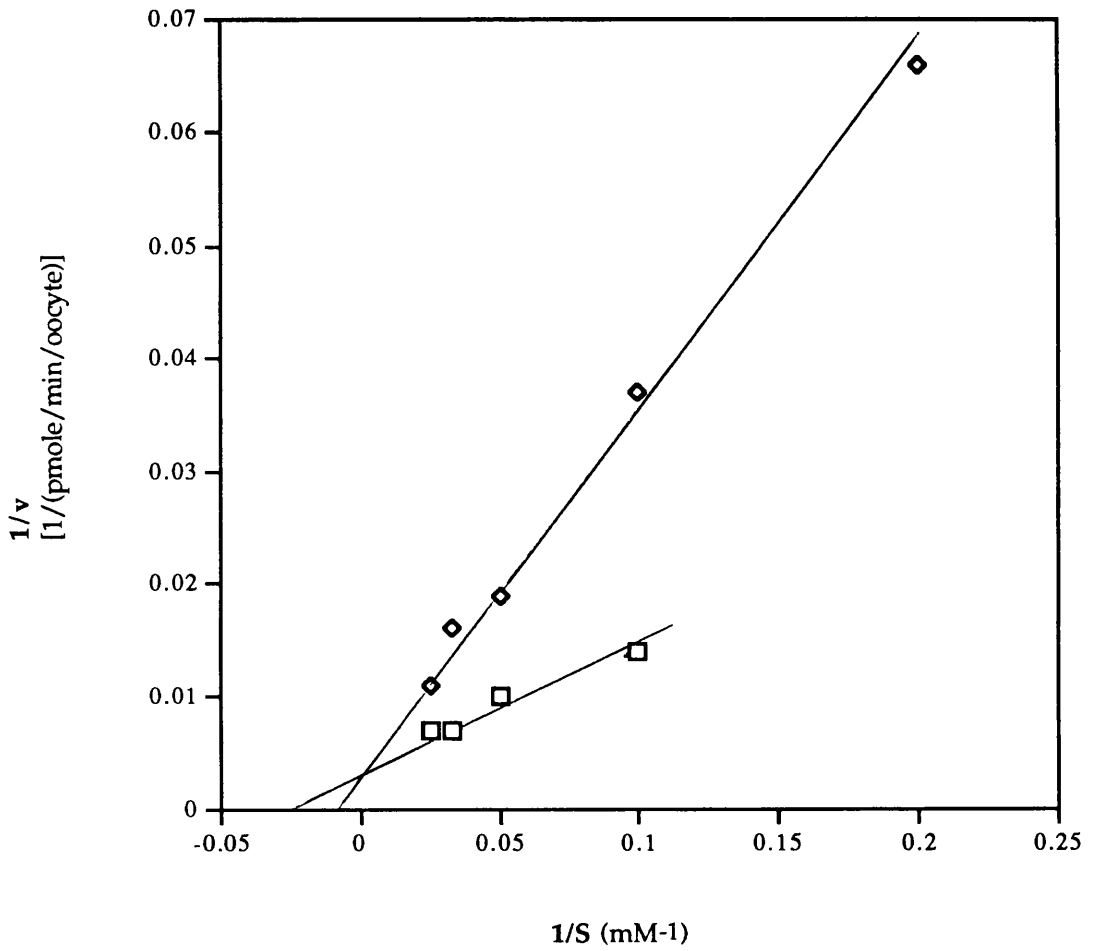


Figure 3.7

Transport rates of D-fructose into oocytes expressing GLUT2 were determined as described. Each point is the mean of six separate oocytes at each concentration of sugar. Values presented are corrected for the transport of fructose by non-injected oocytes as described in Figure 3.2 for 2-deoxy-D-glucose. In the representative experiment shown, (\diamond) represents the plot obtained in the absence of inhibitors and (\square) in the presence of 10 mM D-glucose. The range of error was typically $\pm 10\%$ at each point. Error bars are omitted for clarity.

Figure 3.7
Lineweaver-Burk Plot of Transport of D-Fructose by
GLUT2-Injected oocytes in the Presence and Absence of
D-Glucose.

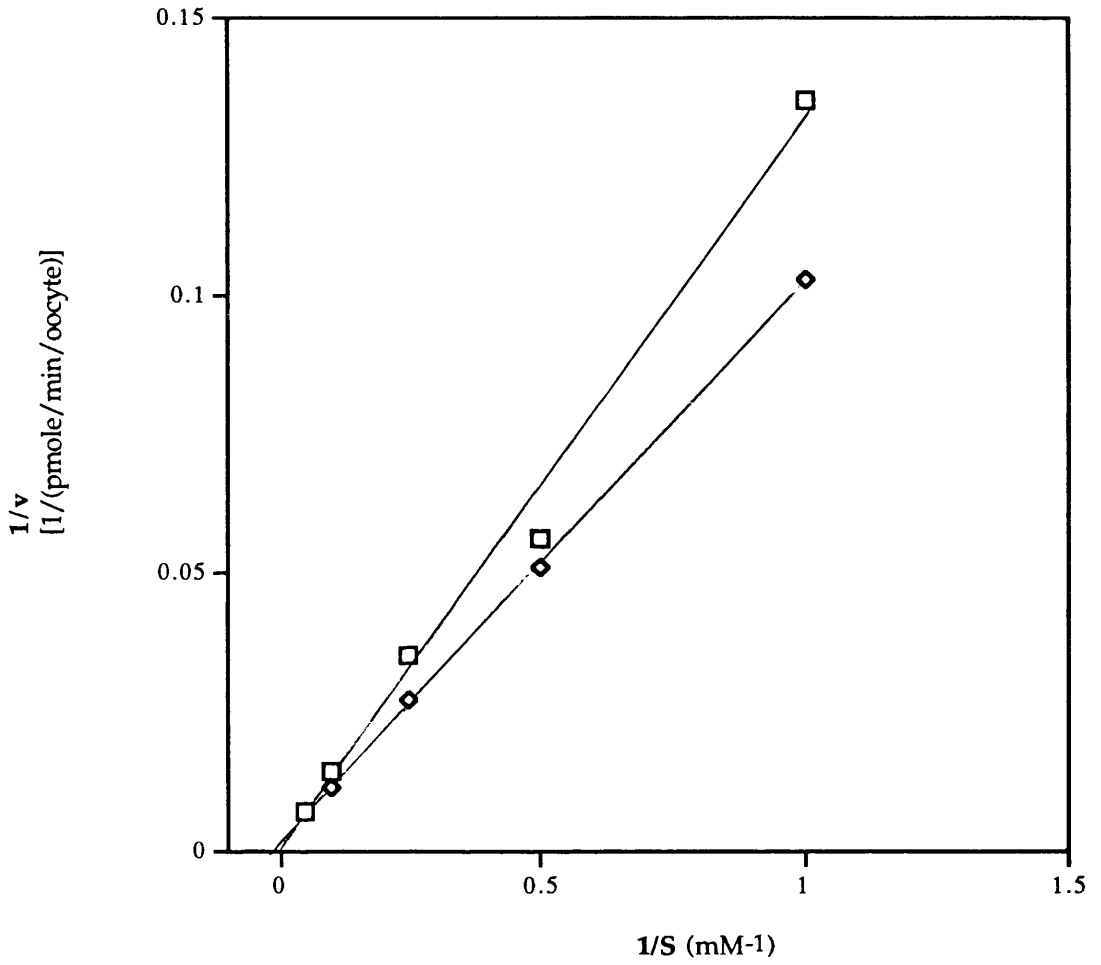


Figure 3.8

Oocytes expressing GLUT2 were assayed for 2-deoxy-D-glucose and D-fructose transport, and oocytes expressing GLUT3 assayed for 2-deoxy-D-glucose and D-galactose transport (by Carol Colville) as described. Transport rates were determined in the absence or presence of cytochalasin B in the bathing media at the indicated concentrations. Groups of 6 oocytes were assayed as described in section 2.4, and the mean rate per oocyte is presented. Transport rates were expressed as a percentage of the rate obtained in the absence of cytochalasin B.

(●) 2-deoxy-D-glucose by GLUT2; (◐) D-fructose by GLUT2; (▲) 2-deoxy-D-glucose by GLUT3; (▲) D-galactose by GLUT3. For clarity, error bars have been included only for one of the curves, the errors in the other experiments were similar.

Figure 3.8

Dose-Response of Cytochalasin B on the Inhibition of Transport Rates in GLUT2 and GLUT3-Injected Oocytes.

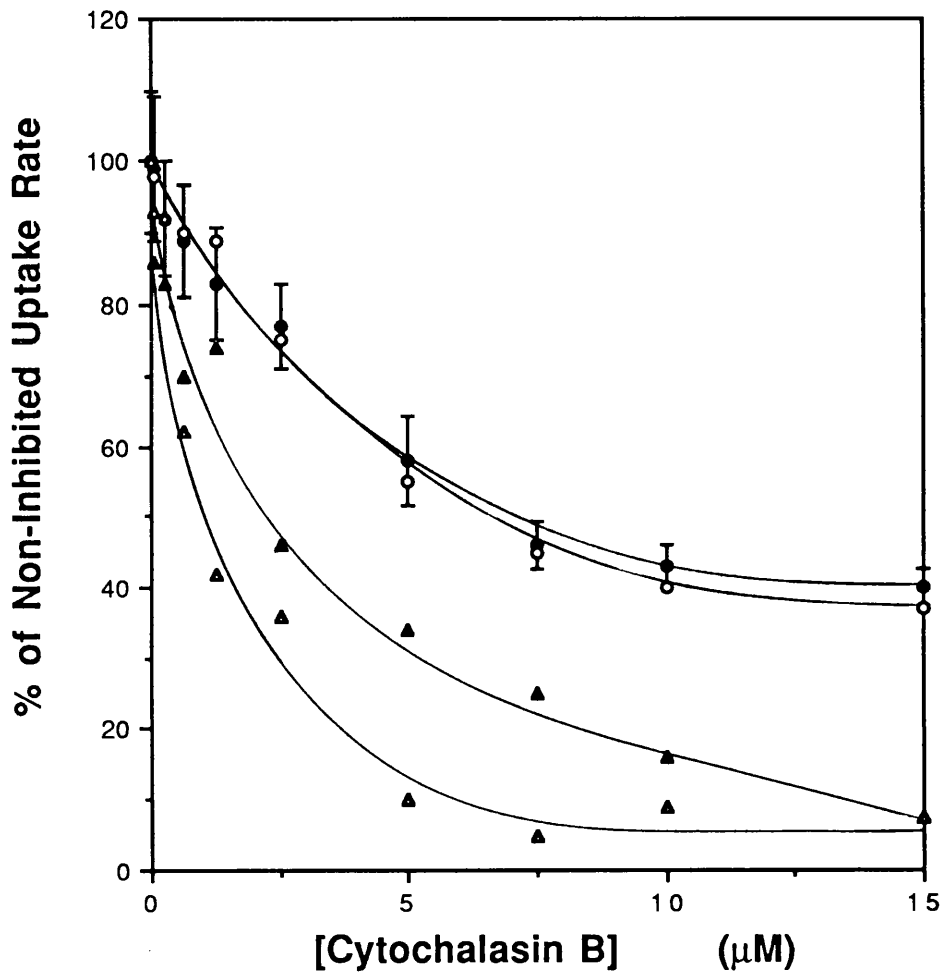


Figure 3.9

Transport rates of 2-deoxy-D-glucose into oocytes expressing GLUT2 were determined as described. Each point is the mean of six separate oocytes at each concentration of sugar. Values presented are corrected for the transport of 2-deoxy-D-glucose by non-injected oocytes as described in Figure 3.2. In the representative experiment shown, (○) represents the plot obtained in the absence of inhibitors, (◻) in the presence of 25 mM 2,5-anhydro-D-mannitol, and (◊) in the presence of 25 mM L-sorbose. The range of error was typically $\pm 10\%$ at each point. Error bars are omitted for clarity.

Figure 3.9
Lineweaver-Burk Plot of Transport of 2-Deoxy-D-glucose
in the Presence of 2,5-Anhydro-D-Mannitol or L-Sorbose
or in the Absence of Inhibitors.

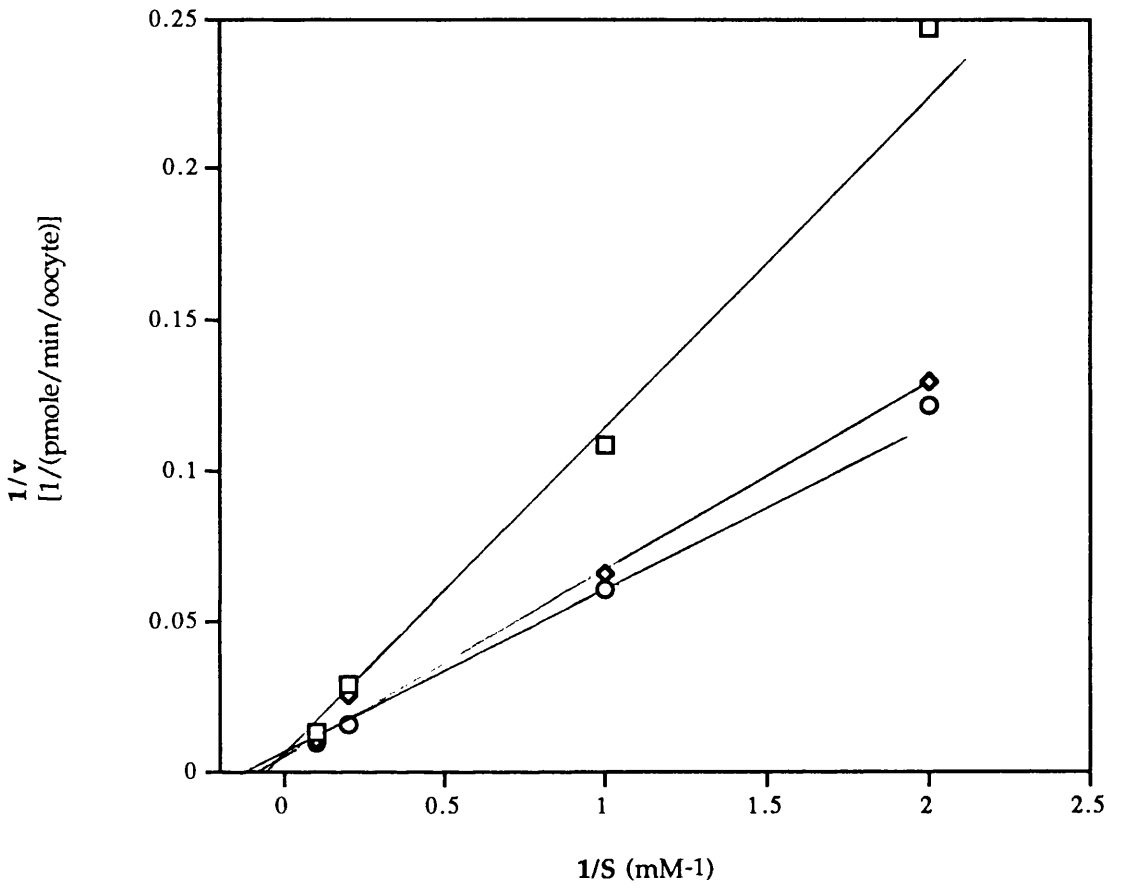


Figure 3. 10

Structures of pyranose and furanose sugars.

Structural comparisons of pyranose and furanose sugars used in the analysis of substrate binding to the transporters. Compound I is β -D-glucose, compound II is β -D-fructopyranose, compound III is α -L-sorbopyranose, compound IV is β -D-fructofuranose and compound V is 2,5-anhydro-D-mannitol.

Figure 3.10

Structures of some Pyranose and Furanose Sugars.

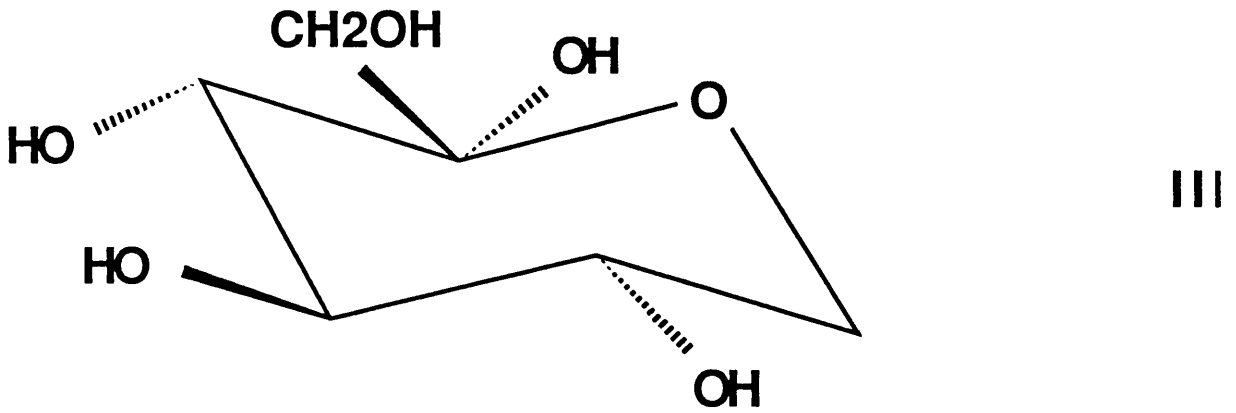
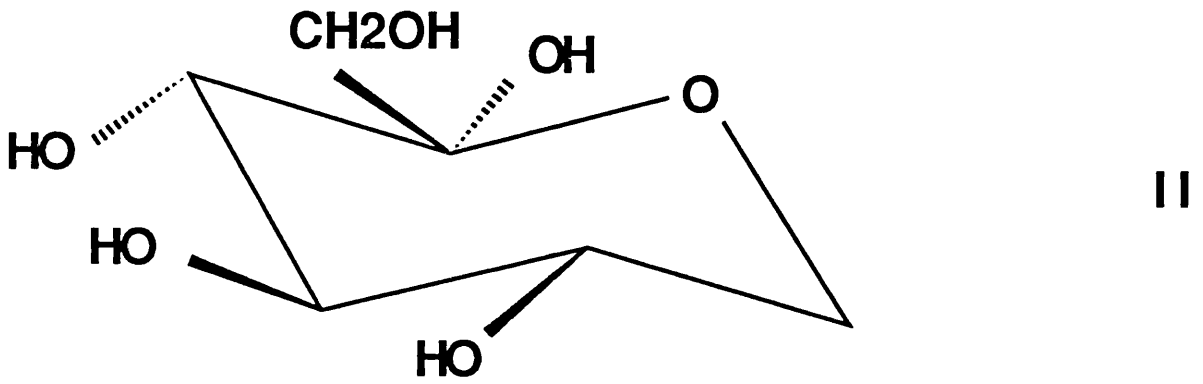
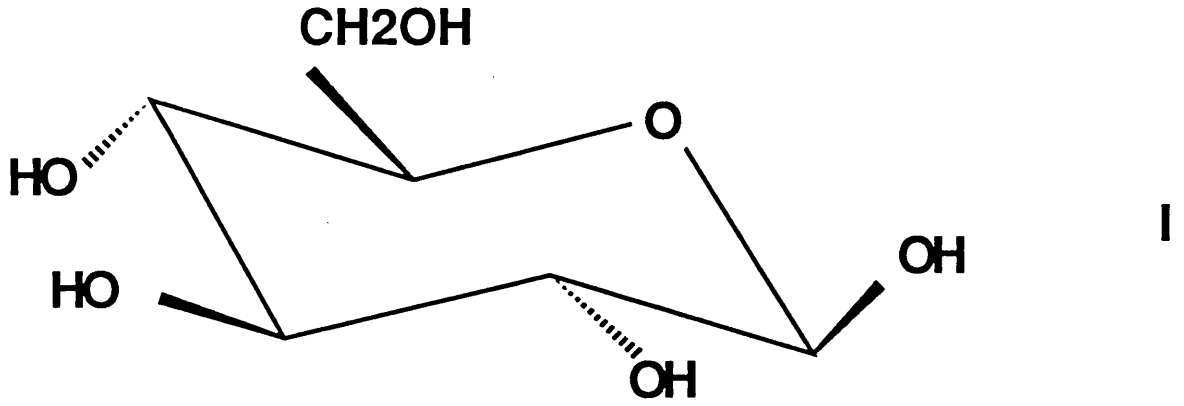


Figure 3.10 (cont.)

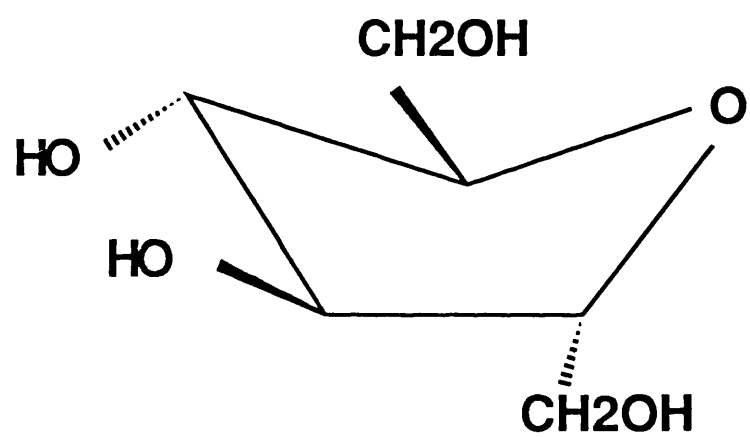
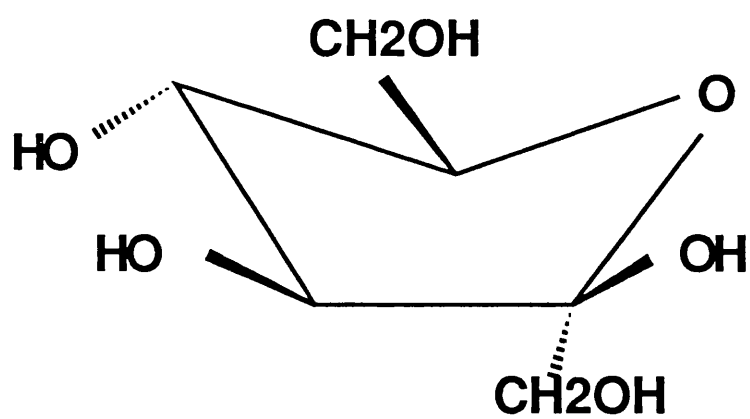


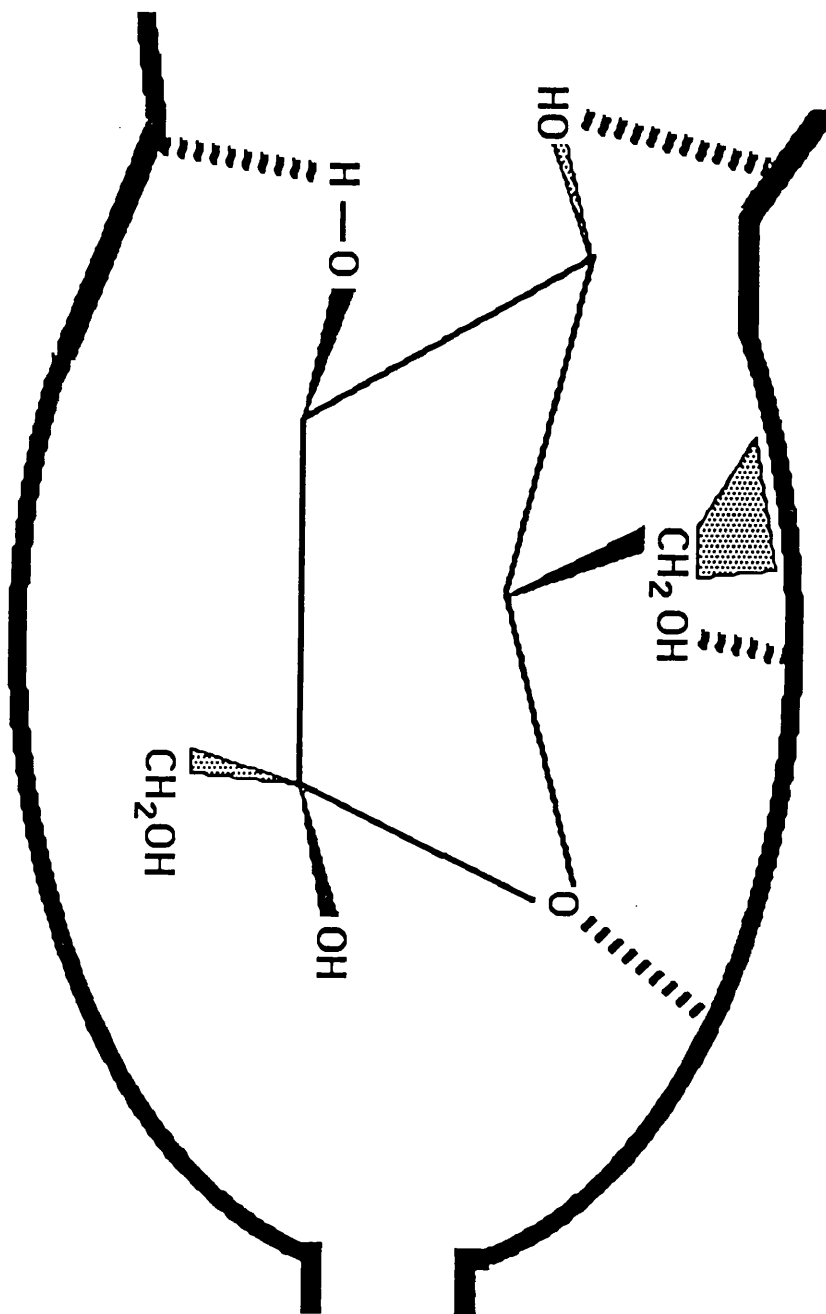
Figure 3.11

Model for the Interaction of β -D-Fructose with GLUT2.

The proposed interaction of the furanose ring form of β -D-fructose and GLUT2 is shown.

Figure 3.11

Model for the Interaction of β -D-Fructose with GLUT2.



3.4 Conclusions.

3.4.1 Effects of Various Sugars on Zero-*trans* Entry of 2-Deoxy-D-glucose and D-Fructose by GLUT2 and D-Galactose by GLUT3.

Previous work from this laboratory has demonstrated that as well as transporting D-glucose, GLUT2 is capable of mediating the transport of both D-galactose and D-fructose, and that GLUT3 also mediates the transport of D-galactose (Gould *et al.*, 1991; Colville *et al.*, 1993).

Here, K_m values for zero-*trans* entry of 2-deoxy-D-glucose into *Xenopus* oocytes by GLUT2 in the presence and absence of transport inhibitors have been determined. GLUT2 has a K_m for 2-deoxy-D-glucose of about 11 mM. The corresponding K_m value for GLUT3 is 1.4 mM. The ratio of these values are comparable to those obtained for 3-O-methyl-D-glucose of 45 mM and 10 mM for GLUTs 2 and 3 respectively (determined under equilibrium exchange conditions). Thus, it is interesting to note that the relative affinities of both analogues for these isoforms are similar, i.e. GLUT3 has about a 4- to 6-fold higher affinity than GLUT2. These values are significantly different from each other and that of GLUT1. The values are in agreement with parallel studies carried out with oocytes in other laboratories (Burant *et al.*, 1992; Nishimura *et al.*, 1993; Keller *et al.*, 1989).

The K_m value of 11 mM for 2-deoxy-D-glucose transport by GLUT2 is consistent with its proposed function as a bidirectional, high capacity glucose transporter in the liver, where it can export as well as import glucose. It is also present in the basolateral membranes of the transepithelial cells of the small intestine and the proximal tubules of the kidney, where it is proposed to transport glucose down its concentration gradient into the blood, after active transport by sodium-linked symporters into these cells. This high K_m

coupled to its expression in pancreatic β -cells has been proposed to enable GLUT2 to act as a "blood glucose sensor" but this is an unresolved issue (section 1.2.3).

The relatively low K_m of 1.4 mM for 2-deoxy-D-glucose transport by GLUT3 closely correlates with data from GLUT3 expressed in Chinese hamster ovary cells (Asano *et al.*, 1992) and conforms with its proposed role as a high affinity glucose transporter in the brain and neural tissue.

Of course, these values are not necessarily identical to the values found in the native cells, since different patterns of glycosylation might occur in oocytes and influence transport kinetics. Additionally, we are looking at the transport of an analogue of D-glucose rather than the sugar itself, at 25°C rather than at 37°C. 2-deoxy-D-glucose was used as a substrate rather than glucose since it cannot be completely metabolised by the cell but is phosphorylated enforcing its retention. Hence the K_m value being measured is a function of the affinity of the substrate for the outward facing binding site alone. Nevertheless it is likely that the K_m values approximate actual values in native cells.

K_m values for D-fructose and D-galactose transport by GLUT2 have been measured, and the K_m value for D-galactose transport by GLUT3 has also been calculated (Colville *et al.*, 1993). The data show that for GLUT2, the relative affinity for sugars is 2-deoxy-D-glucose \gg D-fructose $>$ D-galactose (K_m values of 11 mM, 67 mM and 85 mM respectively- Table 3.1). Similarly, for GLUT3, the K_m for D-galactose (8.5 mM) is much higher than that of 2-deoxy-D-glucose (1.4 mM) (Table 3.1).

Ideally it would be more instructive to measure k_{cat} values in addition to K_m values since they would provide a fuller description of the kinetics of the transporters, giving both affinity of the transporter binding site to the sugar and a rate of transporter turnover rather than just a measure of the

affinity. However, to do this an accurate method of determining the number of transporters at the cell surface would be required in order to calculate the turnover number from the overall V_{\max} . This could be achieved by applying Scatchard analysis to data generated by equilibrium binding of [^3H]cytochalasin B to isolated oocyte plasma membranes, or [^3H]ATB-BMPA equilibrium binding with intact oocytes, to determine the number of transporter molecules at the cell surface. Alternatively, the amount of transporter in oocyte plasma membrane fractions could be determined by SDS-PAGE, blotting onto nitrocellulose, addition of a specific anti-human-GLUT2 or -GLUT3 antibody, and a radiolabelled secondary antibody. Comparison of these samples with standard membrane preparations containing known quantities of transporter protein, measured by the above methods, would determine the amount of transporter present. This is possible for GLUT3 since membranes from a cell-line engineered to stably express GLUT3, containing known quantities of GLUT3, are available (Maher *et al.*, 1992). Unfortunately, the lack of a suitable standard for GLUT2 makes it impossible to accurately quantitate this isoform. This is due to the high K_d value of cytochalasin B for GLUT2 (Axelrod & Pilch, 1983) which makes it technically difficult to perform equilibrium studies with this transporter isoform. Additionally, it has so far proved impossible to obtain pure plasma membrane fractions from oocytes, which is necessary when using cytochalasin B binding studies. This and the non-commercial availability of ATB-BMPA has made quantification of transporters difficult, so K_m and K_i values alone were measured.

The effect of the fungal metabolite cytochalasin B, a well characterised inhibitor of glucose transport, on the transport of 2-deoxy-D-glucose and D-fructose by GLUT2 was examined (Figures 3.2 and 3.5). This was performed in parallel for 2-deoxy-D-glucose and D-galactose by Dr. Carol Colville for

GLUT3. Cytochalasin B is known to be non-competitive for glucose entry mediated by GLUT1, GLUT2 and GLUT4, and Deves and Krupka found that it competitively inhibited efflux of sugar in zero-*trans* exit studies performed in erythrocytes, suggesting that its site of action is the endofacial sugar binding site (Deves & Krupka, 1978). It is well established that GLUTs 1 and 4 can be irreversibly photolabelled with cytochalasin B, and that this labelling may be prevented by D- but not L-glucose. Photolabelling of GLUT2 with cytochalasin B has been reported, though under modified conditions (Axelrod and Pilch, 1983). It has also been shown that GLUT3 can be photolabelled with cytochalasin B in the presence of L- but not D-glucose (Thomas *et al.*, 1993). There is a compelling body of evidence to suggest that this labelling occurs at, or close to, the endofacial glucose binding site (Deves & Krupka, 1978). Here it is shown that cytochalasin B displayed a non-competitive inhibitory effect with 2-deoxy-D-glucose transport by both GLUT2 and GLUT3, consistent with the hypothesis that it binds the endofacial binding site. Moreover, as can be seen from Table 3.1, as previously reported, the K_i for cytochalasin B inhibition of 2-deoxy-D-glucose is higher for GLUT2 than either GLUT1 or GLUT4, and the value for GLUT3 is intermediate. It is interesting to note that the K_i values of cytochalasin B on the inhibition of transport of D-fructose and D-galactose by GLUT2 and GLUT3, respectively, are similar, if not identical, to K_i values on the inhibition of transport of 2-deoxy-D-glucose with the same transporter (Table 3.1). Thus, one interpretation of these results is that since cytochalasin B exhibits identical K_i values regardless of the substrate, then the inward-facing substrate binding sites used by 2-deoxy-D-glucose and D-galactose (GLUT3) or 2-deoxy-D-glucose and D-fructose (GLUT2) are the same.

The effects of maltose on sugar uptake by GLUT2 were also investigated. Maltose is proposed to inhibit transport by binding to the

exofacial binding site (Appleman & Lienhard, 1989). It cannot be transported itself since it is a disaccharide, but could possibly bind reversibly to the exofacial binding site and competitively block glucose uptake. Indeed, maltose was determined to be a competitive inhibitor of both 2-deoxy-D-glucose transport and that of D-fructose. The K_i values obtained are presented in Table 3.1. Similarly, D-glucose itself was found to inhibit 2-deoxy-D-glucose and D-fructose competitively (Table 3.1). Similar findings were reported with maltose and D-glucose competitive inhibition of 2-deoxy-D-glucose and D-galactose transport by GLUT3 (Colville *et al.*, 1993). These observations are interpreted to imply that the alternative substrates tested in these analyses utilise the same outward facing substrate binding site as the preferred substrate (2-deoxy-D-glucose). This conclusion is further supported by the observations that D-fructose is a competitive inhibitor of 2-deoxy-D-glucose transport by GLUT2 (Figure 3.4), and D-galactose is a competitive inhibitor of 2-deoxy-D-glucose transport by GLUT3 (Colville *et al.*, 1993).

It is also interesting to note that D-galactose is a more potent inhibitor of GLUT3 than GLUT2, and D-fructose is more effective at inhibiting transport mediated by GLUT2 than GLUT3 (Table 3.2), consistent with the relative K_m values reported above (Table 3.1).

3.4.2 β -D-Fructose Transport Conformation.

A recent study (Fry *et al.*, 1993) has shown that the sugar transporter of the parasite *Trypanosoma brucei* transports both D-glucose and D-fructose with equal efficiency. Various furanose and pyranose sugars were used to inhibit 6-deoxy-D-glucose *zero-trans* entry and it was discovered that D-

glucose is transported in the pyranose form, but D-fructose is transported in the furanose conformation.

It has been reported that GLUT2 can also effectively transport D-fructose, albeit with low efficiency (Gould *et al.*, 1991). As noted in this chapter, D-glucose is a competitive inhibitor of D-fructose *zero-trans* entry, and D-fructose a competitive inhibitor of 2-deoxy-D-glucose *zero-trans* entry. This suggests that D-glucose and D-fructose probably share the same exofacial binding site. It has been shown that 4,6-O-ethylidene-D-glucose [a glucose analogue known to interact only with the outward-facing binding site (Appleman & Lienhard, 1989)] and 2,5-anhydro-D-mannitol (a reduced fructose analogue) inhibited both 2-deoxy-D-glucose and D-fructose transport by GLUT2 (Colville *et al.*, 1993). While these data do indicate that the transport of D-fructose and D-glucose are mediated by the same exofacial binding site on GLUT2, it is not clear which of the ring forms of D-fructose are transported. In aqueous solutions, D-fructose exists predominantly (about 70%) in the pyranose form; 2,5-anhydro-D-mannitol is however, locked in the furanose form (Figure 3.10).

In order to address this, L-sorbose and 2,5-anhydro-D-mannitol, which are fructose analogues, were used to inhibit 2-deoxy-D-glucose transport by GLUT2. L-sorbose exists naturally predominantly in the pyranose ring form (>98%), whereas 2,5-anhydro-D-mannitol has a locked furanose ring. It was found that 2,5-anhydro-D-mannitol has a much lower K_i (26 mM) than L-sorbose (170 mM) (Figure 3.9), or D-fructose (200 mM) (Table 3.1), on 2-deoxy-D-glucose transport. This indicates that the furanose ring binds preferentially to GLUT2, since the two inhibitors are identical in other aspects (Figure 3.10). The low affinity of D-fructose itself is likely to be due to the fact that only 30% of the population are in the furanose form at any given point in time (Fry *et al.*, 1993). Thus, for fructose binding, hydrogen bonding at C-3 and C-4

positions are important, but not at C-2. Compared to the binding of D-glucose, the most significant difference is likely to be the absence of a hydrogen bond between the transporter and the C-1 position of D-glucose. This may account in part for the lower affinity of D-fructose for the transporter. A model depicting the interaction of β -D-fructofuranose with the exofacial binding site of GLUT2 is shown as Figure 3.11 (also Figure 4.4). It is interesting to note that the sequence QLS, which is highly conserved in transmembrane helix 7 of GLUTs 1, 3 and 4, which accept D-glucose with high affinity, is not present in those transporters which accept D-fructose, such as GLUT2, GLUT5, or the trypanosome transporter (Fry *et al.*, 1993). The QLS residues may therefore be involved in the hydrogen bonding to the C-1 position of D-glucopyranose.

3.5 Summary.

In conclusion, some kinetic properties of the human liver-type facilitative glucose transporter (GLUT2) have been analysed and the results compared with those obtained by Dr. Carol Colville with the brain-type transporter (GLUT3). These data show that GLUT3 has a significantly lower K_m for 2-deoxy-D-glucose than that recorded for GLUT2. The relative affinities of D-fructose and D-galactose for GLUT2 have also been determined, and the affinity of D-galactose for GLUT3 analysed by Dr. Carol Colville. These had been determined to be the major alternative substrates of these isoforms (Gould *et al.*, 1991). It was found that cytochalasin B is a non-competitive inhibitor of the transport of 2-deoxy-D-glucose and D-fructose uptake by GLUT2, and that the K_i values for inhibition of 2-deoxy-D-glucose and D-fructose are similar (about 7 μ M). Indeed, although GLUT3 had lower K_i values for cytochalasin B inhibition of 2-deoxy-D-glucose and D-galactose uptake, the K_i values were similar for both transported sugars (about 2 μ M).

These results suggest that the endofacial substrate binding sites used by 2-deoxy-D-glucose and D-fructose (GLUT2) or D-galactose (GLUT3) are similar or overlap. D-glucose and maltose are competitive inhibitors of both 2-deoxy-D-glucose and D-fructose transport by GLUT2, and 2-deoxy-D-glucose and D-galactose transport by GLUT3, suggesting that all transported sugars are likely to use the same exofacial sugar binding site on the transporter molecule. Furthermore, each of the alternative substrates for each isoform is a competitive inhibitor of 2-deoxy-D-glucose transport, and D-glucose is a competitive inhibitor of the transport of the alternative substrates. 2,5-anhydro-D-mannitol has a significantly lower K_i value than L-sorbose for inhibition of 2-deoxy-D-glucose transport by GLUT2, indicating that D-fructose is probably transported in the furanose ring form whilst D-glucose is transported in the pyranose ring form.

CHAPTER 4.

Analysis of the Structural Requirements of Sugar Binding to the Liver-type Glucose Transporter (GLUT2) Expressed in *Xenopus* Oocytes.

4.1 Aims.

1. To investigate the structural basis of sugar binding to GLUT2 using a range of hexoses, halogeno- and deoxy-glucose analogues to inhibit the transport of 2-deoxy-D-glucose by GLUT2 expressed heterologously in *Xenopus* oocytes.

2. To compare the results obtained for GLUT2 with those published for GLUT1 and GLUT4, and with GLUT3 in oocytes.

3. To produce a model for the interactions of D-glucose and D-fructose with the exofacial binding site of GLUT2.

4.2 Background.

Although GLUTs 1 to 4 all function to transport glucose, the nature of the glucose binding sites on these proteins are subtly different (Gould *et al.*, 1991; Colville *et al.*, 1993). For example, GLUT2 is able to mediate the transport of D-fructose quite efficiently as well as D-glucose. Additionally, although GLUTs 1, 2 and 3 all transport D-galactose (Gould *et al.*, 1991; Colville *et al.*, 1993), they do so with distinctly different K_m values. These and other observations suggest that the nature of the interaction of the transported sugars with the transport proteins may be different between isoforms.

Studies attempting to investigate the binding of glucose to the erythrocyte sugar transporter were performed in the early 1970s (Barnett *et al.*, 1973; Barnett *et al.*, 1975; Kahlenberg & Dolansky, 1972). It had been apparent for many years that glucose entry into cells was protein-mediated, as transport in erythrocytes, for example, was found to be saturable, stereospecific and bidirectional. D-glucose was proposed to reversibly bind to a specific protein site, translocate across the plasma membrane in an aqueous pocket by a protein conformational change, and be released into the cytoplasm from an endofacial site. The method of sugar transport was proposed to involve transient association between sugar hydroxyl groups and polar amino acid side-chains of the transporter (LeFevre, 1961). Therefore investigation of the importance of hydrogen bonding at these positions would involve studying relative binding after their removal or modification.

Such methods were employed to characterise the nature of the interaction of D-glucose with the exofacial binding site of GLUT1 (Barnett *et al.*, 1973; Kahlenberg & Dolansky, 1972). Derivatives of D-glucose were synthesised, altering each of the hydroxyl groups in turn. Epimers were

created by exchanging the axial hydroxyl groups for equatorial groups or *vice versa*, deoxy-analogues were produced by the removal of each hydroxyl group and different alkyl groups or halogeno-groups were also used as substituents.

Kahlenberg and Dolansky investigated the ability of these compounds to inhibit radiolabelled D-glucose uptake by isolated human erythrocyte membranes. In a parallel study, Barnett *et al.* measured inhibition constants, K_i 's, for the inhibition of uptake of radiolabelled L-sorbose into erythrocytes by these specifically substituted analogues of D-glucose. Measurements of K_i 's were preferential to K_m 's since the former gives a better description of the dissociation constant of the transporter exofacial binding site even when the rate of translocation is similar to the rate of formation of the sugar-protein complex (LeFevre *et al.*, 1971). L-sorbose had previously been shown to be taken up by erythrocytes, albeit with much lower affinity than D-glucose itself (LeFevre & Davies, 1951; Sen & Widdas, 1962). By using this sugar inhibitory effects with relatively weakly binding analogues could easily be measured. The ability of each analogue to inhibit L-sorbose uptake was investigated, not uptake of the analogue itself.

If a deoxy-analogue (D-glucose lacking a given hydroxyl group) has an impaired ability to bind to the transporter then that deoxy-sugar will inhibit L-sorbose uptake to a lesser extent than D-glucose. However, if the extent of inhibition is similar to that of D-glucose, then the absent hydroxyl group is unlikely to significantly inhibit the binding of D-glucose to the exofacial binding site.

The epimerisation of a group tells us about the spatial requirements of binding. For example, an epimer with a higher K_i for L-sorbose uptake than D-glucose indicates that the hydroxyl group has probably moved to a position which is not optimal for hydrogen bonding to the transporter. Hydrogen bond optimal distances vary depending on the particular hydrogen acceptor,

the average distance being 2.8Å (Stryer, 1981). It is also possible that the new position of the hydroxyl group might cause steric hindrance though this is less likely due to the hydroxyl group's small size.

Substitution of a hydroxyl with fluoride is a test of the directionality of a particular hydrogen bond. Due to their chemical nature, hydroxyl groups can act as hydrogen acceptors through the oxygen atom, or as hydrogen donors via the hydrogen moiety. Hence, consider a hydroxyl position which has proved to be important in transporter binding, i.e. the corresponding deoxy-analogue poorly inhibits L-sorbose transport. If an analogue with a fluoride substitution at this position restores the inhibition of L-sorbose to levels comparable to D-glucose then binding to the transporter has been restored. That would indicate that the hydrogen is donated by the transporter. Conversely, if the pattern of inhibition resembled that of the deoxy-analogue then the direction of the hydrogen bond would be predicted to be from the sugar hydrogen to some electronegative transporter residue side-chain. Of course, steric hindrance could also play a part in the lack of inhibition of L-sorbose binding by halogen analogues. This is unlikely for fluoride-substituted sugars, as fluoride is similar in size to the replaced hydroxyl group. However, the substitution of hydroxyl group by bromide or iodide groups might cause more steric problems. Steric effects can also be analysed by substitution with alkyl groups of various sizes for each of the sugar hydroxyl groups; with the aim of giving some indication of the shape of the exofacial binding site.

In an analysis of GLUT1, Barnett *et al.* found that the hydroxyl groups at the C-1 and C-3 positions and to a lesser extent, the C-4 and C-6 ring positions, were important for hydrogen bonding to GLUT1 although no single position was critical for binding (Barnett *et al.*, 1973). The binding of 1-deoxy-D-glucose to the transporter confirmed that sugars are transported in the

pyranose ring form. They discovered that a large substituent group could be added at positions C-4 and, to a lesser extent, at C-6 and C-3 without any further loss of affinity for the transporter. This indicated large spaces at these positions. These workers also noted that analogues with alkyl substituents at C-6 had a greater affinity for the transporter than D-xylose. D-xylose has identical stereochemistry to D-glucose except it lacks the $-\text{CH}_2\text{OH}$ at the C-5 position. Hence, it was postulated that hydrophobic interactions at the C-5/C-6 position were likely to be important in the binding of D-glucose. A model was constructed where glucose enters the transporter binding site C-1 first with the C-4 position last, utilising hydrogen bonding and hydrophobic interactions but forming no covalent bonds (Figure 4.1). A similar model was also proposed independently (Kahlenberg and Dolansky, 1972) who also found that substitution of the ring oxygen by sulphur led to a decrease in binding.

The model was reinforced by a later study (Barnett *et al.*, 1975) where it was found that D-glucose and L-sorbose entry into, and exit from erythrocytes was blocked by analogues with large C-4 and C-6 substituents only when present outside the cells. Moreover, analogues substituted at the C-1 position, such as propyl- β -D-glucopyranoside, were found to competitively inhibit exit of D-glucose but not affect entry (Barnett *et al.*, 1975). Hence, it was concluded that the transporter has two distinct asymmetric binding sites. Effects of the presence of various sugars on 1-fluoro-2,4-dinitrobenzene inactivation of the transporter showed that some sugars stimulated inactivation whilst others protected against inactivation, depending whether they bound the exofacial binding site or the endofacial one. It was concluded that the transporter undergoes a conformational change upon sugar binding from one asymmetric state to another, exposing or burying the 1-fluoro-2,4-dinitrobenzene inactivation site. The presence of two conformational states

had previously been proposed by other groups (Bowyer & Widdas, 1958; Krupka 1971; Krupka, 1972; Shimmin & Stein, 1970; Edwards, 1973).

This approach has also been used successfully to examine the nature of the binding site for glucose in insulin-stimulated rat adipocytes (GLUT4) (Holman *et al.*, 1981; Rees & Holman, 1981; Holman & Rees, 1982). The same techniques were used, measuring K_i values for the inhibition of radiolabelled D-allose uptake by substituted analogues of D-glucose. D-allose is the C-3 position epimer of D-glucose and has a relatively poor affinity for both GLUTs 1 and 4. Hence, as was the case with L-sorbose, relatively weak binding by an analogue can lead to a measurable decrease in D-allose uptake by GLUT4. To summarise their results, a model was predicted where the C-3 and C-4 hydroxyl groups are important for sugar/transporter interaction; there are hydrophobic interactions at C-6: and the ring oxygen also plays a part in transporter binding. Experiments were also performed with a series of 6-O-alkyl-D-glucose and 6-O-alkyl-D-galactose analogues in addition to propyl- β -D-glucopyranoside. Their behaviour with GLUT4 was found to be similar to that found with GLUT1 (Barnett *et al.*, 1975) in that these C-6 position substituents inhibited D-allose uptake only when present outside the cells, and propyl- β -D-glucopyranoside again had inhibitory effects only when preincubated with the cells so that it was present internally. So the final mode of D-glucose binding by GLUT4 was shown to be almost identical to that of GLUT1, where the sugar enters the exofacial binding pocket C-1 first and binds the endofacial binding site C-6 first during sugar exit. This general sugar orientation is predicted to vary little during transport, whilst conformational changes in the transporter cause the translocation of D-glucose across the membrane.

The results of a similar analysis of GLUT2, expressed heterologously in *Xenopus* oocytes is presented here. In addition, results obtained from parallel

experiments performed by Carol Colville with GLUT3 are shown, and models depicting the interaction of the substrate, D-glucose, with these different transporter isoforms are proposed.

4.3 Results.

In all the following analysis, the effects of different analogues of D-glucose on the transport of 2-deoxy-D-glucose into oocytes expressing GLUT2 have been measured. The transport of 100 μM radiolabelled 2-deoxy-D-glucose into oocytes was determined for 30 min (see section 2.4). It has previously been shown that under these conditions, the transport of 2-deoxy-D-glucose is rate limiting, and not its subsequent phosphorylation by hexokinase (Thomas *et al.*, 1993; Colville *et al.*, 1993). 2-deoxy-D-glucose was chosen as the substrate for this analysis since it is only partially metabolisable and because it has been shown to inhibit L-sorbose and D-glucose uptake by GLUT1 (Barnett *et al.*, 1973; Kahlenberg and Dolansky, 1972) and D-allose uptake by GLUT4 (Holman *et al.*, 1981) as well as D-glucose itself. These observations, together with the previous demonstration that 2-deoxy-D-glucose is transported with a lower K_m than other sugar analogues such as 3-O-methyl-D-glucose (Gould *et al.*, 1991; Colville *et al.*, 1993) all point to an insignificant role of hydrogen bonding at the C-2 position in the recognition of the transported sugar by all transporter isoforms (see below). Moreover, the use of 2-deoxy-D-glucose rather than 3-O-methyl-D-glucose enables an analysis of the outward-facing binding site of the transporter, since 2-deoxy-D-glucose is rapidly phosphorylated by hexokinase, and thus, unlike 3-O-methyl-D-glucose, is trapped inside the oocyte resulting in a negligible efflux

of sugar. Thus, the results of this study are interpreted in terms of inhibition at the exofacial binding site.

4.3.1 Effects of C-1 and C-2 Position Analogues on 2-Deoxy-D-glucose Transport.

The ability of 1-deoxy-D-glucose, D-mannose, 2-chloro-D-glucose and 2-deoxy-D-glucose to inhibit the transport of 0.1 mM radiolabelled 2-deoxy-D-glucose mediated by GLUT2 were examined. The results of this analysis are presented in Table 4.1. In this table and each of the others, results obtained for GLUT3 by Dr. Carol Colville are presented for the purpose of comparison.

4.3.2 Effects of C-3 Position Analogues on 2-Deoxy-D-glucose Transport.

The effects of C-3 position analogues on the transport of 2-deoxy-D-glucose by GLUT2 are shown in Table 4.2. The analogues studied were D-allose (the C-3 epimer of D-glucose), 3-deoxy-D-glucose, 3-bromo-D-glucose, 3-fluoro-D-glucose, 3-O-methyl-D-glucose and 3-O-propyl-D-glucose. Table 4.5 shows a comparison of the effects of both 2 mM and 10 mM 3-fluoro-D-glucose and 3-deoxy-D-glucose on transport mediated by GLUT2 and GLUT3.

4.3.3 Effects of C-4 and C-6 Position Analogues on 2-Deoxy-D-glucose Transport.

Table 4.3 shows the effect of D-galactose, maltose, cellobiose, lactose and 4,6-O-ethylidene-D-glucose on the transport of 2-deoxy-D-glucose by GLUT2. It has been established that GLUT2 transports D-galactose (Gould *et al.*, 1991; Burant & Bell, 1992) as does GLUT3, but note that the disaccharides are not

transported substrates, neither is 4,6-*O*-ethylidene-D-glucose (Barnett *et al.*, 1973; Holman *et al.*, 1981). Table 4.4 shows the effects of a range of C-6 position analogues on 2-deoxy-D-glucose transport.

Table 4.1

Groups of 6 oocytes expressing the transporter of interest were incubated in Barths buffer containing the competing sugar for approximately 5 min prior to the addition of [2,6-³H]2-deoxy-D-glucose (100 μM, 1 μCi/ml). Transport was determined for 60 min. After this time, the oocytes were washed and the radiolabel associated with each oocyte determined as described in section 2.4. The data shown above are from typical experiments, repeated at least twice for each analogue/transporter. Rates are expressed as a percentage of the rate measured in the presence of 10 mM L-glucose, and are the mean of six oocytes for each analogue (± SD). Note that the inclusion of L-glucose did not alter the transport rate compared to oocytes assayed in the absence of any other sugars. Values which are significantly different from the L-glucose rates (determined by an unpaired t-test) are indicated by *. Transport rates were between 3 and 5 pmoles/min/oocyte for both GLUT2 and GLUT3.

Table 4.1**Effects of C-1 and C-2 Position Analogues on 2-Deoxy-D-glucose Transport by GLUTs 2 and 3.**

Competing Sugar	2-deoxyglucose transport rate	
	GLUT2	GLUT3
10 mM L-glucose	100%	100%
10 mM D-glucose	24 ± 4%*	10 ± 2%*
10 mM 1-deoxy-D-glucose	109 ± 10%	104 ± 12%
10 mM 2-chloro-D-glucose	76 ± 5%*	42 ± 3%*
10 mM 2-deoxy-D-glucose	20 ± 2%*	12 ± 2%*
10 mM D-mannose	29 ± 3%*	14 ± 2%*

Table 4.2

The data shown is from a typical experiment, repeated at least two times for each analogue/transporter. In all cases, competing sugars were at 10 mM in the assay, and the assay conditions were as described in the legend to Table 4.1. Values which are significantly different from the L-glucose rates (determined by an unpaired t-test) are indicated by *.

Table 4.2**Effects of C-3 Position Analogues on 2-Deoxy-D-glucose Transport by GLUTs 2 and 3.**

Competing sugar (all at 10 mM)	2-deoxyglucose transport rate	
	GLUT2	GLUT3
L-glucose	100%	100%
D-glucose	18 ± 3%*	8 ± 2%*
3-deoxy-D-glucose	103 ± 12%	85 ± 7%
3-bromo-D-glucose	95 ± 10%	75 ± 4%*
3-fluoro-D-glucose	85 ± 5%*	14 ± 2%*
3-O-methyl-D-glucose	73 ± 6%*	17 ± 3%*
3-O-propyl-D-glucose	100 ± 12%	80 ± 7%
D-allose	59 ± 6%*	96 ± 7%

Table 4.3

The data shown is from a typical experiment, repeated at least two times for each analogue/transporter. Rates are expressed as a percentage of the rate measured in the presence of 10 mM L-glucose, and are the mean of at least six oocytes for each analogue (\pm SD). Values which are significantly different from the L-glucose rates (determined by t-test analysis) are indicated by *.

Table 4.3**Effects of C-4 Position Analogues on 2-Deoxy-D-glucose Transport by GLUTs 2 and 3.**

	2-deoxyglucose transport rate	
	GLUT2	GLUT3
Competing sugar		
10 mM L-glucose	100%	100%
10 mM D-glucose	17 ± 2%*	9 ± 2%*
10 mM D-galactose	110 ± 12%	57 ± 5%*
10 mM 4,6-O-ethylidene-D-glucose	102 ± 9%	73 ± 6%*
20 mM maltose	105 ± 8%	75 ± 7%*
20 mM lactose	110 ± 9%	112 ± 9%
20 mM cellobiose	113 ± 12%	82 ± 6%*

Table 4.4

The data shown is from a typical experiment, repeated at least two times for each analogue/transporter. Rates are expressed as a percentage of the rate measured in the presence of L-glucose, and are the mean of six oocytes for each analogue (SD was typically between 5 and 15%). Note however, that the concentration of competing sugars used in these analyses were 50 mM for GLUT2, and 25 mM for GLUT3. Values which are significantly different from the L-glucose rates (determined by an unpaired t-test) are indicated by *.

Table 4.4**Effects of C-6 Position Analogues on 2-Deoxy-D-glucose Transport by GLUTs 2 and 3.**

Competing sugar	2-deoxyglucose transport.	
	GLUT2	GLUT3
L-glucose	100%	100%
D-glucose	24 ± 5%*	10 ± 1%*
6-deoxy-D-glucose	33 ± 9%*	46 ± 7%*
D-xylose	106 ± 9%	78 ± 6%*
L-arabinose	138 ± 22%	63 ± 7%*
D-fucose	65 ± 18%*	25 ± 2%*
D-galactose	63 ± 7%*	16 ± 2%*
6-O -methyl-D-galactose	57 ± 10%*	109 ± 11%
6-O -propyl-D-galactose	n.d.	93 ± 17%
6-fluoro-D-galactose	50 ± 12%*	30 ± 9%*

Table 4.5

Comparison of the Inhibitions of 2-deoxy-D-glucose Transport mediated by GLUT2 and GLUT3 induced by C-3-substituted sugars.

Competing Sugar	Relative 2-deoxy-D-glucose transport (%)			
	GLUT2		GLUT3	
	2 mM	10 mM	2 mM	10mM
L-glucose	100	100	100	100
3-deoxy-D-glucose	102 ± 4	100 ± 5	101 ± 7	85 ± 7
3-fluoro-D-glucose	96 ± 5	85 ± 5	60 ± 6	18 ± 3

Transport of 2-deoxy-D-glucose was measured in oocytes expressing GLUT2 or GLUT3 as described in section 2.4. The extent of inhibition in the presence of either of two concentrations of 3-fluoro-D-glucose or 3-deoxy-D-glucose was determined and the result expressed as a percentage of the transport in the presence of an equal concentration of L-glucose. Results from a representative experiment are shown each value representing the mean ± SD for six oocytes at each point.

Figure 4.1

Model for the Interaction of β -D-Glucose with GLUT1.

A model for the hydrogen bonding of D-glucose to GLUT1 is shown as proposed by Barnett *et al.*. Hydrogen bonds are illustrated by dotted lines and the C-6 hydrophobic interactions are shown by a dashed area.

Figure 4.1

Model of the Interaction of β -D-Glucose with GLUT1.

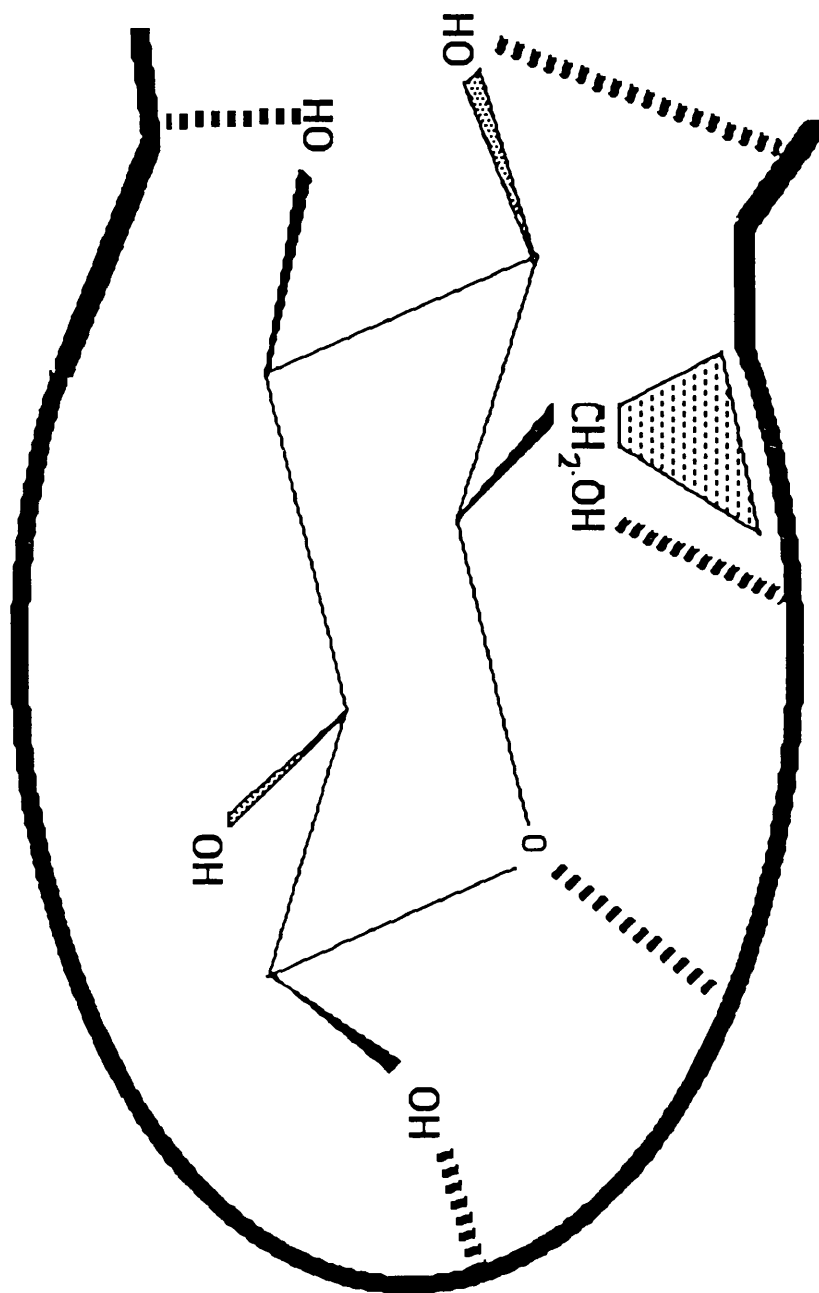


Figure 4.2

Model of the Interaction of β -D-Glucose with GLUT2.

A model for the hydrogen bonding of β -D-glucose to GLUT2 is illustrated. Hydrogen bonds are represented by dotted lines and the hydrophobic interaction between the transporter and the C-6 position methylene group is indicated by dashed lines.

Figure 4.2

Model of the Interaction of β -D-Glucose with GLUT2.

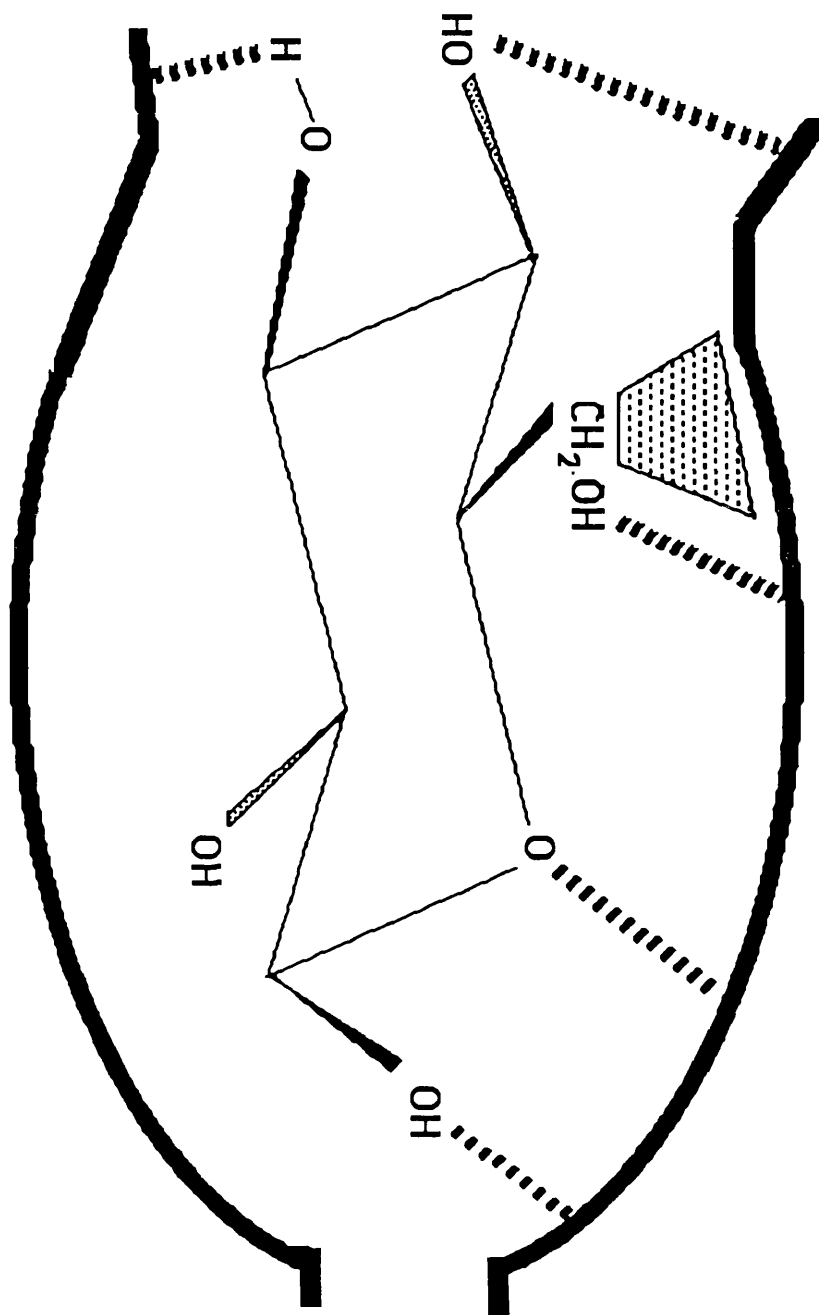


Figure 4.3

Model of the Interaction of β -D-Glucose with GLUT3.

A generalised model showing β -D-glucose binding to GLUT3. Note that the hydrogen bond at the C-3 position hydroxyl has a different nature to that of GLUT2. Also, the C-4 position hydrogen bond is likely to be less significant in substrate binding than with the other transporter isoforms since GLUT3 binds D-galactose, the C-4 epimer of D-glucose.

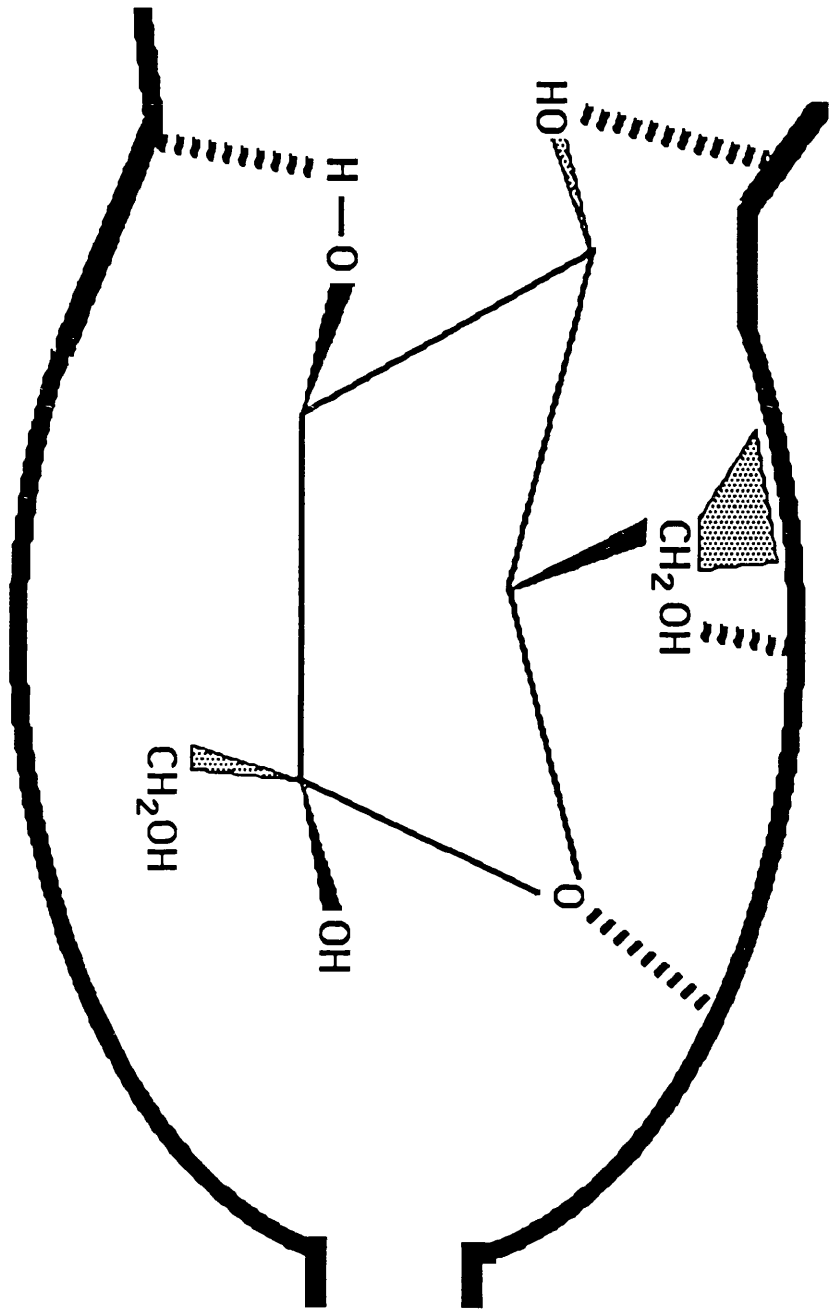
Figure 4.4

Model for the Interaction of β -D-Fructose with GLUT2.

The proposed interaction of the furanose ring form of β -D-fructose and GLUT2 is shown.

Figure 4.4

Model for the Interaction of β -D-Fructose with GLUT2.



4.4 Discussion.

The nature of the interaction of D-glucose with the various glucose transporters is proposed to involve hydrogen bonds between the sugar hydroxyl groups and polar side chains of the transporter. However, there might also be associations between water and the sugar binding site of the transporter. The dissociation constant for the D-glucose/transporter complex may also represent an equilibrium between solvated sugar in bulk solution, and sugar bound to the transporter. If the hydroxyl groups on the sugar are in the appropriate stereochemical configuration for binding, that is, they occupy the correct regions in space for interaction with the appropriate groups within the transporter binding site, then the activation energy required for binding will be reduced such that the equilibrium will lie towards transporter/sugar complex formation.

Analysis of the participation of each hydroxyl group can be examined by the effective replacement of that group by hydrogen (i.e. the deoxy-analogue). If a hydroxyl group important for binding is removed then the affinity of this analogue for the transporter will be significantly reduced. This sugar should inhibit the transport of 2-deoxy-D-glucose to a lesser degree than D-glucose itself does. Replacement of the hydroxyl with a strongly electronegative atom such as fluorine should restore the affinity of the sugar for the transporter if the protein is the hydrogen atom donor, but not if the that sugar hydroxyl group is the donor. To presume this it must be assumed that the stereochemistry is retained, and that the fluorine substituent is not too large, avoiding steric hindrance. The ability of fluoro-, alkoxy-, chloro- and bromo-substituted analogues, altered at specific sites in the hexose ring, to inhibit transport by GLUT2 have been examined.

Ideally, a complete analysis of the K_i values of each sugar analogue on 2-deoxy-D-glucose transport by GLUT2 into oocytes would have been performed. However, this was impractical due to the small amounts of some sugar analogues available for this study. Instead, the percentage inhibition of 2-deoxy-D-glucose transport by these analogues has been measured, and compared with the relative extents of inhibition using D-glucose and L-glucose within the same experiment. The extent of inhibition is a reflection of the K_i for the different analogues. When the K_i is high, the percentage inhibition will be small. It has previously been shown that at positions where hydrogen bonds appear important for the binding of D-glucose to GLUT1, substitution of a hydroxyl by hydrogen results in an approximate 10-fold increase in K_i (Kahlenberg and Dolansky, 1972; Barnett *et al.*, 1973).

It would also have been preferable to use a substrate such as L-sorbose or D-allose rather than 2-deoxy-D-glucose. These sugars have been shown to bind GLUT1 and GLUT4, respectively, with relatively poor affinity compared to 2-deoxy-D-glucose, so that inhibition by D-glucose analogues would give more measurable results. However, the expense of obtaining radiolabelled L-sorbose proved to be prohibitive.

The results of this analysis have been interpreted to reflect sugar interaction at the exofacial sugar binding site of the transporter molecule. This assumption is based upon the fact that changes in the rates of 2-deoxy-D-glucose transport are measured. Since this glucose analogue is phosphorylated by hexokinase and hence trapped inside the oocyte, the rate of sugar exit is assumed to be minimal. No significant accumulation of non-phosphorylated 2-deoxy-D-glucose has been observed in oocytes with concentrations of 2-deoxy-D-glucose far in excess of the 100 μM used in this analysis. This indicates that hexokinase is not rate limiting under these conditions (Thomas *et al.*, 1993; Colville *et al.*, 1993).

4.4.1 Binding at the C-1 Position.

10 mM 1-deoxy-D-glucose did not inhibit 2-deoxy-D-glucose transport to any significant extent by GLUT2. This suggests the presence of a hydrogen bond at this position in the transporter which is important for substrate recognition/binding. 20 mM 1-deoxy-D-glucose produced a small level of inhibition (less than 20%- data not shown). Therefore although the C-1 hydroxyl group is important, it is not essential for sugar transport. 1-deoxy-D-glucose has a ring which is locked in the pyranose form, indicating that, as was expected based on studies of GLUTs 1 and 4 (Barnett *et al.*, 1973; Rees & Holman, 1981), the pyranose form of glucose binds to the carrier. Similar results were found with GLUT3 (Table 4.1).

4.4.2 Binding at the C-2 Position.

Studies of GLUT1 have suggested that the C-2 position is not important for hydrogen bonding (Kahlenberg & Dolansky, 1972; Barnett *et al.*, 1973). This was also confirmed to be the case for GLUT4 (Rees & Holman, 1981). The affinity of 2-deoxy-D-glucose for both GLUT2 and GLUT3 is higher than that of 3-O-methyl-D-glucose, and β -D-mannose (the C-2 epimer of D-glucose) is as effective as D-glucose in inhibiting transport by both isoforms (Table 4.1; see also Gould *et al.*, 1991). Additionally, 2-chloro-D-glucose did not bind to the transporter with any greater affinity than 2-deoxy-D-glucose itself. This can be seen by comparing the inhibition of 0.1 mM 2-deoxy-D-glucose by 10 mM 2-chloro-D-glucose with the effective inhibition of 2-deoxy-D-glucose isotopically diluted to 10 mM (Table 4.1). The possibility that the reduction of affinity for the transporter caused by the chloride substitution, relative to 2-

deoxy-D-glucose, is due to steric hindrance cannot be ruled out. The space surrounding the C-2 position of GLUT1 was shown to be limited (Barnett *et al.*, 1973), so it is possible that this is also true in the case of GLUT2. However, the C-2 position is not important for binding to GLUT2, suggesting that hydrogen bonding at this position is unlikely to play a significant role in sugar binding. Again these results were identical to those obtained in a parallel analysis of GLUT3.

4.4.3 Binding at the C-3 Position.

See Table 4.2. 3-deoxy-D-glucose was found to be a poor inhibitor of 2-deoxy-D-glucose transport by GLUT2, indicating that hydrogen bonding at the C-3 position is important for sugar binding to this transporter. However, comparison of the extent of inhibition of transport in the presence of identical concentrations of either 3-deoxy-D-glucose or 3-fluoro-D-glucose indicated no significant difference in the affinity for GLUT2 (Tables 4.2 and 4.5). Unless the replacement of the hydroxyl with a fluoro-substituent has caused the analogue to be sterically incompatible with the binding site, then the relative lack of affinity for the transporter must be attributable to impaired hydrogen bonding. Therefore it is likely that the hydrogen bond formed at position C-3 is formed by donation of the hydrogen atom from the sugar hydroxyl, not from the transporter. The observation that 3-halogeno substituted sugars are better inhibitors of GLUTs 1, 3 and 4 than 3-deoxy-D-glucose (Barnett *et al.*, 1973; Rees & Holman, 1981; and Table 4.2) would suggest that steric constraints are unlikely, since binding to these transporters shows no steric hindrance. In addition, the fluoro-group is not much bigger than a hydrogen. Seemingly, the C-3 position hydroxyl is involved in hydrogen bonding of the transported sugar to GLUT2, but the nature of this hydrogen bonding is

unique, since 3-halogeno substituted sugars have higher affinity for the GLUTs 1, 3 and 4 than 3-deoxy-D-glucose.

D-allose, the C-3 position epimer of D-glucose, is an effective inhibitor of 2-deoxy-D-glucose transport by GLUT2 (Table 4.2). This is not the case with GLUTs 1, 3 or 4 (Barnett *et al.*, 1973; Rees & Holman, 1981; and Table 4.2). With GLUT2, the displacement of the C-3 hydroxyl in space has not reduced the affinity of the sugar for the transporter to the same extent as its removal, i.e. 3-deoxy-D-glucose. It is possible that the C-3 hydroxyl is able to weakly participate in hydrogen bonding in the allo-configuration. This does not appear to be the case with the other transporter isoforms.

3-deoxy-D-glucose was found to be a poor inhibitor of transport mediated by GLUT3 (Carol Colville, Table 4.2), indicating that the C-3 position is involved in hydrogen bonding. Replacement of the hydrogen with a fluoride restored the affinity of the analogue for the transporter, suggesting the direction of the hydrogen bond is such that the transporter is the hydrogen donor. Comparison of 2 mM and 10 mM 3-deoxy- and 3-fluoro-analogues (Table 4.5) demonstrate that the fluoro-analogue inhibits the rate of 2-deoxy-D-glucose transport to a greater extent than the deoxy-analogue. With GLUT2, the inhibition in the presence 3-deoxy-D-glucose was comparable to that with 3-fluoro-D-glucose at concentrations of 10 mM and 20 mM.

3-O-methyl-D-glucose and 3-O-propyl-D-glucose have been shown to bind to GLUTs 1, 3 and 4 and inhibit transport by these isoforms to a greater extent than 3-deoxy-D-glucose (Barnett *et al.*, 1973; Rees & Holman, 1981; and Table 4.2), presumably since hydrogen bonds at the C-3 position can still be formed. The C-3 position is able to accommodate relatively large substitutions before steric effects significantly effect binding with these isoforms. Although GLUT2 transports 3-O-methyl-D-glucose with reasonable

affinity (K_m for equilibrium exchange is 30 mM, Gould *et al.*, 1991) it has lower affinity for this sugar than GLUT3. Additionally, at the concentrations tested (10 mM), 3-O-propyl-D-glucose did not bind appreciably to GLUT2 at all. This confirms the difference observed in binding exhibited at the C-3 position between GLUT2 and the other transporter isoforms.

4.4.4 Binding at the C-4 Position.

4-deoxy-D-glucose was not available for this analysis. Instead, D-galactose, the C-4 position epimer of D-glucose was used. D-galactose is a transported substrate of GLUT2 having a K_m value of about 85 mM (see Table 3.1). However, no inhibition of 2-deoxy-D-glucose transport by GLUT2 was observed in the presence of 10 mM D-galactose (Table 4.3), in contrast to a marked inhibition in the presence of 10 mM D-glucose. A greater inhibition was observed by 50 mM D-galactose (Table 4.4). In contrast, GLUT3, which has a relatively high affinity for D-galactose (K_m of 8.5 mM), was effectively inhibited by 10 mM D-galactose, but to a significantly lesser extent than that measured in the presence of 10 mM D-glucose (Table 4.3). This is confirmed by comparison of the K_i values of D-glucose and D-galactose inhibition of 2-deoxy-D-glucose transport by GLUT3 (1.6 mM and 15.5 mM respectively, see Table 3.1). The interpretation of these results suggests the presence of a hydrogen bond between the C-4 position hydroxyl in the gluco-configuration of D-glucose and GLUT2, similar to the results proposed by Barnett *et al.* for GLUT1 (Barnett *et al.*, 1973) and confirmed for GLUT4 (Rees & Holman, 1981). However, the interaction of the C-4 position hydroxyl with GLUT3 seems to be much less important than with GLUTs 1, 2 or 4 since D-galactose is an effective inhibitor of transport. This result is consistent with the observed decreasing order of affinities of D-galactose reported to date, GLUT3 > GLUT1

> GLUT2 (Burant & Bell, 1992; Colville *et al.*, 1993). The model of D-glucose binding to the exofacial binding site of GLUT1 envisaged by Barnett *et al.* showed a large space at the C-4 position and hydrogen bonding to the C-4 hydroxyl was proposed to be relatively important but not vital. Perhaps the C-4 hydroxyl is required to the same extent in GLUT3 as the other isoforms, but the repositioning of the C-4 hydroxyl does not affect the interaction of D-galactose with GLUT3 because the stereochemistry of the appropriate bonding group of that transporter is such that hydrogen bonding is still possible although not to the extent as with D-glucose itself.

20 mM maltose, cellobiose and 4,6-*O*-ethylidine-D-glucose (which can be regarded as C-4 analogues of D-glucose) are not good inhibitors of 2-deoxy-D-glucose transport by GLUT2, unlike GLUT3 (Table 4.3). Maltose has been shown to be a competitive inhibitor of 2-deoxy-D-glucose transport by GLUTs 2 and 3, albeit with relatively high K_i values of 124 mM and 37 mM, respectively (Table 3.1). It is therefore likely that the regions of the exofacial binding sites of GLUTs 2 and 3 responsible for interacting with the C-4 position of the D-glucose, like that of GLUT1, each incorporate a relatively large 'space' which is able to accommodate bulky derivatives. Again, these results suggest that the model of Barnett *et al.* for GLUT1 where the sugar enters the binding site C-1 position first, with C-4 oriented such that it faces out of the sugar binding site, is also valid for both GLUT2 and GLUT3. This has also been proposed for GLUT4 (Holman & Rees, 1982).

4.4.5 Binding at the C-6 Position.

50 mM 6-deoxy-D-glucose is a good inhibitor of 2-deoxy-D-glucose transport by GLUT2 (Table 4.4). Likewise, 25 mM 6-deoxy-D-glucose is a good inhibitor of 2-deoxy-D-glucose transport by GLUT3. This suggests that

hydrogen bonding at the C-6 position with either isoform is not crucial for transport. Nevertheless, the lower affinity of 6-deoxy-D-glucose than D-glucose itself does suggest the presence of a hydrogen bond at this position. The same concentration of D-xylose (which lacks the C-5 hydroxymethyl group of D-glucose) elicited significantly less inhibition than 6-deoxy-D-glucose with GLUT2 and GLUT3. The potential for hydrophobic interactions between the transported sugar and the protein around the C-6 position has been suggested for GLUT1 (Barnett *et al.*, 1973). The above results support a similar interaction between D-glucose and GLUTs 2 and 3.

A similar pattern of inhibition was seen using a series of C-6 substituted analogues of D-galactose to inhibit 2-deoxy-D-glucose transport by GLUT2. 50 mM D-galactose itself produced a measurable level of inhibition and was used as a standard to compare with inhibition by L-arabinose (D-galactose without the C-5 hydroxymethyl group), D-fucose (6-deoxy-D-galactose), 6-O-methyl-D-galactose, and 6-fluoro-D-glucose. Replacement of the C-6 hydroxymethyl group with a hydrogen (L-arabinose) resulted in a complete loss of affinity for the transporter. In contrast, removal of the C-6 hydroxyl group (D-fucose) resulted in no loss of affinity for the transporter relative to D-galactose itself. This suggests that a C-5 substituent is important for binding, and hydrogen bonding plays comparatively little part. Addition of methyl and fluoro- substituents to the C-6 hydroxyl did not lead to any significant decrease of inhibition of 2-deoxy-D-glucose transport relative to D-galactose or any significant increase relative to D-fucose. This again suggests the unimportance of the C-6 hydroxyl and also shows that a methyl group can be accommodated at this position by GLUT2. Unfortunately, insufficient 6-O-propyl-D-galactose was available to test the size of the pocket at this position.

Similar results were obtained for GLUT3 (Carol Colville). In this case, D-galactose is a better inhibitor of transport (consistent with the less

significant role of the gluco-C-4 in hydrogen bonding suggested above). As can be seen in Table 4.4, inhibition of 2-deoxy-D-glucose transport by 25 mM D-fucose than is slightly less than that observed with 25 mM D-galactose, but 25 mM L-arabinose is a significantly weaker inhibitor than D-fucose itself. Again this suggests that hydrophobic interactions are more important than hydrogen bonding at this position with GLUT3, at least when the C-4 hydroxyl is in the galacto-conformation.

One notable difference between the isoforms is that 6-O-methyl-D-galactose is not an effective inhibitor of GLUT3 but is with GLUT2 (Table 4.4). Similar studies by this group also suggest that 6-O-methyl-D-galactose is a better inhibitor of 2-deoxy-D-glucose than D-galactose itself (Colville *et al.*, 1993b), however this result is in contrast to the results of Holman & Rees (1981) who found that 6-O-methyl-D-galactose was a poor inhibitor of GLUT4. Presumably, the alkoxy-analogues are not effective inhibitors of GLUT3 due to steric considerations, and the space might be larger at this position of the GLUT2 exofacial binding site.

4.4.6 Models of the Interaction of β -D-Glucose with the Exofacial Binding Sites of GLUT2 and GLUT3 .

Transport of glucose is restricted to the β -D-enantiomer, since L-glucose does not bind appreciably to any known transporter. β -D-glucose has also been proposed to be transported in the pyranose ring form (LeFevre, 1961). In addition, it has been noted that the most favourable conformation consists of a ring in the 4C_1 chair conformation with the hydroxyls in the equatorial position (Kahlenberg & Dolansky, 1972). Models for the interaction of β -D-glucopyranose with GLUT2 and GLUT3 are presented in Figure 4.2 and 4.3, respectively. These are based on the data obtained in this chapter and the

model of the GLUT1/D-glucose complex proposed by Barnett *et al.* (Figure 4.1) is included for comparison. For both GLUT2 and GLUT3, some degree of hydrogen bonding between the C-1, C-3 and C-4 positions is indicated by the results presented above. One significant difference between the action of the transporters involves the direction of the hydrogen bond at the C-3 position of GLUT2 compared to GLUTs 1, 3, or 4 (see above; Barnett *et al.*, 1973; Rees & Holman, 1981). Another notable difference between transporter isoforms is hydrogen bonding at the C-4 position. This position plays a relatively minor role in sugar binding by GLUT3, consistent with the ability of this transporter to transport D-galactose, the C-4 epimer of D-glucose, with relatively high affinity.

The ability of 6-deoxy-D-glucose to inhibit 2-deoxy-D-glucose uptake by both GLUT2 and GLUT3 suggests that hydrogen bonding is not important at the C-6 position of either isoform. Hydrophobic interactions have been established using a series of C-6 D-galactose analogues. Since D-fucose is as effective as D-galactose in inhibiting glucose transport, hydrophobic interactions at this position seem to be more important than hydrogen bonds. Similar results have also been obtained for GLUTs 1 and 4 (Barnett *et al.*, 1973; Rees & Holman, 1981).

A proposed model for the interaction of β -D-fructose and the exofacial binding site of GLUT2 is shown in Figure 4.4. This is based on the model for D-glucose binding to GLUT2 and results obtained with D-fructose analogues (section 3.3.2). These suggest that D-fructose binds and is transported by GLUT2 in the furanose ring form. Hydrogen bonding at the C-3 and C-4 positions are probably important, but not at C-2. Compared to the binding of D-glucose, the most significant difference is likely to be the absence of a hydrogen bond between the transporter and the C-1 position of D-glucose.

This model is reasonably speculative and more fructose-analogue studies need to be carried out to investigate whether this model is correct.

4.5 Summary.

The patterns of hydrogen bonding of β -D-glucose to GLUT2 and GLUT3 (Carol Colville) have been investigated. The results indicate that hydrogen bonding at the C-1, C-3 and C-4 positions occur during glucose binding and transport, and that hydrophobic interactions between the C-6 position of the sugar and each transporter also occur. Slight differences in the pattern of binding were found between isoforms, as was predicted by the individual specific range of substrates transported by each isoform.

CHAPTER 5.

Analysis of the Role of Putative Transmembrane Helix 8 in GLUT3, the Brain- Type Transporter.

5.1 Aims.

1. To use Site-directed mutagenesis and Recombinant Polymerase Chain Reaction (PCR) technology to construct a series of nineteen mutant GLUT3 cDNAs. These will contain single codon changes such that each cDNA will encode a protein with a particular amino acid, located in putative transmembrane helix 8, altered to alanine.
2. These transporter cDNAs will then be used as a template for *in vitro* synthesis of mRNA which will be injected into *Xenopus* oocytes.
3. By investigating the transport kinetics of each mutant in relation to kinetics of wild-type GLUT3, it should be possible to determine whether or not each amino acid residue is directly involved in sugar uptake.

5.2 Introduction.

5.2.1 Structure-Function Analyses of GLUT1 using Mutagenic Techniques.

Specific substitution of individual amino acids in protein sequences has recently emerged as a powerful tool for the investigation of reaction mechanisms. The availability of the cloned cDNAs for each of the sugar transporters and powerful expression systems (such as *Xenopus* oocytes), allow the expression of heterologous transporter proteins, providing an excellent basis for the investigation of transporter structure and function by the mutagenesis of specific amino acid residues. Residues of interest can be changed to determine whether they are functionally important, a loss of transport activity or a perturbation of certain ligand binding indicating that they are somehow involved in the transport process. Obviously, residues are not chosen randomly for mutagenesis. Those which are invariant, i.e. they occur at the same position in all transporter isoforms, or at least highly conserved are good candidates (for example see Figure 5.1.a). The bulk of mutagenic studies of this nature have been carried out on GLUT1.

5.2.1.1 Substitution of Conserved Polar Residues.

Conserved polar residues in the transmembrane helices are prime targets for substitution since they are most likely to interact with glucose, especially if they are capable of forming hydrogen bonds. Hydropathy analysis of the sequence of GLUT1 (Mueckler *et al.*, 1985) predicts that putative transmembrane helices 3, 5, 7, 8, and 11 are moderately amphipathic and have been proposed to bundle together forming a protein pore, enabling glucose to traverse the membrane through a polar environment. These helices contain

several conserved serine, threonine, asparagine, glutamine, and tyrosine residues which have polar side chains capable of hydrogen bonding with D-glucose.

The bis-mannose derivative, ATB-BMPA, which has been shown to interact specifically with the transporter exofacial binding site (section 1.7.2), has been shown to bind in the proximity of putative transmembrane helices 7 and 8 (Davies *et al.*, 1991). In addition, helices 7 and 8 contain many conserved polar residues, for example helix 7 contains the motif, QXSGXNXXYY.

Three of these residues in GLUT1 were substituted in one study: asparagine-288 (Asn²⁸⁸) and glutamine-282 (Gln²⁸²), in transmembrane helix 7, were replaced by isoleucine (Ile) and leucine (Leu), respectively (Hashiramoto *et al.*, 1992). In transmembrane helix 8, asparagine-317 (Asn³¹⁷) was replaced by isoleucine. It was discovered that the Asn²⁸⁸ -> Ile and Gln²⁸² -> Leu mutants exhibited 2-deoxy-D-glucose uptakes reduced to about 50% of wild-type levels. Although all three clones were labelled by cytochalasin B at levels equivalent to wild-type GLUT1, only the two asparagine mutants were labelled with ATB-BMPA at levels comparable with wild-type. The Gln²⁸² -> Leu mutant was labelled at only 5% of wild-type levels. Also the K_i value for 4,6-O-ethylidene-D-glucose inhibition of 2-deoxy-D-glucose transport increased from about 12 mM for wild-type GLUT1 to 120 mM for this mutant alone. Both these findings pointed to the fact that glutamine-282, which is located in putative transmembrane helix 7, is located in the exofacial binding site. The lack of perturbation of cytochalasin B binding in relation to wild-type levels suggests that, as postulated, the exofacial and endofacial glucose binding sites are structurally distinct (see chapter 1).

A similar approach was adopted to investigate the properties of conserved GLUT1 residues Asn¹⁰⁰, Gln¹⁶¹, Gln²⁰⁰, Tyr²⁹², and Tyr²⁹³

(Mueckler *et al.*, 1994a) which were sequentially replaced by various hydrophobic or polar residues. 2-deoxy-D-glucose transport was largely impaired only with the substitution of Gln¹⁶¹, which is located in transmembrane helix 5. Replacement of this residue with leucine or asparagine reduced 2-deoxy-D-glucose transport into *Xenopus* oocytes by 50-fold and 5-fold, respectively, when compared with wild-type GLUT1 transport levels. Further characterisation of the Gln¹⁶¹ → Asn mutant revealed that although no alteration of K_m for zero-*trans* entry of 2-deoxy-D-glucose was detected, the turnover number was decreased by 7.5-fold and the K_i for binding the exofacial ligand 4,6-O-ethylidene-D-glucose was increased by 18-fold. The authors concluded from these data that Gln¹⁶¹ must comprise part of the exofacial binding site of GLUT1, since the affinity for 4,6-O-ethylidene-D-glucose is greatly reduced, but the rate-limiting conformational changes of sugar translocation must also be affected since the transport rate is also markedly reduced.

GLUT4 residues Tyr²⁸, Tyr¹⁴³, Tyr²⁹², Tyr²⁹³, Tyr³⁰⁸, and Tyr⁴³² have all individually been substituted with phenylalanine (Wandel *et al.*, 1994). It was found that their subcellular distribution and expression levels when transiently expressed in COS-7 cells were comparable with wild-type levels. [¹²⁵I]IAPS-forskolin binding was not affected by each mutation. Glucose transport activity was reduced in the Tyr¹⁴³ and Tyr²⁹³ mutants but not in any of the others. Cytochalasin B binding was reduced with the Tyr¹⁴³, Tyr²⁹² and Tyr²⁹³ mutants. The authors concluded that Tyr¹⁴³ and Tyr²⁹³ might be important for transporter function and that Tyr²⁹² might be part of the cytochalasin B binding site.

Another residue which appears to be important is asparagine-415 in transmembrane helix 11 of GLUT1, as indicated by the mutation, Asn⁴¹⁵ → Asp (Ishihara *et al.*, 1991), which severely impaired transport activity.

However, this loss of activity might be due to a perturbation of transporter tertiary structure caused by the introduction of a positive charge into a membrane-spanning helix.

5.2.1.2 Substitution of Conserved Tryptophan Residues.

Attention was again drawn to transmembrane helix 11 by a study investigating the effects of sequentially mutating all the tryptophan residues in GLUT1 to glycine or leucine (Garcia *et al.*, 1992). The rationale for this approach was that a tryptophan residue has been implicated as being near the cytochalasin B binding site. Only the Trp³⁸⁸ -> Leu and Trp⁴¹² -> Leu mutants showed any disruption of transport activity in *Xenopus* oocytes. Immunolabelling with confocal microscopy showed that the targeting of the Trp³⁸⁸ -> Leu mutant to the plasma membrane was impaired, accounting for most of the reduction of transport associated with this mutant. Western blotting of plasma membranes showed that the Trp⁴¹² -> Leu mutant, however, was expressed at the same quantities as wild-type transporter levels, and therefore loss of 2-deoxy-D-glucose transport was attributed to a loss of intrinsic activity. A dose response of the ability of cytochalasin B to inhibit 2-deoxy-D-glucose transport by the Trp³⁸⁸ -> Leu mutant showed a decrease in affinity of that mutant for cytochalasin B relative to wild-type levels. The authors concluded that Trp⁴¹², which is located in transmembrane helix 11, might comprise part of the aqueous channel utilised for the passage of D-glucose, and that Trp³⁸⁸, in helix 10, must comprise part of, or lie near to, the endofacial glucose binding site.

Parallel studies were carried out investigating the Trp⁴¹² -> Leu (Katagiri *et al.*, 1991) and Trp³⁸⁸ -> Leu (Katagiri *et al.*, 1993) mutations. These workers observed that the 2-deoxy-D-glucose transport was reduced to 15-30%

of wild-type levels with the Trp⁴¹² mutant, displaying a 2.5-fold increase in K_m and a 3-fold decrease in turnover number. ATB-BMPA binding of this mutant was identical with wild-type GLUT1, but cytochalasin B labelling was 40% lower, contrasting to the results of Garcia *et al.*. Since Trp³⁸⁸ had been proposed to be involved in forskolin binding (Wadzinski *et al.*, 1990), Katagiri *et al.* tested this hypothesis by attempting to photoaffinity-label this mutant with [¹²⁵I]IAPS-forskolin. It was discovered that this residue was not photolabelled, but 3-*O*-methyl-D-glucose zero-*trans* entry was impaired, with an increase in K_m and decrease in turnover number relative to wild-type. In contrast, zero-*trans* exit was not altered. These authors concluded that this residue is not the site of forskolin binding, but subsequent cytochalasin B labelling experiments showed that labelling was reduced relative to wild-type GLUT1 (Inukai *et al.*, 1994). However, contrary to the result of Garcia *et al.*, no decrease in targeting to the plasma membrane was observed with the Trp³⁸⁸ mutant. This work was followed by a study in which both Trp⁴¹² and Trp³⁸⁸ were altered to leucine in the same GLUT1 protein (Inukai *et al.*, 1994). Glucose transport was reduced to similar levels as found with the Trp⁴¹² mutant. Cytochalasin B labelling of the Trp⁴¹²Trp³⁸⁸ mutant was abolished and cytochalasin B binding reduced to 30% of wild-type levels. These authors concluded that cytochalasin B binds to GLUT1 in the helix 10-11 region and can covalently bind to the transporter by photolabelling at either residue Trp⁴¹² or Trp³⁸⁸.

Similarly, the mutation of Trp⁴¹⁰ of GLUT3 has been reported (Burant & Bell, 1992). This mutation led to a large loss of 2-deoxy-D-glucose transport activity relative to wild-type GLUT3 when expressed heterologously in *Xenopus* oocytes.

5.2.1.3 Substitution of Conserved Proline Residues.

Diverse studies investigating both the protection of GLUT1 from proteases by ligand binding, and the quenching of tryptophan fluorescence by D-glucose transport and specific ligands by GLUT1, have suggested that the conformational change associated with sugar transport is sufficiently large that it cannot be accounted for by localised movement of amino acid side-chains alone (reviewed in Gould & Holman, 1993). Molecular modelling and molecular dynamics techniques suggest that transmembrane helix 10 of GLUT1 may undergo large conformational changes which could account for the ability of the transporter to assume two distinct glucose-binding conformations (Gould and Holman, 1993). The same modelling predicts that Pro³⁸³, Pro³⁸⁵ and Pro³⁸⁷ would probably act as the pivot necessary for this conformational change. The putative transmembrane domains of several membrane transporters are reported to contain a larger number of membrane-buried proline residues than other integral membrane proteins which do not function as transporters (Brandl & Deber, 1986) and the *cis-trans* isomerism of these prolines could provide the transporter with sufficient flexibility to undergo conformational change.

Pro³⁸⁵ has been substituted with isoleucine, alanine, glutamine or glycine (Tamori *et al.*, 1994; Wellner *et al.*, 1994b). Tamori *et al.* found that transport activity was markedly reduced by substitution with isoleucine but unaffected by substitution by glycine. In addition ATB-BMPA labelling was abolished in the Pro³⁸⁵-> Ile mutant relative to wild-type GLUT1, but cytochalasin B labelling was unaltered, suggesting that this mutant transporter is locked into an inward-facing conformation.

Substitution of Pro³⁸⁵, Pro³⁸³ and Pro³⁸⁷ with alanine had no effect on transport activity, but substitution of any of these residues with glutamine

almost abolished transport activity (Wellner *et al.*, 1994b). It therefore appears that the substitution of one of these proline residues with an amino acid possessing a large side-chain hinders transport and presumably transporter conformational changes, but substitution of a single proline with an amino acid possessing a small side-chain does not affect transport. Tamori *et al.* suggested that the substitution of Pro³⁸⁵ with glycine did not affect transporter operation since glycine's side chain is small enough not to hinder mobility of the adjacent Pro³⁸³ and Pro³⁸⁷ residues, unlike that of isoleucine. Presumably the effects of substitution of either of Pro³⁸³ and Pro³⁸⁷ with alanine (Wellner *et al.*, 1994b) did not affect the mobility of the remaining two prolines.

Three proline residues in GLUT1 helix 6 are conserved in the other transporter isoforms, with the exception of GLUT2. The effects of substituting GLUT1 residues Pro¹⁸⁷, Pro¹⁹⁶ and Pro²⁰⁵ with either alanine or the equivalent GLUT2 residue, histidine, arginine or phenylalanine, respectively, have also been investigated (Wellner *et al.*, 1994b). None of these mutants displayed any differences in transport activity with respect to wild-type levels except the Pro¹⁹⁶-> Arg mutant, which caused a decrease in transport activity. This might be due to the insertion of a polar amino acid into a non-polar environment, but this residue occurs naturally in GLUT2. It is possible that the presence of the arginine residue in GLUT2 might contribute to its lower affinity for transported substrates by destabilising the protein, though this is unlikely.

5.2.1.4 Substitution of GLUT1 Cysteine Residues.

Cysteine residues have been postulated to be involved in protein conformational stability (reviewed by Walmsley, 1988; Carruthers, 1990) and also might have a role in oligomerisation of glucose transporters (Herbert &

Carruthers, 1992). Wellner *et al.* instituted the following changes by site-directed mutagenesis into six different GLUT1 proteins: Cys¹³³ -> Ser, Cys²⁰¹ -> Gly, Cys²⁰⁷ -> Ser, Cys³⁴⁷ -> Ser, Cys⁴²¹ -> Arg, and Cys⁴²⁹ -> Ser (Wellner *et al.*, 1994a). None of these mutants exhibited any perturbation of transport activity. Binding of the thiol-group-reactive reagent *p*-chloromercuribenzenesulphonate (pCMBS) to either the endofacial or exofacial surface of plasma membranes containing these mutants showed that only Cys⁴²⁹, in the sixth external loop, and Cys²⁰⁷, in the large intracellular loop, are the residues which are involved in the inhibition of transport by various thiol-group-reactive agents.

5.2.1.5 Substitution of Residues Predicted to Lie in Extramembranous Loops.

Not all studies are restricted to the transmembrane helices. It has been demonstrated that the substitution of Asn⁴⁵ by Asp, Trp or Gln abolished *N*-linked glycosylation of GLUT1 (Asano *et al.*, 1991), and that this led to a 2-fold loss of affinity for D-glucose. Therefore, this raises the possibility that the glycosylation state of the transporter affects its ability to transport glucose. Thus, in systems such as *Xenopus* oocytes where the glycosylation pattern of heterologously expressed transporters has been shown to be different from that found in native cells, the kinetic parameters of transport may be affected.

The C-terminal cytoplasmic domain has also been implicated in sugar transport. In an important study, Oka *et al.* showed that the deletion of the C-terminal 37 amino-acids of GLUT1 resulted in a transporter which lost all transport activity and appeared to be locked into an inward-facing conformation, since ATB-BMPA binding was abolished but cytochalasin B was still able to bind (Oka *et al.*, 1990). Removal of only the last 12 amino acids had no effect on GLUT1 activity (Lin *et al.*, 1992), so one region of the

GLUT1 sequence responsible for proper activity must lie between residues 460 and 480. Since the C-terminal domain is very variable in length and sequence between transporter isoforms, Katagiri *et al.* decided to test whether this region accounts for the difference in transporter kinetics between GLUTs 1 and 2 (Katagiri *et al.*, 1992). GLUT2 had previously been shown to have much higher K_m and V_{max} values than other isoforms (Craik & Elliot, 1979; Johnson *et al.*, 1990; Bell *et al.*, 1990), and bind cytochalasin B with a K_d in the order of 10-fold higher than GLUT1 (Axelrod & Pilch, 1983). Katagiri *et al.* expressed a GLUT1 clone in Chinese hamster ovary cells which had its C-terminal domain replaced with that of GLUT2. This chimera displayed 3.8-fold increase of K_m and a 4.3-fold increase in V_{max} values for 2-deoxy-D-glucose uptake compared to wild-type GLUT1. However, the K_d value for cytochalasin B binding was unchanged relative to GLUT1. This suggests that the C-terminal domain might at least partially confer some of the kinetic properties specific to each isoform, although how this is achieved is unknown.

5.2.1.6 Naturally-Occurring Mutations.

Two polymorphisms in the GLUT2 gene that result in amino acid changes have recently been described (Tanizawa *et al.*, 1994). One of these, Thr¹¹⁰ -> Ile, has been found at equal frequencies in patients with non-insulin-dependent diabetes (NIDDM) and control subjects. In all other members of the facilitative glucose transporter family, residue-110 is normally isoleucine. The other polymorphism, Val¹⁹⁷-> Ile, was discovered in one female patient with gestational diabetes, who recovered after pregnancy. Both these mutations were individually created in plasmid encoded GLUT2, and expressed in *Xenopus* oocytes (Mueckler *et al.*, 1994b). The Thr¹¹⁰ -> Ile

mutant had identical 2-deoxy-D-glucose transport activity to wild-type GLUT2, but the Val¹⁹⁷-> Ile mutation completely abolished 2-deoxy-D-glucose transport. This is surprising given the conservative nature of the substitution, but the increased size of the isoleucine side chain relative to the wild-type residue may block the transport of glucose. Interestingly, in GLUT1, Val¹⁶⁵ was also altered to isoleucine, again resulting in a large loss of transport activity. This residue is predicted to lie one helical turn from the conserved residue Gln¹⁶¹ which is also important in transport (Mueckler *et al.*, 1994a).

5.2.1.7 Mutations Induced in the Yeast SNF3 Transporter.

The yeast glucose transporter, SNF3, which is structurally related to the mammalian glucose transporter family, has also been mutated (Marshall-Carlson *et al.*, 1990). Mutations included substitutions of two conserved glycine residues located in transmembrane helices 1 and 2, which correspond to Gly²⁷ and Gly⁷⁵ of GLUT1, with Asp and Arg, respectively. The effect of each mutation resulted in a transporter which was not targeted to the plasma membrane. This is either due to the importance of the glycine residues, or the effects of inserting a polar or charged amino acid into a hydrophobic environment, or both. Replacement of the non-conserved helix 8 residue, Val⁴⁰², with Ile caused a large decrease in the protein's transport ability. This is somewhat surprising, considering both the lack of conservation of this residue between different transporters and the conservative nature of the substitution. It also contrasts strongly with the substitution of GLUT1 helix 8 residue Asn³¹⁷, which has no observed effects (Hashiramoto *et al.*, 1992).

5.2.2 Transmembrane Helix 8.

Although hydropathy analysis predicts twelve transmembrane helices in GLUT1 and the other members of the glucose transporter family, only five are predicted to be amphipathic. These are helices 3, 5, 7, 8 and 11. Helices 7 and 11 have been implicated in sugar binding and translocation by ligand binding and mutagenesis studies with GLUT1 (see above). These two helices are proposed to lie in close proximity in transporter tertiary structure, perhaps forming a sugar binding cleft. Helix 8 obviously lies next to the supposedly important helix 7 in transporter tertiary structure due to the short length of the stretch of connecting residues. Helices 7 and 8 have been proposed to be the photolabelling site of the exofacial-specific ligand ATB-BMPA (Gould & Holman, 1993). Helix 8 also contains several residues conserved throughout the glucose transporter family, including one tyrosine, one asparagine and two threonines (Figure 5.1.a), of which Thr³⁰⁸, Asn³¹⁵ and Thr³¹⁹ (GLUT3 residue numbers) are predicted to lie on the polar face of the putative transmembrane helix (Figure 5.1.b).

To investigate the importance of these residues, an approach was utilised that was identical to that used to investigate various residues in GLUT1, namely site-directed mutagenesis. Each residue in putative helix 8 of GLUT3 was sequentially altered to alanine.

GLUT3 was chosen in preference to GLUT1 simply due to the relative lack of investigation of this isoform. GLUT3 also has distinct advantages over GLUT2 as a template for amino acid substitution. Firstly, any alteration of transport kinetics induced by mutagenesis would be more measurable in the case of GLUT3, since it displays a relatively low K_m value for zero-*trans* 2-deoxy-D-glucose entry into *Xenopus* oocytes compared to that of GLUT2. Secondly, the inhibitory effects cytochalasin B on 2-deoxy-D-glucose transport

by GLUT3 have been demonstrated to be greater than by GLUT2, suggesting tighter binding to GLUT3. Again, any perturbation of cytochalasin B binding, induced by mutagenesis, should be more easily measurable in the case of GLUT3. A third concern is that, to date, successful photolabelling of GLUT2 by cytochalasin B has not been reported, except under vastly modified conditions (Axelrod & Pilch, 1983). Immunoprecipitation of GLUT2 is also problematical (Jordan & Holman, 1992; and Gwyn Gould, personal communication). In order to calculate the quantity of mutant or wild-type transporters expressed in oocyte plasma membrane fractions by comparative immunoblotting procedures, a standard sample of protein with a known concentration of transporter is required. The concentration of transporter in this sample also requires to be quantified. This would typically be attained by performing an equilibrium binding study with [³H]cytochalasin B, in the presence of various concentrations of non-labelled cytochalasin B, with D-glucose present or absent. The number of available D-glucose-sensitive cytochalasin B binding sites, which is equivalent to the number of transporters, would then be calculated by Scatchard analysis. This can be performed successfully with GLUT3, but not GLUT2 since the K_d of GLUT2 for cytochalasin B is so high (1.7 μ M- Axelrod & Pilch, 1983) that concentrations required for equilibrium binding studies exceed the solubility limit of cytochalasin B in aqueous solution (about 50 μ M).

5.3 Mutagenesis, Subcloning and Sequencing of cDNA.

Two very different methods have been used for the production of mutant GLUT3 cDNAs, each differing from wild-type GLUT3 sequence by 1-3

base pairs, encoding a single amino acid change from a particular transmembrane helix 8 residue to alanine.

One method was site-directed mutagenesis, using Amersham's "RPN 1526 Oligonucleotide Directed Mutagenesis kit".

The second method used was the recombinant polymerase chain reaction (PCR) technique, using sets of primers incorporating the mutations to be introduced into the GLUT3 cDNA.

5.3.1 Vectors.

There are several vectors incorporating cDNAs, each encoding individual members of the human facilitative transporter family (GLUT) available in the laboratory. These have been described in section 2.5.1. These cDNAs are linearised by restriction digestion (section 2.5.2) and used as templates for the synthesis of transporter mRNAs to be injected into *Xenopus laevis* oocytes. In this chapter, only mutagenic techniques carried out using GLUT3 cDNA as a template will be discussed.

Two constructs have been used - M13mp18GT3 and pSPGT3, which are constructs with GLUT3 cDNA cloned into the multiple cloning sites of M13mp18 and pSP64T (described by Kayano *et al.*, 1990), respectively. These are shown in diagrammatic format in Figures 2.2 and 2.3. In pSPGT3, the GLUT3 cDNA is under the transcriptional control of the powerful SP6 promoter. SP6 RNA polymerase is commercially available.

5.3.2 Site-directed Mutagenesis.

The method used for site-directed mutagenesis utilised the Amersham "Sculptor *in vitro* mutagenesis system- RPN 1526" kit. The basis of this

method is shown in Figure 5.2 (see also section 2.6 for methodology). M13mp18GT3 single-stranded DNA (ssDNA) was used as a template for mutagenesis. A series of oligonucleotides with sequences complementary to part of the GLUT3 putative helix 8 sequence were constructed (Dr. V. Math-Dept. of Biochemistry, University of Glasgow), except having bases altered to encode alanine instead of the native residue (Table 5.1). These oligonucleotides were 5'-phosphorylated using polynucleotide kinase and then annealed to the ssDNA M13mp18GT3 template and used as primers for the production of second cDNA strands using T7 DNA polymerase, T4 DNA ligase and dNTPs. One of the nucleotides used in this extension was dCTP α -S, which contains a sulphur atom in place of an oxygen at the α -phosphate group. When incorporated into a DNA strand this nucleotide conveys resistance to restriction digestion as the phosphate backbone cannot be hydrolysed. Hence, what was produced was replicating form DNA (rfDNA) with one wild-type strand and one mutated strand incorporating dCTP α -S. T5 exonuclease was used to remove remaining ssDNA. Digestion of the rfDNA with *Nci* I produced a single "nick" in the wild-type strand only. Exonuclease III was then used to digest the vulnerable wild-type strand until it was judged that only a small fragment remained to act as a primer for re-extension. This was performed using DNA polymerase I, T4 DNA ligase and dNTPs.

This DNA was then transformed into XL1-blue MRF' *E. coli* (section 2.5.8), plaques isolated and propagated to produce small amounts of ssDNA (section 2.5.13). Single-stranded DNA was chosen for the purpose of screening mutants, by automated sequencing, although double-stranded DNA is also a perfectly good template for this method (section 2.8). An oligonucleotide complementary to sequence at the 3' side of the intended mutation was used as a sequencing primer (G3 2B+, Table 5.2 and Figure 5.8). Positive clones

were further propagated (section 2.5.11) and larger quantities of double-stranded DNA produced (section 2.5.12.a).

Positive clones were then restricted with *Bst*X I/*Apa* I or *Bst*X I/*Eco*R V (section 2.5.4) to produce fragments which contained the mutant GLUT3 sequence which were then ligated (section 2.5.6) into similarly restricted and alkaline phosphatase-treated (section 2.5.5) pSPGT3 vector with the wild type sequence fragment removed. This was necessary since M13mp18GT3 has no promoter for the production of mRNA. The ligation mix was again transformed into XL1-blue *E. coli* (section 2.5.9), colonies were selected for by virtue of ampicillin resistance, isolated and small amounts of dsDNA produced (section 2.5.10). Colonies were then screened by sequencing this cDNA using the same oligonucleotide primer as previously used (G3 2B+, Table 5.2 and Figure 5.8). The insert region of positive clones was completely sequenced (section 2.8; Table 5.2; Figure 5.8). If no misincorporations were found, the clones were propagated to produce large amounts of dsDNA (section 2.5.12.b) and portions linearised with *Xba* I (section 2.5.2) to be used as a template for the synthesis of mRNA (section 2.2).

5.3.2.1 Results.

Eight of the nineteen mutant cDNAs were obtained by this method. Although the cDNA sequence of each subclone isolated by this method was error-free, the ratio of mutant/wild-type M13mp18GT3-containing plaques was extremely low. Theoretically, no wild-type cDNA should remain after the digestion of single-stranded cDNA by T5 exonuclease, but this was never the case in practice. Even treatment of the reaction with higher concentrations of T5 exonuclease for extended periods did not increase the ratio of mutants to wild-type colonies. Similarly, alteration of any of the

other reaction steps did not increase the yield of mutant colonies. Additionally, it was necessary to screen plaques/colonies twice- initially in M13mp18GT3, and then after subcloning into pSPGT3. This second screening step was necessary due to inevitable incomplete digestion of pSPGT3 vector prior to ligation which seemed to be due to a low efficiency of the *EcoR V* and *Apa I* enzymes. Since the size of the fragment being excised is small relative to the size of the vector, single-cut and double-cut cDNA migrate practically identically on agarose gel electrophoresis. This makes contamination of double-cut cDNA with single-cut cDNA unavoidable. Since self-ligation of single-cut vector is much more efficient than ligation of vector and insert, this also reduces the ratio of mutant colonies to wild-type colonies on this second screen. The problem of vector self-ligation was reduced by alkaline phosphatase treatment of the vector (see section 2.5.5), but even this process was never 100% efficient. The final ratio of mutant/wild-type GLUT3 colonies in this second screen, using these methods, averaged at 1:3.

5.3.3. Recombinant Polymerase Chain Reaction.

This a modification of the method described by Katagiri *et al.* (Katagiri *et al.*, 1992). This approach was used as an attempt to address the inefficiency problems encountered with the previous method. Oligonucleotides (20-24'mers) were constructed with sequences corresponding to positive strand GLUT3 cDNA sequence of putative transmembrane helix 8 with base changes introduced to encode a protein with alanine substituted for a particular amino acid. These oligonucleotides were complementary in sequence to oligonucleotides constructed for use with the site directed mutagenesis method which correspond to GLUT3 negative strand sequence (Table 5.1). Two 37'mer oligonucleotides were also constructed with sequences corresponding

to untranslated regions of the GLUT3 cDNA at the 5' sides of the positive and negative strands, named G3-Start and G3-End, respectively (Table 5.1).

5.3.3.1 Primary Reactions.

See Figure 5.3.a. In initial polymerase chain reactions, G3-Start, which is complementary to the negative strand in the 3' untranslated region of GLUT3, and a mutagenic oligonucleotide complementary to the GLUT3 positive strand in the region encoding putative transmembrane helix 8, were added to pSPGT3 plasmid dsDNA. Under certain conditions, (sections 2.7.1.b; 2.7.3.a) a PCR fragment "a" was produced (Figure 5.3.a)

Likewise, identical reactions were performed using G3-End, which binds the 3' untranslated region of the GLUT3 positive strand, a mutagenic oligonucleotide complementary to GLUT3 negative strand in the region complementary to that encoding transmembrane helix 8, and pSPGT3. This led to the production of a PCR fragment "b" (Figure 5.3.a). Mutagenic oligonucleotides used in parallel reactions were complementary to each other but differed from the wild-type GLUT3 sequence by 1-3 base pairs, encoding alanine (Table 5.1).

PCR reactions were separated by electrophoresis in agarose gels and the correct bands corresponding to the primary products identified by size and excised. The sizes of reaction products "a" and "b" were 900 and 700 base pairs long, respectively. These were purified (as described in sections 2.7.4, 2.7.5, and 2.7.6) and used as templates for secondary polymerase chain reactions.

5.3.3.2 Secondary Reactions.

Purified primary PCR products "a" and "b" from reactions incorporating identical mutations were included as template cDNA for secondary PCR reactions (sections 2.7.2 and 2.7.3.b). The sequences of the primary products were such that the final 20-24 bp of the product "a" were repeated as the initial bases of product "b". This sequence overlap is the basis of the secondary PCR reaction. As can be seen in Figure 5.3.b, melting of the cDNA double helix and subsequent cooling allows the 3' end of the "a" positive strand to bind to the 3' end of the "b" strand. Each strand acts as a primer for extension of the opposite strand with *Taq* or *Pfu* polymerase, resulting in a full length GLUT3 mutant cDNA. This acts as a template for further PCR extension using G3-Start and G3-End primers.

This final linear cDNA product (Figure 5.4) must be cloned into an expression vector to enable production of mRNA. As with the site-directed mutagenesis procedure, the enzymes chosen were *Bst*X I and *Eco*R V. pSPGT3 vector was also restricted with these enzymes and the fragments ligated and transformed into XL1-Blue *E. coli* (Figure 5.5). Colonies were screened for mutant cDNAs by sequencing as described above (G3 2B+; Table 5.2, Figure 5.8 and section 2.8).

5.3.3.3 Results using *Taq* DNA Polymerase.

The majority of the point mutants (ten) were created by this method using *Taq* DNA polymerase. After cloning into pSPGT3, the frequency of mutant colonies/wild-type colonies averaged about 1:3 but varied dramatically between different mutants, being as high as 5:1 and as low as 1:40.

However, although many mutant colonies were isolated by this method, complete sequencing of each cDNA between the *Bst*X I and *Eco*R V restriction sites (section 2.8) revealed that the error rate of *Taq* polymerase was such that two base pairs in every thousand, on average, were misincorporated into the final product. Hence, the amino acid sequence was frequently altered by these random changes. This is due to the absence of a 3' to 5' proof-reading exonuclease element within *Taq*. Thus, it was frequently necessary to excise these erroneous mutations by restriction digestion of the cDNA, if possible. This involved searching the cDNA sequence of pSPGT3 for unique restriction sites to excise either the erroneous misincorporations from the mutant cDNA, or excise the intended mutation out of this cDNA and insert this fragment into a similarly cut pSPGT3 vector which was free of the misincorporation (see Figures 5.6 and 5.7). This technique was only possible where the misincorporations were few or clustered together in a position reasonably far from the helix 8 mutation such that a suitable restriction site was present in the intervening sequence.

5.3.3.4 Further Subcloning.

Only cDNAs which possessed misincorporations to the 3' of the *Stu* I site at position 1265 or to the 5' side of the *Sac* I site at position 1029 were considered for restriction digestion (Figure 2.2). The former were digested with *Stu* I and *Pvu* I to produce a vector backbone and an insert of 2596 base pairs containing the desired alanine mutation (Figure 5.6) which was purified as described previously (sections 2.7.4-2.7.6). This was then ligated with similarly digested wild-type pSPGT3 vector backbone to produce a misincorporation-free mutant. Likewise, mutants possessing misincorporations to the 5' side of position 1029 were digested with *Sac* I,

which also cuts at position 2312. This generates an insert of 1283 base pairs containing the alanine mutation (Figure 5.7) which again can be ligated to the vector backbone of similarly digested wild-type pSPGT3. These ligations were once more transformed into XL1-Blue *E. coli* and screened by automated sequencing (G3 2B+; Table 5.2, Figure 5.8 and section 2.8).

As is usual with cloning procedures, the efficiency of production of the desired product was never 100%. Colonies containing wild-type GLUT3 and GLUT3 with misincorporations still present were produced in addition to those which contained the desired mutation alone. The overall efficiency of this process was typically about 30% although this varied from mutant to mutant.

5.3.3.5 Results using *Pfu* DNA Polymerase.

Pfu DNA polymerase was used to attempt to address the infidelity problems encountered with *Taq* polymerase. One mutant (the last one) was created using this enzyme. The procedure for use of *Pfu* polymerase was similar to that used with *Taq* polymerase but there were differences in protocols (sections 2.7.1-2.7.3). A major difference in the procedures was the step at which the enzyme was added to the reaction. Due to its low thermostability (relative to *Taq*), *Pfu* polymerase was added only after the initial 95°C melting step. This had been found to increase its activity. Since *Pfu* was less stable than *Taq*, the quantity of PCR product obtained was noticeably less when using the former enzyme rather than the latter. This was especially true of the yields of secondary PCR reactions, which tend to be poorer than those of primary PCR reactions in any case (Figure 5.4). In general, it proved difficult to produce sufficient secondary PCR product for cloning into pSPGT3, and this problem was elevated by the poor yields from

reactions using *Pfu*. However, upon cloning, the ratio of mutants to wild-type colonies was 9:1. In addition, sequencing of the entire *EcoR V/BstX I* "insert" in four separate clones of the same point mutant revealed no misincorporations. The fidelity of this enzyme is due to a 3' to 5' exonuclease proof-reading activity which is lacked by the more thermostable *Taq* polymerase.

5.3.4 Sequencing of Subclones.

Automated DNA sequencing was carried out as described in section 2.8. This method can be used to sequence up to 500 bp of single-stranded or double-stranded cDNA from the site of primer binding, although only the first 300-350 bp is generally accurate. Therefore, although only a single oligonucleotide primer was necessary for screening of mutants (G3 2B+; Table 5.2 and Figure 5.8), the length of the cloned mutant *EcoR V/BstX I* or *Apa I/BstX I* insert (871 bp and 678 bp, respectively) in pSPGT3 required several oligonucleotide primers for complete sequencing (Table 5.2). Due to the nature of sequencing, such as band compressions on the gel due to GC-rich regions, sequencing one DNA strand alone often produces specific recurring errors in the sequence. This problem can be averted by individually sequencing both strands and comparing sequences. The annealing sites of the primers used are such that the sequence obtained from use of one primer overlaps that of another, which allows further comparison of sequences (Figure 5.8). Sequence alignments and comparisons were analysed using the Biosoft GeneJockey II software package on an Apple Macintosh LCIII computer.

5.4 Transport of 2-Deoxy-D-glucose by GLUT3 Mutants into *Xenopus* Oocytes.

After isolating and checking each mutant (section 5.3), these cDNAs were linearised with *Xba* I (section 2.5.2) and an *in vitro* synthesis of mRNA was carried out (section 2.2). In addition, wild-type GLUT3 mRNA was also synthesised. The concentrations of mRNA were assessed by comparison on a 1% agarose gel and each adjusted to ~1 mg/ ml (section 2.5.3 and Figure 2.1). 50 nl of each mRNA was then injected into *Xenopus* oocytes (section 2.3.4), incubated in Barths buffer (Table 2.1) for 48 hours, and oocytes were assayed for transport of [³H]2-deoxy-D-glucose (0.1 mM, 2 µCi/ml) for a period of 30 min (section 2.4).

Since the nineteen mutants were isolated over a period of time, only four or five mutant mRNAs were individually injected into oocytes isolated from a single toad. Groups of seven oocytes were assayed for 2-deoxy-D-glucose transport. In each case, oocytes were also assayed which had been injected with an identical quantity of wild-type GLUT3 mRNA or not injected. Non-injected oocytes were used to measure non-specific transport and that of the native oocyte transporter(s) (section 2.4). Wild-type GLUT3-injected oocytes provided some means with which to compare the transport associated with mutant-injected oocytes. The results can be seen in Figure 5.9. Since not all GLUT3 mutant mRNAs were assayed in a single oocyte preparation and concentrations of mutant and wild-type GLUT3 protein in oocyte plasma membranes were not measured, transport levels cannot be directly compared. Therefore the level of 2-deoxy-D-glucose transport by each mutant is expressed as a percentage of transport by wild-type GLUT3, after the subtraction of transport values for non-injected oocytes. Typical rates of wild-type GLUT3 2-deoxy-D-glucose transport were 4.5-5.0 pmoles/min/oocyte.

Rates of 2-deoxy-D-glucose transport by non-injected oocytes averaged 0.7 pmoles/min/oocyte. Transport rates by mutants were in the range of 2-9 pmoles/min/oocyte.

It must be stressed that since the protein levels of each transporter in oocyte plasma membranes and kinetic parameters, such as K_m and V_{max} values for 2-deoxy-D-glucose entry and exit, have not yet been measured, no conclusions regarding the binding affinities or intrinsic activities possessed by these mutant proteins can be derived. Analysis of these properties must await a more exhaustive study. However, since oocytes expressing each mutant transported 2-deoxy-D-glucose at least twice as well as non-injected oocytes, it can be concluded that each mutant transporter has been successfully expressed, although no information on the relative targeting of these transporters can be derived from this preliminary transport data.

Table 5.1

This lists the oligonucleotides used in the site-directed mutagenesis and PCR protocols. The sequences are shown reading from the 5' end to the 3' end. The codon which encodes the substituting alanine residue is underlined. Each sense-strand oligonucleotide is exactly complementary to one antisense oligonucleotide, and these are used individually to generate primary PCR products which are combined as templates for a secondary PCR reaction.

Table 5.1-**Mutagenesis Oligonucleotides.**

Oligonucleotide	Sequence	Mutation
1453c (antisense strand)	GGTGGCATA <u>TGCG</u> GGCTCTTG	Ile ³⁰⁵ ->Ala
1454 (antisense strand)	GATGGTGGC <u>GGCG</u> ATGGGCTC	Tyr ³⁰⁶ ->Ala
1455 (antisense strand)	CGCGCCGAT <u>TGCG</u> GCATAGAT	Thr ³⁰⁸ ->Ala
1456 (antisense strand)	CGCGCCT <u>GCGGTG</u> GCATA	Ile ³⁰⁹ ->Ala
1457 (antisense strand)	GATAGTATT <u>TGCC</u> ACACCCGC	Val ³¹⁴ ->Ala
1460 (antisense strand)	AAGATAGTT <u>GCA</u> ACCACACC	Asn ³¹⁵ ->Ala
1461 (antisense strand)	GTGAAGATT <u>GCA</u> TAACCAC	Thr ³¹⁶ ->Ala
1462 (antisense strand)	TACAGTGAAT <u>GCA</u> GTATTAAC	Ile ³¹⁷ ->Ala
1463 (antisense strand)	CCCTTCCACT <u>GCA</u> AATAGAGAAA	Leu ³²⁵ ->Ala
1466 (antisense strand)	CCTTCCACCAGT <u>G</u> <u>C</u> TAGAGAAAC	Phe ³²⁴ ->Ala
1467 (antisense strand)	AACTACAGTT <u>GCG</u> ATAGTATT	Phe ³¹⁸ ->Ala

Table 5.1 (cont)

Oligonucleotide	Sequence	Mutation/ Complementary oligonucleotide
1468 (antisense strand)	AGAAACTACT <u>TGCG</u> AAGATAGT	Thr ³¹⁹ ->Ala
1470 (antisense strand)	AAATAGAGAT <u>TGC</u> TACAGTGAA	Val ³¹² ->Ala
1471 (antisense strand)	CAGAAATAGT <u>TGC</u> AACTACAGT	Ser ³²² ->Ala
1473 (antisense strand)	CACCAGAAAT <u>TGCA</u> GAAACTAC	Leu ³²³ ->Ala
1474 (antisense strand)	TAGAGAAACT <u>TGC</u> AGTGAA	Val ³²⁰ ->Ala
1476 (antisense strand)	CACACCCGCT <u>TGCG</u> ATGGTGGC	Gly ³¹⁰ ->Ala
1477 (antisense strand)	AGTATTAACT <u>TGCA</u> CCCGCGCC	Val ³¹³ ->Ala
1478 (antisense strand)	ATTAACCACT <u>TGCC</u> GCGCCGAT	Gly ³¹² ->Ala
1643 (sense strand)	CAAGAGCCC <u>GCAT</u> ATGCCACC	1453c
1644 (sense strand)	GAGCCCATC <u>GCCG</u> CCACCATC	1454
1645 (sense strand)	ATCTATGCC <u>GCAA</u> TCGGCGCG	1455

Table 5.1 (cont.)

Oligonucleotide	Sequence	Complementary oligonucleotide
46 (sense strand)	GCGGGTGTGGCAA ATACTATC	1457
47 (sense strand)	TTTCTCTATTTGCA GTGGAAAGGG	1460
48 (sense strand)	GGTGTGGTTGCAA CTATCTT	1461
49 (sense strand)	GTGGTTAATGCAA TCTTCAC	1463
50 (sense strand)	AATACTATCGCAA CTGTAGTT	1467
51 (sense strand)	GTTTCTCTAGCACT GGTGGAAAGG	1466
52 (sense strand)	TTCAGTGTAGCAT CTCTATTT	1470
53 (sense strand)	GTAGTTTCTGCAT TTCTGGTG	1473
3' End (antisense strand)	GTCGACGTCGACG AGGGAGAGGTGGC TTCCCATGCC	Binds GLUT3 sense strand at 3' UTR.
3' Start (sense strand)	GTCGACGTCGACT CACCCCTAGATCT TTCTTGAAGAC	Binds GLUT3 antisense strand at 3' UTR.

Table 5.2

This lists the oligonucleotides used as primers for automated DNA sequencing. The sequences are shown reading from the 5' end to the 3' end. Oligonucleotides designated "T" bind to the antisense strand of GLUT3 and generate sequences corresponding to the GLUT3 sense strand. Oligonucleotides designated "B" bind to the sense strand of GLUT3 and generate sequences corresponding to the GLUT3 antisense strand.

Table 5.2-
Sequencing Oligonucleotides.

G3 2T	ACTGGACCTCCAAC
G3 3T	TCGGCGCGGGTGTGG
G3 3T+	ATCTATGCCACCATC
G3 4T	CCAGATTTTTGCTCA
G3 5T	GACTGTGTAAAGTAG
G3 1B	GGGAGAGGTGGCTTT
G3 2B+	ACAGTCATGAGCGTG
G3 3B+	GTAGCTGGACACTCT
G3 4B	TGAGCAAAAATCTGG

Figure 5.1.a

This show an alignment of the protein sequences of human (h), mouse (m), rat (r) and rabbit (rb) facilitative glucose transporters in the region of putative transmembrane helix 8. Residues which are identical in all transporter isoforms are shown in **bold type**. A consensus sequence of GLUTs 1- 4 is shown below. Residues which vary between isoforms are shown as "X", and those which are predicted to lie on the polar face of transmembrane helix 8 are marked with an asterisk (*) -see Figure 5.1.b.

Figure 5.1.a-

Comparison of Amino Acid Sequences in Putative Transmembrane Helix 8 of the Facilitative Glucose Transporter Family.

hGLUT1	V	Y	A	T	I	G	S	G	I	V	N	T	A	F	T	V	V	S	L	F	V
mGLUT1	V	Y	A	T	I	G	S	G	I	V	N	T	A	F	T	V	V	S	L	F	V
rGLUT1	V	Y	A	T	I	G	S	G	I	V	N	T	A	F	T	V	V	S	L	F	V
rbGLUT1	V	Y	A	T	I	G	S	G	I	V	N	T	A	F	T	V	V	S	L	F	V
hGLUT2	V	Y	A	T	I	G	V	G	A	V	N	M	V	F	T	A	V	S	V	F	L
mGLUT2	V	Y	A	T	I	G	V	G	A	I	N	M	I	L	T	A	V	S	V	L	L
rGLUT2	V	Y	A	T	I	G	V	G	A	I	N	M	I	F	T	A	V	S	V	L	L
hGLUT3	I	Y	A	T	I	G	A	G	V	V	N	T	I	F	T	V	V	S	L	F	L
mGLUT3	I	Y	A	T	I	G	A	G	V	V	N	T	I	F	T	V	V	S	L	F	L
hGLUT4	A	Y	A	T	I	G	A	G	V	V	N	T	V	F	T	L	V	S	V	L	L
mGLUT4	A	Y	A	T	I	G	A	G	V	V	N	T	V	F	T	L	V	S	V	L	L
rGLUT4	A	Y	A	T	I	G	A	G	V	V	N	T	V	F	T	L	V	S	V	L	L
hGLUT5	Q	Y	V	T	A	G	T	G	A	V	N	V	V	M	T	F	C	A	V	F	V
rGLUT7	A	Y	V	T	L	G	S	G	S	V	N	F	L	T	T	V	V	S	L	I	V
GLUT1-4	X	Y	A	T	I	G	X	G	X	X	N	X	X	X	T	X	V	S	X	X	X
	*		*			*	*			*	*			*		*		*	*		

Figure 5.1.b

This shows the predicted secondary structure of GLUT3 putative transmembrane helix 8. The α - helix is viewed from above. The amino acid sequence begins at Ile³⁰⁵ at the "bottom" of the helix (numbered 1), and the positions of the following residues rotate upward in a clockwise direction until the last residue, Leu³²⁵ (numbered 21) is reached.

Figure 5.1.b-

Predicted α - Helical Structure of GLUT3 Transmembrane Helix 8.

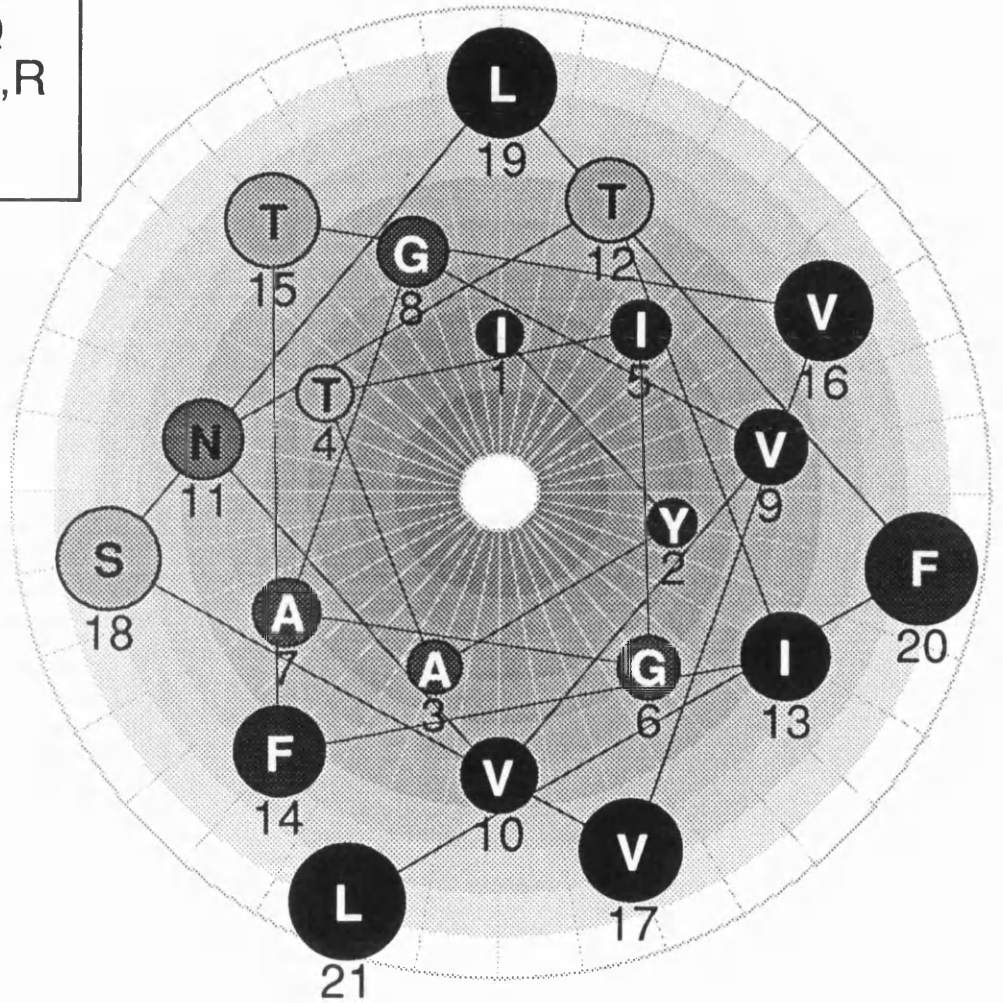
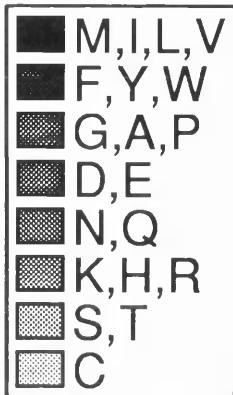


Figure 5.2

This is a diagrammatic representation of the site-directed mutagenesis reaction (section 2.6). Note that the purpose of the T5 exonuclease step is the removal of remaining single-stranded cDNA, which has not been represented in this diagram for the sake of clarity.

Figure 5.2-

Diagram showing Sculptor™ Site-Directed Mutagenesis.

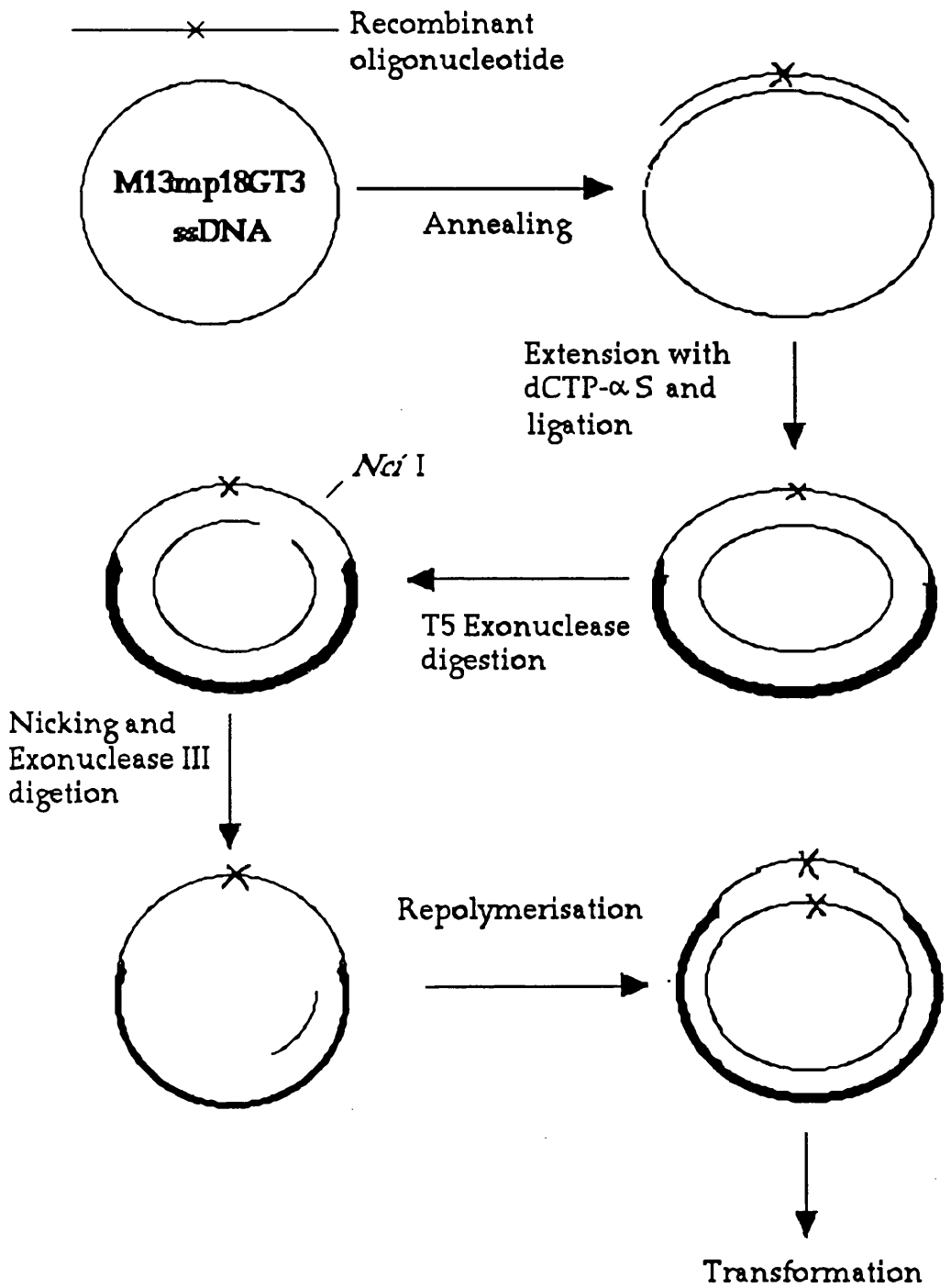


Figure 5.3.a

This diagram shows where the reaction primers bind to pSPGT3 (upper plasmid) and shows the sequence of events in both primary PCR reactions (section 2.7.1 or 2.7.3.a). In reaction 1, G3-Start and the mutagenic primer, corresponding to the antisense cDNA strand in the helix 8-encoding region, bind to melted GLUT3 antisense and sense strands, respectively. New strands are then extended from these primers in the 5' to 3' direction by *Taq* or *Pfu* DNA polymerase (dotted lines). Melting, reannealing and extension occur 30 times producing the ~1000 bp fragment "a". This fragment has a *Sal* I site just 5' to the coding sequence and the alanine mutation is at the 3' end (corresponding to the sense cDNA strand). In reaction 2, the second mutagenic primer (which is complementary to that used in reaction 1) and G3-End, bind to melted GLUT3 antisense and sense strands, respectively. New strands are then extended from these primers in the 5' to 3' direction by *Taq* or *Pfu* DNA polymerase (dotted lines). This time a ~600 bp fragment "b" is produced. This fragment has a *Sal* I site just 3' to the coding sequence and the alanine mutation is at the 5' end (corresponding to the sense cDNA strand).

Figure 5.3.a-

Recombinant PCR used for the Construction of GLUT3 Helix 8 Mutants.

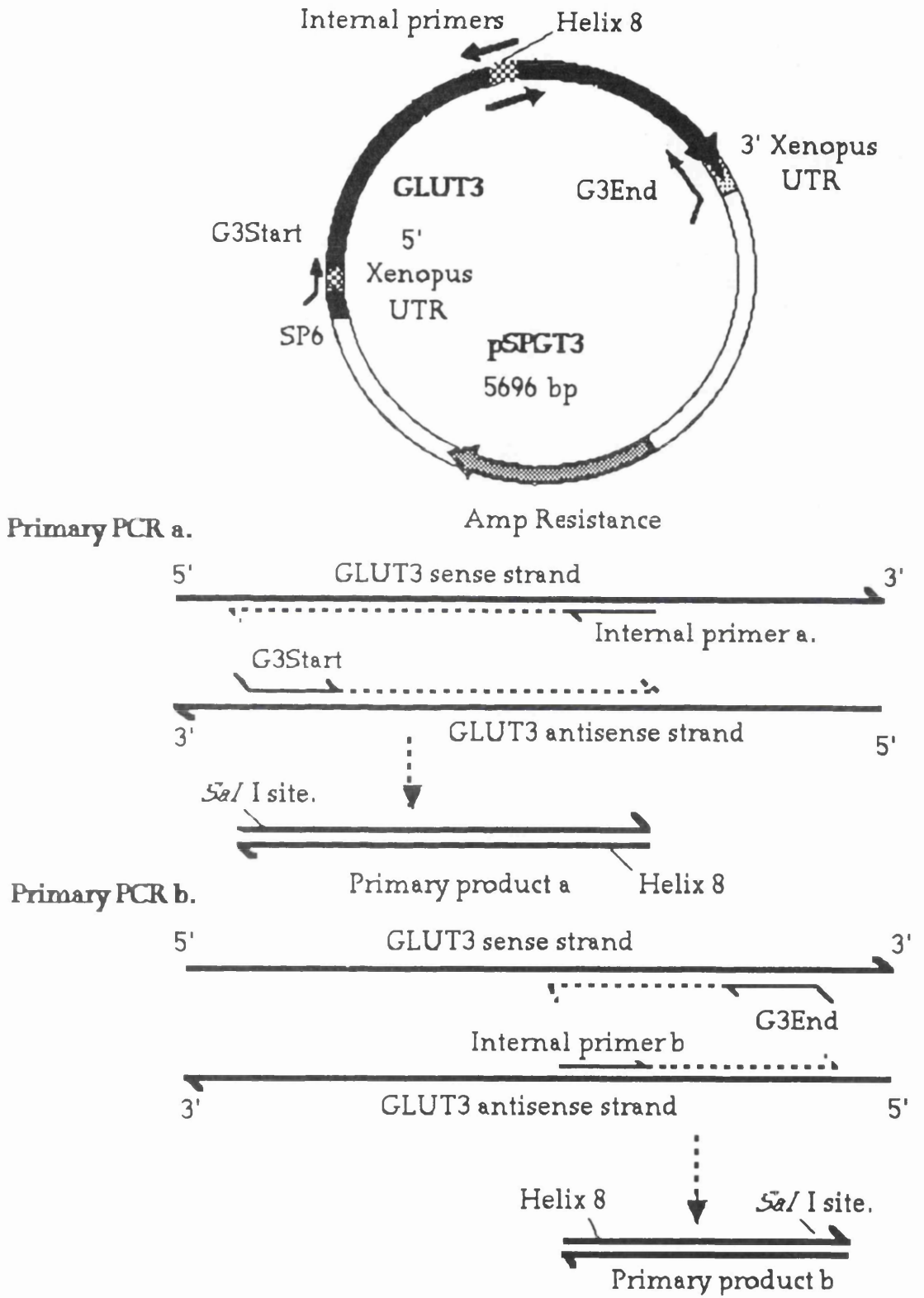


Figure 5.3.b

This shows the events occurring during a secondary PCR reaction (section 2.7.2 or 2.7.3.b). This time equal quantities of products "a" and "b" are used as the templates for a second set of cycles with both G3-Start and G3-End primers. For amplification to occur, the two templates must melt and anneal to form a single template. This is possible since there is a short overlap of 18-24 bp between the two templates at the 3' end of the sense cDNA strand of primary product "a" and the antisense strand of primary product "b", corresponding to the mutated helix 8 region. In the first few cycles of PCR, these strands can anneal and extend in a 5' to 3' direction (dotted lines) to form a full length secondary product "ab", which can act as a template for amplification with G3-Start and G3-End. Note that only the sense strand of "a" and antisense strand of "b" can be extended after association, since binding of the antisense strand of "a" and sense strand of "b" leads to a complex which cannot be extended in a 5' to 3' direction. The formation of "a"/"b" complexes is also a relatively infrequent event when compared to the frequency of self-association of "a" and "b" strands. Both these factors make secondary PCR yields much lower than those obtained from primary PCR.

Figure 5.3.b-

Diagram showing Secondary PCR Reactions.

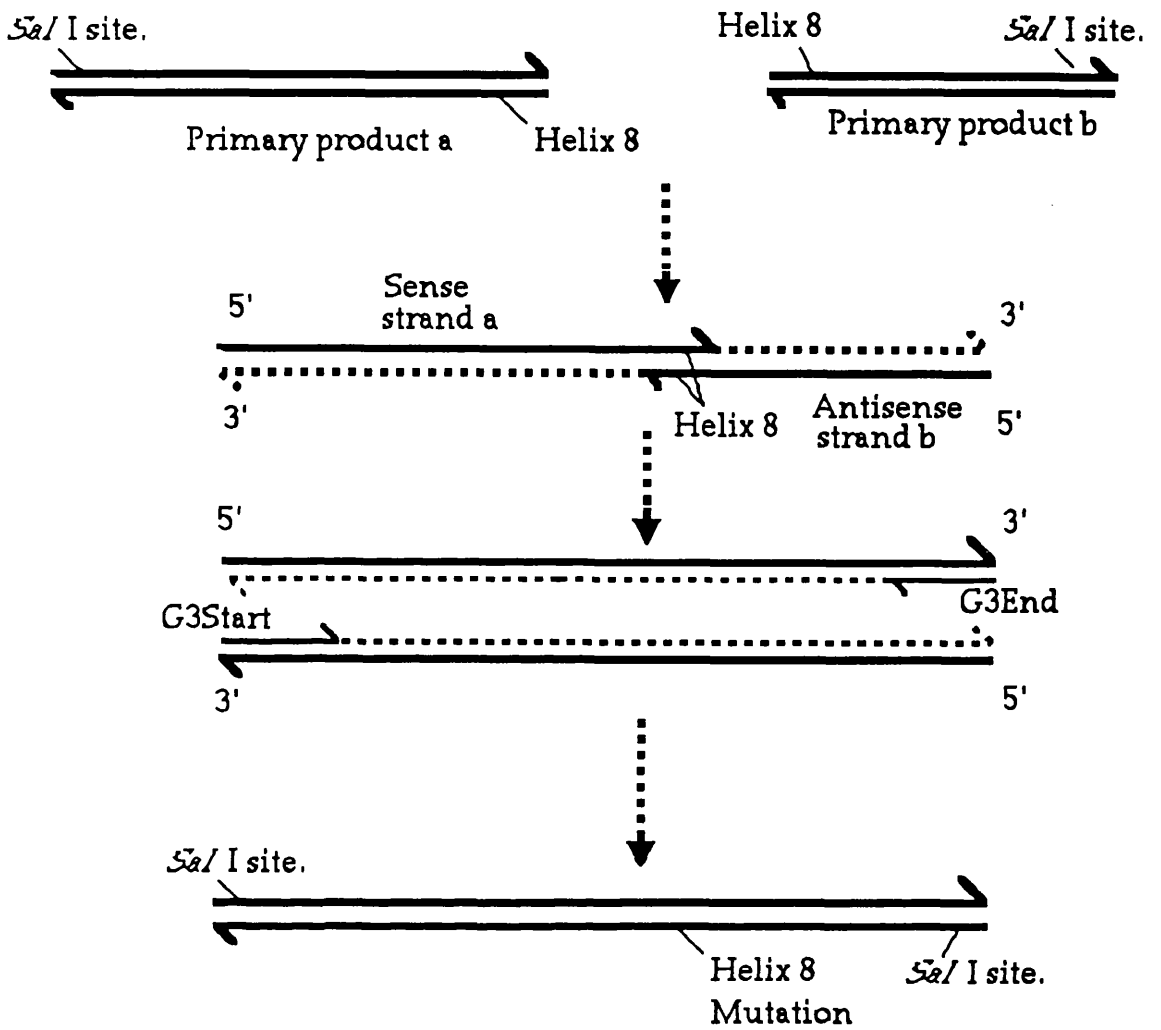


Figure 5.4

This shows a photograph of samples of various PCR products and vector cDNAs which have been electrophoresed on a 1% agarose gel and stained with ethidium bromide (section 2.5.3). Lanes 1 and 8 contain 0.625 μg of *Bst*E II-digested lambda DNA. Lane 2 contains 1 μl (from a total of 30 μl) of primary PCR product "b" generated using *Pfu* DNA polymerase (Figure 5.3.a). Lane 3 contains 1 μl (from a total of 30 μl) of primary PCR product "a" generated using *Pfu* DNA polymerase (Figure 5.3.a). Lane 4 contains 1 μl (from a total of 10 μl) of secondary PCR product "ab" generated using *Pfu* DNA polymerase and 1 μl each of 1/10-diluted products "a" and "b" (Figure 5.3.b). Lane 5 contains 1 μl (from a total of 5 μl) of *Eco*R V/*Bst*X I-digested and purified secondary product "ab". Lane 6 contains 1 μl (from a total of 10 μl) of *Eco*R V/*Bst*X I-digested and purified pSPGT3 vector backbone. Lane 8 contains 1 μl of 2 mg/ml dsDNA isolated from a subclone transformed with a ligation containing 0.5 μl of *Eco*R V/*Bst*X I-digested and purified pSPGT3 vector backbone and 5 μl of *Eco*R V/*Bst*X I-digested and purified secondary product "ab". This cDNA subclone was sequenced and found to be pSPGT3 containing the desired mutation.

Lane	Band sizes (in base pairs)
2	~600
3	~1000
4	~1600
5	871
6	4825
7	5696

Figure 5.4 -

A 1% Agarose gel showing various P.C.R. products and vectors used in cloning.

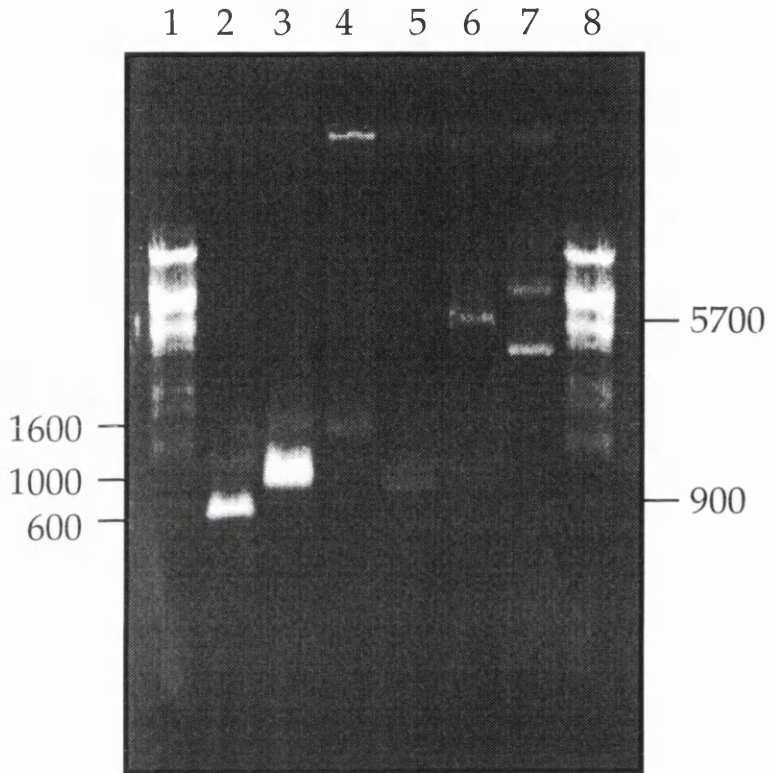


Figure 5.5

This diagram shows the *EcoR* V/*Bst*X I digestion of pSPGT3 and secondary PCR product, and the ligation of the purified vector backbone and the 871 bp PCR insert to produce an intact pSPGT3 vector incorporating a mutated GLUT3 codon in the sequence region encoding putative helix 8.

Figure 5.5-

Digestion of Secondary PCR Products and Subcloning into pSPGT3.

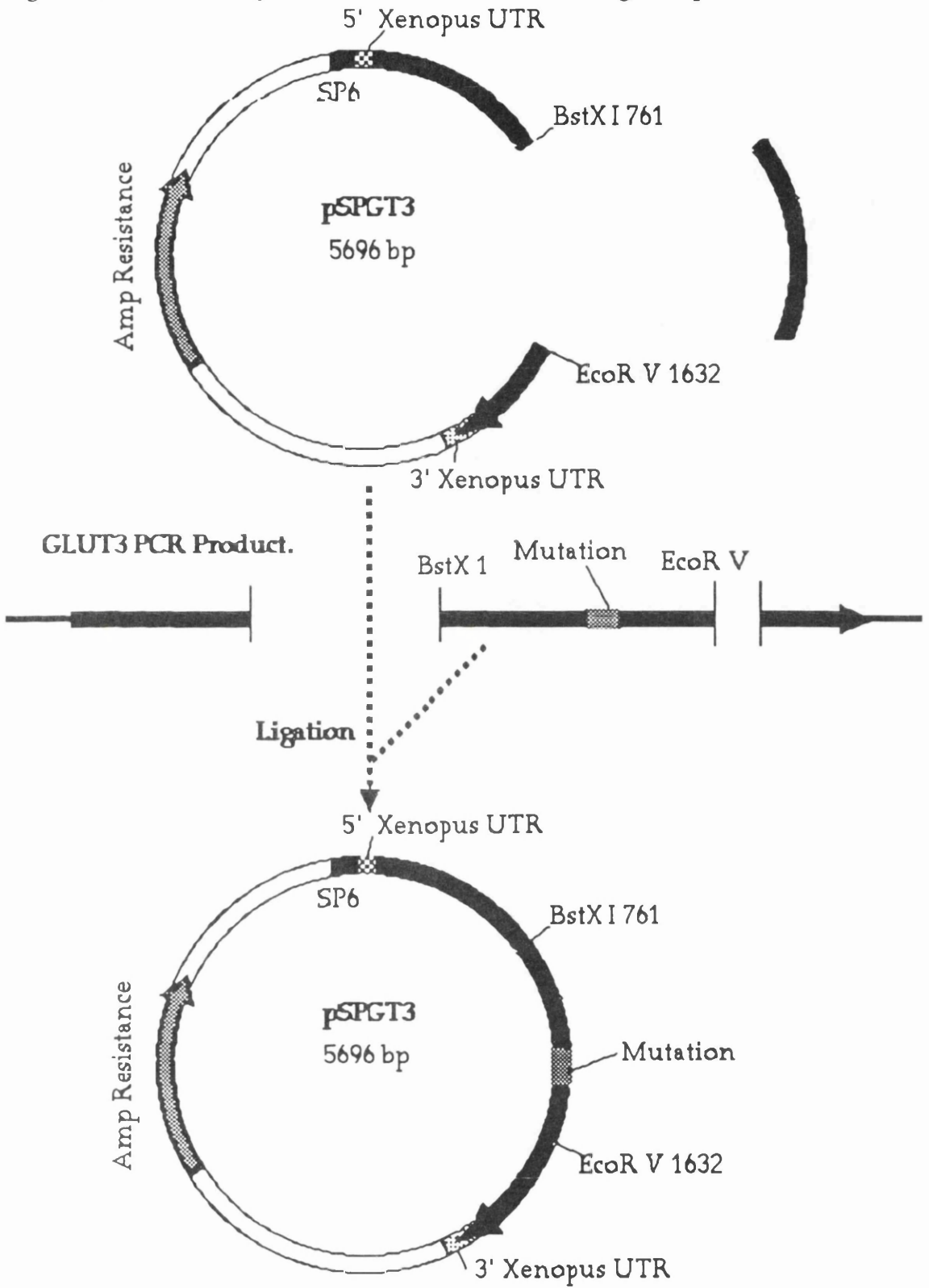


Figure 5.6

This diagram shows the *Stu* I/*Pvu* I digestion of both "mutant" and wild-type GLUT3 sequences in pSPGT3, and the ligation of the 3100 bp purified vector backbone from the wild-type GLUT3-containing construct and the 2596 bp "mutant" insert to produce an intact pSPGT3 vector incorporating a mutated GLUT3 codon in the sequence region encoding putative helix 8, but without any other altered sequences. This process is designed to excise any misincorporated bases from the region between the *Stu* I and *EcoR* V restriction sites, introduced by *Taq* DNA polymerase.

Figure 5.6-

Excision of Misincorporated Bases using *Stu* I and *Pvu* I.

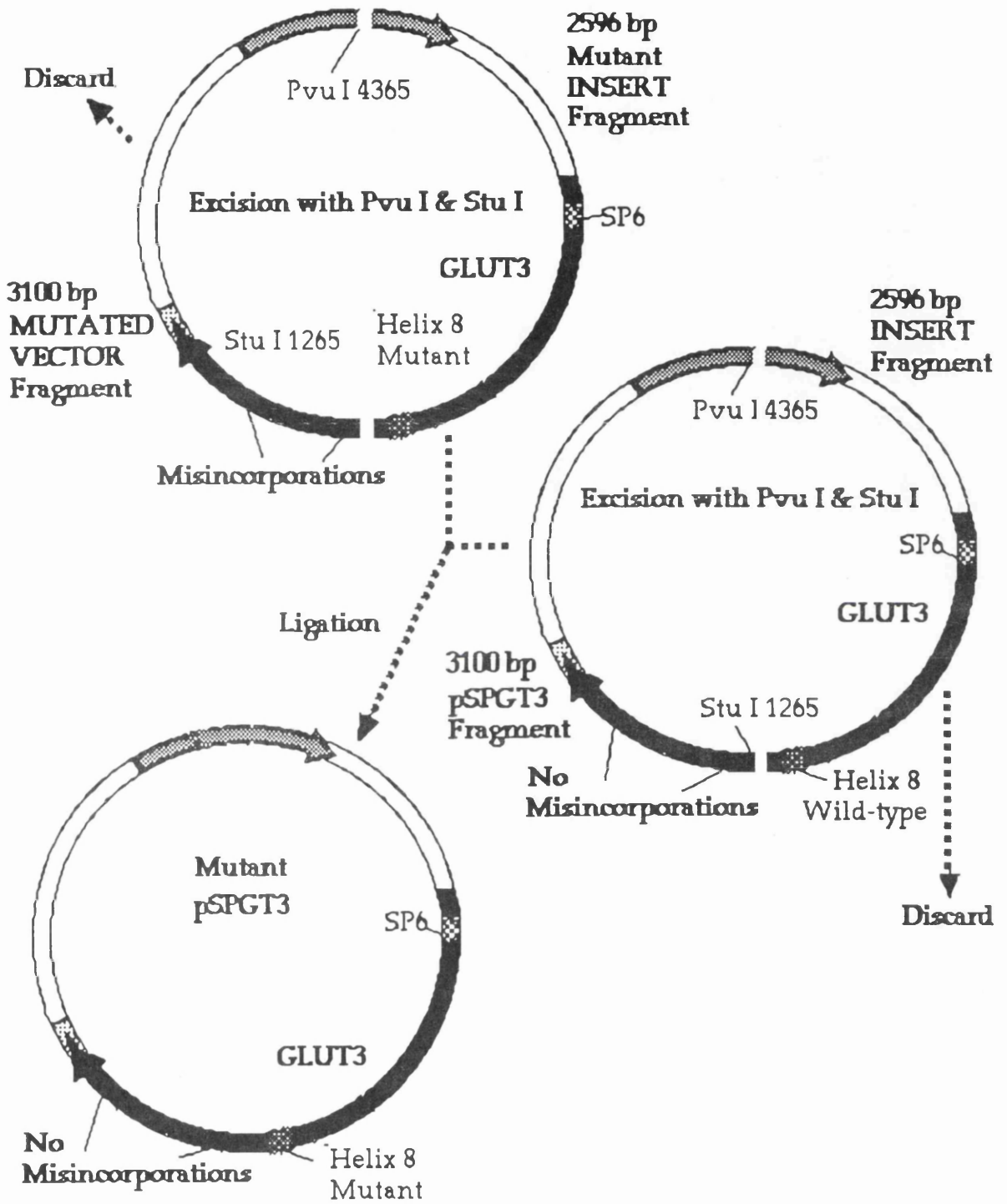


Figure 5.7

This diagram shows the *Sac* I digestion of both "mutant" and wild-type GLUT3 sequences in pSPGT3, and the ligation of the 4413 bp purified vector backbone from the wild-type GLUT3-containing construct and the 1283 bp "mutant" insert to produce an intact pSPGT3 vector incorporating a mutated GLUT3 codon in the sequence region encoding putative helix 8, but without any other altered sequences. This process is designed to excise any misincorporated bases from the region between the *Bst*X I and first *Sac* I restriction sites, introduced by *Taq* DNA polymerase.

Figure 5.7-

Excision of Misincorporated Bases using *Sac* I Digestion.

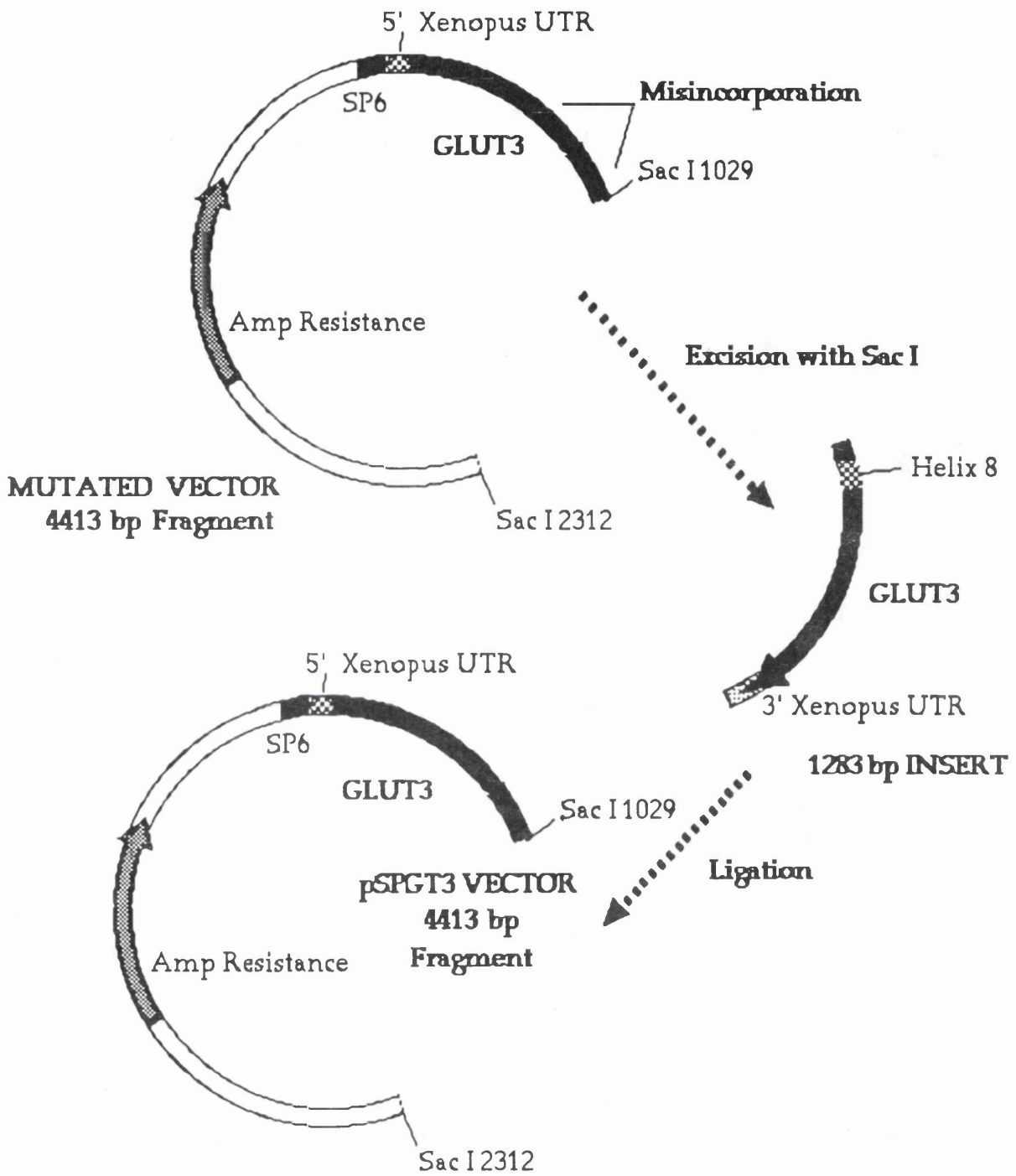


Figure 5.8

This is a diagrammatic representation of the GLUT3 coding sequence from the 5' end of the sense cDNA strand to the 3' end. Position "0" corresponds to base "0" in pSPGT3. The GLUT3 open reading frame (ORF) begins at position 255 and ends (STOP) at position 1743. The approximate locations of several restriction sites are shown and the sequence encoding putative transmembrane helix 8 bordered by vertical dashed lines. The annealing positions of all sequencing primers (Table 5. 2) and G3-Start and G3-End are shown. Sequencing primers (dotted lines) pointing from left to right and depicted above the GLUT3 cDNA bind the antisense strand and yield 300-350 bp sequences of the cDNA to their right. Primers pointing from right to left and depicted below the GLUT3 cDNA bind the sense strand and yield 300-350 bp sequences of the cDNA to their left. Comparison of sequences using all the primers is sufficient to accurately describe the sequence between the *EcoR*V and *Bst*X I restriction sites. All initial screening of possible "mutant" clones was achieved using primer G3 2B+. This was found to yield accurate sequences of the helix 8-encoding region. This primer was also chosen since it binds the GLUT3 cDNA sense strand, which is the only one present when sequencing M13mp18GT3 ssDNA.

Figure 5.8-

Diagram showing the Binding Positions of Various Sequencing and Mutagenesis Oligonucleotides in the GLUT3 cDNA.

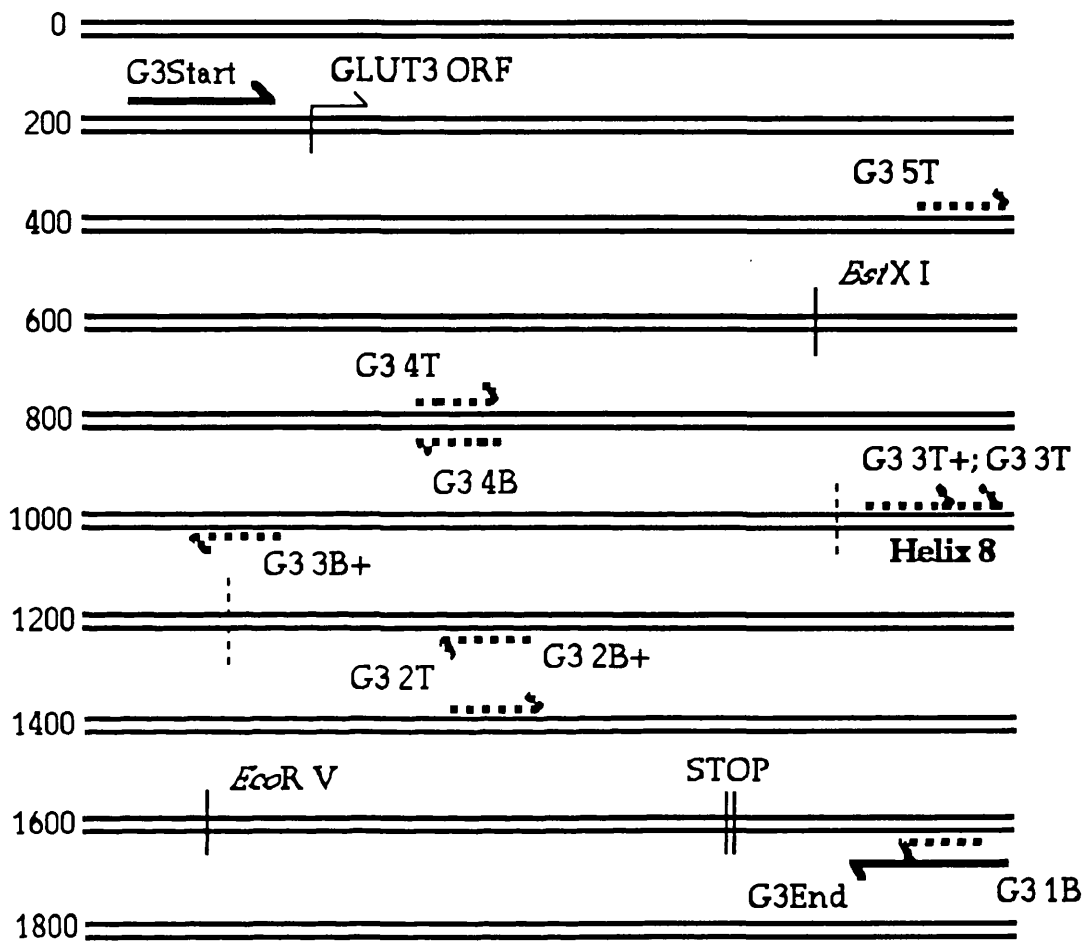
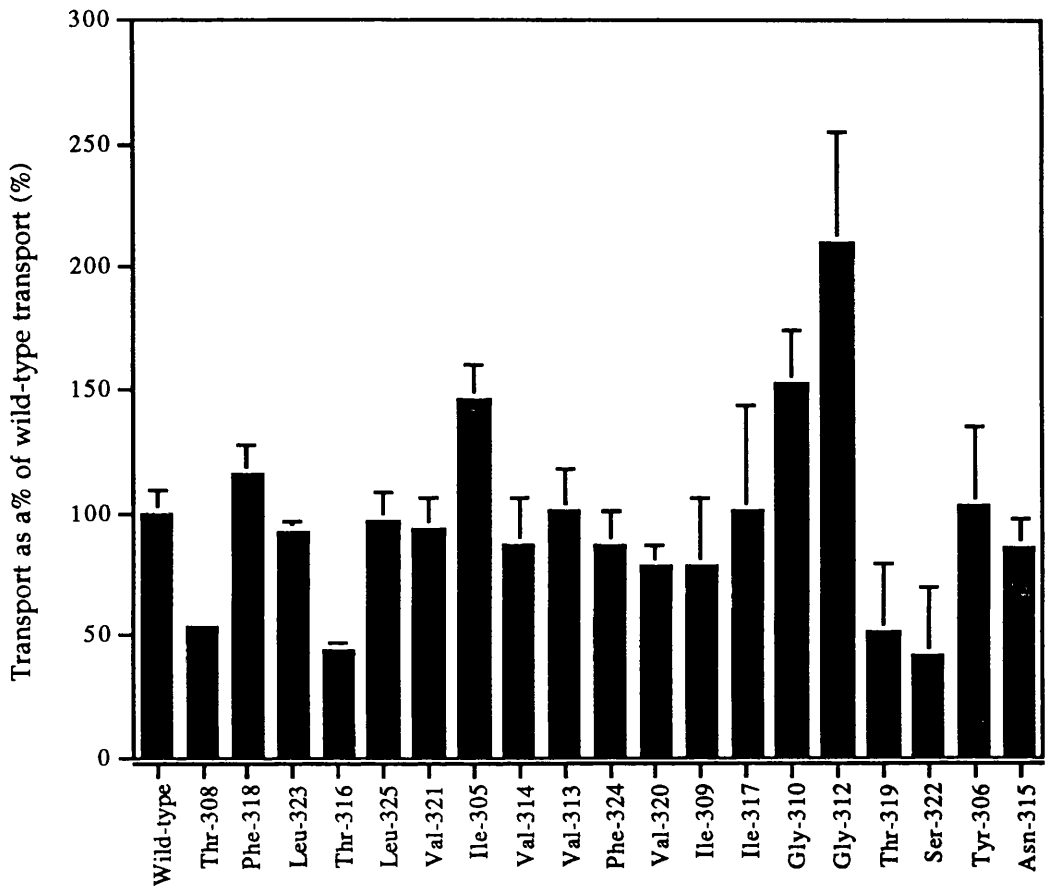


Figure 5.9

This is a graph showing transport of [³H]2-deoxy-D-glucose into *Xenopus* oocytes injected with either wild-type, or one of nineteen mutant GLUT3 mRNAs. Rates of transport into non-injected oocytes were deducted from each injected rate, and the adjusted rate expressed as a percentage of the adjusted transport rate into wild-type GLUT3-injected oocytes. Each column represents the adjusted transport rate into 7 oocytes \pm standard deviations from a representative experiment (if n > 1). Typical rates of wild-type GLUT3 2-deoxy-D-glucose transport were 4.5-5.0 pmoles/min/oocyte.

Figure 5. 9-
2-deoxy-D-glucose Transport Rates of Various GLUT3 Mutants
as a Percentage of Wild-type GLUT3 Transport Levels.



5.5 Discussion.

The importance of various conserved amino acid residues in GLUT1 have been extensively investigated by mutagenesis. These studies have shown that substitution of some of these residues by other amino acids has led to changes in the behaviour of the transporter protein. These changes include reductions of transporter intrinsic activity and reduction of the affinity of various sugars and ligands for the transporter (reviewed in section 5.2.1). However the mutagenesis of other transporters has generally been limited to construction of chimeric GLUT1/ GLUT4 transporters for the study of GLUT4 targeting (reviewed James *et al.*, 1993), with the exceptions being the GLUT1/ GLUT2 chimera which was constructed for the study of kinetic differences between the two transporter isoforms (Katagiri *et al.*, 1992), and a few site-directed mutagenesis studies described in section 5.2.1.

This study investigates the importance of the residues of putative transmembrane helix 8 in GLUT3. Although work on helix 7 in GLUT1 has been extensive, the only other helix 8 residues which have been investigated are GLUT1 residue asparagine-317 (Asn³¹⁷-> Ile; Hashiramoto *et al.*, 1992) and GLUT4 residue tyrosine-308 (Tyr³⁰⁸->Phe; Wandel *et al.*, 1994). Asn³¹⁷-> Ile exhibited no decrease of 2-deoxy-D-glucose uptake relative to wild-type levels. Cytochalasin B and ATB-BMPA labelling levels were also equivalent to wild-type GLUT1. Likewise, the Tyr³⁰⁸->Phe mutant showed no differences in glucose transport activity and ligand binding from wild-type GLUT4.

Figure 5.1.a shows an alignment of protein sequences of human, mouse, rat and rabbit facilitative glucose transporters in the region of putative transmembrane helix 8. As can be seen the sequence is highly conserved between transporter isoforms. Residues Tyr³⁰⁶, Thr³⁰⁸, Gly³¹⁰, Gly³¹², Asn³¹⁵, and Thr³¹⁹ (GLUT3 nomenclature) are identical between all isoforms. Note

that residues Ala³⁰⁷, Ile³⁰⁹, Val³²¹, and Ser³²² are also identical in GLUTs 1-4, which are D-glucose transporters, unlike GLUT5 which transports D-fructose. Val³¹⁴, Thr³¹⁶, and Phe³¹⁸ are identical in GLUTs 1, 3 and 4 but are altered in GLUT2. Indeed, GLUT2 shows the greatest diversity between isoforms from different species, with four non-identical residues in this region alone. All other transporter isoforms have complete identity of protein sequence between species in this helix.

A possible orientation of GLUT3 helix 8 is shown in Figure 5.1.b. This shows a view looking down through the α -helix from above, where residue Ile³⁰⁵ is at the "bottom" and the helix progresses upwards in a clockwise direction to residue Leu³²⁵. The amphipathic nature of the helix can be seen as the majority of the polar residues are situated at one side of the helix, and the hydrophobic residues are present on the other side. Invariant residues Thr³⁰⁸, Asn³¹⁵, and Thr³¹⁹ are found on the "polar side", but residue Tyr³⁰⁶ is predicted to lie directly opposite these which would infer that it is presumably in contact with lipid rather than part of a protein pore. The polar residues Ser³²² and Thr³¹⁶ are also predicted to lie on the "polar side" of the α -helix.

Preliminary studies revealed that GLUT3 2-deoxy-D-glucose transport rates were seemingly unaltered by most substitutions (Figure 5.9). However, substitution of Thr³⁰⁸, Thr³¹⁶, Thr³¹⁹, and Ser³²² by Ala led to a 50% reduction in 2-deoxy-D-glucose transport relative to wild-type levels, and residues Ile³⁰⁵, Gly³¹⁰, and Gly³¹² by Ala led to a 150% to 200% increase in transport. Of course, the effects of the latter mutations are most probably due to an increased concentration of transporter protein but an increase in intrinsic activity cannot be ruled out. Likewise the observed decreased transport in the Thr³⁰⁸, Thr³¹⁶, Thr³¹⁹, and Ser³²² mutants are quite possibly due to reduced expression of these transporter isoforms rather than decreased intrinsic activity. These questions can only be answered by measuring protein levels in

mutant and wild-type oocyte plasma membranes. Targeting of each mutant to the plasma membrane should also be assessed.

In addition, other kinetic parameters need to be measured. These include K_m and V_{max} values for the *zero-trans* entry of 2-deoxy-D-glucose and D-galactose, the secondary substrate of GLUT3. K_i values for the inhibition of 2-deoxy-D-glucose or D-galactose transport by D-glucose, maltose and 4,6-O-ethylidene-D-glucose transport should be measured as these will give an indication of any changes of affinity of the exofacial binding site for these sugars. Binding studies with [3H]ATB-BMPA should also be undertaken to determine effects mutation on its binding site. ATB-BMPA has been proposed to bind to GLUT1 helix 8 (Davies *et al.*, 1991). The site of the covalent bond formed between glucose transporters and ATB-BMPA by photolabelling might also be discovered by assaying each mutant for binding (if the site of interaction is in helix 8).

Cytochalasin B binding studies on oocyte plasma membranes which express mutant transporters, and measurement of the K_i values for this compound's inhibition of 2-deoxy-D-glucose and D-galactose transport by mutant GLUT3 isoforms should also be undertaken to assess whether the endofacial sugar binding site has been affected by substitution of these residues. This is unlikely since the site of cytochalasin B binding has been localised to helices 10 and 11, but it is possible that other regions also contribute to the binding properties of this inhibitor.

It is interesting to note that no reduction of transport activity was observed with the Asn³¹⁵->Ala and Tyr³⁰⁶->Ala mutants relative to wild-type GLUT3 levels, since these results were also found with substitution of the equivalent residues in GLUT1 (Asn³¹⁷; Hashiramoto *et al.*, 1992) and GLUT4 (Tyr³⁰⁸; Wandel *et al.*, 1994). However the results of this study are by no means conclusive.

Although many transporter residues have been substituted in a number of studies, the frequency of finding one which affects transport activity or ligand binding is low. However, many residues, which have been found not to affect transport, are highly conserved between transporter isoforms. As speculated by Mueckler (Mueckler *et al.*, 1994a), these residues must play an important role in some aspect of transporter structure, that is not measured by the assays performed. Mutations might cause an alteration of the kinetic properties under physiological conditions that is not measurable in *Xenopus* oocytes, or may affect protein stability or regulation by unknown factors.

On the other hand, substitution of non-conserved residues has frequently led to a large reduction in transport activity. For example, replacement of the non-conserved helix 8 residue, Val⁴⁰², of SNF3 with Ile (Marshall-Carlson *et al.*, 1990) and the replacement of Val¹⁹⁷ (GLUT2) and Val¹⁶⁵ (GLUT1) with Ile (Mueckler *et al.*, 1994b) completely abolish sugar transport. This is surprising given the conservative nature of the substitutions, but the increased size of the isoleucine side chain relative to the wild-type residue may block the transport of glucose.

5.6 Summary

GLUT3 residues 305-325 have individually been substituted with alanine by alteration of the sequence of the GLUT3 cDNA. These mutants have been expressed heterologously in *Xenopus* oocytes, by injection with *in vitro*-synthesised mRNA. All mutants have been successfully expressed and at least partially successfully targeted to the plasma membrane, as determined by the transport of radiolabelled 2-deoxy-D-glucose. Further studies are required to quantitate the expression levels and plasma membrane targeting

of each mutant transporter. In addition, kinetic parameters for transport of 2-deoxy-D-glucose and D-galactose need to be measured and the inhibitory effects of various sugars and ligands determined.

CHAPTER 6

Discussion

Understanding the structural basis of glucose transporter function is a key issue when trying to understand glucose transporter dysfunction, which may play a causal role in some forms of diabetes. For example, peripheral insulin resistance may be caused by GLUT4 depletion or inactivation in skeletal muscle and fat, and lead to non-insulin dependent diabetes. Moreover, GLUT2 is likely to be an important factor in insulin secretion and whole-body glucose homeostasis, due to its presence in the β -cells of the pancreas and in the liver, respectively.

Many structural studies have been carried out on GLUT1, due to its availability and the ability to obtain this isoform in a purified, functional form. Investigation of the kinetic profile of this transporter and use of physical techniques to directly probe its structure have elucidated a structure comprising 12 transmembrane helices which seem to form a pore structure, passively transporting D-glucose by virtue of a conformational change which re-orientates glucose from an exofacial to an endofacial binding site, where it is released inside the cell. Use of specific probes and mutagenic techniques have identified certain regions of the primary sequence and specific amino acid residues which may be important in the interaction of the transporter and D-glucose and also regions involved in the conformational changes.

Comparison of the primary sequences of other members of the facilitative glucose transporter family reveals high identity with GLUT1. In addition, hydropathy analysis of these other isoforms yields a pattern virtually identical to that of GLUT1. These factors and the similarities of substrate specificity, kinetic profile, and ligand binding between isoforms reveals that all transporters share a similar structure and mode of action. However, the transporters are distributed in a tissue-specific manner, suggesting that they have subtly evolved to meet the different glucose requirements of these tissues. Indeed expression of glucose transporters in

oocytes reveals that not only are the kinetic parameters of each transporter different, but also the substrate selectivity. For example, GLUT2 has been shown to transport both D-fructose and D-glucose, whilst GLUT5 seems primarily to be a D-fructose transporter.

The purpose of this study is the characterisation of the kinetic properties of GLUT2 and GLUT3, whilst expressed in *Xenopus* oocytes, and, using these values as a guideline, to investigate the structural/functional properties of amino acid residues in a region which have been implicated as the exofacial site of glucose binding in GLUT1, transmembrane helix 8. This helix contains several polar residues which are highly conserved between glucose transporter isoforms, and also occur in related transporters from diverse organisms. These residues have the capacity to form hydrogen bonds with the hydroxyl groups of D-glucose, allowing D-glucose to reversibly bind to the exofacial binding site. A mutagenic approach was selected, whereby each of the nineteen amino acid residues of helix 8 was individually substituted with alanine, removing the ability of that residue to form hydrogen bonds. A parallel study was carried out investigating the effects of effectively removing or substituting the hydroxyl groups of D-glucose on the interaction of that sugar with either GLUT2 or GLUT3, whilst expressed in *Xenopus* oocytes.

The kinetic parameters of *zero-trans* entry of 2-deoxy-D-glucose into GLUT2- and GLUT3-expressing oocytes, and the inhibitory effects of other sugars on that transport confirm previous findings that GLUT2 and GLUT3 are low affinity and high affinity transporters, respectively (reviewed in Gould & Holman, 1993). In addition, GLUT2 transports β -D-fructose with lower affinity. Analysis of the effects of D-fructopyranose and D-fructofuranose fixed-ring analogues indicate that whilst D-glucose is known to bind in the pyranose ring form, the furanose form of D-fructose seems to

bind to GLUT2. This is in agreement with a study of the trypanosome transporter which also transports these configurations of D-glucose and D-fructose (Fry *et al.*, 1993).

Following investigations of the molecular basis of the interactions of D-glucose with GLUT1 (Barnett *et al.*, 1973; Kahlenberg & Dolansky, 1972) and GLUT4 (Rees & Holman, 1981), similar, if less extensive, studies were performed with GLUT2 and GLUT3 expressed in *Xenopus* oocytes. The results indicate that hydrogen bonding at the C-1, C-3 and C-4 positions of D-glucose occur during binding and transport with both isoforms, and that hydrophobic interactions between the C-6 position of the sugar and each transporter also occur. The nature of the bond between the C-3 hydroxyl group of D-glucose and GLUT2 is proposed to be different from that formed by other transporter isoforms. In addition, the formation of the bond between the C-4 hydroxyl group of D-glucose and GLUT3 is less essential for transport than required by other transporter isoforms. Differences in the interaction of D-glucose with each transporter are predicted by the different substrate specificities of each isoform. For example, the relative high affinity of GLUT3 for D-galactose, the C-4 epimer of D-glucose, is reflected by the different nature of that transporter in the region which interacts with the C-4 position of D-glucose. The interactions of the transporter/sugar which are measured above probably occur in the exofacial binding site, due to the nature of the assay (see chapter 4) but it cannot be ruled out that some of the measured interactions may be influenced by affinities of transporter/sugar during transport itself.

Until it is possible to functionally purify and crystallise all of the facilitative glucose transporters, the only means to study their structure, more fully than has been done already, is use of molecular biological techniques to study which regions and residues are important for transporter function.

One approach utilises the construction of cDNAs which encode GLUT2/GLUT3 chimeric proteins, with varying proportions of GLUT2 and GLUT3 sequence, and expression of these in *Xenopus* oocytes. For example, the ability of each protein to transport D-fructose should indicate which part(s) of the GLUT2 sequence is responsible for binding that sugar. Chimeric approaches have already been used and have demonstrated that replacement of the C-terminal domain of GLUT1 with that of GLUT2 leads to an increase of K_m and V_{max} values for 2-deoxy-D-glucose transport compared to wild-type GLUT1 (Katagiri *et al.*, 1992), suggesting that the C-terminal domain might at least partially confer some of the kinetic properties specific to each isoform. More localised site-directed mutagenesis within the C-terminal domains of GLUTs 1 and 2 might reveal which amino acid residues of this domain are responsible for interaction with D-glucose or producing conformational effects such that the intrinsic activity of the transporter is affected.

The use of chimeras is complemented by studies involving mutagenesis of individual amino acids, such as this study. Here, the injection of various mRNAs encoding GLUT3, each with one helix 8 amino acid residue substituted with alanine, into *Xenopus* oocytes, all resulted in some degree of functional expression, as determined the ability to transport 2-deoxy-D-glucose. Preliminary comparison of transport levels with oocytes injected with a similar quantity of wild-type GLUT3, suggest that substitution of any of three threonine residues results in a decrease in the ability of GLUT3 to transport 2-deoxy-D-glucose. However, increases in the level of transport, relative to wild-type levels, were observed with other mutants, which are unlikely to be attributable to increased transporter catalytic activity. This issue requires to be addressed by measurement of transporter numbers at the cell surface and by a more extensive kinetic analysis, including determination of the affinities of each mutant for 2-deoxy-D-glucose, D-galactose, D-glucose and

exofacial ligands such as maltose and 4,6-*O*-ethylidene-D-glucose. These values should indicate whether or not each mutant shows impaired binding and/or transport ability. Photoaffinity labelling of mutant transporters with ATB-BMPA or cytochalasin B and comparison with relative wild-type labelling should indicate the potential participation of each helix 8 residue in either the exofacial or endofacial binding sites, respectively. Disruption of ATB-BMPA labelling is much more likely, since this probe has been proposed to bind helix 8 of GLUT1 (Davies *et al.*, 1991), whereas cytochalasin B labelling occurs in region of helices 10-11 (Holman & Rees, 1987).

The results of this and other mutagenic studies, past and future, could be combined with investigations of the specificity of each isoform for D-glucose analogues, as determined for wild-type transporters, to discover which transporter residues interact with each sugar hydroxyl group, or are involved in hydrophobic interactions. This approach could also be used to determine which GLUT2 and GLUT5 residues are responsible for interaction with each hydroxyl group of D-fructose. Use of mutagenesis and domain-swapping in the same protein, after the characterisation of the non-mutant construct might also prove informative. With extensive application of molecular biological techniques to construct numerous mutant transporters, and careful analysis of the properties of each, it should be possible to build a picture of the binding sites of each transporter.

References.

- Allard, W. J. and Lienhard, G. E. (1985) *J. Biol. Chem.* **260**, 8668-8675.
- Alvarez, J., Lee, D. C., Baldwin S. A. and Chapman, D. (1987) *J. Biol. Chem.* **261**, 7101-7104.
- Appleman, J.R. & Lienhard, G.E. (1989) *Biochemistry* **28**, 8221-8227.
- Asano, T., Shibasaki, Y., Kasuga, M., Kanazawa, Y., Takaku, F., Akanuma, Y. and Oka, Y. (1988) *Biochem. Biophys. Res. Commun.* **154**, 1204-1211.
- Asano, T., Katagiri, H., Takata, K., Lin, J. -L., Ishihara, H., Inukai, K., Tsukuda, K., Kikuchi, M., Hirano, H., Yazaki, Y. and Oka, Y. (1991) *J. Biol. Chem.* **266**, 246322-24636.
- Asano, T., Takata, K., Katagiri, H., Tsukuda, K., Lin, J.-L., Ishikara, H., Inukai, K., Hirano, H., Yazaki, Y. and Oka, Y. (1992) *J. Biol. Chem.* **267**, 19636-19641.
- Axelrod, J. D. and Pilch, P. F. (1983) *Biochemistry* **22**, 2222-2227.
- Baker, G. F. and Widdas, W. F. (1973) *J. Physiol. (Lond)*. **231**, 143-165.
- Baldwin, S. A., Baldwin, J. M., Gorga, F. R. and Lienhard, G. E. (1979) *Biochim. Biophys. Acta* **552**, 183-188.
- Baldwin, J. M., Gorga, J. C. and Lienhard, G. E. (1981) *J. Biol. Chem.* **256**, 3685-3689.
- Baldwin, S. A. and Henderson, P. J. F. (1989) *Annu. Rev. Physiol.* **51**, 459-471.
- Baldwin, S. A. and Lienhard, G. E. (1989) *Methods Enzymol.* **174**, 39-50.
- Baldwin, S. A. (1993) *Biochim. Biophys. Acta* **1154**, 17-49.
- Barnett, J.E.G., Holman, G.D. & Munday, K.A. (1973) *Biochem. J.* **131**, 211-221.

- Barnett, J.E.G., Holman, G.D., Chalkley, R.A. & Munday, K.A. (1975) *Biochem. J.* **145**, 417-429.
- Bell, G. I., Kayano, T., Buse, J. B., Burant, C. F., Takeda, J., Lin, D., Fukumoto, H. and Seino, S. (1990) *Diabetes Care* **13**, 13276-13282.
- Bell, G. I., Burant, C. F., Takeda, J. and Gould, G. W. (1993) *J. Biol. Chem.* **268**, 19161-19164.
- Birnbaum, M. J., Haspel, H. C. and Rosen, O. M. (1986) *Proc. Natl. Acad. Sci. U.S.A.* **83**, 5784-5788.
- Birnbaum, M.J. (1989) *Cell* **57**, 305-315.
- Bloch, R. (1971) *Biochemistry* **12**, 4799-4801.
- Brandl, C. J. and Deber, C. M. (1986) *Proc. Natl. Acad. Sci. USA* **83**, 917-921.
- Brant, A. M., Jess, T. J., Milligan, G., Brown, C. M. and Gould, G. W. (1993) *Biochem. Biophys. Res. Commun.* **192**, 1297-1302.
- Bowyer, F. and Widdas, W. F. (1958) *J. Physiol. (Lond.)* **141**, 219-232.
- Büchel, D. E., Gronenborn, B. and Müller-Hill, B. (1980) *Nature (Lond.)* **283**, 541-545.
- Burant, C.F. & Bell, G.I. (1992) *Biochemistry* **31**, 10414-10420.
- Burant, C. F., Takeda, J., Brot-Laroche, E., Bell, G. I. and Davidson, N. O. (1992) *J. Biol. Chem.* **267**, 14523-14526.
- Cairns, M. T., Elliot, D. A., Scudder, P. R. and Baldwin, S. A. (1984) *Biochem J.* **221**, 179-188.
- Cairns, M. T., Alvarez, J., Panico, M., Gibbs, A. F., Morris, H. R., Chapman, D. and Baldwin, S. A. (1987) *Biochim. Biophys. Acta.* **905**, 295-310.

- Carruthers, A. and Helgerson, A. L. (1989) *Biochemistry* **28**, 8337-8346.
- Carruthers, A. (1990) *Physiol. Rev.* **70**, 1135-1176.
- Carruthers, A. (1991) *Biochemistry* **30**, 3898-3906.
- Carruthers, A. and Helgerson, A. L. (1991) *Biochemistry* **30**, 3907-3915.
- Charron, M. J., Brosius III, F. C., Alper, S. L. and Lodish, H. F. (1989) *Proc. Natl. Acad. Sci. U.S.A.* **86**, 2535-2539.
- Chin, J. J., Jung, E. K. Y. and Jung, C. Y. (1986) *J. Biol. Chem.* **261**, 7101-7104.
- Chin, J. J., Jung, E. K. Y., Chen, V. and Jung, C. Y. (1987) *Proc. Natl. Acad. Sci. U.S.A.* **84**, 4113-4116.
- Chin, J. J., Jhun, B. H. and Jung, C. Y. (1992) *Biochemistry* **31**, 1945-1951.
- Clark, A. E. and Holman, G. D. (1990) *Biochem. J.* **269**, 615-622.
- Colville, C. A., Seatter, M. J., Jess, T. J., Gould, G. W. and Thomas, H. M. (1993) *Biochem. J.* **290**, 701-706.
- Colville, C. A., Seatter, M. J. and Gould, G. W. (1993b) *Biochem. J.* **294**, 753-760.
- Craik, J. D. and Elliott, K. R. F. (1979) *Biochem. J.* **182**, 503-508.
- Cushman, S. W. and Wardzala, L. J. (1980) *J. Biol. Chem.* **255**, 4758-4762.
- Davidson, N. O., Hausman, A. M. L., Ifkovits, C. A., Buse, J. B., Gould, G. W., Burant, C. F. and Bell, G. I. (1992) *J. Biol. Chem.* **267**, C795-C800.
- Davies, A., Meeran, K., Cairns, M. T. and Baldwin, S. A. (1987) *J. Biol. Chem.* **262**, 9347-9352.

Davies, A., Ciardelli, T. L., Lienhard, G. E., Boyle, J. M., Wheton, A. D. and Baldwin, S. A. (1990) *Biochem. J.* **266**, 799-808.

Davies, A. F., Davies, A., Preston, R. A. J., Clark, A. E., Holman, G. D. and Baldwin, S. A. (1991) Molecular Basis of Biological Membrane Function meeting, abs S. E. R. C. (UK)

Deves, R. & Krupka, R.M. (1978) *Biochim. Biophys. Acta.* **510**, 339-348.

Deziel, M. R. and Rothstein, A. (1984) *Biochim. Biophys. Acta* **776**, 10-20.

Dohm, G. L., Tapscott, E. B., W.J., P., Flichinger, E. G., Meelheim, P., Fushiki, T., Atkinson, S. M., Elton, C. W. and Caro, J. F. (1988) *J. Clin. Invest.* **82**, 486-494.

Edwards, P. A. W. (1973) *Biochim. Biophys. Acta* **307**, 415-418.

Elliott, K.R.F. & Craik, J.D. (1982) *Biochem. Soc. Trans.* **10**, 12-13.

Fischbarg, J., Cheung, M., Czegledy, F., Li, J., Iserovich, P., Kuang, K., Hubbard, J., Garner, M., Rosen, O. M., Golde, D. W. and Vera, J. C. (1993) *Proc. Natl. Acad. Sci. USA* **90**, 11658-11662.

Fry, A. J., Towner, P., Holman, G. D. & Eienthal, R. (1993) *Mol. Biochem. Paraistol.* **60**, 9-18

Fukamoto, H., Seino, S., Imura, H., Seino, Y., Eddy, R. L., Fukushima, Y., Byers, M. G., Shows, T. B. and Bell, G. I. (1988) *Proc. Natl. Acad. Sci. USA* **85**, 5434-5438.

Fukumoto, H., Kayano, T., Buse, J. B., Edwards, Y., Pilch, P. F., Bell, G. I. & Seino, S. (1989) *J. Biol. Chem.* **264**, 7776-7779.

Garcia, J. C., Strube, M., Leingang, K., Keller, K. and Mueckler, M. M. (1992) *J. Biol. Chem.* **267**, 7770-7776.

Geck, P. (1971) *Biochim. Biophys. Acta* **241**, 462-472.

- Gibbs, A. F., Chapman, D. and Baldwin, S. A. (1988) *Biochem. J.* **27**, 6681-6685.
- Gorga, F. R. & Lienhard, G. E. (1982) *Biochemistry*, **21**, 1905-1908.
- Gould, G.W. & Lienhard, G.E. (1989) *Biochemistry*, **28**, 9447-9452.
- Gould, G. W., Thomas, H. M., Jess, T. J. and Bell, G. I. (1991) *Biochem. J.* **30**, 5139-5145.
- Gould, G.W., Brant, A.M., Shepherd, P.R., Kahn, B.B., McCoid, S. & Gibbs, E.M. (1992) *Diabetologia* **35**, 304-309.
- Gould, G. W. and Holman, G. D. (1993) *Biochem. J.* **295**, 329-341.
- Griffith, J. K., Baker, M. E., Rouch, D. A., Page, M. G. P., Skurray, R. A., Paulsen, I., Chater, K. F., Baldwin, S. A. and Henderson, P. J. F. (1992) *Curr. Opin. Cell Biol.* **4**, 684-695.
- Hacker, H. J., Thorens, B. and Gobholz, R. (1991) *Histochemistry* **96**, 435-439.
- Hashiramoto, M., Clark, A. E., Muraoka, A., Sakura, H., Holman, G. D. and Kasuga, M. (1992) *Diabetes* **41** Suppl. 1, 44A.
- Haspel, H. C., Rosenfeld, M. G. and Rosen, O. M. (1988) *J. Biol. Chem.* **263**, 398-403.
- Henderson, P. J. F., Baldwin, S. A., Cairns, M. T., Charalambous, B. M., Dent, H. C., Gunn, F. J., Liang, W. J., Lucas, V. A., Martin, G. E., McDonald, T. P., McKeown, B. J., Muiry, J. A. R., Petro, K. R., Roberts, P. E., Shatwell, K. P., Smith, G. and Tate, C. G. (1992) *Int. Rev. Cytol.* **137**, 149-208.
- Herbert, D. N., and Carruthers, A. (1991) *Curr. Opin. Cell Biol.* **3**, 702-709.
- Herbert, D. N. and Carruthers, A. (1992) *J. Biol. Chem.* **267**, 23829-23838.
- Helgerson, A. L., and Carruthers, A. (1987) *J. Biol. Chem.* **262**, 5464-5475.

Hirshman, M. F., Goodyear, L. J., Wardzala, L. J., Horton, E. D. and Horton, E. S. (1990) *J. Biol. Chem.* **265**, 987-991.

Hodgson, P. A., Osguthorpe, D. J. and Holman, G. D. (1992) Molecular Modelling of the Human Erythrocyte Glucose Transporter, 11th Annual Molecular Graphics, Society Meeting Abstract.

Holman, G.D., Pierce, E.J. & Rees, W.D. (1981) *Biochim. Biophys. Acta.* **646**, 382-388.

Holman, G. D. and Rees, W. D. (1982) *Biochim. Biophys. Acta.* **685**, 78-86.

Holman, G. D. and Midgley, P. J. W. (1985) *Carbohydr. Res.* **135**, 337-341.

Holman, G. D., Parkar, B. A. and Midgley, P. J. W. (1986) *Biochim. Biophys. Acta* **855**, 115-126.

Holman, G. D. and Rees, W. D. (1987) *Biochim. Biophys. Acta.* **897**, 395-405.

Holman, G. D., Kozka, I. J., Clark, A. E., Flower, C. J., Saltis, J., Habberfield, A. D., Simpson, I. A. and Cushman, S. W. (1990) *J. Biol. Chem.* **265**, 18172-18179.

Holman, G. D., Lo Leggio, L. and Cushman, S. W. (1994) *J. Biol. Chem.* **269**, 17516-17524.

Hresko, R. C., Kruse, M., Strube, M. and Mueckler, M. (1994) *J. Biol. Chem.* **269**, 20482-20488.

Inukai, K., Asano, T., Katagiri, H., Anai, M., Funaki, M., Ishihara, H., Tsukuda, K., Kikuchi, M., Yazaki, Y. and Oka, Y. (1994) *Biochem. J.* **302**, 355-361.

Ishihara, H., Asano, T., Katagiri, H., Lin, J. L., Tsukuda, K., Shibasaki, Y. and Oka, Y. (1991) *Biochem. Biophys. Res. Commun.* **176**, 922-930.

Jacquez, J. A. (1984) *Am. J. Physiol.* **246**, R289-298.

- James, D. E., Brown, R., Navarro, J. and Pilch, P. F. (1988) *Nature, London* **333**, 183-185.
- James, D. E., Strube, M. and Mueckler, M. (1989) *Nature, London* **338**, 83-87.
- Johnson, J. H., Ogawa, A., Chen, L., Orci, L., Newgard, C. B. and Unger, R. H. (1990) *Science* **250**, 546-549.
- Jordan, N. J. and Holman, G. D. (1992) *Biochem. J.* **286**, 649-656.
- Jung, C. Y. (1971) *J. Membr. Biol.* **5**, 2300-2314.
- Jung, E. K. Y., Chin, J. J. and Jung, C. Y. (1986) *J. Biol. Chem.* **261**, 9155-9160.
- Kaestner, K. H., Christy, R. J., McLenithan, J. C., Braiterman, L. H., Cornelius, P., Pekala, P. H. and Lane, M. D. (1989) *Proc. Natl. Sci. USA* **86**, 3150-3154.
- Kahlenberg, A. & Dolansky, D. (1972) *Can. J. Biochem* **50**, 638-6643.
- Karim, A. R., Rees, W. D. and Holman, G. D. (1987) *Biochim. Biophys. Acta* **902**, 402-405.
- Kasahara, M. and Hinkle, P. C. (1977) *J. Biol. Chem.* **252**, 7384-7390.
- Katagiri, H., Asano, T., Shibasaki, Y., Lin, J.-L., Tsukuda, K., Ishihara, H., Akanuma, Y., Takaku, F. and Oka, Y. (1991) *J. Biol. Chem.* **266**, 7769-7773.
- Katagiri, H., Asano, T., Ishihara, H., Tsukuda, K., Lin, J.-L., Inukai, K., Kikuchi, M., Yazaki, Y. and Oka, Y. (1992) *J. Biol. Chem.* **267**, 22550-22555.
- Katagiri, H., Asano, T., Ishihara, H., Lin, J.-L., Inukai, K., Shanahan, M. F., Tsukuda, K., Kikuchi, M., Yazaki, Y. and Oka, Y. (1993) *Biochem. J.* **291**, 861-867.
- Kayano, T., Fukumoto, H., Eddy, R. L., Fan, Y.-S., Byers, M. G., Shows, T. B. and Bell, G. I. (1988) *J. Biol. Chem.* **263**, 15245-15248.

- Kayano, T., Burant, C. F., Fukomoto, H., Gould, G. W., Fan, Y., Eddy, R. L., Byers, M. G., Shows, T. B., Seino, S. and Bell, G. I. (1990) *J. Biol. Chem.* **265**, 13276-13282.
- Keller, K., Strube, M. and Mueckler, M. (1989) *J. Biol. Chem.* **264**, 18884-18889.
- King, A.P.J, Tai, P-K. K. & Carter-Su, C. (1991) *Biochemistry* **30**, 11546-11553.
- Klip, A., Rampall, T., Young, D. and Holloszy, J. O. (1987) *FEBS. Lett.* **224**, 224-230.
- Klip, A., Marette, A., Dimitrakoudis, D., Rampal, T., Gicca, A., Shi, Z.-Q. and Vranic, M. (1992) *Diabetes Care* **15**, 1747-1776.
- Krieg, P. A. and Melton, D. A. (1984) *Nucleic Acids Res.* **12**, 7057-7070.
- Krupka, R.M. (1971) *Biochemistry* **10**, 1143-1153.
- Krupka, R. M. (1972) *Biochim. Biophys. Acta* **282**, 326-336.
- LeFevre P. G. and Davies, R. I. (1951) *J. Gen. Physiol.* **34**, 515-524.
- LeFevre P. G. and Marshall, J. K. (1959) *J. Biol. Chem.* **234**, 3022-3027.
- LeFevre, P. G. (1961) *Pharmacol. Rev.* **13**, 39-70.
- Levine, M., Levine, S. and Jones, M. N. (1971) *Biochim. Biophys. Acta.* **265**, 291-300.
- Li, J. and Tooth, P. (1987) *Biochemistry* **26**, 4816-4823.
- Lin, J.-L., Asano, T., Katagiri, H., Tsukuda, K., Ishihara, H., Inukai, K., Yazaki, Y. and Oka, Y. (1992) *Biochem. Biophys. Res. Commun.* **184**, 865-870.
- Lowe, A. G. & Walmsley, A. R. (1986) *Biochim. Biophys. Acta.* **857**, 146-154.
- Lowe, A. G. & Walmsley, A. R. (1987) *Biochim. Biophys. Acta.* **903**, 547-550.

Lund-Andersen, H. (1979) *Physiol. Rev.* **59**, 305-352.

Maher, F., Vannucci, S., Takeda, J. and Simpson, I. (1992)
Biochem. Biophys. Res. Commun. **182**, 703-711.

Maiden, M. C. J., Davis, E. O., Baldwin, S. A., Moore, D. C. M. and Henderson, P. J. F. (1987) *Nature(Lond)*. **325**, 641-643.

Marshall-Carlson, L., Celenza, J. L., Laurent, B. C. and Carlson, M. (1990)
Mol. Cell Biol. **10**, 1105-1115.

May, J. M. and Mikulecky, D. C. (1982) *J. Biol. Chem.* **257**, 11601-11608.

May, J. M. (1988) *J. Biol. Chem.* **263**, 13635-13640.

May, J. M. (1989) *J. Biol. Chem.* **263**, 875-881.

May, J. M., Buchs, A. and Carter-Su, C. (1990) *Biochemistry* **29**, 10393-10398.

Merrall, N. W., Plevin, R. and Gould, G. W. (1993) *Cellular Signalling* **5**,
667-675.

Midgley, P. J. W., Parkar, B. A. and Holman, G. D. (1985)
Biochim. Biophys. Acta **812**, 33-41.

Miyazaki, J., Araki, K., Yamato, E., Ikegami, H., Asano, T., Shibasaki, Y., Oka, Y.
and Yamamura, K. (1990) *Endocrinology* **127**, 126-132.

Mueckler, M., Caruso, C., Baldwin, S. A., Panico, M., Blench, I., Morris, H. R.,
Allard, W. J., Lienhard, G. E. and Lodish, H. F. (1985) *Science* **229**, 941-945.

Mueckler, M., Kruse, M., Strube, M., Riggs, A. C., Chiu, C. K. and Permutt, M.
A. (1994a) *J. Biol. Chem.* **269**, 17765-17767.

Mueckler, M., Weng, W. and Kruse, M. (1994b) *J. Biol. Chem.* **269**, 20533-20538.

- Nagamatsu, S., Kornhauser, J. M., Burant, C. F., Seino, S., Mayo, K. E. and Bell, G. I. (1992) *J. Biol. Chem.* **267**, 467-472.
- Nishimura, H., Pallardo, F. V., Seidner, G. A., Vannucci, S., Simpson, I. A. and Birnbaum, M. J. (1993) *J. Biol. Chem.* **268**, 8514-8520.
- Oka, Y., Asano, T., Shibasaki, Y., Lin, J. L., Tsukuda, K., Katagiri, H., Akanuma, Y. and Takaku, F. (1990) *Nature (Lond)*. **345**, 550-553.
- Orci, L., Thorens, B., Ravazzola, M. and Lodish, H. F. (1989) *Science* **245**, 295-297.
- Pawagi, A. B. and Deber, C. M. (1990) *Biochemistry* **29**, 950-955.
- Pederson, O. and Gliemann, J. (1981) *Diabetologia* **20**, 630-635.
- Pessino, J. M., Carruthers, A. and Czech, M. P. (1991) *J. Biol. Chem.* **266**, 20213-20217.
- Ploug, T., Galbo, H., Vinten, J., Jorgenson, M. and Richter, E. A. (1987) *Am. J. Physiol.* **253**, E12-E20.
- Preston, R. A. and Baldwin, S. A (1993) *Biochem. Soc. Trans.* **21**, 309-312.
- Rees, W.D. & Holman, G.D. (1981) *Biochim. Biophys. Acta.* **646**, 251-260.
- Santalucia, T., Camps, M., Castello, A., Munoz, P., Nuel, A., Testar, X., Palacin, M., and Zorzano, A. (1992) *Endocrinology.* **130**, 837-846.
- Sen, A. K. and Widdas, W. F. (1962) *J. Physiol. (London)* **160**, 392-403.
- Sergeant, S. and Kim, H. D. (1985) *J. Biol. Chem.* **260**, 14677-14682.
- Shepherd, P. R., Gibbs, E. M., Wesslau, C., Gould, G. W. and Kahn, B. B. (1992) *Diabetes* **41**, 1360-1364.
- Shimmin, E. R. A. and Stein, W. D. (1970) *Biochim. Biophys. Acta.* **211**,

308-312.

Simpson, I. A. and Cushman, S. W. (1986) *Annu. Rev. Biochem.* **55**, 1059-1089.

Sogin, D. C. and Hinkle, P. C. (1978) *J. Supramol. Struct.* **8**, 447-453.

Stryer, L. *Biochemistry* (1981) 2nd Edn., Freeman.

Suzue, K., Lodish, H. F. and Thorens, B. (1989) *Nucleic Acids Res.* **17**, 10099.

Suzuki, K. and Kono, T. (1980) *Proc. Natl. Sci. USA* **77**, 2542-2545.

Takata, K., Kasahara, T., Kasahara, M., Ezaki, O. and Hirano, H. (1990) *Biochem. Biophys. Res. Commun.* **173**, 67-73.

Tamori, Y., Hashiramoto, M., Clark, A. E., Mori, H., Muraoka, A., Kadowaki, T., Holman, G. D. and Kasuga, M. (1994) *J. Biol. Chem.* **269**, 2982-2986.

Tanizawa, Y., Riggs, A. C., Chiu, K. C., Janssen R. C., Bell, D. S. H., Go, R. P. C., Roseman, J. M., Acton, R. T. and Permutt, M. A. (1994) *Diabetologia* **37**, 420-427.

Taylor, L. P. and Holman, G. D. (1981) *Biochim . Biophys. Acta* **642**, 325-335.

Thomas, H. M., Takeda, J. and Gould, G. W. (1993) *Biochem. J.* **290**, 707-715.

Thorens, B., Sahar, H. K., Kaback, H. R. and Lodish, H. F. (1988) *Cell* **55**, 281-290.

Thorens, B., Cheng, Z.-Q., Brown, D. and Lodish, H. F. (1990) *Am. J. Physiol.* **259**, C279-C285.

Vischer, U., Blondel, B., Wollheim, C. B., Hoppner, E., Seitz, H. J. and Lypedjian, P. B. (1987) *Biochem. J.* **241**, 249-255.

Waddell, I. D., Scott, H., Grant, A. and Burchell, A. (1991) *Biochem. J.* **275**, 363-369.

- Waddell, I. D., Zomerschoe, A. G., Voice, M. W. and Burchell, A. (1992) *Biochem. J.* **286**, 173-177.
- Wadzinski, B. E., Shanahan, M. F., Seamon, K. B. and Ruoho, A. E. (1990) *Biochem. J.* **272**, 151-158.
- Walmsley, A. R. and Lowe, A. G. (1987) *Biochim . Biophys. Acta* **901**, 229-238.
- Walmsley, A.R. (1988) *Trends Biochem. Sci.* **13**, 226-231.
- Wandel, S., Schuermann, A., Becker, W. and Joost, H. G. (1994) *Naunyn-Schmied.Arch. Pharmacol.* **349**, Suppl. R7.
- Wang, J-F., Falke, J. J. and Chan, S. I. (1986) *Proc. Natl. Acad. Sci. USA* **83**, 3277-3281.
- Weiler Guttler, H., Zinke, H., Mockel, B., Frey, Gassen, H. G., (1989) *Biol. Chem. Hoppe. Seyler.* **370**, 467-473.
- Wellner, M., Monden, I. and Keller, K. (1992) *FEBS Lett.* **309**, 293-296.
- Wellner, M. Monden, I. and Keller, K. (1994a) *Biochem. J.* **299**, 813-817.
- Wellner, M., Monden, I. and Keller, K. (1994b) *Naunyn-Schmied.Arch. Pharmacol.* **349**, Suppl. R35.
- Wheeler, T. J., and Hinkle, P. C. (1981) *J. Biol. Chem.* **256**, 8907-8914.
- Whitesell, R. R. and Gliemann, J. (1979) *J. Biol. Chem.* **254**, 5276-5283.
- Widdas, W. F. (1952) *J. Physiol. (Lond).* **118**, 23-39.
- Widdas, W. F. (1955) *J. Physiol. (Lond).* **127**, 318-327.
- White, M. K., Rall, T. B. and Weber, M. J. (1991) *Mol. Cell Biol.* **11**, 4448-4454.

Yano, H., Seino, Y., Inagaki, N., Hinokio, Y., Yamamoto, T., Yasuda, K., Masuda, K., Someya, Y. and Imura, H. (1991) *Biochem. Biophys. Res. Commun.* 174, 470-477.

Zoccoli, M. A., Baldwin, S. A. and Lienhard, G. E. (1978) *J. Biol. Chem.* 253, 6923-6930.

